University of Huddersfield Repository

Myers, Alan

The Effect of Concrete Foundations and Machine Thermal Conditions on the Accuracy of Large Machine Tools

Original Citation

Myers, Alan (2017) The Effect of Concrete Foundations and Machine Thermal Conditions on the Accuracy of Large Machine Tools. Doctoral thesis, University of Huddersfield.

This version is available at http://eprints.hud.ac.uk/id/eprint/34454/

THE EFFECT OF

CONCRETE FOUNDATIONS

AND

MACHINE THERMAL CONDITIONS

ON THE ACCURACY OF

LARGE MACHINE TOOLS

ALAN MYERS

A thesis submitted to the University of Huddersfield in partial fulfilment of the requirements for the degree of Doctor of Philosophy

UNIVERSITY OF HUDDERSFIELD

SCHOOL OF COMPUTING AND ENGINEERING

CENTRE FOR PRECISION TECHNOLOGIES

DECEMBER 2017

DEDICATIONS

To my family, in particular my wife, daughter and son who have been extremely
understanding, encouraging and supportive
of me whilst I have been completing this
Thesis

COPYRIGHT STATEMENT

The author of this thesis (including any appendices and/or schedules to this thesis) owns any copyright in it (the "Copyright") and s/he has given The University of Huddersfield the right to use such copyright for any administrative, promotional, educational and/or teaching purposes.

Copies of this thesis, either in full or in extracts, may be made only in accordance with the regulations of the University Library. Details of these regulations may be obtained from the Librarian. This page must form part of any such copies made.

The ownership of any patents, designs, trademarks and any and all other intellectual property rights except for the Copyright (the "Intellectual Property Rights") and any reproductions of copyright works, for example graphs and tables ("Reproductions"), which may be described in this thesis, may not be owned by the author and may be owned by third parties. Such Intellectual Property Rights and Reproductions cannot and must not be made available for use without the prior written permission of the owner(s) of the relevant Intellectual Property Rights and/or Reproductions

ABSTRACT

Thesis

This thesis comprises of eighteen publications which describe research work which has been carried out into two aspects regarding the accuracy of large machine tools. The first six papers discuss the concrete foundations on which the machines are supported and the remaining twelve papers describe the consequences of thermal effects on machines. The publications are all ones of joint authorship, with the candidate being one of the named authors.

Manufacturing industry and the precision requirements of large machine tools

The thesis reviews the range of errors and their causes that effect large machine tools and then specifically addresses what are considered to be two of the most significant contributors to these inaccuracies, namely those caused by the concrete foundations which support the machines and those caused by thermal effects. Both can cause problems that can be very difficult and extremely expensive to resolve. After a concrete foundation has been cast, if it is found to be inadequate it cannot, of course, be easily modified and thermal effects such as environmental temperature changes for instance can require the use of factory air conditioning systems which are expensive to install, operate and maintain. The publications included in the thesis show a systematic contribution to significantly improving the accuracy of large machine tools with respect to the two mentioned subjects.

Modern components

Components used in modern equipment such as cars, trains, aircraft, robots, household appliances etc. require good functionality, reliability, long life, light weight etc. A significant contributor to these requirements is the high degree of precision [1] that these components are manufactured to in terms of their dimensions, form and surface finish. Production of virtually all of these components is achieved either directly or indirectly by use of machine tools. Therefore the machine tools need to perform extremely accurately, even more so than the components they produce since other factors such as fixtures, tooling etc. cause additional inaccuracies.

Machine tool Accuracy

To achieve high accuracy performance, the machines need to move in a precise manner in terms of their straightness of movement, positional accuracy, rotational orientation and the

relationship of one axis to another etc. It is also important that the accuracy is repeatable in order to guarantee the level of performance at all times.

Large machine tools:-

Large machine tools can weigh hundreds of tonnes, have traverses of eighty metres length or more and are used for machining a vast variety of components such as nuclear reactor vessels, marine diesel engines, valve bodies, rolls for steel mills, aircraft wing components such as skins, ribs, stringers and spars and large undercarriage components.

Foundations

Because the machines being considered are large and heavy their influence on the concrete foundations that support them is considerable and as a machine moves through its traverses the position of the center of gravity changes. The consequence is the foundation changes both shape (bends) and vertical position (sinks and rises). The six foundation papers describe the research and developement of techniques that can be used to ensure the distortions and deflections values are acceptable such that a machine will be capable of performing to its intended functionality. Also described is the research, development and performance testing of a taut wire and optical senors instrumentation for efficiently measuring the change of shape of the foundation.

Thermal Effects

The machines and the workpieces they produce, can be constructed from a variety of materials such as steel, aluminium, carbon fibre, concrete etc all of which have coefficients of linear expansion that when subjected to modest temperature changes can result in contractions and expansions that can cause workpiece to cutting tool relative positions to vary more than the workpiece dimensional tolerances. The twelve thermal publications describe the research and developement that has been carried out into machine tool thermal characteristics and the positional compensation techniques that have been developed to minimise the resulting positional errors. Using artifical intelligence methods this has been achieved so successfully that the errors can be reduced by 95%.

LIST OF CONTENTS

LIST OF FIGURES

ACKNOWLEDGEMENTS

I would like to state my sincere gratitude to Professor Andrew Ball, Pro-Vice Chancellor of Research and Enterprise at the University of Huddersfield, for his kind and considerate help and guidance, given to me during the preparation of this thesis.

My sincere gratitude is also to be passed to the Joint-Authors of the publications that are shown here as justification for my submission of this thesis for the award of PhD by Publication. Namely my colleagues and friends, Dr Andrew Longstaff, Dr Simon Fletcher, Professor Derek Ford, Dr Naeem Mian, Dr Simon Barrans, Dr Qiang Xu, Dr Oleg Borisov and Dr Ali Abdulshahed who all work or have worked within the Engineering Control and Machine Performance Research Group of the Centre for Precision Technologies. Their exceptional blend of academic and practical skills and abilities enabled the projects and publications to be completed so successfully.

Additionally, my thanks are also due to the many other people who have supported the compilation of the original publications such as the technicians and academics who have all played their part in the projects that produced the content for the publications. Namely they are Andrew Bell and Allan Kennedy, both Machine Tool Application Engineers and Dennis Town the Chief Technician for the School of Computing and Engineering whose experience, knowledge and skills helped to ensure successful outcomes to the various projects.

DECLARATIONS

The entire work presented in this thesis has been carried out whilst the candidate has been employed by the University of Huddersfield.

No part of this thesis has been submitted by the candidate in support of an application for any other degree either at the University of Huddersfield or at any other establishment.

AUTHOR DETAILS

Personal and Correspondence Information

Gender: Male

Marital Status: Married with two children

Date of Birth: 09-August-1946

Nationality: British

Work Address: -   Home Address:-

Centre for Precision Technologies   Badger House

School of Computing and Engineering   14, Dewsbury Road,

The University of Huddersfield, HD1 3DH   Rastrick, Brighouse HD6 3QB

Email: a.myers@hud.ac.uk

Current Title:

Professor of Machine Tool Technology

Current Post:

Technical Director of the Centre for Precision Technologies and Engineering Control and Machine Performance Research Group Leader

Education and Training

Middlesex University (formerly Hendon College of Technology)

1968-1973 – BSc Hons 2-1 Degree

Company sponsored four year degree sandwich course with three industrial placements involving experience in the planning, production and jig and tool departments.

Percival Whitley College of Further Education.

Higher National Certificate Mechanical Engineering (Endorsements in Thermodynamics, Structural Analysis and Industrial Administration.)

ONC Mechanical Engineering (Endorsement in Electrical Engineering).

'A' Level General Certificate of Education: - Computer Science.

Halifax Technical High School

Ordinary Level General Certificate of Education: - Mathematics, Physics, Geography, English Language, Engineering Drawing, Metal Work and Art

Employment History and Training

2002 – to present

PROFESSOR (Machine Tool Technology) University of Huddersfield

As Technical Director of the Centre for Precision Technologies and head of the Engineering Control and Machine Performance Research Group (ECMPG) duties include supervision of the research, enterprise and teaching activities of the groups 31 personnel, 7 of whom are Post-Doctoral, 16 are currently carrying out PhD studies, 2 administration and 5 technical staff.

Emeritus Professor D.G.Ford is a consultant to the group.

Prof Chris Holmes is a visiting Research Fellow to the group.

Research:-

Areas of activity and expertise are Precision Engineering Metrology, Machine Tool design and analysis, Control systems, Spindle and feed drives, Structures, Concrete Foundations, Hydrostatics, Hydraulics, Finite Element Analysis, Error avoidance, reduction and compensation techniques.

These activities are carried out in collaboration with industrial partners including Airbus UK, Rolls Royce, Siemens, Heidenhain, Hardinge/Bridgeport, BAeSystems, Mazak, Northrop Grumman Corporation (Los Angeles), Lockheed Martin (Fort Worth) and GKN Aerospace.

Publications:- 90 to date with further 6 recently submitted, approved and awaiting publication.

Enterprise:-Responsibilities include

First NPL measurement facility at a British University – The author was instrumental in the signing of a MoU between NPL & UoH. The facility provides a framework for business collaboration in the field of engineering measurement in support of UK manufacturing industry.

European funded Framework Programme 7 projects:-

Principal Investigator:

ADAMOD (€348k): Plug-in ADAptronic MODules for real-time errors (Thermal and Vibration) compensation & superfine positioning in reconfigurable high precision machine tools

SOMMACT (€415k): Self Optimising Measuring Machine Tools

HARCO (€330k): Hierarchical Adaptive Smart Components for Precision Production Systems

VCS – Development of low cost integrated control unit for compensation of machine tool geometric and thermal errors. Modular design enables retrofit onto nearly all new and existing machines. Capable of reducing geometric errors by 97% and thermal by 75%. Licence agreement with Singapore based company (Dapatech) to market the system globally

Knowledge Transfer Partnerships (KTP) – responsible for 4 schemes in collaboration with Craftsman Tools Ltd , Northern Tool Reclamation Ltd and Machine Tool Technologies Ltd (2)

Industrial Training Courses – Seven modules for CNC maintenance ranging from 2 days to 2 weeks have been written and delivered to Rolls-Royce and BAeSystems personnel.

Industrial Consultancy: - Typical activities are involved with Rolls-Royce SAMULET project – work is being currently being carried out at the following sites Barnoldswick, Derby, Hucknall, Annesly, Ansty and with Sheffield Forgemasters to calibrate of their largest machines.

Teaching:-

Teaching responsibilities include 5 Masters modules provided by the group.

2001 - 2002   CONSULTANT ENGINEER   (AMBAS Engineering Consultants)

Engineering consultant providing services such as 'expert witness', machine design, foundation design, Finite Element analysis, European Standards work and 'CE' marking etc.

1998- 2001   CHIEF ENGINEER   (Hargreaves Machine Tools Ltd)

Responsible for all aspects of the mechanical, hydraulic and pneumatic design and development of large machine tools, including setting of test procedures, specification of concrete foundations and ensuring the machines meet the latest safety standards.

The most significant aspect of this work has been the design of a £2.3 million, 270 Tonne die sinking machine for the American steel industry to be used for producing structural, under carriage parts for Boeing aircraft.

The design process involved the use of 2D and 3D design software (i.e. AutoCAD and Pro/Eng.), as well as Pro Mechanica Finite Element Analysis software.

1993-2000   TECHNICAL MANAGER   (AsquithButler Ltd)

In charge of the development and the inspection departments and responsible for the design, development and quality control of the company product range of CNC machine tools.

During this period the company introduced six different new designs of machining centres and a new design of spline rolling machine for sale to the automotive industry

1981-1993   CHIEF RESEARCH AND DEVELOPMENT ENGINEER   (William Asquith 1981 Ltd)

Responsible for research and development of the company range of a variety of special purpose machine tools supplied to such customers as BAe, GEC, and British Rail

This work involved virtually all aspects of machine tool design from detailed structural analysis to the mechanical, hydraulic, pneumatic and electrical design of test rigs using both CNC and PLC controllers.

1973-1981 DEVELOPMENT ENGINEER   (William Asquith Ltd)

Design and development of a varied range of machine tools from radial drilling machines to large (150 tonne) ram type milling, drilling and boring machines supplied to the heavy engineering industry such as Parsons, British Steel and GEC.

1963-1968   DRAWING OFFICE / SHOP FLOOR APPRENTICESHIP (Kitchen / Wade)

One year at apprentice training school

One-year shop floor experience in the machine shops and fitting departments

Three year Design Office Apprenticeship.

Current and Previously held Professional Posts and Responsibilities

Chairman of the BSI Machine Tool Standards Committee MTE1/2

Member of the ISO TC 39 SC 02 Machine Tool Standards Committee

Member of the Manufacturing Technologies Association (MTA) Technical Committee

Member of the Executive Board of Trustees for Kirkdale Industrial Training Services

Member of the EPSRC Peer Review College

Co-organiser of the Lamdamap International Conferences.

Member of UK Precision Engineering Network Committee and MTA Technical Committee.

Reviewer for Institute of Mech. Eng. and Int. Journal of Advanced Mfg. Tech. publications.

Grant reviewer for the Swiss National Science Foundation

School Computing &Engineering award for Enterprise 2008.

Principal Investigator EU Framework 7 International grant ADAMOD

Principal Investigator EU Framework 7 International grant SOMMACT

Principal Investigator EU Framework 7 International grant HARCO

Co-Investigator EU Framework 7 International grant EASE R^3

Co-Investigator, EPSRC Centre for Innovative Manufacturing in Advanced Metrology (£7.8M)

Co-investigator on 2 completed EPSRC Research Grants (CAPM and REDUCE)

Principal investigator on 1 EPSRC Research Grant (ROBCON) rated Tending to Outstanding.

Patent: Named inventor on patent of a heavy-duty foundation connector used for precision levelling of large machine tools and used extensively on Asquith Ltd machine tools.

External lecturing: -   Have given individual lectures on various aspects of machine tool design to the Institute of Mechanical Engineers, Design Council, AMTRI and UMIST.

Research Experience and Expertise

Prior to commencing employment at the UoH the author had worked at four different companies in the UK Machine Tool industry, manufacturing machines for a global market. The machines were individually valued at up to £2M and could weigh 200Tonnes with concrete foundations weighing 1,000 Tonnes. Over a forty year period and holding a number of senior positions within the companies led to significant experience both at home and abroad in the field of Research and Development of extremely large, complex, and precise machine tools.

Holding posts such as Chief Research and Development Engineer and with responsibilities for Quality Control and Inspection enabled the author to gain expertise and skills in many disciplines such as:-

Prototype projects and Test Rigs

Extensive machine design experience with particular emphasis on the following areas:

Spindle transmission design – high speed (10000rpm) – electro spindles

Structural static and dynamic design, analysis and testing.

Feed axes design and analysis

Journal and linear bearing technology.

Hydrostatic bearing system design.

Materials selection.

Value analysis.

Hydraulic, pneumatic, coolant, lubrication and electrical circuit design

Fatigue testing

Specification of machine testing procedures.

'CE' marking requirements, technical manuals.

Microsoft Office,

AutoCAD

Simulink systems analysis software

Pro/Eng 3D CAD

Pro/Mechanica Finite Element Analysis software.

SolidWorks 3D CAD

Concrete foundations specification, design and testing.

Journal & Peer Reviewed Conference Publications Full List

2015

2015 – 03 (Thermal - Journal):   Abdulshahed, Ali, Longstaff, Andrew P., Fletcher, Simon and Myers, Alan (2015) *Thermal error modelling of machine tools based on ANFIS with fuzzy c-means clustering using a thermal imaging camera.* Applied Mathematical Modelling, 39 (7). pp. 1837-1852. ISSN 0307-904X

Mian, Naeem S., Fletcher, Simon, Longstaff, Andrew P. and Myers, Alan (2015) *FEA-based design study for optimising non-rigid error detection on machine tools.* In: Laser Metrology and Machine Performance XI, LAMDAMAP 2015, University of Huddersfield.

Alzarok, Hamza, Fletcher, Simon, Longstaff, Andrew P. and Myers, Alan (2015) *Investigation of a new method for improving image resolution for camera tracking applications.* In: Laser Metrology and Machine Performance XI, LAMDAMAP 2015. University of Huddersfield, UK, pp. 40-50. ISBN 978-0-9566790-5-5

2014

 Li, Feng, Longstaff, Andrew P., Fletcher, Simon and Myers, Alan (2014) *Rapid and accurate reverse engineering of geometry based on a multi-sensor system.* International Journal of Advanced Manufacturing Technology, 74 (1-4). pp. 369-382. ISSN 0268-3768

Ford, Derek G., Castaneda, Veimar Yobany Moreno, Longstaff, Andrew P., Pislaru, Crinela and Myers, Alan (2014) *Computer numerical control vertical machining centre feed drive modelling using the transmission line technique.* Proceedings of the Institution of Mechanical Engineers Part C Journal of Mechanical Engineering Science. pp. 1-22. ISSN 09544062

2014 – 06 (Foundation - Journal):   Borisov, Oleg, Fletcher, Simon, Longstaff, Andrew P. and Myers, Alan (2014) *Performance evaluation of a new taut wire system for straightness measurement of machine tools.* Precision Engineering, 38 (3). pp. 492-498. ISSN 0141-6359

Chen, Xiaomei, Longstaff, Andrew P., Fletcher, Simon and Myers, Alan (2014) *Deployment and evaluation of a dual-sensor autofocusing method for on-machine measurement of patterns of small holes on freeform surfaces.* Applied Optics, 53 (10). pp. 2246-2255. ISSN 1559-128X

Chen, Xiaomei, Longstaff, Andrew P., Fletcher, Simon and Myers, Alan (2014) *Analysing and evaluating a dual-sensor autofocusing method for measuring the position of patterns of small holes on complex curved surfaces.* Sensors and Actuators A: Physical, 210. pp. 86-94. ISSN 0924-4247

Longstaff, Andrew P., Fletcher, Simon, Parkinson, Simon and Myers, Alan (2014) *The Role of Measurement and Modelling of Machine Tools in Improving Product Quality.* International Journal of Metrology and Quality Engineering, 4 (03). pp. 177-184. ISSN 2107-6839

Chen, Xiaomei, Longstaff, Andrew P., Parkinson, Simon and Myers, Alan (2014) *A Method for Rapid Detection and Evaluation of Position Errors of Patterns of Small Holes on Complex Curved and Freeform Surfaces.* International Journal of Precision Engineering and Manufacturing, 15 (2). pp. 209-217. ISSN 2234-7593

Ford, Derek G., Widiyarto, Muhammad Helmi Nur, Myers, Alan, Longstaff, Andrew P. and Fletcher, Simon (2014) *Structural analysis and chracterisation technique applied to a CNC vertical machining centre.* Journal of Mechanical Engineering Science. ISSN 0954-4062

2013

Alzarok, Hamza, Fletcher, Simon, Longstaff, Andrew P. and Myers, Alan (2013) *Assessment of the positioning accuracy of a small articulated robot during machining operations.* In: Proceedings of Computing and Engineering Annual Researchers' Conference 2013 : CEARC'13. University of Huddersfield, Huddersfield, pp. 106-111. ISBN 9781862181212

Shagluf, Abubaker, Longstaff, Andrew P., Fletcher, Simon, Denton, Paul and Myers, Alan (2013) *The importance of assessing downtime cost related factors towards an optimised machine tool calibration schedule.* In: Proceedings of Computing and Engineering Annual Researchers' Conference 2013 : CEARC'13. University of Huddersfield, Huddersfield, pp. 182-187. ISBN 9781862181212

Li, Feng, Longstaff, Andrew P., Fletcher, Simon and Myers, Alan (2013) *A Practical Coordinate Unification Method for Integrated Tactile-Optical Measuring System.* Optics and lasers in engineering. ISSN 0143-8166

2013 – 13 (Thermal - Conference): Abdulshahed, Ali, Longstaff, Andrew P., Fletcher, Simon and Myers, Alan (2013) *Application of GNNMCI(1, N) to environmental thermal error modelling of CNC machine tools.* In: The 3rd International Conference on Advanced Manufacturing Engineering and Technologies. KTH Royal Institute of Technology, Stockholm, Sweden, pp. 253-262. ISBN 9789175018928

Mian, Naeem S., Fletcher, Simon, Longstaff, Andrew P. and Myers, Alan (2013) *Towards obtaining robust boundary condition parameters to aid accuracy in FEA thermal error predictions.* In: 2nd Annual EPSRC Manufacturing the Future Conference, 17-18 September 2013, Cranfield University, UK.

Li, Feng, Longstaff, Andrew P., Fletcher, Simon and Myers, Alan (2013) *Multiple-sensor integration for efficient reverse engineering of geometry.* Proceedings of the 11th International Conference on Manufacturing Research. pp. 319-324. ISSN 978-1-907413-23-0

Shagluf, Abubaker, Longstaff, Andrew P., Fletcher, Simon, Denton, Paul and Myers, Alan (2013) *Predictive Calibration-Based Tolerance Boundaries for Arresting Deterioration of Machine Tool Accuracy.* In: 2nd Annual EPSRC Manufacturing the Future Conference, 17-18 September 2013, Cranfield University, UK.

2013 – 09 (FJ) : Borisov, Oleg, Fletcher, Simon, Longstaff, Andrew P. and Myers, Alan (2013) *New low cost sensing head and taut wire method for automated straightness measurement of machine tool axes.* Optics and lasers in engineering, 51 (8). pp. 978-985. ISSN 0143-8166

Rubio Rodriguez, Luis, De la Sen Parte, Manuel, Longstaff, Andrew P. and Myers, Alan (2013) *Analysis of discrete time schemes for milling forces control under fractional order holds.* International Journal of Precision Engineering and Manufacturing, 14 (5). pp. 735-744. ISSN 2234-7593

Ford, Derek G., Myers, Alan, Haase, Frerk, Lockwood, Stephen and Longstaff, Andrew P. (2013) *Active Vibration Control for a CNC Milling Machine.* Proceedings of the Institute of Mechanical Engineering Part C, Journal of Mechanical Engineering Science. ISSN 0954-4062

2013 – 06 (TJ) : Mian, Naeem S., Fletcher, Simon, Longstaff, Andrew P. and Myers, Alan (2013) *Efficient estimation by FEA of machine tool distortion due to environmental temperature perturbations.* Precision Engineering, 37 (2). pp. 372-379. ISSN 0141-6359

2013 – 05 (TC) : Abdulshahed, Ali, Longstaff, Andrew P., Fletcher, Simon and Myers, Alan (2013) *Comparative study of ANN and ANFIS prediction models for thermal error compensation on CNC machine tools.* In: Laser Metrology and Machine Performance X. LAMDAMAP 2013. EUSPEN, Bedfordshire, UK, pp. 79-89. ISBN 978-0-9566790-1-7

Chen, Xiaomei, Longstaff, Andrew P., Fletcher, Simon and Myers, Alan (2013) *Evaluation of measurement technique for a precision aspheric artefact using a nano-measuring machine.*, In: Laser Metrology and Machine Performance X. LAMDAMAP 2013, EUSPEN, Bedfordshire, UK, pp. 357-364. ISBN 978-0-9566790-1-7

Rubio Rodriguez, Luis, Longstaff, Andrew P., Fletcher, Simon and Myers, Alan (2013) *Towards self-optimizing and self-adaptive milling processes.* In: Laser Metrology and Machine Performance X. LAMDAMAP 2013, EUSPEN, Bedfordshire, UK

2013 – 02 (TC): Mian, Naeem S., Fletcher, Simon, Longstaff, Andrew P. and Myers, Alan (2013) *The significance of air pockets for modelling thermal errors of machine tools..* In: Laser Metrology and Machine Performance X. LAMDAMAP 2013, EUSPEN, Bedfordshire, UK, pp. 189-198. ISBN 978-0-9566790-1-7

Li, Feng, Longstaff, Andrew P., Fletcher, Simon and Myers, Alan (2013) *Integrated Tactile-Optical Coordinate System for the Reverse Engineering of Complex Geometry.* In: Proceedings of the 37th International MATADOR Conference. Springer, pp. 41-44. ISBN 9781447144793

2012

Leung, AYT, Guo, Zhongjin and Myers, Alan (2012) *Steady state bifurcation of a periodically excited system under delayed feedback controls.* Communications in Nonlinear Science and Numerical Simulation, 17 (12). pp. 5256-5272. ISSN 1007-5704

2012 – 06 (TC): Mian, Naeem S., Fletcher, Simon, Longstaff, Andrew P. and Myers, Alan (2012) *An efficient offline method for determining the thermally sensitive points of a machine tool structure.* In: 37th International Matador Conference, 25th-27th July 2012, Manchester, England.

Sztendel, S., Pislaru, Crinela, Longstaff, Andrew P., Myers, Alan, Fletcher, Simon and Ford, Derek G. (2012) *Analysis of complex interactions between mechanical elements using ansys and simulink.* In: Proceedings of The Queen's Diamond Jubilee Computing and Engineering Annual Researchers' Conference 2012: CEARC'12. University of Huddersfield, Huddersfield, pp. 136-141. ISBN 978-1-86218-106-9

Parkinson, S., Longstaff, Andrew P., Crampton, Andrew, Fletcher, Simon, Allen, Gary and Myers, Alan (2012) *Automation as a Solution for Machine Tool Calibration Planning.* In: Proceedings of The Queen's Diamond Jubilee Computing and Engineering Annual Researchers' Conference 2012: CEARC'12. University of Huddersfield, Huddersfield, pp. 57-62. ISBN 978-1-86218-106-9

Li, Feng, Longstaff, Andrew P., Fletcher, Simon and Myers, Alan (2012) *Integrated Tactile and Optical Measuring Systems in Three Dimensional Metrology.* In: Proceedings of The Queen's Diamond Jubilee Computing and Engineering Annual Researchers' Conference 2012: CEARC'12. University of Huddersfield, Huddersfield, pp. 1-6. ISBN 978-1-86218-106-9

Parkinson, Simon, Longstaff, Andrew P., Crampton, Andrew, Allen, Gary, Fletcher, Simon and Myers, Alan (2012) *The use of Cryptographic Principles within Metrology Software.* In: Advanced Mathematical and Computational Tools in Metrology and Testing. Series on Advances in Mathematics for Applied Sciences, 9 (84). World Scientific, Singapore, China, pp. 292-296.

Sztendel, S., Pislaru, Crinela, Longstaff, Andrew P., Fletcher, Simon and Myers, Alan (2012) *Five-Axis Machine Tool Condition Monitoring Using dSPACE Real-Time System.* Journal of Physics: Conference Series, 364. 012091. ISSN 1742-6596

2011

Parkinson, Simon, Longstaff, Andrew P., Allen, Gary, Crampton, Andrew, Fletcher, Simon and Myers, Alan (2011) *Hierarchical Task Based Process Planning For Machine Tool Calibration.* Proceedings of The 29th Workshop of the UK Planning and Scheduling Special Interest Group (PlanSIG2011). pp. 53-60. ISSN 1368-5708

Parkinson, Simon, Longstaff, Andrew P., Crampton, Andrew, Fletcher, Simon, Allen, Gary and Myers, Alan (2011) *Representing the Process of Machine Tool Calibration in First-order Logic.* In: Proceedings of the 17th International Conference on Automation & Computing. Chinese Automation and Computing Society, Huddersfield, UK. ISBN 978-1-86218-098-7

Li, Feng, Longstaff, Andrew P., Fletcher, Simon and Myers, Alan (2011) *A fast and effective way to improve the merging accuracy of multi-view point cloud data.* In: Proceedings of the 17th International Conference on Automation & Computing. Chinese Automation and Computing Society, Huddersfield, UK, pp. 18-21. ISBN 978-1-86218-098-7

2011 – 05 (TJ): Mian, Naeem S., Fletcher, Simon, Longstaff, Andrew P. and Myers, Alan (2011) *Efficient thermal error prediction in a machine tool using finite element analysis.* Measurement Science and Technology, 22 (8). 085107. ISSN 0957-0233

Parkinson, Simon, Longstaff, Andrew P., Fletcher, Simon, Allen, Gary, Crampton, Andrew and Myers, Alan (2011) *Controlling Machine Tool Accuracy through a Robust Calibration Process.* In: Yorkshire and North East Vitae Public Engagement Competition, 6th April 2011, Durham town hall.

Borisov, Oleg, Fletcher, Simon, Longstaff, Andrew P. and Myers, Alan (2011) *Efficient machine error measurement.* In: Yorkshire and North East Vitae Public Engagement Competition, 6 April 2011, Durham town hall, UK.

Feng, Li, Longstaff, Andrew P., Fletcher, Simon and Myers, Alan (2011) *Integrated tactile-optical coordinate measuring system.* In: University of Huddersfield Annual Research Festival School of Computing and Engineering, March 2011, University of Huddersfield.

Parkinson, Simon, Longstaff, Andrew P., Fletcher, Simon, Crampton, Andrew, Allen, Gary and Myers, Alan (2011) *Cryptographic Techniques in Metrology Software.* In: University of Huddersfield Annual Research Festival School of Computing and Engineering 12th March 2010, Friday 12th March 2010, University of Huddersfield.

2010

Borisov, Oleg, Fletcher, Simon, Longstaff, Andrew P. and Myers, Alan (2010) *Efficient Machine Error Measurement.* In: Future Technologies in Computing and Engineering: Proceedings of Computing and Engineering Annual Researchers' Conference 2010: CEARC'10. University of Huddersfield, Huddersfield. ISBN 9781862180932

Wright, Daniel, Murgatroyd, S., Longstaff, Andrew P., Myers, Alan and Fletcher, Simon (2010) *Process control within an SME to increase output and achieve consistent manufacture of components.* In: Future Technologies in Computing and Engineering: Proceedings of Computing and Engineering Annual Researchers' Conference 2010: CEARC'10. University of Huddersfield, Huddersfield. ISBN 9781862180932

Parkinson, Simon, Longstaff, Andrew P., Fletcher, Simon, Allen, Gary, Crampton, Andrew and Myers, Alan (2010) *A novel framework for establishing a machine tool quality metric.* In: Future Technologies in Computing and Engineering: Proceedings of Computing and Engineering Annual Researchers' Conference 2010: CEARC'10. University of Huddersfield, Huddersfield. ISBN 9781862180932

Sztendel, S., Pislaru, Crinela, Longstaff, Andrew P., Ford, Derek G., Myers, Alan and Poxton, Anthony (2010) *Linking fed drive model with structural models for CNC machine tools.* In: University of Huddersfield Annual Research Festival School of Computing and Engineering 12th March 2010, Friday 12th March 2010, University of Huddersfield.

Mian, Naeem S., Fletcher, Simon, Longstaff, Andrew P., Myers, Alan and Pislaru, Crinela (2010) *Novel and efficient thermal error reduction strategy for machine tool performance improvement.* In: University of Huddersfield Annual Research Festival School of Computing and Engineering 12th March 2010, Friday 12th March 2010, University of Huddersfield.

Poxton, Anthony, Longstaff, Andrew P., Barrans, Simon, Myers, Alan, Fletcher, Simon and Pislaru, Crinela (2010) *Off-line investigation of machine tool non-rigid errors.* In: University of Huddersfield Annual Research Festival School of Computing and Engineering 12th March 2010, Friday 12th March 2010, University of Huddersfield.

2009

Mian, Naeem S., Fletcher, Simon, Longstaff, Andrew P., Myers, Alan and Pislaru, Crinela (2009) *Efficient offline thermal error modelling strategy for accurate thermal behaviour assessment of the machine tool.* In: Proceedings of Computing and Engineering Annual Researchers' Conference 2009: CEARC'09. University of Huddersfield, Huddersfield, pp. 26-32. ISBN 9781862180857

Aldawi, Fouad, Longstaff, Andrew P., Fletcher, Simon, Mather, Peter, Myers, Alan and Briggs, Jack (2009) *A Low-cost Ultrasonic 3D Measurement Device for Calibration for Cartesian and Non-Cartesian Machines.* Journal of the Japanese Society of Experimental Mechanics, 9 (S). pp. 77-80. ISSN 1346-4930

Lobato, H, Fletcher, Simon, Myers, Alan, Orchard, N and Charlesworth, A (2009) *Using a Kinematic Model of a Machine Tool to Predict Component Feature Capability.* In: Laser Metrology and Machine Performance IX, LAMDAMAP 2009, Brunel University, ISBN 9780955308277

Longstaff, Andrew P., Fletcher, Simon, Poxton, Anthony and Myers, Alan (2009) *Comparison of Volumetric Analysis Methods for Machine Tools with Rotary Axes.* In: Laser Metrology and Machine Performance IX, LAMDAMAP 2009, Brunel University, pp. 87-96. ISBN 978-0-9553082-7-7

Fletcher, Simon, Longstaff, Andrew P. and Myers, Alan (2009) *Defining and Computing Machine Tool Accuracy.* In: Laser Metrology and Machine Performance IX, LAMDAMAP 2009, Brunel University, pp. 77-86. ISBN 978-0-9553082-7-7

Mian, Naeem S., Fletcher, Simon, Longstaff, Andrew P., Myers, Alan and Pislaru, Crinela (2009) *Efficient Offline Thermal Modelling for Accurate Assessment of Machine Tool Thermal Behaviour.* In: Laser Metrology and Machine Performance IX, LAMDAMAP 2009, Brunel University, pp. 9-18. ISBN 978-0-9553082-7-7

2009 – 04 (FC): Myers, Alan, Barrans, Simon, Longstaff, Andrew P., Fletcher, Simon and Ford, Derek G. (2009) *Evaluation and Comparison of a Large Machine Tool Structure with ISO Standard Alignment Tests.* In: Laser Metrology and Machine Performance IX, LAMDAMAP 2009, Brunel University, pp. 57-66. ISBN 978-0-9553082-7-7

Pislaru, Crinela, Ford, Derek G. and Myers, Alan (2009) *Novel condition monitoring technique used for improved CNC machine tool performance.* In: Laser metrology and machine performance IX, LAMDAMAP 2009, Brunel University, pp. 176-186. ISBN 9780955308277

Aldawi, Fouad, Longstaff, Andrew P., Fletcher, Simon, Pislaru, Crinela, Myers, Alan and Briggs, Jack (2009) *A high accuracy ultrasonic system for measurement of air temperature.* In: Proceedings of the 9th International Conference - San Sebastian, Spain, 2009. EUSPEN, pp. 134-137. ISBN 978-0-9553082-6-0

Mian, Naeem S., Fletcher, Simon, Longstaff, Andrew P., Myers, Alan and Pislaru, Crinela (2009) *Novel and Efficient Thermal Error Reduction Strategy For Machine Tool Performance Improvement.* In: University of Huddersfield Research Festival, 23rd March - 2nd April 2009, University of Huddersfield.

2008

Aldawi, Fouad, Longstaff, Andrew P., Fletcher, Simon, Mather, Peter and Myers, Alan (2008) *A Low Cost Ultrasonic 3D Measurement Device for Calibration for Cartesian and Non-Cartesian Machines.* In: Third International Symposium on Advanced Fluid/Solid Science

and Technology in Experimental Mechanics ISEM 2008, 7th - 10th December 2008, National Cheng Kung University, Tainan, Taiwan.

Mian, Naeem S., Fletcher, Simon, Longstaff, Andrew P., Myers, Alan and Pislaru, Crinela (2008) *Novel and efficient thermal error reduction strategy for machine tool performance improvement.* In: Proceedings of Computing and Engineering Annual Researchers' Conference 2008: CEARC'08. University of Huddersfield, Huddersfield, pp. 15-22. ISBN 978-1-86218-067-3

Poxton, Anthony, Longstaff, Andrew P., Barrans, Simon, Myers, Alan, Fletcher, Simon and Pislaru, Crinela (2008) *Simulation of the structural elements of a three axis VMC for machine tool error compensation.* In: Proceedings of Computing and Engineering Annual Researchers' Conference 2008: CEARC'08. University of Huddersfield, Huddersfield, pp. 23-27. ISBN 978-1-86218-067-3

Aldawi, Fouad, Longstaff, Andrew P., Fletcher, Simon, Mather, Peter, Myers, Alan and Briggs, Jack (2008) *A multifrequency FM-based ultrasonic system for accuracy 3D measurement.* In: Proceedings of Computing and Engineering Annual Researchers' Conference 2008: CEARC'08. University of Huddersfield, Huddersfield, pp. 9-14. ISBN 978-1-86218-067-3

Sztendel, S., Pislaru, Crinela, Ford, Derek G. and Myers, Alan (2008) *Development of experiment control graphical user interface for Hardware in the Loop (HIL) simulations.* In: MATAR 2008, 15th-18th September 2008, Prague University.

Pislaru, Crinela, Sztendel, S., Ford, Derek G. and Myers, Alan (2008) *Real-time implementation of a novel transmission line matrix (TLM) model for high speed feed drives.* In: MATAR 2008, 15th-18th September 2008, Prague University.

Myers, Alan, Pislaru, Crinela, Longstaff, Andrew P. and Fletcher, Simon (2008) *Machine Tool Accuracy and Real-Time Control.* In: Research Festival - School of Computing and Engineering Research Open Day, Friday 7th March 2008, University of Huddersfield.

2007

Aldawi, Fouad, Longstaff, Andrew P., Fletcher, Simon, Mather, Peter and Myers, Alan (2007) *A high accuracy ultrasound distance measurement system using binary frequency shift-keyed signal and phase detection.* In: Proceedings of Computing and Engineering Annual Researchers' Conference 2007: CEARC'07. University of Huddersfield, Huddersfield, pp. 1-7.

Poxton, Anthony, Longstaff, Andrew P., Barrans, Simon, Myers, Alan, Fletcher, C. and Pislaru, Crinela (2007) *Analysis and reduction of machine tool non-rigid errors.* In: School of Computing and Engineering Annual Researchers' Conference 2007, 14th December 2007, University of Huddersfield.

2007 – 05 (TC): Longstaff, Andrew P., Fletcher, Simon and Myers, Alan (2007) *Flexible compensation of thermal errors.* In: EUSPEN Topical Meeting "Thermal Effects in Precision Engineering", 3 - 4 December 2007, Maastricht, The Netherlands.

2007 - 04 (TC): Fletcher, Simon, Longstaff, Andrew P. and Myers, Alan (2007) *Measurement methods for efficient thermal assessment and error compensation.* In: EUSPEN Topical Meeting "Thermal Effects in Precision Engineering", 3 - 4 December 2007, Maastricht, The Netherlands.

Pislaru, Crinela, Ford, Derek G., Widiyarto, Muhammad Helmi Nur, Longstaff, Andrew P. and Myers, Alan (2007) *Hardware-in-the-loop implementation of modern CNC machine tool feed drive models.* In: Laser Metrology and Machine Performance VIII, LAMDAMAP 2007, Cardiff University.

2007 – 02 (FC): Myers, Alan, Barrans, Simon and Ford, Derek G. (2007) *Structural Analysis of a Large Moving Gantry Milling Machine including its Work Support System and Foundation.* In: Laser Metrology and Machine Performance VIII, LAMDAMAP 2007, Cardiff University, pp. 63-72. ISBN 9780955308239

Pislaru, Crinela, Widiyarto, Muhammad Helmi Nur, Ford, Derek G. and Myers, Alan (2007) *Theoretical and experimental approach for the evaluation of structural dynamics of CNC machine tools.* In: Laser Metrology and Machine Performance VIII, LAMDAMAP 2007, Cardiff University, Wales.

2006

Pislaru, Crinela, Myers, Alan and Ford, Derek G. (2006) *Methods for modelling and simulating the dynamic behaviour of CNC machine tool feed drives.* In: EUSPEN 2006, 28th May - 1st June 2006, Baden bei Wien, Austria.

Pislaru, Crinela, Myers, Alan, Ford, Derek G. and Moreno-Castaneda, V.Y. (2006) *Modelling the Dynamic Behaviour of CNC Machine Tool Feed Drives by Using a Novel 2D Transmission Line Model.* In: EUSPEN 2006, 28th May- 1st June 2006, Baden bei Wien, Austria.

2005

2005 – 12 (TC): Fletcher, Simon, Longstaff, Andrew P. and Myers, Alan (2005) *Practical compensation of all significant thermal errors in machine tools.* In: 3rd International Congress on Precision Machining, Vienna, Austria, October 2005, Vienna, Austria.

Longstaff, Andrew P., Fletcher, Simon and Myers, Alan (2005) *Volumetric compensation of machine tools makes geometric errors negligible.* In: 3rd International Congress on Precision Machining, October 2005, Vienna, Austria.

2005 – 10 (TC): Fletcher, Simon, Longstaff, Andrew P. and Myers, Alan (2005) *Flexible modelling and compensation of machine tool thermal errors.* In: 20th Annual Meeting of American Society for Precision Engineering, 9th -14th October 2005, Norfolk, VA.

Fletcher, Simon, Longstaff, Andrew P. and Myers, Alan (2005) *Investigation into the accuracy of a proposed laser diode based multilateration machine tool calibration system.* Journal Paper of Physics: Conference Series, 13. pp. 398-401. ISSN 1742-6588

Longstaff, Andrew P., Fletcher, Simon and Myers, Alan (2005) *Volumetric compensation for precision manufacture through a standard CNC controller.* In: 20th Annual Meeting of the American Society for Precision Engineering, 9th-14th October 2005, Norfolk, VA.

2005 – 07 (TC):   Fletcher, Simon, Longstaff, Andrew P. and Myers, Alan (2005) *Compensation of thermal errors on a small vertical milling machine.*, In: Laser Metrology and Machine Performance VII, LAMDAMAP 2005, Cranfield University pp. 432-441. ISBN 1861941188

2005 – 06 (FC):   Myers, Alan, Ford, Derek G. and Barrans, Simon (2005) *Finite element analysis of the static stiffness of a foundation for large machine tool.*. In: Laser Metrology and Machine Performance VII, LAMDAMAP 2005, Cranfield University

Widiyarto, Muhammad Helmi Nur, Pislaru, Crinela, Ford, Derek G., Longstaff, Andrew P. and Myers, Alan (2005) *Hybrid modelling technique applied to digital feed drives.* In: Laser Metrology and Machine Performance VII, LAMDAMAP 2005, Cranfield University, pp. 454-463. ISBN 1861941188

Pislaru, Crinela, Ford, Derek G., Widiyarto, Muhammad Helmi Nur and Myers, Alan (2005) *Methods for modal parameters identification applied to CNC machine tool feed drives.* In: Laser Metrology and Machine Performance VII, LAMDAMAP 2005, Cranfield University.

Holroyd, Geoffrey, Fletcher, Simon and Myers, Alan (2005) *Modelling the dynamic behaviour of a ballscrew system taking into account the changing position of the ballscrew nut.* In: Laser Metrology and Machine Performance VII, LAMDAMAP 2005, Cranfield University.

Longstaff, Andrew P., Fletcher, Simon and Myers, Alan (2005) *Volumetric error compensation through a Siemens controller.* In: Laser Metrology and Machine Performance VII, LAMDAMAP 2005, Cranfield University, pp. 422-431. ISBN 1861941188

2005 – 01 (FJ): Myers, Alan, Ford, Derek G. and Xu, Q. (2005) *Measurement techniques for determining the static stiffness of foundations for machine tools.* Journal Paper of Physics: Conference Series, 13. pp. 410-413. ISSN 1742-6588

2004

Myers, Alan (2004) *Firm foundations for sure.* Machinery, 162 (4. p. 48.)

2003

Myers, Alan, Ford, Derek G. and Xu, Q. (2003) *Finite element analysis of the structural dynamics of a vertical milling machine.* In: Laser Metrology and Machine Performance VI. Southampton University, pp. 431-440. ISBN 9781853129902

LIST OF PUBLICATIONS TO BE CONSIDERED FOR PhD

Eighteen papers are being submitted in support of consideration for the PhD award. Six related to research of machine tool errors due to concrete foundations (three journal and three peer reviewed conferences) and twelve related to thermally induced machine tool errors (three journal and nine peer reviewed conferences). For convenience they have been listed in chronological order. The first number is the year and the second number is the order within the year taken from the University of Huddersfield repository list of publications for the candidate.

Foundation related papers:-

2005 – 01 (Journal): Myers, Alan, Ford, Derek G. and Xu Q (2005) *Measurement techniques for determining the static stiffness of foundations for machine tools.* Journal Paper of Physics Conference Series 13. pp. 410-413 ISSN 1742-6588

2005 – 06 (Conference): Myers, Alan, Ford, Derek G. and Barrans, Simon (2005) *Finite element analysis of the static stiffness of a foundation for large machine tool.* In: Laser Metrology and Machine Performance VII, LAMDAMAP 2005, Cranfield University

2007 – 02 (Conference): Myers, Alan, Barrans, Simon and Ford, Derek G. (2007), *Structural Analysis of a large Moving Gantry Milling Machine including its Work Support System and Foundation.* In: Laser Metrology and Machine Performance VIII, LAMDAMAP 2007, Cardiff University, pp. 63-72. ISBN 9780955308239

2009 – 04 (Conference): Myers, Alan, Barrans, Simon, Longstaff, Andrew P., Fletcher, Simon and Ford, Derek G. (2009) *Evaluation and Comparison of a Large Machine Tool Structure with ISO Standard Alignment tests.* In: Laser Metrology and Machine Performance IX, LAMDAMAP 2009, Brunel University, pp. 57-66 ISBN 978-09553082-7-7

2013 – 09 (Journal): Borisov, Oleg, Fletcher, Simon, Longstaff, Andrew P. and Myers, Alan (2013), *New low cost sensing head and taut wire method for automated straightness measurement of machine tool axes* Optics and lasers in engineering 51 (8). Pp. 978-985. ISSN 0143-8166

2014 – 06 (Journal): Borisov, Oleg, Fletcher, Simon, Longstaff, Andrew P. and Myers, Alan (2014), <u>*Performance evaluation of a new taut wire system for straightness measurement of machine tools*</u> Precision Engineering, 38 (3), pp. 492-298. ISSN 0141-6359

Thermal error related papers:-

2005 – 07 (Conference): Fletcher, Simon, Longstaff, Andrew P. and Myers, Alan (2005) *Compensation of thermal errors on a small vertical milling machine.* In: Laser Metrology and Machine Performance VII, LAMDAMAP 2005, Cranfield University. pp. 432-441. ISBN 1861941188

2005 – 10 (Conference): Fletcher, Simon, Longstaff, Andrew P. and Myers, Alan (2005) *Flexible modelling and compensation of machine tool thermal errors.* In: 20th Annual Meeting of American Society for Precision Engineering, 9th -14th October 2005, Norfolk, VA.

2005 – 12 (Conference): Fletcher, Simon, Longstaff, Andrew P. and Myers, Alan (2005) *Practical compensation of all significant thermal errors in machine tools.* In: 3rd International Congress on Precision Machining, Vienna, Austria, October 2005, Vienna, Austria.

2007 – 04 (Conference): Fletcher, Simon, Longstaff, Andrew P. and Myers, Alan (2007) *Measurement methods for efficient thermal assessment and error compensation.* In: EUSPEN Topical Meeting "Thermal Effects in Precision Engineering", 3 - 4 December 2007, Maastricht, The Netherlands.

2007 – 05 (Journal): Longstaff, Andrew P., Fletcher, Simon and Myers, Alan (2007) *Flexible compensation of thermal errors.* In: EUSPEN Topical Meeting "Thermal Effects in Precision Engineering", 3 - 4 December 2007, Maastricht, The Netherlands.

2011 – 05 (Conference): Mian, Naeem S., Fletcher, Simon, Longstaff, Andrew P. and Myers, Alan (2011) *Efficient thermal error prediction in a machine tool using finite element analysis.* Measurement Science and Technology, 22 (8) 085107. ISSN 0957-0233

2012 – 06 (Conference): Mian, Naeem S., Fletcher, Simon, Longstaff, Andrew P. and Myers, Alan (2012) *An efficient offline method for determining the thermally sensitive points of a machine tool structure.* In: 37th International Matador Conference, University of Manchester

2013 – 02 (Conference): Mian, Naeem S., Fletcher, Simon, Longstaff, Andrew P. and Myers, Alan (2013) *The significance of air pockets for modelling thermal errors of machine tools.* In: Laser Metrology and Machine Performance X, LAMDAMAP 2013. EUSPEN, pp. 189-198. ISBN 978-0-9566790-1-7

2013 – 05 (Conference): Abdulshahed, Ali, Longstaff, Andrew P., Fletcher, Simon and Myers, Alan (2013) *Comparative study of ANN and ANFIS prediction models for thermal error compensation on CNC machine tools.* In: Laser Metrology and Machine Performance X. LAMDAMAP 2013, EUSPEN, pp. 79-89. ISBN 978-0-9566790-1-7

2013 – 06 (Journal): Mian, Naeem S., Fletcher, Simon, Longstaff, Andrew P. and Myers, Alan (2013) *Efficient estimation by FEA of machine tool distortion due to environmental temperature perturbations.* Precision Engineering, 37 (2). pp. 372-379. ISSN 0141-6359

2013 – 13 (Conference): Abdulshahed, Ali, Longstaff, Andrew P., Fletcher, Simon and Myers, Alan (2013) *Application of GNNMCI (1, N) to environmental thermal modelling of CNC machine tools.* In: The 3rd International Conference on Advanced Manufacturing Engineering and Technologies. KTH Royal Institute of Technology, Stockholm, Sweden, pp. 253-262. ISBN9789175018928

2015 – 03 (Journal): Abdulshahed, Ali, Longstaff, Andrew P., Fletcher, Simon and Myers, Alan (2015) *Thermal error modelling on machine tools based on ANFIS with fuzzy c-means clustering using a thermal imaging camera.* Applied Mathematical Modelling, 39 (7). pp. 1837-1852. ISSN 0307-094X

CONTRIBUTION TO THE PAPERS

All the publications are of Joint-Authorship and were published from 2005 to 2015 whilst the candidate was Director of the Centre for Precision Technologies and Leader of the Engineering Control and Machine Performance Research Group (ECMPG). All authors, either were or are, employed within the ECMPG and with the exception of Prof Ford and Dr Barrans, they reported directly to the Candidate who was, or is, their line manager and as such has overall responsibility for the group's research activities. The research was mainly carried out under EPSRC, EU FP7 or Industrial Consultancy such as the Rolls-Royce SAMULET project and the candidate was the Principal Investigator.

Foundation Papers

Four of the foundation papers were written by the candidate as first author.
The other two were written under the candidate's overall supervision as Group leader of the Engineering control and Machine Performance Research Group within the Centre for Precision Technologies. Percentage contribution per publication is based on the number of joint-authors.

Thermal papers

The twelve thermal papers were all written under the overall supervision of the candidate whilst Group Leader of the Engineering Control and Machine Performance Research Group. Percentage contribution per publication is based on the number of joint authors.

I. AN OVERALL SUMMARY OF THE RESEARCH

MACHINE TOOL ACCURACY:

For many large machine tool installations two of the most significant contributors to inaccuracy are the concrete foundations on which the machines are supported and the effects of thermal sources on the machine structure. Both can cause millimetres of positional error of the spindle with respect to the workpiece.

Manufacturing industry and the precision requirements of large machine tools

This thesis will review the range of errors and their causes that effect large machine tools and then specifically address what are considered to be two of the most significant contributors to these inaccuracies, namely those caused by the concrete foundations which support the machines and those caused by thermal effects. Both can cause problems that can be very difficult and extremely expensive to resolve. After a concrete foundation has been cast, if it is found to be insufficient it cannot easily be modified and thermal effects such as environmental temperature changes can require factory air conditioning systems which are expensive to install, operate and maintain. The publications to be included in the thesis show a systematic approach to significantly improving the accuracy of large machine tools.

Modern components

Components used in modern equipment such as cars, trains, aircraft, robots, household appliances etc. require good functionality, reliability, long life, light weight etc. A significant contributor to these requirements is the high degree of precision [1] that these components are manufactured to in terms of their dimensions, form and surface finish. Production of virtually all of these components is achieved either directly or indirectly by use of machine tools. Therefore the machine tools need to perform extremely accurately, even more so than the components they produce since other factors such as fixtures, tooling etc. cause additional inaccuracies.

Machine tool Accuracy To achieve high accuracy performance, the machines need to move in a precise manner in terms of their straightness of movement, positional accuracy, rotational

orientation and the relationship of one axis to another etc. It is also important that the
accuracy is repeatable in order to guarantee the level of performance at all times.

Large machine tools:-

Large machine tools can weigh hundreds of Tonnes, and have moving parts that weigh 100
Tonnes, they typically have movements of 20 metres and spindle power ratings of 100KW
The workpieces they machine are also large and heavy thus setting a requirement for
substantial foundation support to maintain accuracy of straightness of movement which might
typically be 50
. They are used for machining a vast variety of components such as nuclear reactor vessels,
marine diesel engines, valve bodies, rolls for steel mills, aircraft wing skins.

Typical large machine tool configurations

The configurations are often such that the workpiece support structure such as a rotary table
or static workplates is not directly connected to the machine, but both are supported on the
concrete foundation. The concrete foundation in such cases is absolutely essential to the
integrity of the system with the force loop between tool and workpiece passing through the
concrete foundation. Figure "1" below shows a large moving gantry machine tool and the
workpiece which has been machined on it. The workpiece is a side panel for a Eurostar train
carriage. Whilst being machined the workpiece can change in length by 6mm due to
environmental temperature changes during a day which emphasises

Figure 1 - Moving gantry vertical ram type machine and workpiece.

Error types

There are many types of inaccuracies affecting machine tools mainly such as geometric errors, thermal errors, load errors, dynamic errors, etc.

a. Geometric errors are the inaccuracies of the individual axes straightness, squareness of each axis to the others, orientation of the moving elements as they move either translation or rotation (pitch, roll and yaw errors). A three axis machine has twenty one individual geometric errors. Five axis machines can have in excess of forty geometric errors depending on their exact configuration.

b. Thermal errors [3] are the variation of the size and the shape of the machine when temperature changes and temperature gradients occur causing differential expansions.

c. Load errors are the deflections that occur in the machine when forces are applied to the machine.

d. Dynamic errors are the inaccuracies of tool position that occur when the machine is moving or vibrating.

Error causes:-

The causes of the above mentioned errors are shown below|:-

a. Geometric errors are the result of manufacturing inadequacies in the machining and assembly processes. They can be caused by machining and assembly inaccuracies.

b. Thermal errors are caused by temperature changes of the machine due to self-generated or environmental thermal sources

c. Load or non-rigid errors are due to compliance of the machine structure or drives causing displacements when forces such as gravity or cutting are applied [2]

d. Dynamic errors are a response to variable loads, accelerations, servo drive velocity lags etc.

Accuracy tolerances:-

The accuracy requirements are extremely high with linear tolerances specified in microns, angular tolerances in arc seconds and which require specialist equipment to measure them such as Laser Interferometers, Gravity Based Inclinometers. ISO standards are used as the basis for quantifying the tolerance values, the methods of test and the equipment to use for specific machine configurations e.g. ISO 3070, ISO 8636. Generic test methods applicable to all machine tools are specified by the ISO-230 series of standards.

1. CONCRETE FOUNDATIONS FOR MACHINE TOOLS (background and literature review)

Concrete foundation errors:-

Concrete foundations for large machine tools can be extremely large, massive and expensive. Typically a foundation might weigh 500 tonnes with a depth of between 1metre to 2metres and a plan area of 150 square metres. In the majority of cases it is the concrete foundation that connects the machine tool to the work-piece and it is therefore an integral part of the structure [1]. Foundation errors are the static deflections or displacements that occur to the concrete foundation which supports a machine tool. They can be displacements due to rigid body movement of the foundation or deflections due to distortion such as bending of the foundation. The displacements are caused by changes in the position of the centre of gravity of the machine as it is traversed horizontally from one position to another. This can cause the vertical orientation of the foundation to change due to tilting as the pressure distribution on the sub-soil changes. The deflections are caused by changes in shape of the foundation due to bending and/or shear as the machine is traversed horizontally. Both displacements and deflections can also be caused by other factors such as temperature changes of the concrete (which are discussed later), the ingress of water into the concrete caused by a changing level of water tables and settlement of the sub-soil beneath the foundation with time. Measurement of errors [2] is difficult due to the small but significant values which are normally encountered and the irregular nature of the concrete surfaces. The methodology for measurement and the equipment that is used is very specific to the task and involves the use and adaption of a variety of metrology instruments which are deployed in an innovative manner. Reduction of these errors is achieved by careful specification of the foundation stiffness based on the machine accuracy tolerances. The specification is then used to dictate the design of the foundation using Finite Element Analysis following sub-soil stiffness measurements carried out using test bore holes and surface plates stiffness measurements to ensure the foundation stiffness meets the requirements. The use of impervious tanking membranes to prevent the ingress of water is provided around the sides and based of the concreted.

It is an interesting observation that Concrete foundations for Machine Tools appear to be a relatively under researched area possibly because the two disciplines do not have too much in common i.e. civil engineers seldom deal with microns and machine tool engineers seldom deal with hydraulic concrete or soil mechanics.

1.1 Foundation Specification

1.1.1 Found Stiffness Specification

No BSI or ISO standards are available

Evaluation comparison paper 2009-04

1.1.1 Found General Specification

 Screeds (facilitates ease of carrying out the steel fixing)

 Creep

 Ingress of water/moisture

 Tanking

 Water tables

 Bituminous membranes

 Visqueen 100

 Upper surface needs treating to prevent dusting

 Monolithic construction

 No vertical joints

 Sufficient re-enforcement to be included

1.2 Foundation Design

1.2.1 Considerations

Cost of foundations

Excavations

Subsoil

Piling:-

   a. Radichy piling – non vertical piles – simulating tree roots

   b. Vertical piling

   c. Skin friction piles

   d. End bearing piles

   e. Raft constructions

   f. Mixture strength (cement, Sand and water ratio)

   g. Variations in Modulus of Rigidity Value due to various causes

1.2.2 Design Criteria

Traditionally designed on a stress based criterion only

For this application a stiffness based criterion should also be used which will almost always over-ride the stress based.

1.2.3 Design Process Parameters

Loads and positions (including movable ones) specified

Machine alignment tolerances specified

BSI – ISO – Company standards

Excavations to depth or test bore holes drilled

Plate tests done to determine subsoil surface stiffness characteristics

Coefficient of Uniform Elastic Compressions (Coeff. of UEC)

FEA carried out using values from plate tests

Depth of concrete calculated

Deflections

Gravitational effects

Machine CofG movement effect

Distortion

"E" and "G" values

Steel re-enforcement design – rebar - mesh

1.3   Foundation Connectors

1.3.1 Types and requirements

Pull down bolts

Vertical jacking adjustment

Many different types

     a.   Co-axial

     b.   Adjacent/offset

     c.   Wedgemounts – Farrat – BWFixaors – Homemade designs

     d.   Chemical anchors

Non-pocket types

     a.   Adheres to the concrete surface

     b.   Surface needs degreasing with chemical agent

Pockets:-

     a.   Precast

   b.   Diamond trepanned

   c.   Dovetailed for mechanical grip

   d.   Scabbled for mechanical grip

Grout:-

   a.   Different types

        i.   Epoxy

        ii.   Cementitious

        iii. Expanding

   b.   Suppliers

        i.   Pagel Ltd

        ii.   CBP

        iii. Chemical Building Products Ltd

        iv.   Master Builders

        v.   Homemade with expanding additive

1.4   Foundation Testing

1.4.1 Testing of final stiffness prior to machine installation

   a.   Load testing for static stiffness

   b.   Use of specialist equipment

   c.   Water pots

   d.   Dial test indicators

   e.   Depth micrometers

   f.   Precision Engineering Inclinometers

   g.   Roll Steel Joists

   h.   Measurement of change in topography of the surface

1.4.2 Curing Process Considerations

   a.   Time to reach full strength

   b.   Time to reach maximum stiffness

   c.   Chemical reaction

   d.   High temperatures generated

        i.   50 Degree C

   e.   Time to return to ambient is months

1.5 Foundation problems – Case studies

    a. RMC Machine at ROF Barnbow Leeds had 1mm overall concrete deflection

    b. Baker Perkins – Walker anti-vibration matting caused high static errors

    c. John Brown Stroud machine and workpiece areas separated vertical joint

    d. Kindcaids machine – foundation had to be excavated & replaced with new

    e. Isles of white – Elliot Turbo Machinery – foundation too compliant

1.6 Publication Specific Commentary

The following publications described in the this section were written in an attempt to address some of the more concerning aspects of machine tool inaccuracies caused by inadequate foundations that have been outlined above namely.

Large machine tools rely on their concrete foundations to provide sufficient stiffness for the machines to maintain accuracy of movement in terms of straightness, rotational orientation and squareness to other axes. Typically the cast iron or fabricated bed of a machine tool by itself would only have 10% of the stiffness required. It is therefore essential to know the stiffness of the concrete foundation because the machine accuracy of movement is so dependent upon it.

The first publication 2005-01 is the description of an attempt to verify what the actual value of stiffness is for a foundation of a large machine tool, specifically a moving gantry machine. The paper describes the tests carried out on a machine tool in a railway locomotive factory and how they are structured to simulate the behaviour of the machine when it is in machining mode. The test also simulated the effect of placement of the intended work-piece onto the concrete foundation.. The procedure is explained, the equipment is described and the concrete foundation with its re-enforcement is clearly shown. The results show that the small be in context significant displacements and distortions that took place within the concrete foundation.

The second publication 2005-06 follows on logically from the previous one by describing the analysis of a typical foundation using Finite Element Analysis software in an attempt to

understand the behaviour of a foundation in terms of its stiffness characteristics such that the results can be compared with those obtained for the one previously measured. This analysis highlights the need for the subsoil properties to be known, particularly the stiffness at the surface of the subsoil and suggests that these properties should be determined in practice by site tests using test bore holes before the site is excavated or plate tests after the site has been excavated down to the anticipated level of the underside of the intended concrete foundation.

The third publication 2007-02 describes the analysis of a complete moving gantry type machine tool including the concrete foundation in order to assess the overall stiffness of the full system. This then allowed the significance of the foundation as a % of the overall system to be assessed confirming the requirement for a full understanding of the behaviour to be obtained so predictable accurate assessments could be made of foundations in the future to ensure foundations are specified to have the correct values to ensure they provide sufficient support that the machines can move with accuracies that allow components to be manufactured within tolerances.

The fourth publication 2009-04 describes a review and assessment of typical values taken from the appropriate ISO standard accuracy of a moving gantry machine tool such that they can be compared with the stiffness values that can be achieved in reality with reasonable costs for foundations. Conclusions are drawn as to how effective the current approach is.

The fifth publication 2013-09 describes a novel method for measurement needed for determining the accuracy of straightness of large machine tools using current technology. This method is much quicker and efficient than current techniques and uses less expensive equipment. The straightness values are used to determine the required stiffness of the concrete foundations.

The sixth publication 2017-06 describes the performance evaluation of the equipment and technique presented in the previous publication to determine its scope of usage and applicability to machine tool measurement.

2. THERMAL EFFECTS ON MACHINE TOOL ACCURACY (background and literature review)

1. Thermal effects cause significant errors of machine tools [1] due to the expansion and contraction of the various materials that the machines comprise of, as their temperatures change.

2. If the temperature of a machine changes in a uniform manner throughout the structure it will change size but not shape. The change of size will cause the machine to produce parts that are either too big or too small dependent whether the temperature increases or decreases respectively. If the temperature changes non-uniformly throughout the structure the temperature gradients will in turn produce distortions of the structure. The parts produced will subsequently not be the exact shape that is required, e.g., surfaces that should be flat will become concave or convex and surfaces that should be parallel will have angular misalignment to each other etc.

3. The two main causes of temperature change are either environmental or machine self - induced. Environmental changes are caused by variations of the factory temperature usually maintained within limits set only by the comfort levels required by the occupants. These levels are usually far greater than those needed to ensure parts are produced within satisfactory tolerances of precision. Machine self-induced heat sources are such as motors, pumps sliding friction of guide-ways etc.

4. Measurement of these errors is carried out in a similar way as the geometric errors but with additional measurement of ambient temperature and the temperatures of the structure. Generally this is done over longer periods of time to take into account daily and even weekly changes.

5. Reduction of thermal errors is achieved by a number of techniques involving such as environmental temperature control, heat removal by good design, liquid cooling and coolant systems and error compensation methods [3] etc.

6. It is worthy of note that the thermal errors should be minimised before any attempt is made to improve geometric errors since they simply add to them. If at all possible thermal compensation should be applied before geometric.

7. Overall thermal volumetric error values can be in the order of millimetres on large machine tools.

2.1 Thermal Error Measurements

The dimensional errors produced by thermal causes are measured by a wide range of metrology equipment.

Temperature gradients cause differential thermal expansion which in turn causes shape distortion of the machine tool structure.

Saturated temperatures create steady state conditions

Measurement of the errors of machine tools – ISO Stds.

2.2 Thermal Error Sources

2.2.1 Environmental sources

Factory temperature variations due to opening and closing access doors, heat received through windows radiated heat from factory wall mounted heaters ectc.

2.2.2 Machine self-induced sources

Heat sources such as motors, pumps, slide-ways, refrigeration unit exhausts, spindle bearings, the cutting process and standing swarf.

2.3 Temperature measurement considerations

Position of sensors etc.

Numbers of sensors

Reliability of sensors

Three wire bus – Dallas sensors

Flair imaging systems

Dallas single spot temperature measurement

2.4 Error Elimination by Design

Good design practice

Analysis of machine tool thermal behaviour using FEA

Differential material expansion

Linear expansion

Reduced Friction Bearings

Rolling element bearings

Hydrostatic bearings

Air bearings

Careful selection of bearing preload

Linear encoder feedback

Symmetrical design

Spindle cooling

Refrigeration

Airblast coolers

Minimum coefficients of expansion materials

Carbon fibre

Zerodur

Invar

Air pockets

2.5 Thermal Error Compensation

2.5.1 Controller based

The compensation software is based within the CNC Controller and usually provided by the CNC builder.

2.5.2 Remote based

Stand alone units provided by third party companies often retrofitted to legacy machines.

2.5.3 Thermal error compensation based on classical physics algorithms

Theoretical approach using physics based analytical tools to predict thermal errors.

2.5.4 Thermal error compensation based on Artificial Intelligence

An empirical approach using a number of different methods and proving to give better results than the traditional systems.

2.6 Thermal Error Testing and Verification

Machine calibration is essential

Calibration techniques:-

Etalon

Laser Trackers

6 DoF

Typical error reduction has been 70%

AI now achieving c.95%

Warm up times reduce machine efficiency

Thermal drift

2.7 Case Studies

Installations include:-

Micro-Metalsmiths

Rolls-Royce

Renishaw HongKong   Foxconn

Renishaw Singapore   ASM

Renishaw San Francisco   Apple

Typical error reduction has been 70%

AI now achieving c.95%

2.8 Thermal Paper Specific Commentary

The first paper 2005-07 describes the application of a thermal compensation system onto a small vertical spindle milling machine. The system was implemented within the machine controller and used an algorithm s based on classical physics to calculate the positional error values from temperature measurements taken of the machine structure. Errors were shown to have been reduced by 70%.

The second paper 2005-10 describes an enhanced compensation system developed using a novel programming language to provide a flexible modelling technique combine with comprehensive measurement of the machine temperatures. The techniques described provide robust modelling development and the minimisation of machine downtime in comparison with the previous approach.

The third paper 2005-12 describes further development of a more practical compensation system for systematic thermal errors in an open architecture controller which reduces the hardware required whilst using component offsets to compensate for differential expansion

between feedback method and component. Results showed an average error reduction 80% for position dependant and environmental errors.

Fourth paper 2007-04 discusses the development of improve methods for temperature measurement using thermal imaging equipment capturing radiated temperature information with a much improved accuracy over previous methods. It has enabled the detailed on line measurement of thermal gradients and hence the ability to compensate for complex structural distortions with further reduced downtime.

The fifth paper 2007-05 explains further development of thermal compensation with more flexibility and achieved by creation of a novel compensation language. This enables at the machine program e modifications without offline software re-writes and allows for machine operation parameters to be readily updated thus providing significant further improvement in flexibility.

The sixth paper 2011-05 describes further progress towards thermal error reduction by research into the nature of heat transfer characteristics of specific machine tool features such as linkages and joint interfaces. Finite Element Analysis has been used to develop offline novel techniques to accurately reproduce the effects of significant internal heat generation sources. The result show when applied to compensation systems there would be significant further reduction in thermal errors of circa 80%.

The seventh paper 2012-06 concentrates on prediction techniques for finding the thermally sensitive areas of machine tool structures. Matlab and FEA have been used to develop rapid and efficient optimisation methods for determining the significant locations on machine tool structures for most effective temperature measurements. Thus simplifying and reducing the time for installation of temperature sensors.

The eighth paper 2013-02 describes further research to understand and quantify the significance of air pockets on machine tool structures and to enable more accurate modelling of their effect. It was shown to improve the accuracy of modelling of certain structural aspects by circa 55%.

The ninth paper 2013-05 discusses a significant change in modelling methods away from a physics based approach to an empirical one. Artificial Intelligence techniques were used to produce four thermal analysis models for comparison of performance. The results strongly indicated that ANFIS models were consistently superior to ANN models for accurate prediction of thermal errors.

The tenth paper 2013-06 continued the direction of research towards the development of superior compensation systems by investigation of thermal errors caused by machine structural distortion due to environmental temperature changes. FEA was used to determine the errors and the results compared with measurements taken at the modelled machine. The accuracy was such that if applied to a compensation system the errors could be reduced to less than 12 microns.

The eleventh paper 2013-13 continues the research into novel empirical techniques. A novel method is proposed that enables determination of the system behaviour. This will result in a more cost effective and practical solution to error predication with the corresponding benefits for compensation systems.

The twelfth paper 2015-03 is a further extension of the Artificial Intelligence research based on the use of thermal imaging equipment and ANFIS with fuzzy c-clustering. The resultant performance was such that the thermal error could be predicted within 5% thus having the potential when used with a compensation system to reduce the thermal errors by 95%.

3. AIMS, OBJECTIVES AND TIMELINE OF THE RESEARCH

3.1 The aim of the research

The overarching aim of the research being described here was to improve the accuracy of large products typically such as nuclear reactor vessels, marine diesel engine components (e.g. crankshafts and crankcases), aircraft components such as undercarriage structural members, wing members (e.g. spars, stringers, ribs and wing skins), all of which are manufactured by the many different configurations of large machine tools such as the one shown in figure 2.
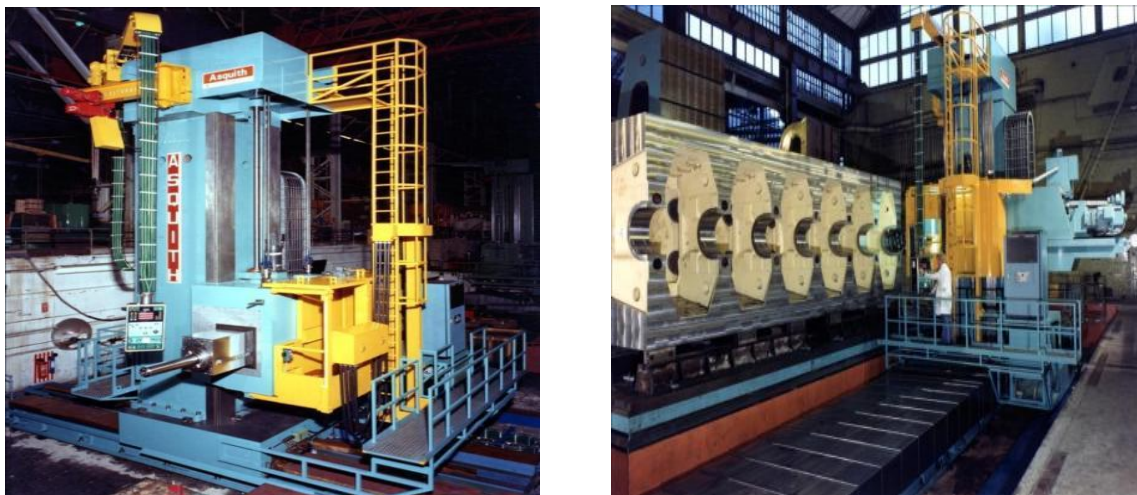
Figure 2 - Moving column horiz. ram type machine and marine diesel engine crankcase

The requirement for more accurate components is a result of the need to improve their functionality, reliability, strength, performance and life. An example of this is that air craft components need to be as light as possible and are therefore manufactured to extremely tight tolerances which can only be achieved by extremely accurate machine tools.

3.2 The Philosophy and Objectives of the Research

The philosophy is to continually strive to improve the accuracy of machine tools and therefore the accuracy of the components they produce.

Machine tools are complex machines with many technical requirements that need to be met to ensure they function satisfactorily. In particular the static and dynamic accuracy of the movement of the machines is dependent on numerous factors. The research described in the

thesis deals with the static performance. Of the many factors involved in machine tool static accuracy the research being discussed here deals with the two subjects that cause the maximum errors and difficulty in the manufacture and operation of large machine tools; namely the foundations which supports the machines and the thermal conditions under which they operate.

There are many ways in which a machine tool's performance is assessed which range from the quality of the components it is capable of producing to the direct measurements of the machine's movements as it traverses along its axes.

3.3   Concrete Foundations

The objective of the foundation research has been to investigate the overall process used to produce concrete foundations for machine tools in order to determine a best practice procedure which will provide a high level of certainty of foundation performance in order to ensure that the machine tool will be capable of producing work-pieces to the required level of precision.

3.3.1 Existing design and build procedural practice

Existing practice is for the machine tool manufacturer to provide a basic specification for the foundation to the purchaser of the machine (i.e. the customer). The customer will in turn engage the services of a civil engineering consultant and also a civil engineering construction company. The specification is passed to the consultant who then designs the concrete foundation which the construction company subsequently build. The machine tool manufacturer will then install the machine on the concrete foundation, commission it and carry out a series of pass off tests which have previously been agreed with the customer. The pass off tests will normally comprise of verification measurements of the machine's accuracy and also the machining of a typical component based on the customers range of products.

In the event of a failure to pass certain tests, actions are taken to try to decide on the cause of the problem and where the responsibility lies. In the case of a problem caused by an inadequate foundation it can be very difficult after the machine has been installed to ascertain whether it is caused by the foundation or the machine.

The above procedure is fundamentally flawed for the following reasons:-

It does not provide enough information for the foundation to be designed correctly

It does not collect the information needed to design the base correctly.

It uses the wrong criterion for assessing the foundations adequacy as fit for purpose.

It does not test the foundation to confirm that it is satisfactory before machine installation.

3.3.2 Preferred design and build procedure

3.3.2.1 Foundation specification and format

Typical current practice is for the machine tool manufacturer to specify a minimum depth of concrete for the foundation and the static and moving weights of the machine tool.

The minimum depth is almost arbitrarily chosen based previous experience with other machines or the depth needed to give satisfactory cover for the lengths of the holding down bolts that are to be used to secure the machine to the concrete.

The final depth, if greater than the minimum required for bolts, will therefore be based on the stress levels in the concrete due to the moving and static loads. In practice this criterion will usually result in a depth that is less than that required to ensure that minimum deflection tolerances are not exceeded.

Straightness Tolerances
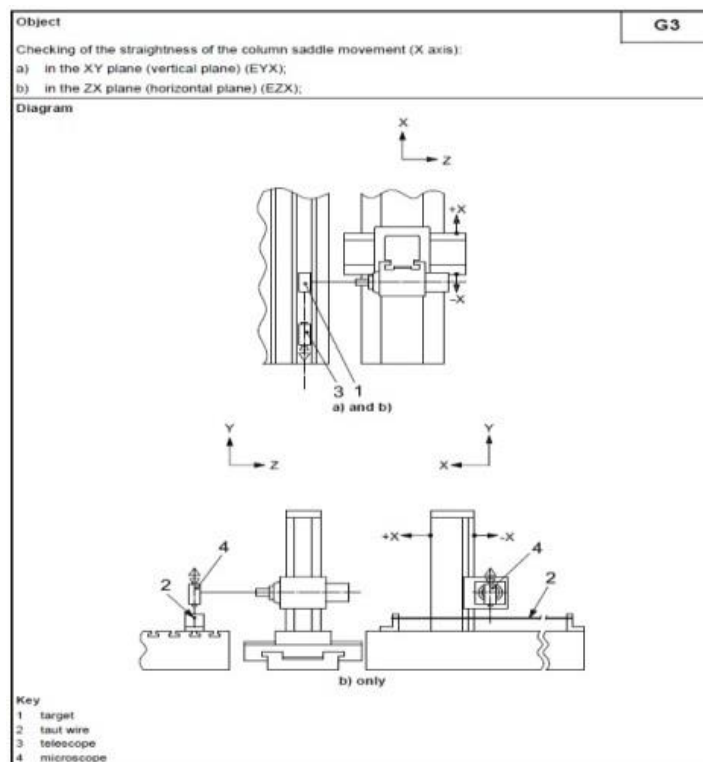
Figure 3 - Moving column horiz. ram machine typical alignment test to ISO 3070 Pt 2: 2007

The above procedure has a fundamental flaw since it is essentially based on a stress criterion rather than stiffness and does not ensure that the foundation provides sufficient support to the machine structure to prevent excess deflection occurring and this can cause alignment tolerances not to be achievable.

The foundation specification should provide the information on the required stiffness at the upper surface of the concrete needed to ensure maximum acceptable pseudo static deflections are not exceeded. The maximum deflections should be based on the machine manufacturer's alignment tests sheets for the particular machine or the ISO Standard tests for the particular machine configuration. See a typical example test shown in figure 3 above which specifies the maximum straightness tolerance allowed for the "X" axis longitudinal traverse of a typical large machine tool.

 The static accuracies are stipulated in a range of standards for large machine tools and generated by a number of ISO Standards Sub-Committees which fall under the overall responsibility of the International Standards Organisation Technical Committee TC39.

These standards when issued are administered by national standards bodies such as in the UK the British Standards Organisation and in particular Machine Tool Committee MTE1-2 for machine accuracy.

The above information can be subsequently converted into the maximum deflections allowed at the surface of the concrete and specified as in figure 4 below.

Publication 2009-04 describes the evaluation of the alignment tolerances for configurations of large machine tools which can be used to create a machine tool foundation specification and how they have been compared with FEA results for a large moving gantry machine.

FOUNDATION SPECIFICATION
Distortion Tolerances
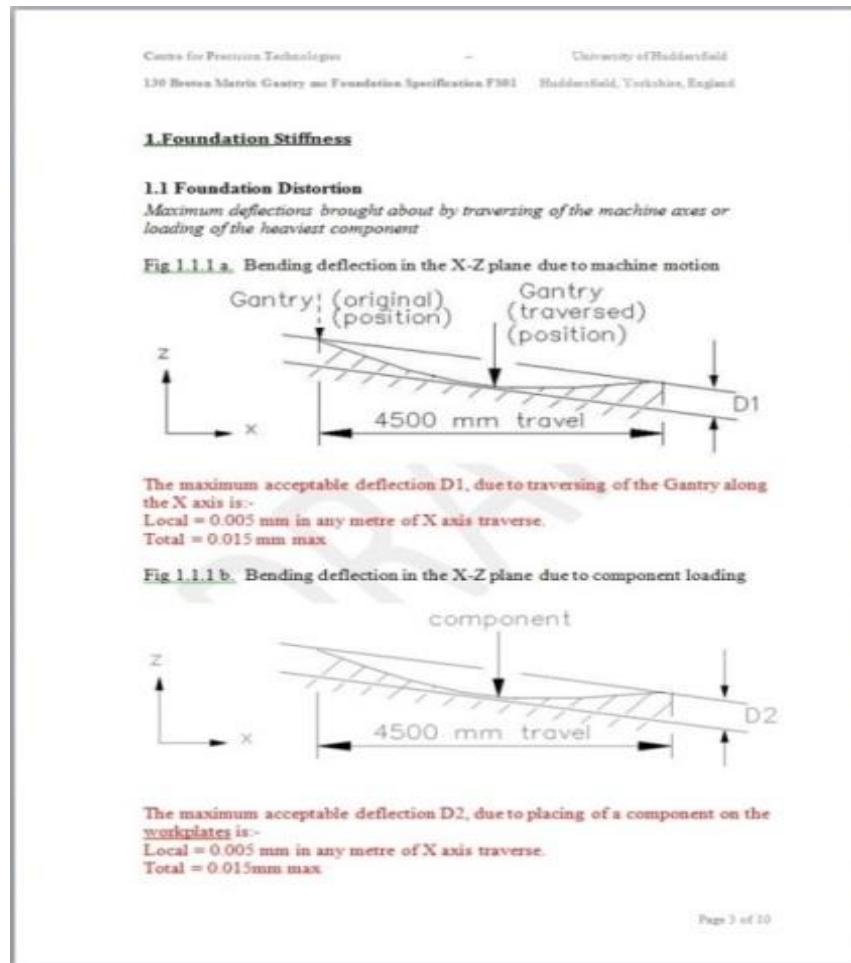
Figure 4 - Moving column horizontal ram type machine foundation specifications

3.3.2.2 Foundation Design

The foundation design procedure should be based on the above format of foundation
specification where stiffness rather than stress is the criterion used under the loading values
and conditions that are specified.

Finite Element Analysis (FEA) should be used to determine the necessary depth of the
concrete foundation.

Because the stiffness of the concrete is very much dependant on the nature of the subsoil
which supports it, then it is an essential part of the procedure to know the characteristics of
the subsoil, in particular the value of the Coefficient of Uniform Elastic Compression (C_u).

This can be determined by a plate test carried out on the surface of the exposed subsoil which should be carried out after an initial excavation of the site to remove the upper layers of subsoil down to an appropriate level determined after bore hole samples have been taken. The plate test would involve cyclical loading after an initial preload which is related to the maximum weight of the machine, has been applied.

When the above information has been determined FEA can be carried out to determine the depth of the concrete needed to provide sufficient stiffness at its surface to ensure the maximum deflections do not exceed the ones specified under the applied loading conditions.

Figure 5 – Partially constructed foundation for a large machine tool installation
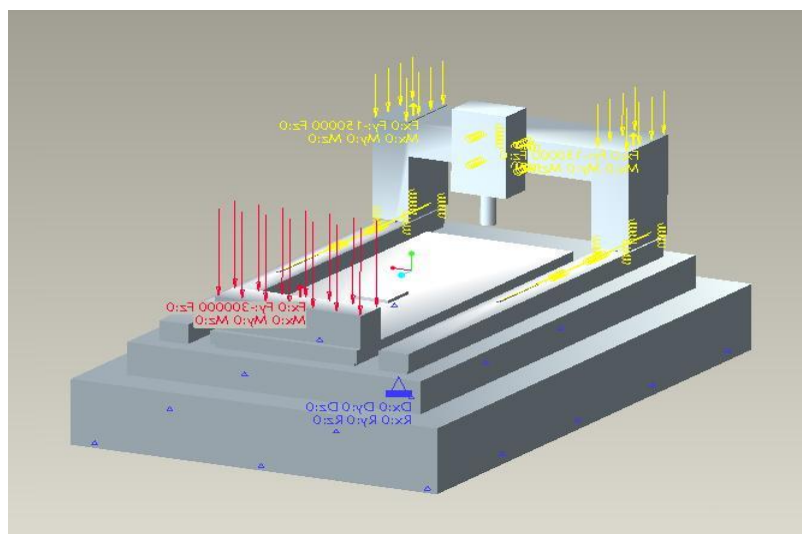
Figure 6 – FEM of a moving column gantry machine installation including the foundation

Publication 2005-06 describes the FEA of a foundation for a large moving gantry foundation.

Publication 2007-02 describes the FEA of a large moving gantry machine and its foundation.

3.3.2.3 Foundation testing

After construction it is essential that the concrete foundation should be tested to confirm the specified stiffness has been achieved under the corresponding loading conditions. This should be carried out before the machine is installed in order to minimise confusion when interpreting the results and facilitate determining where the responsibility lies in the event of a problem.

However, a period of one month should be allowed after pouring before any tests take place in order to allow the concrete to cure and reach maximum strength and stiffness. One such foundation test is shown in figure 7 below where a foundation is being loaded with 90 tonnes to assess its behaviour when workpieces are placed on it.

Figure 7 - Moving column horizontal ram type machine foundation testing

Publication 2005-01 describes a concrete foundation test as carried out on foundation for a moving gantry machine tool. The publication describes the procedure which had been developed, the equipment, instrumentation, the loads that were used and the results obtained.

3.3.2.4 Foundation testing equipment

The instrumentation used for testing machine tool foundations to measure the stiffness at the upper surface is currently based on traditional equipment such as Dial Test Indicators, Inclinometers and hydraulic levelling units in conjunction with a reference frame comprising

of steel beams. The taut wire/optical sensor would provide a more suitable alternative being less expensive, considerably lighter and much easier to use.

In cases were the machine has been installed on the foundation the straightness of the longitudinal axis traverse needs to be measured as part of the final inspection protocol. This test is carried out with a taut wire and microscope which on large machine tools can typically involve 100 individual measurements and can take an entire shift i.e. circa. 8 hours.

The taut wire with the optical sensor would reduce this time considerably because the measurements can be taken as the machine is moving and automatically recorded electronically reducing the time to less than one hour.

Alternatively the measurements are often taken using laser interferometry instrumentation which is expensive and time consuming to set up whereas the taut/wire & optical sensor equipment is extremely inexpensive in comparison and relatively easy to set up.
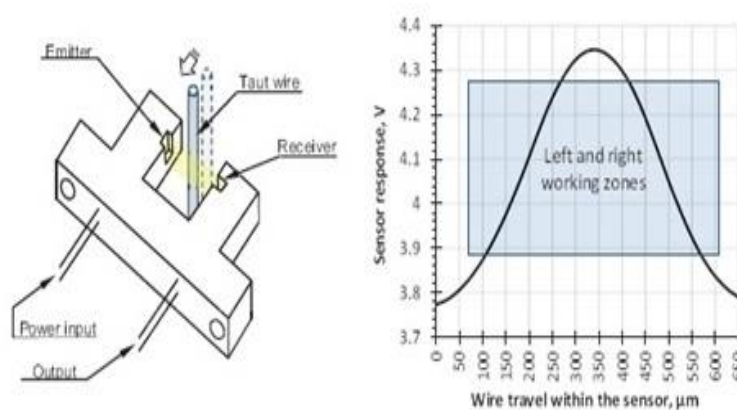
Figure 2. Omron photomicrosensor and its sensitivity graph.

Figure 8 – Taut wire / Optical Sensor for deflection and straightness measurement

Publication 2013-09 describes the research and development carried out on an optical sensor/taut wire based instrument and process for measuring deflections and straightness discussed above.

Publication 2014-06 describes the performance tests carried out on the instrumentation and process discussed above.

3.3.2.4 Graphical representation of the overall design and build procedure

The preceding work is described graphically below in figure 9 to show the recommended process in detail.
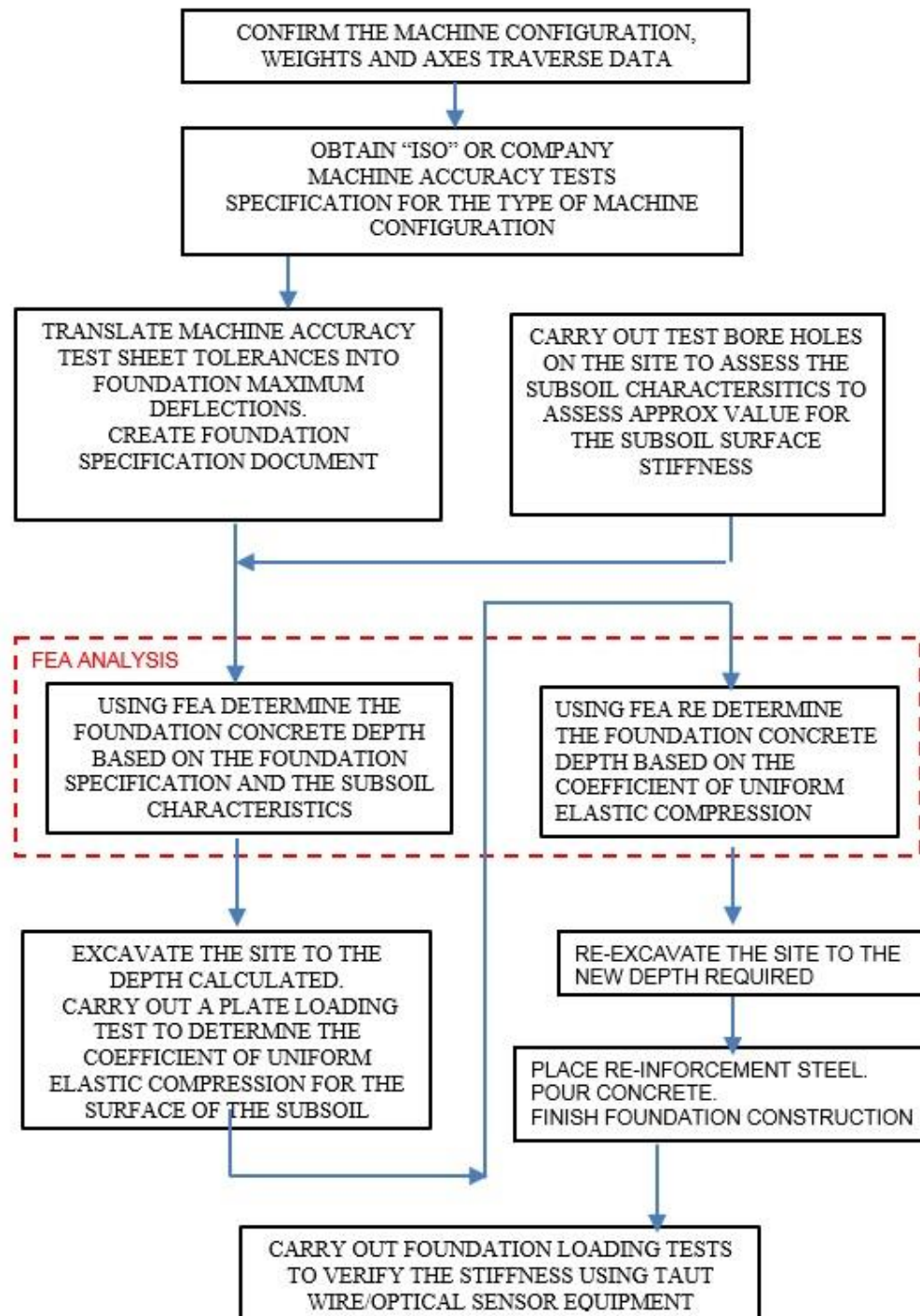
Figure 9 - Flow chart for recommended procedure for design & build of machine foundation

3.4   Thermal error reduction

Twelve papers are presented in this thesis that have been published on the subject of thermal error reduction. Thermal errors significantly affect the accuracy of machine tools and therefore the precision of the components they produce. The errors are caused by temperature changes of the machine tool structure due to environmental temperature changes and self-induced heat sources within the machine itself.

Under steady state conditions they simply expand or contract the structure without changing its shape, whereas under transient conditions they cause temperature gradients within the structure which in turn produce distortions of the structural shape in addition to the change of size.

It is good practice to design the machines such that the effect of the temperature changes cause minimum effect using passive means such as choice of materials, direction of exhaust of hot air from motors away from the structure etc.

Additionally active means are also used such as spindle jackets carrying cooling liquid to remove the often large amounts of heat generated by spindle bearing rotation. For environment issues factory temperature control is used though the costs can be extremely high.

However the above items have a limited effect and for extreme precision it is necessary to use compensation methods. Historically the best achievements have given circa 70% reduction of thermal error.

To this end the work described in these publications has involved the continued research and development of compensation systems in an attempt to improve the percentage level of error reduction to those currently being achieved for compensation of geometric errors i.e. greater than 90% error reduction.

3.4.1 Thermal error, physics based compensation

The publications, 2005-07, 2005-10, 2005-12, and 2011-05 describe the use of the laws of physics to predict the distortions and growth that will occur in machine tool structures when temperatures of the structure change due to either environmental changes or self-induced heat generation within the machine itself.

By the development of algorithms that relate the temperatures of the structure to the errors at the spindle mounted tool cutting point, these errors can be predicted and subsequently negated.

By correctly predicting the errors, these values can be used through the CNC controller to apply positional offsets that are equal and opposite to the errors and which result in cancelling the error out.

Compensation systems using physics based algorithms rely on having sufficient and accurate knowledge of the temperature profile of the structure. This requires the application of temperature sensors that are accurate, reliable and simple to apply. This has been achieved by the development of an inexpensive, digital sensor system which uses a three, wire bus loom.

The four papers describe the temperature compensation research and development of a controller based system, flexible modelling to reduce downtime of the machine, further development within an open architecture controller and the development of a more flexible novel, language which allows program modifications without offline software re-writes.

State of the art at this stage of the research was producing thermal error reductions of circa. 70%.

3.4.2 Temperature measurement

Publication 2007-04 describes the development of the use of thermal imaging equipment to give a much higher level of accuracy enabling thermal gradients to be measured and therefore the ability to compensate for complex structural distortions.

3.4.3 Thermal modelling

Publication 2011-05 presents the further development of enhanced modelling techniques by investigating the thermal behaviour of linkages and joints. Publication 2012-06 describes the research into prediction of the thermally sensitive points on a machine tool structure for most effective temperature measurement. Publication 2013-02 describes research into the significance of air pockets in a machine structure to enable more accurate modelling of their effects. Publication 2013-06 continued the

improvements in modelling techniques by use of FEA to further investigate the structural errors caused by

State of the art at this stage of the research had reached circa. 80% reduction of thermal errors.

3.4.4 Thermal compensation based on Artificial Intelligence

The latest work is described in the three publications 2013-05, 2013-13 and 2015-03 where a significant change in modelling methods has been made away from physics based approach to an empirical one using of Artificial Intelligence methods to predict the thermal growth and distortion of the machine structure. A number of Adaptive Neuro Fuzzy Inference System (ANFIS) models were compared with Artificial Neural Network (ANN) models when verified against test results on CNC machining centre. The test results showed the ANFIS models were consistently superior to the ANN models for accurate prediction of thermal errors.

Subsequently ANFIS models with fuzzy c-clustering models were tested. The performance was such that the thermal errors could be predicted within 5% thus having the potential when used in a compensation system to reduce machine tool thermal errors by 95%.

3.4.5 Graphical representation of overall thermal research

The preceding description of the thermal research is shown graphically below in figure 10
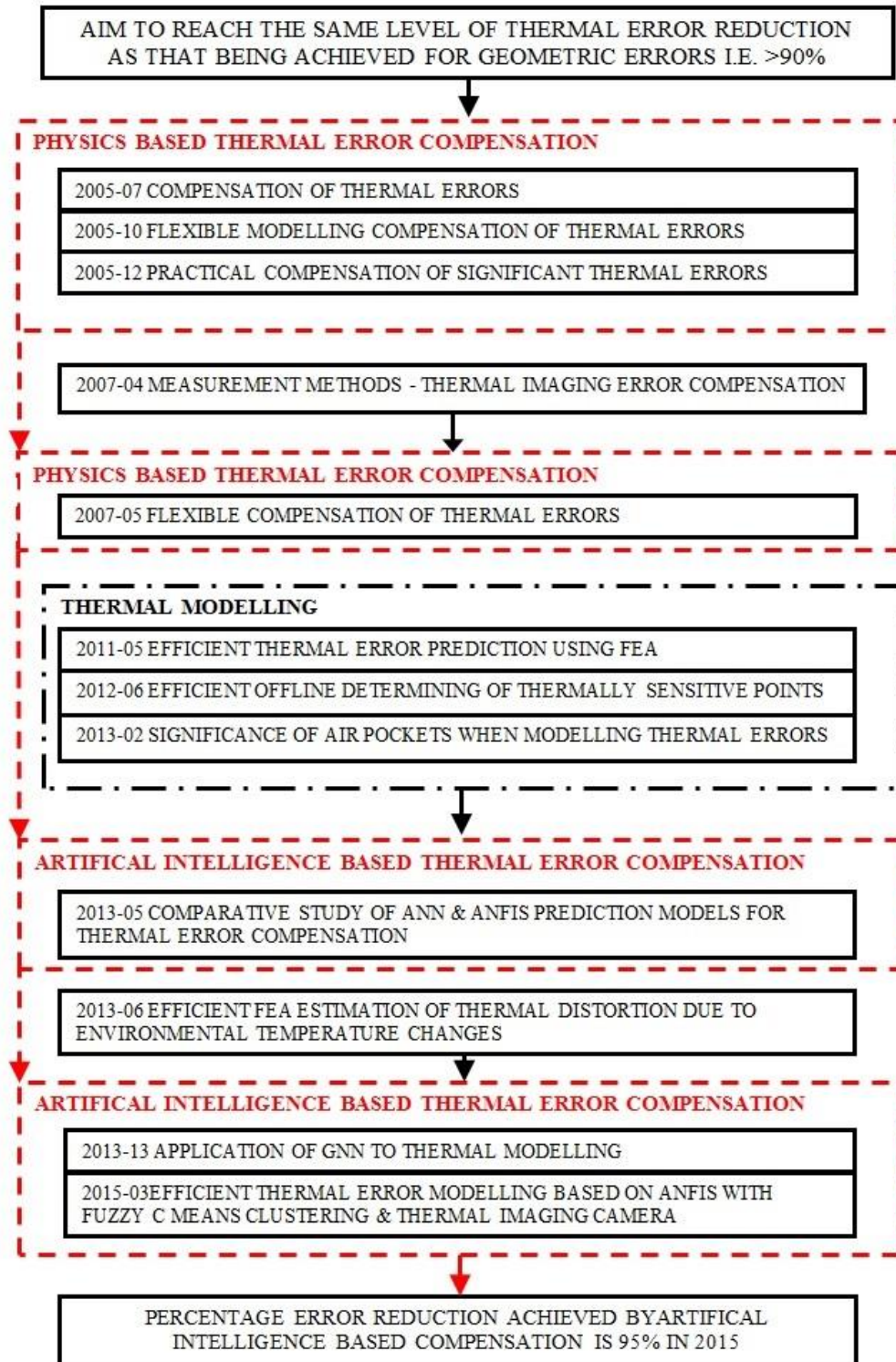
Figure 10 – Graphical chronology of the thermal error research

3. 5   The Timeline of the research

The research described here covers in total an eleven year period the earliest paper being published in 2005 and the latest paper published in 2015.

The six foundation related papers were published over a nine year period from 2005 to 2014.

The twelve thermal related papers were published over an eleven year period from 2005 to 2015.

4. SUMMARY OF THE INVESTIGATIONS

4.1   Foundation

The outcome of the six research papers has been a clear understanding of the process for the design of foundations required to ensure that they are adequate to provide the machines placed upon them with sufficient support that they will be able to function as intended.

4.2   Thermal

The outcome of the twelve thermal research papers is a significant generation of knowledge such that processes and equipment are now available such that large machine tools can be built to accuracy levels that are considerably higher than those previously.

5. IMPACT OF THE RESEARCH

The research described in this thesis up to 2013 was used in the Research Excellence Framework 2014 national government assessment and contributed to the highest ranking award of 4 Star for impact.

The predictive methods and novel techniques developed by the CPT's research into machine tool accuracy have benefited a range of end-users in industry, both nationally and internationally, throughout the REF2014 period.

Leading UK employers such as BAE systems and Rolls-Royce (RR), as well as major local employers such as Yorkshire based Micro Metalsmiths were among the first beneficiares of the CPT's PC based compensation systems and have continued to use increaslingly advanced versions of the technology since 2008.

Collaboration with Siemens on developing the compensation system for industrial CNC has led to a number of high profile installations on machine tools requiring new levels of accuracy for the Joint Strike Fighter (JSF) programme. As a result of its collaboration with the CPT, Siemens has produced a commercial compensation system and are actively marketing it globally.

Under a TSB grant in collaboration with AsquitButler Ltd, the UK's only manufacturer of very large machine tools, the error compensation system (MTC) has been integrated into a PowerCentre 500, 5-axis horizontal ram, moving colum machining centre.

The use of the CPT's new methodologies throughout the manufacturing industry has led to training courses being developed and delivered in collaboration with Machine Tool Technologies Ltd. and is aimed primarily at maintenance engineers employed in advanced manufacturing. Five week courses have been developed and delivered to companies including R-R, BAE and AWE.

6. EXTERNAL REFERENCES

[1] L.Uriarte, M. Zatarain, D. Axinte, J. Yague-Fabra, S. Ihlenfeldt, J. Eguia, A. Olarra, *Machine tools for large parts*, CIRP Annals – Manufacturing Technology 62 (2013) pp. 731-750

[2] Thamir Salah, Subhair G Hussain, Wedad A Azzawy, *Machine Tools Foundation Static and Free vibration analyses,* WSEAS Transactions on Applied and Theoretical Mechanics Issue 2 Vol. 7 (2012) pp. 93-105

[3] R. Ramesh, M. A. Mannan, A. N. Poo, *Error compensation in machine tools – a review, Part 2: thermal errors,* International Journal of Machine Tools & Manufacture 40 (2000) pp. 1257-1284

II. COPIES OF PAPERS IN SUPPORT OF THE PhD DEGREE

This section shows a copy of the papers submitted in support of the PhD. The copies are provided as images of the original publications as shown in the relevant journals or conference proceedings.

For ease of reference they are shown in the appropriate category either "Foundation" or "Thermal" and subsequently in chronological sub-order within each category.

FOUNDATION RELATED PAPERS

2005-01 Measurement techniques for determining the static stiffness of foundations for machine tools

Measurement techniques for determining the static stiffness of foundations for machine tools.

A Myers[1], S M Barrans and D G Ford

Center for Precision Technologies, University of Huddersfield, UK

E-mail: [1]a.myers@hud.ac.uk

Abstract. The paper presents a novel technique for accurately measuring the static stiffness of a machine tool concrete foundation using various items of metrology equipment. The foundation was loaded in a number of different ways which simulated the erection of the machine, traversing of the axes and loading of the heaviest component. The results were compared with the stiffness tolerances specified for the foundation which were deemed necessary in order that the machine alignments could be achieved. This paper is a continuation of research previously published for a FEA of the foundation [1].

Introduction

To perform satisfactorily a machine tool must be both statically and dynamically rigid. Its static stiffness determines its ability to produce dimensionally accurate parts and its dynamic stiffness affects the quality of the component's surface finish and the maximum metal removal rates that can be achieved. Virtually all medium to large machine tools, such as the one shown in Figure 1, rely upon a concrete foundation to provide adequate structural support in-order that the machine is sufficiently rigid to enable it to perform satisfactorily.

Fig.1 Moving gantry milling machine

Large machine tools are used typically for producing component parts for the aircraft and automotive industries and the accuracies to which the many different configurations are built are specified in a wide range of ISO and other standards. The typical tolerance specified for axes straightness for such machines is 5 microns per metre of traverse and since the machine might typically weight as much as 100 tonnes with a foundation weighing 500 tonnes, the stiffness of the concrete base must be extremely high to minimise non rigid errors [2].

410

411

To illustrate how exacting the requirements are, it is interesting to observe that for machines of extremely long traverse the earth's curvature can be a significant proportion of the allowable tolerance. A machine 40metre long might have a 'X' axis straightness tolerance of 160 microns and the earth's curvature over this distance is 32 microns.

Foundation specification
It is essential therefore to be able to specify and subsequently measure the static stiffness of machine tool foundations, such as the one shown under construction in Figure 2, in order to ensure that the correct level of support is provided and that the machine tool alignment accuracies are achieved [3, 4].

Fig.2 Foundation being constructed for a gantry milling machine

For a satisfactory machine installation the foundation stiffness must first be specified based upon the required alignment tolerances for the machine, as specified in the appropriate ISO standard for the particular machine configuration e.g. ISO 3070 Part 2 for a large Moving Column, Horizontal Ram Type milling machine and ISO 8636 Part 2 for a Moving Gantry Vertical Ram Type milling machine. The stiffness specification for the foundation must state a number of criteria and the associated tolerances.

For the above gantry machine with 'X' traverse of 14 metres and 'Y' traverse of 4 metres the values were as shown below: -

a) Maximum bending deflection in longitudinal and transverse planes (typically 5 microns per metre of the corresponding traverse of the machine 'X' and 'Y' axes due to firstly the moving weight of the machine (30 Tonnes) and secondly the maximum weight of component (5 Tonnes)).
   'X-Z' plane maximum deflection 70 microns.
   'Y-Z' plane maximum deflection 20 microns.

b) maximum acceptable rigid body rotation of the foundation in both the longitudinal and transverse planes (typically10 microns / metre of the corresponding tranverse of the machine 'X' and 'Y' axes due firstly to the moving weight of the machine and secondly the heaviest component)
   'X-Z' plane maximum deflection 140 microns.
   'Y-Z' plane maximum deflection 40 microns.

c) maximum vertical deflection that can occur at the boundary between the machine support area and the work support area. (10 microns due to machine movement or loading of heaviest component)

The bending stiffness (a) affects the accuracy of the component since any error would be machined into the part.

The rigid body rotational stiffness (b) does not affect component accuracy but will cause difficulties with the machine installation since movements of the foundation during erection of the machine need to be monitored and taken into account.

The foundation was designed, built and subsequently tested to confirm it met the above specification requirements.

412

Test procedure

A technique has been developed using a combination of metrology equipment, as shown in Figure 3, comprising water level units, electronic levels and dial test indicators that enabled the deflections, distortions and stiffness of the concrete foundation to be measured to the accuracy necessary to satisfy the tolerances stated above.

The procedure involved placement of the required equipment on the foundation surface such that measurements could be taken at sufficient points to enable the distorted shape to be subsequently described by graphical means. This meant taking readings at approximately 20 locations on the foundation surface.

Eight water level units were placed around the foundation periphery and linked by transparent hose filled with water with a wetting agent added. Adjacent to six of the water level units three steel beams were placed transversely across the foundation and mounted on single point supports. Steel tubes are suspended from the beams and dial test indicators (DTI) were placed beneath each tube. Each DTI was attached to a plate grouted to the concrete surface. Additional information was obtained from electronic levels placed onto steel plates mounted directly onto the concrete surface at various positions to suit the loading conditions.

The foundation was loaded in a sequential manner with weights that were approximately equal to the various weights of the machine moving elements. The procedure was such that it firstly simulated the erection of the machine, the subsequent traversing of the machine through its critical axes and finally the weights are removed to monitor that the base returned to its original shape in order to confirm its elasticity.

Fig.3 Gantry milling machine foundation test with loads applied to simulate machine moving weight

The measurements at the water units were achieved using traditional depth micrometers. The repeatability of the reading taken at the water level units was +/- 10 microns. This enabled the vertical deflections and distortions the base to be determined over its entire surface to an accuracy of +/-20 microns, a difficult task to achieve with any other type of metrology equipment e.g. laser / trackers etc.

Results

The results, shown in Table 1, were plotted 3 dimensionally, see Figure 4, to graphically show the distorted foundation shapes under the various loaded states. The results were analysed and compared with the specification to confirm whether or not the distortions and deflections of the base would cause an impediment to either the erection or the subsequent use of the machine.

Table 1. Maximum distortion values of the foundation

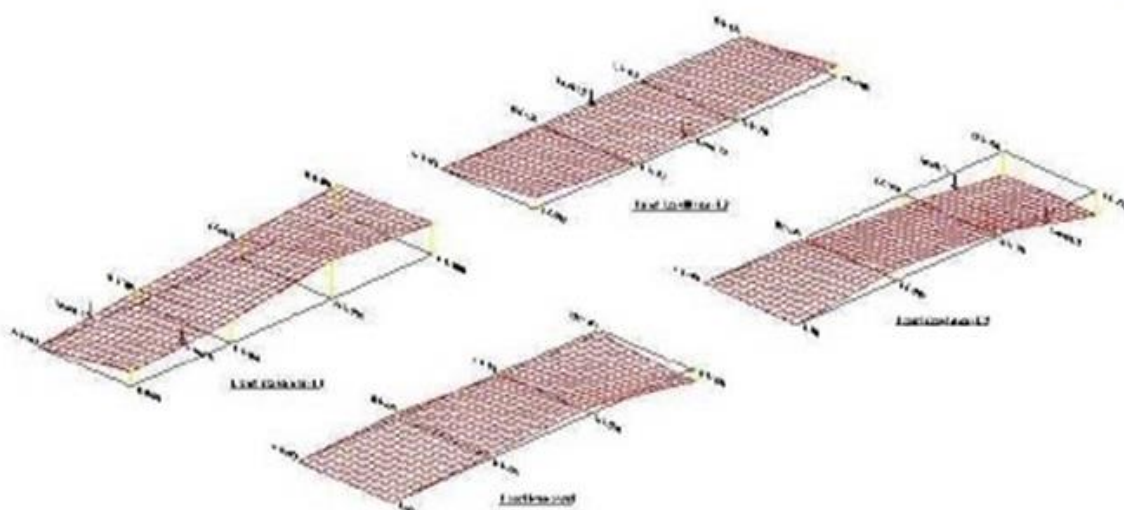| Criteria	Foundation deflections	Tolerance
Max. bending	40 microns ('X-Z' plane – central load)	70 micron
Max. rigid body rotation	100 microns ('X-Z' plane – load at negative X posn.)	140 micron

413

Fig.4 Results of foundation distortions due to 3 loading conditions and subsequent removal of weights

The above results were subsequently compared with a Finite Element Analysis (FEA) of the concrete foundation and which is the subject of another paper [1].

Conclusion

The test was carried out successfully and enabled the stiffness the foundation to be measured to the level of accuracy that was required. The results showed that the foundation met the tolerances laid down in the 'Foundation Specification' thus confirming that the gantry machine tool could be installed to the high level of precision specified by the alignment test sheets and that it would function correctly when in use.

The test procedure took a total of three days to carry out, one day to set up the equipment and two days to carry out the loading and measurements. The equipment used, though relatively inexpensive, met the necessary accuracy requirements.

By testing a foundation in this manner before a machine is installed it is possible to determine whether or not subsequent machining problems will occur after installation and establish where the responsibility lies.

It is envisaged that by comparing the results from these and future tests on other foundations, with the results obtained by FEA, that the accuracy of FEA prediction will be further enhanced to give even higher levels of certainty.

Acknowledgements

References

[1]   Myers A, Ford D G, Barrans S M 2005 *Lamdamap Conference,* Finite element analysis of the static stiffness of a foundation for a large machine tool.
[2]   Ford D G, Postlethwaite S R, Blake M D 1999 *Proc Instn Mech Engrs,* The identification of non rigid error in a vertical machining centre, Vol 213 Part B,
[3]   Brogen T H N 1970 *MTIRA* The stiffness of machine tool foundations, Research Report No 33
[4]   Brogen T H N and Stansfield F M 1970 *International MTDR Conference,* The design of machine tool foundations, Proc 11th pp 333-353

2005-06 Finite element analysis of the static stiffness of a foundation for large machine tool.

Finite element analysis of the static stiffness of a foundation for large machine tool

A. Myers, D. G. Ford, S. Barrans
Centre for Precision Technologies, School of Computing and Engineering, University of Huddersfield, United Kingdom

Abstract

To perform satisfactorily a machine tool must be both statically and dynamically rigid. Its static stiffness determines its ability to produce dimensionally accurate parts and its dynamic stiffness affects both the quality of the component's surface finish and the maximum metal removal rates that can be achieved. Virtually all medium to large machine tools rely upon a concrete foundation to provide adequate structural support in-order that the machine is sufficiently rigid to perform satisfactorily.

This paper describes the theoretical analysis and subsequent validation of an investigation into the static stiffness of the concrete foundation for a large moving gantry machining centre. The analysis was carried out using the latest Finite Element Analysis (FEA) software [1] and the results were physically validated by measurement of the foundation deflections under a variety of applied loading conditions.

1   Introduction

Large machine tools are used typically for producing component parts for the aircraft and automotive industries and the accuracies to which the many different configurations are built are specified in a wide variety of ISO and other standards. The tolerances specified for axes straightness for such machines might typically be 4 microns per meter of traverse and since the machine might weigh as much as 100 tonnes with a foundation weighing 500 tonnes, the stiffness of the concrete base must be extremely high to prevent non rigid [2] errors

To illustrate how exacting the requirements are, it is interesting to observe that for machines of extremely long traverse the earth's curvature is a significant proportion of the allowed tolerance. A machine 40 metres long would have a 'X'

axis straightness tolerance of 160 microns and the earth's curvature over this
distance is 32 microns.

Figure 1 shows a large moving gantry machining centre mounted on two
longitudinal beds which provide the 'X' axis. For a machine of this configuration
the work support units, normally either fixed workplates or a rotary table are
connected to the machine via the concrete foundation. The machine weight is
transferred to the foundation by the beds.

Figure 1: Large moving gantry machining centre

The foundation for such a machine is shown in Figure 2 part way under
construction with the commencement of the steel fixing reinforcement taking
place on top of the screed.

2   Foundation specification

Figure 2: Initial construction phase of foundation for gantry machine

The specification for the foundation stiffness is determined by the machine moving weight [3, 4] and the values of the alignment tolerances. The tolerances are usually based upon accepted ISO or national standards sometimes modified by the machine tool manufacturer to suit the particular machine circumstances.

Three main parameters are used: -

a) Rigid body rotations of the base which are critical during the installation of the machine but do not affect component accuracy.

b) Physical distortions of the base such as bending and twisting which affect the accuracy of the component.

c) The need to ensure the work support area of the base and the machine support area behave as a monolithic structure with no relative movement taking place at the boundaries between them.

3   Finite element model of the concrete foundation

The model used to simulate the foundation comprised of an upper plate whose dimensions matched those of the actual concrete foundation which was 18m long by 7m wide by 2m deep. The plate was assigned the properties of reinforced hydraulic concrete in terms of Young's Modulus and Poisson's ratio.
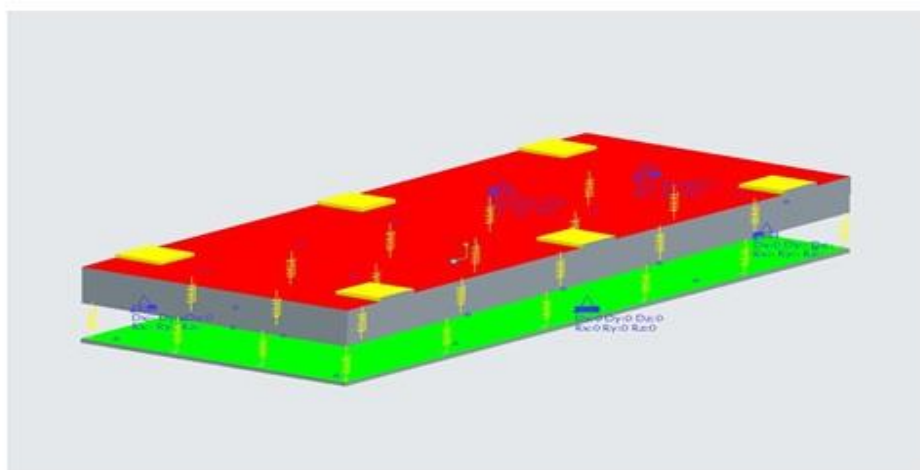
Figure 3: FEA model of the foundation

A second plate of minimum thickness was modelled beneath the upper plate as shown in Figures 3 and 4 to act as an infinitely rigid datum surface.

The two plates were coupled together by 24 elastic spring members placed at suitable intervals across the surfaces of each plate and attached at discrete pads to provide exact locations.

Loads to simulate the machine weight were applied to the upper plate.
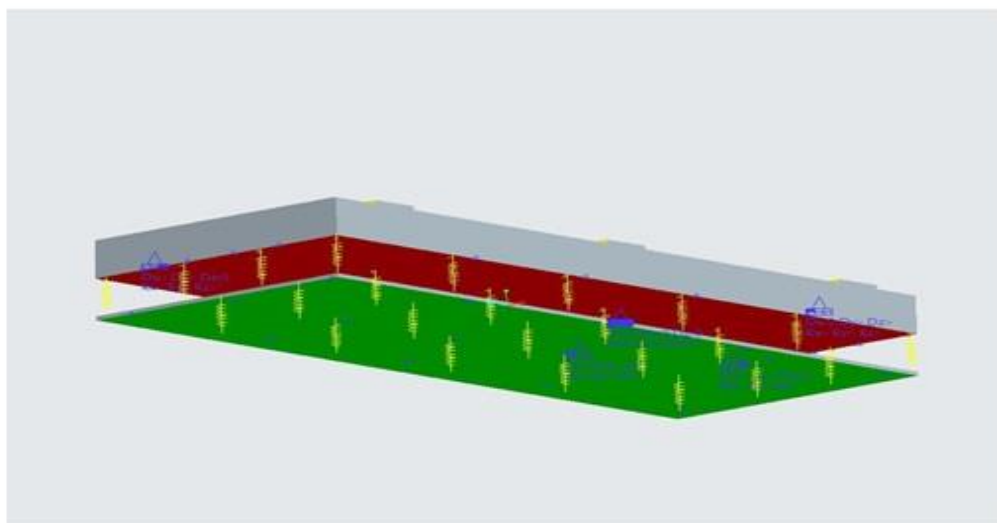
Figure 4: FEA model of the foundation

3.1 Elements

The types of elements used can be shell, beams or solid and the choice of elements used depends upon the nature of the main structural member. In this case the elements were solid ones generated automatically by the FEA software.

3.2 Spring members

Each spring unit was assigned the same spring stiffness constant based upon known values for the sub-soil conditions that applied beneath the actual base taken from test bore hole samples. The values derived were 25,000 N / mm / m**2 based upon the Modulus of Uniform Elastic Compression for the sub-soil a stratified mix of dense gravely sand, stiff red/brown clay and green mudstone.

3.3 Constraints

The upper surface of the lower plate was fully constrained for translation and rotation across its entirety.

The upper plate was constrained at its lower edges to prevent only horizontal translation normal to each side wall of the plate.

No rotational or vertical translational constraints applied to the upper plate.

3.4 Loads

Loads equal to the weight of the entire moving gantry beam (300kN) were applied in sequence at various positions on the top surface of the upper plate to simulate the effect of the gantry on the foundation for 3 different conditions.

A load equal to the weight of the machine headstock (80kN) was applied to simulate the headstock's effect on the foundation as it moves along the 'Y' axis.

4 Static analyses

A basic FEA model was designed to suit the machine configuration and traverse lengths etc using dimensions to match those of the actual concrete. The model was analysed to simulate the erection of the machine. The effects of its weight on the foundation during the machine construction procedure were computed.

Further analyses were undertaken to determine the foundation deflections which occur as the machine is traversed through its 'X' and 'Y' axes.

The analyses obtained the overall elastic deflections of the upper surface of the foundation relative to the datum surface established on the lower plate. However in practice the absolute deflections of a foundation are not of particular interest since they do not directly affect the accuracy of the component. The deflections which are critical are the relative rotations and distortions of the upper surface as these affect installation procedures and component accuracy.

4.1 Load condition '1'

Simulation of the gantry at the X' axis minimum position, (headstock central)
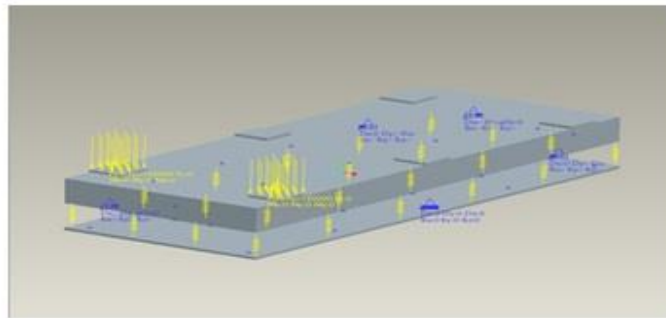
Figure 5: Gantry at 'X' minimum

4.2 Load condition '2'

Simulation of the gantry positioned at mid 'X' axis traverse, (headstock central)
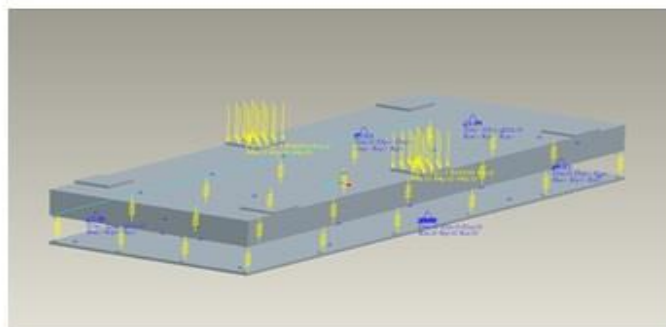
Figure 6: Gantry at mid 'X'

Simulation of the gantry at the 'X' axis maximum position, (headstock central)
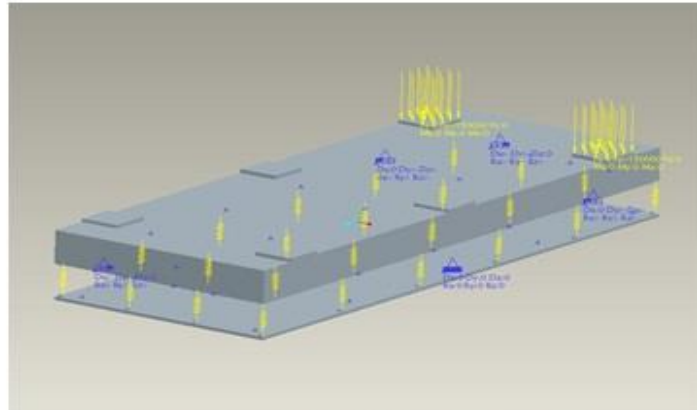
Figure 7: Gantry at full 'X' traverse

4.4 Load condition '4'

Simulation of the effect of the machine headstock being traversed to the extreme of the machine 'Y' axis with gantry positioned at minimum 'X'.
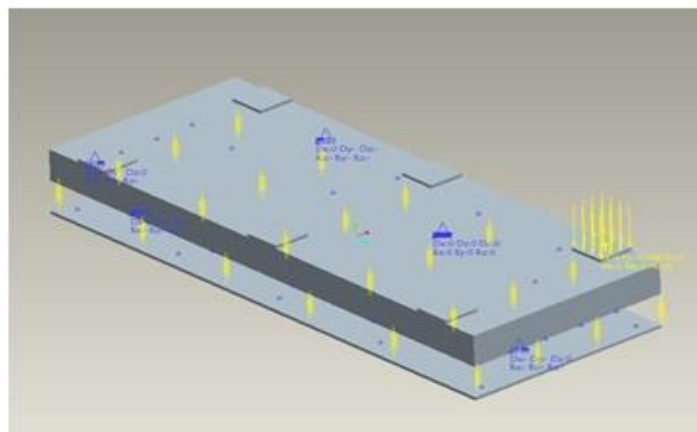
Figure 8: Headstock positioned at 'Y' maximum

5 Results

5.1 FEA Results

For each loading condition the deflections of the upper surface of the concrete foundation have been computed and are shown below as isometric views and side elevations. The deflected shapes through the base are presented in graphical form showing the distortions of the upper surface of the base which are compared with the measured results in Table 1.

5.1.1   Load condition '1'
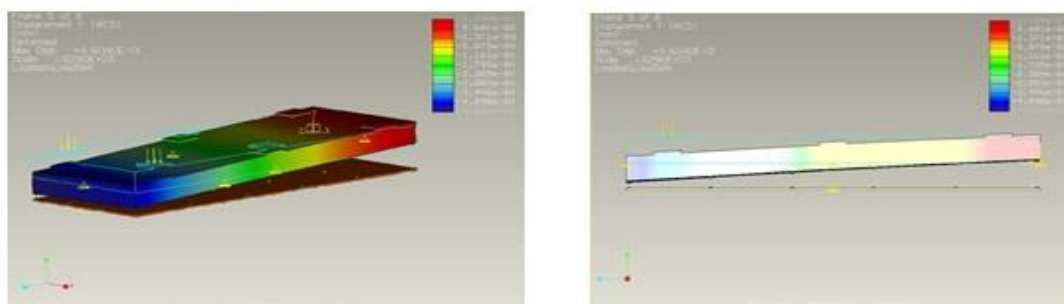
Figure 9: Gantry positioned at 'X' minimum

Maximum absolute deflection beneath the load = 420 microns
Bending distortion = 10 microns
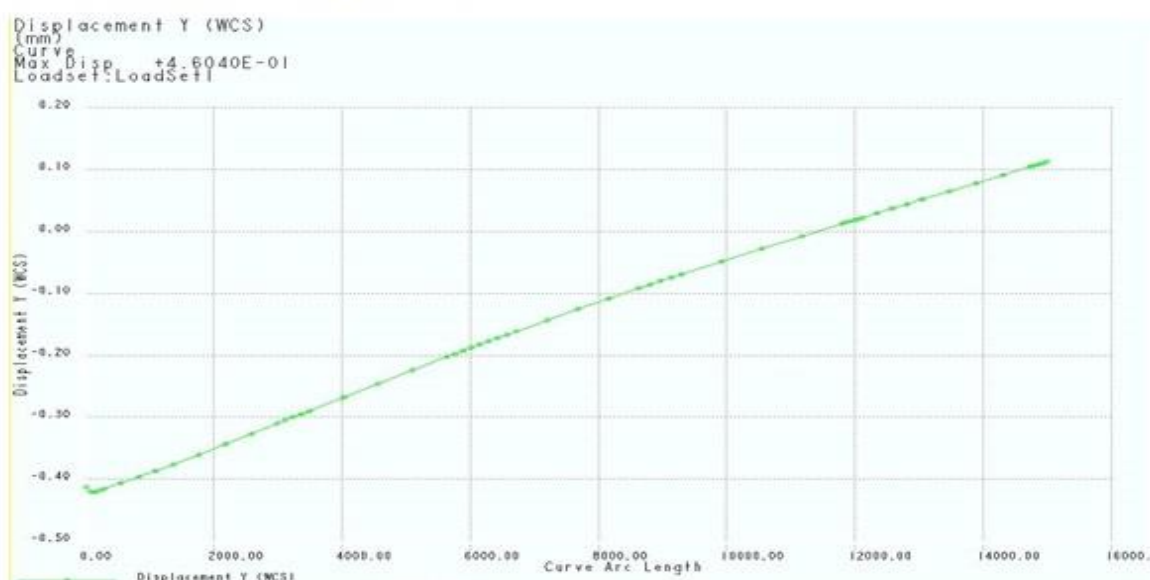
Figure 9a: Gantry positioned at 'X' minimum (upper surface deflected shape)

5.1.2   Load condition '2'

Figure 10: Gantry positioned at mid 'X' traverse

Maximum absolute deflection beneath the load = 200 microns
Bending distortion = 55 microns
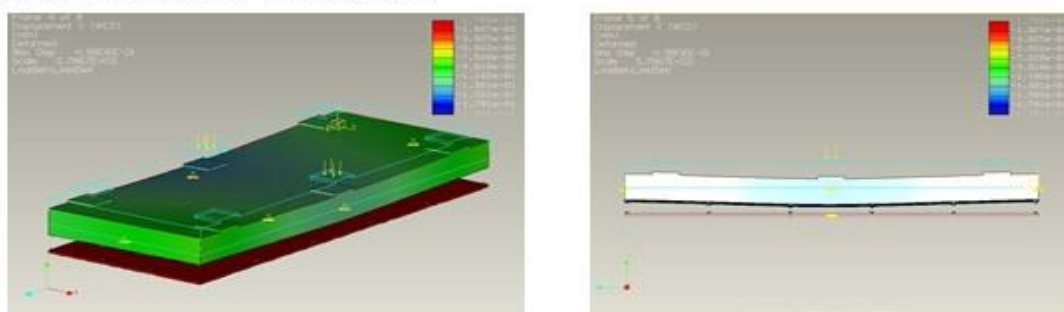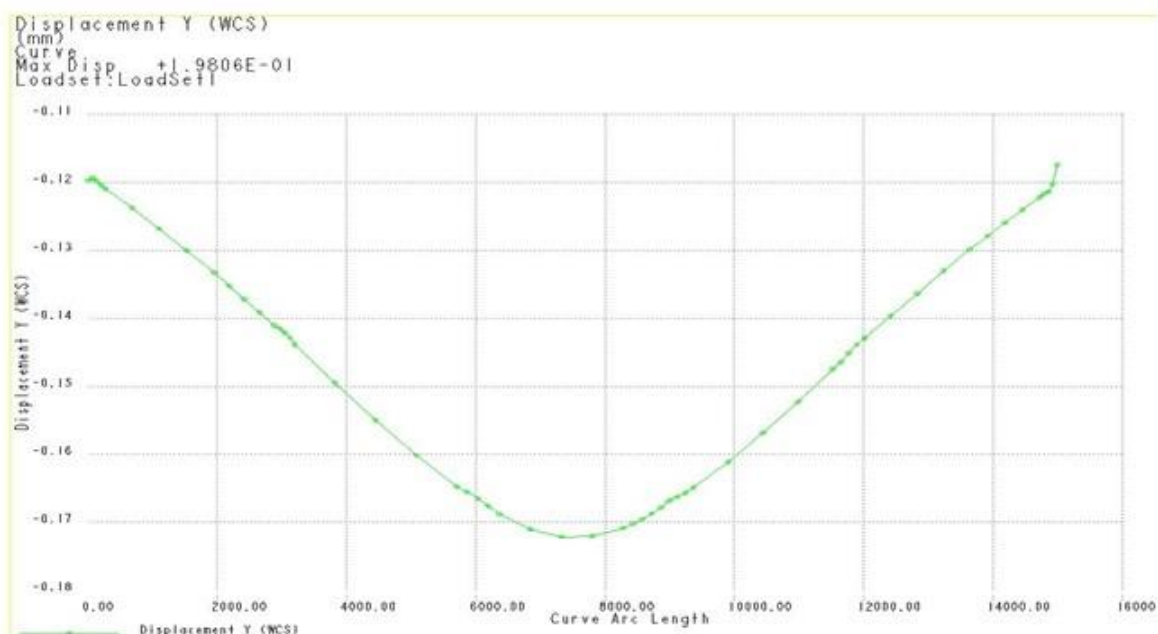
Figure11: Gantry positioned at mid 'X' (upper surface deflected shape)

5.1.3   Load condition '3'

Results values essentially as for load condition '1' therefore graphs not shown
Maximum absolute deflection beneath the load = 420 microns
Bending distortion = 10 microns

5.1.4   Load condition '4'

Gantry beam positioned at 'X' minimum and the headstock at 'Y' maximum
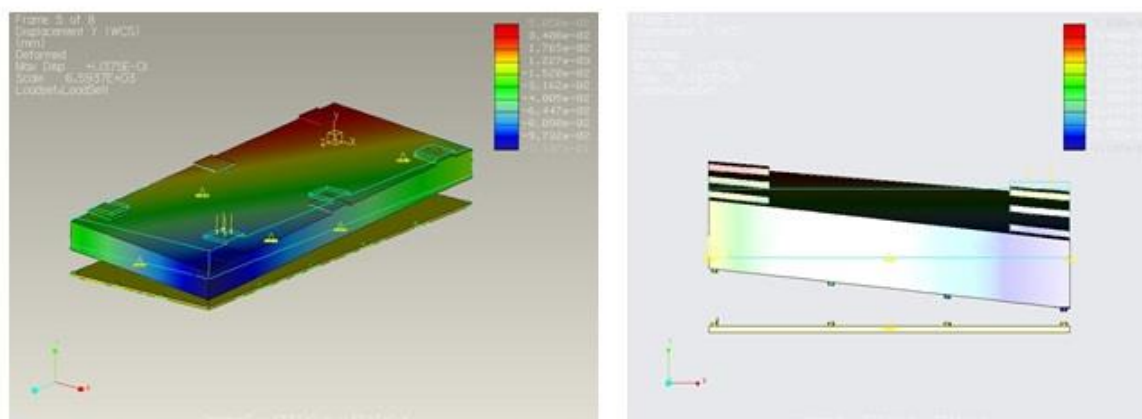
Figure12: Gantry positioned at mid 'X' (upper surface deflected shape)

Maximum absolute deflection beneath the load = 110 microns
Bending distortion = 5 microns

5.2 Physically measured results

The relative vertical deflections of the upper surface of the concrete are shown in Figure 13 below for loading conditions 1, 2 and 3 and are compared with the theoretical ones in Table 1.
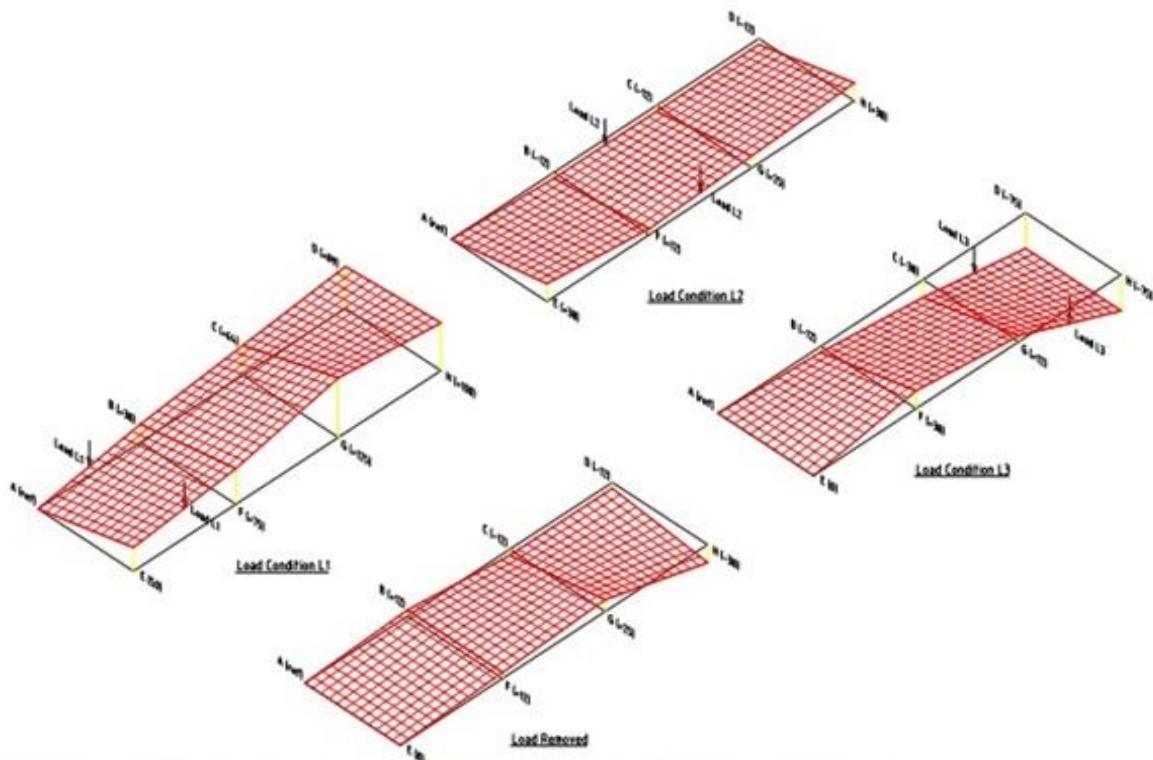
Figure13: Physically measured deflections of the foundation

The technique used to physically measure the deflections of the actual foundation will be the subject of a future paper.

5.3 Validation of the FEA technique

Table 1. Comparison of theoretical and measured results

Load condition	Distortion of upper surface (microns)	
	FEA predicted	Measured
1	10	25
2	50	30
3	5	40
4	5	3

6   Conclusions

The FEA model developed and the subsequent analysis technique proved to be sufficiently robust as to be able to produce results that accurately matched the physical values measured on the actual foundation.

The values measured are approaching the limits of the equipment being used to and as such the variations from predicted to measured are relatively very small.

The technique is dependent upon the accuracy of the assessment of the stiffness values assigned to the sub-oil conditions. In this case this information was gathered from data charts for a variety of sub-soil conditions.

This information can however be confirmed by carrying out a static stiffness test directly onto the sub-soil via a suitable plate after the site has been excavated.

The technique has been shown to be suitable for analysing foundations for large machine tools whatever their weight and configuration. This would enable a machine tool manufacturer to specify the depth of concrete for a machine foundation with a high degree of confidence that the required static stiffness specification will be met and that the machine alignments could be subsequently be achieved.

7   Acknowledgements

References

[1]   Pro/Mechanica –Using Structure with Pro/Engineer, Parametric Technology Corporation

[2]   Ford D.G., Postlethwaite S.R., Blake M.D., The identification of non-rigid errors in a vertical machining centre, *Proc Instn Mech Engrs,* Vol 213 PartB, 1999

[3]   Brogen, T.H.N. The stiffness of Machine Tool Foundations, *MTIRA, 1970 Research Report* No. 33

[4]   Brogen, T.H.N. and Stansfield, F.M. The design of Machine Tool Foundations, Proc 11th International MTDR Conference, 1970, pp 333-353

2007-02 Structural Analysis of a large Moving Gantry Milling Machine including its Work Support System and Foundation

Structural analysis of a large moving gantry milling machine including its work support system and foundation

A Myers, S M Barrans, D G. Ford

Centre for Precsions Engineering, School of Computing and Engineering, The University of Huddersfield, Queensgate, Huddersfield HD1 3DH, UK, Email: a.myers@hud.ac.uk

Abstract

This paper describes the comprehensive analysis of the static structural stiffness of a large moving gantry milling machine of the type typically used to produce large components for the aerospace, shipbuilding and automotive industries.

The need for high static stiffness arises from the requirement to produce parts to a desired size and shape [1] and although finish machining often takes place with small depths of cut and correspondingly light cutting forces, the resulting deflections can still be excessively large if the machine has inadequate static stiffness.

The machining performance and component quality produced by these machines is heavily dependant upon their structural rigidity and it is therefore extremely important to maximise the stiffness of the entire structural force loop.

Machines of the type described above are connected to the work-piece by the concrete foundations which support them and thus the machine's overall rigidity also depends upon the concrete foundation and the sub-soil beneath it.

This research has investigated the contribution of each significant element of the structural loop to the overall static stiffness of the machine, as measured between the ram and the component support system, in this case, fixed work-plates. Emphasis is made on the need to fully consider the concrete foundation and the subsoil beneath it [2, 3] when analysing the force loop for machines of this type. The predicted overall stiffness was compared to the measured value.

The paper clearly shows how modern Finite Element Analysis (FEA) software enables the design of machine tool structures to be carried out quantifiably with significant confidence in the accuracy of the results.

1 Introduction

For a through understanding of the static structural stiffness of a machine tool it is necessary to analyse the full structure, taking into account all significant individual components. This is best carried out using modern Finite Element techniques which not only enable the behaviour of individual fabrications and castings to be determined but almost all aspects of the structure e.g. assemblies, joints, bearings, foundations and subsoil etc.

1.1 Model considerations

The CAD model was produced using Pro/engineer Wildfire [4] to generate the various representations of individual structural components such as subsoil, concrete foundation, foundation connectors, beds, gantry, head-slide, ram and work-plates and to produce the model assembly.

Pro/Mechnica FEA software was used to produce the representations of the X axis linear bearings and Y axis linear bearings.

Appropriate material characteristics were allocated to each structural member to specify such as its Young's Modulus, density and poisson's ratio.

For accurate modelling of the foundation behaviour full translational and rotational external constraint was applied to the base of the sub-soil only [5, 6]. Full kinematic constraints were employed using spring members to represent linear bearings between bed and gantry and gantry and headstock.

Static loads typical of those generated on large Machine Tools were applied to the face of the machine ram and the work-plate simultaneously to simulate the separating forces generated under machining conditions.

1.2 Elements

The types of elements that can be used for the analysis can be shell, beam or solid and choice of appropriate element type depends upon the nature of the main structural member.

In this case the elements were generated automatically using a facility in the Pro/Mechnica [4] FEA software package.

1.3 Types of analyses

The purpose of this paper is to describe the static analysis which was carried out on the machine structure.

The analysis was carried out with loads applied simultaneously to the face of machine ram and the work-piece support system (work-plates) in the vertical direction. The corresponding static deflections of the ram and work-plate were computed and used to calculate the static stiffness of the structure between ram and work-plates.

The contribution of each significant individual component to the overall stiffness was computed and recorded in tabular form.

2 Machine configuration

2.1 Overall structural layout

The construction of the main machine basic structural members was as shown in Figure 1, with each individual component being made from a welded steel fabrication.

For the purposes of this analysis the structural members were assumed to be rigidly connected to each other at each joint interface except where supported by the X axis and Y axis linear bearings which were represented by linear spring members

The X axis gearboxes and the Y axis and Z axis ballscrews were simulated by linear spring members.

The continuous nature of the foundation connectors used to support the machine bed and the work-plates was simulated by a continuous layer of material having the same overall spring stiffness per square metre as the connectors.
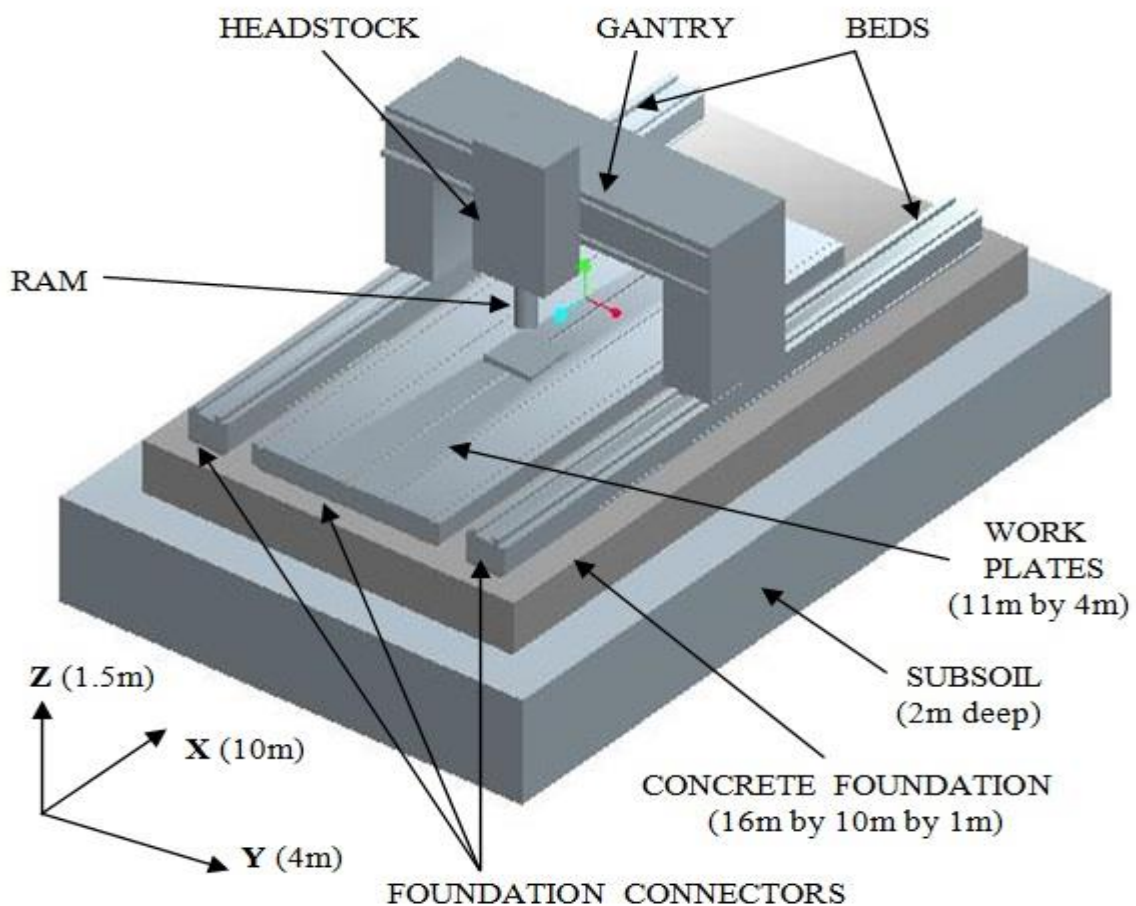
Figure 1: Large moving gantry milling machine structural configuration

2.2 Individual structural layout

Each of the eleven main structural components was modelled in a 3D solid modelling software package [4] using dimensional information obtained from the corresponding original manufacturing drawing.

The significant features were modelled in detail as shown in Figure 2 and Figure 3 below in order to maintain overall accuracy of result. Cosmetic features with no obvious contribution to stiffness were omitted.

The welds were modelled as if continuous and with full width penetration of each plate.
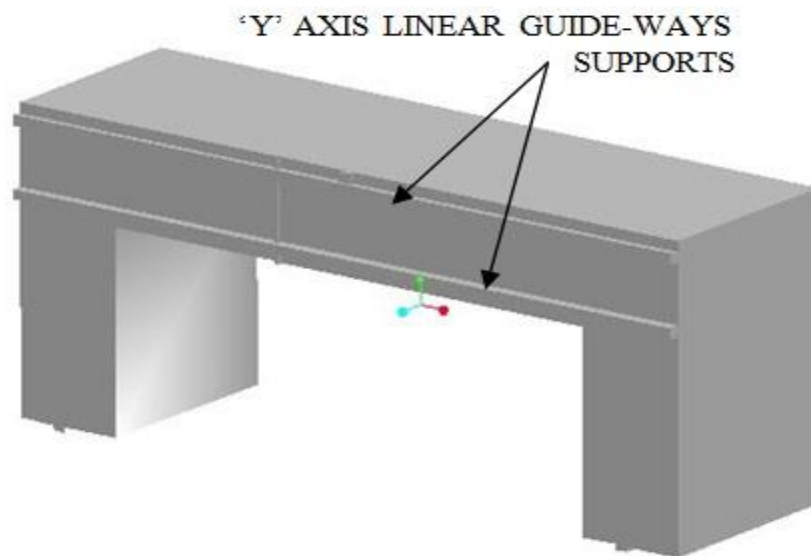
Figure 2: Gantry fabrication
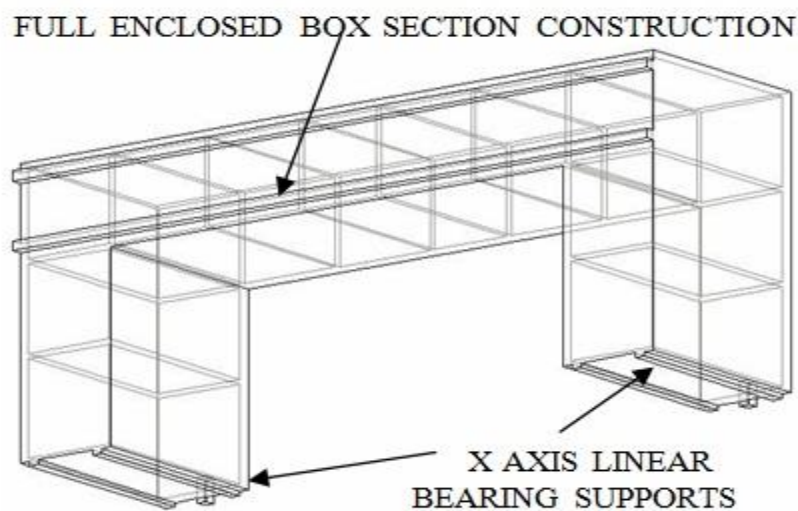
Figure 3: Gantry fabrication (underside view)

2.3 Model assembly

After each component had been modelled separately an assembly model was constructed from the individual members to give the machine configuration as shown in Figure 1.

3 Loads and constraints

Figure 4 shows the Finite Element Model with loads and constraints applied and linear bearings representations added.

3.1 Loads

For the static analysis the load was applied to the lower face of the machine ram and the upper surface of the work-plates simultaneously to represent the separating forces produced by the machining process.

The statically applied force was 10,000N, typical of the cutting forces generated by machines of this type.

3.2 Constraints

The Finite Element Model (FEM) was externally fully constrained for translation and rotation at the underside of the subsoil as would be the case for the actual machine.
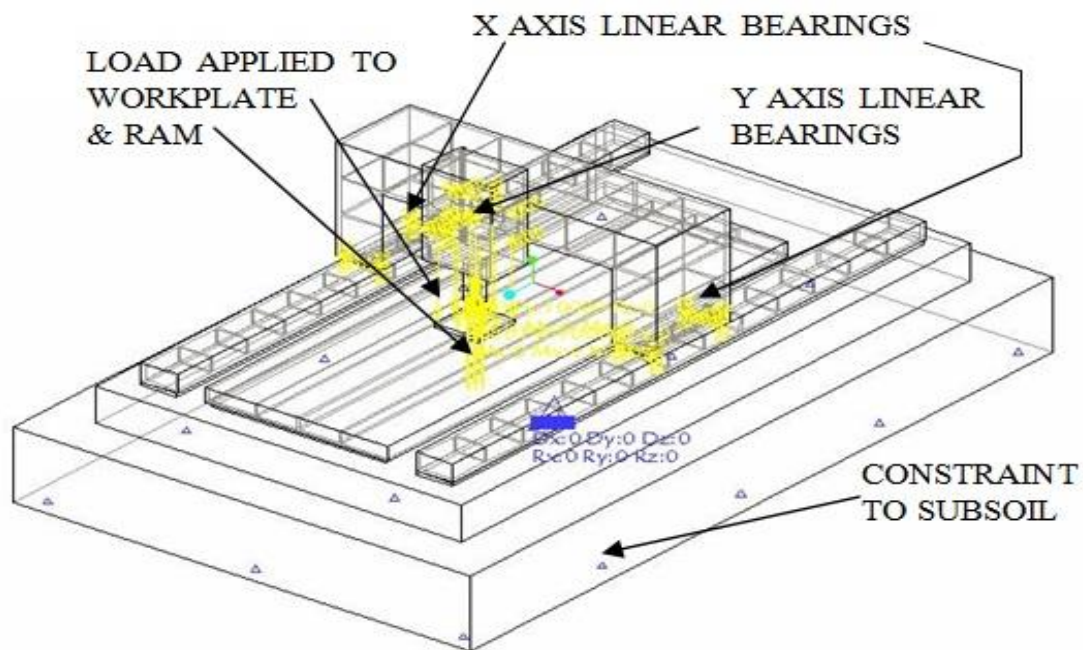
Figure 4: FEM with loads, external constraints and linear bearing constraints

4 Analyses

4.1 Static stiffness

The static analysis calculated the magnitude and direction of the deflections of the structure due to the applied loads and thus enabled the static stiffness of the machine to be determined. The analysis was carried out in single pass adaptive mode.

4.2 Overall structural loop (ram to work-plate) stiffness

The overall stiffness measured between the end of the machine ram and the upper surface of the work-plate was computed by measuring the deflection of the ram relative to the work-plate due to a separating load of 10,000N applied between them. This is the stiffness criterion which determines a machine's ability to achieve dimensional tolerance of the work-piece.

To assess the stiffness of each structural component referred to the ram and work-plates the model was analysed systematically with each component in turn being assigned quasi-infinite stiffness by increasing its E value by a factor of one thousand. The reduction in deflection at the ram/work-plate was a measure of the stiffness of that particular component. This procedure was carried out for the subsoil, concrete foundation, bed foundation connectors, all five machine main structural elements, the X axis linear guide-way bearings, the Y axis linear guide-way bearings, X axis gearbox, Y and Z axis ballscrews, the work-plate foundation connectors and the work-plate.

The overall loop stiffness value is shown in Table 1 and the results were compared and tabulated as percentages of the overall in Table 2.

4.3 Deflections due to machine self weight

The distortion of the machine due to the weight of its main moving member i.e. the 30 Tonne gantry was computed as it moves through the X axis traverse. This stiffness criterion is important in order to maintain alignment tolerances as specified typically by the final inspection test sheets for the machine. These tests are often based upon the appropriate international standard ISO 8636-2: 1988 or national standard BSI 4656-37: 1989 for this particular machine configuration.

To some extent this distortion can be accounted for by deliberately aligning the machine beds with a countering bias on installation. However the value of this bias needs to be measured by tests or predicted by methods such as FEA.

4.4 Deflections due to work-piece weight

The effect on the distortion of the machine due to the heaviest envisaged component being placed on the work-plate was assessed by loading the work-plates with a static uniformly distributed load of 30 Tonne. The effect of this distortion cannot be compensated for because of variation in work-piece weight.

5 Results

5.1 Overall structural loop static stiffness

The following Figure 5 and Figure 6 show the static deflections of the machine structure due to the simulated machining forces being applied to ram and work-plate with the corresponding loop stiffness value being shown in Table 1.
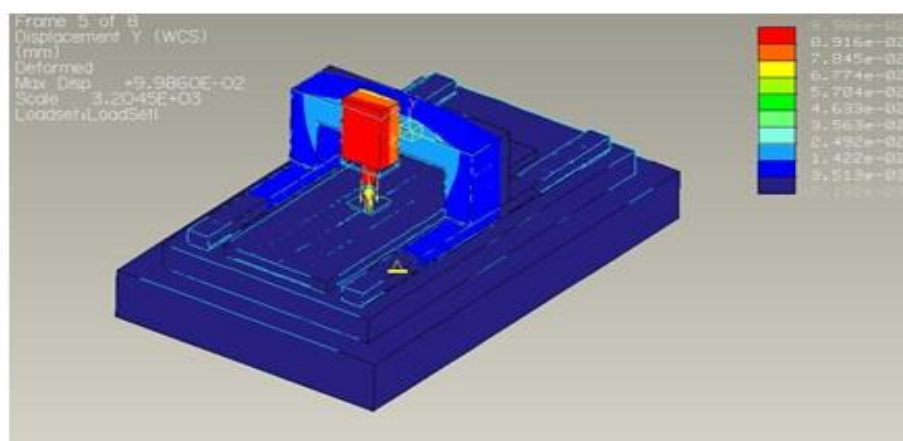

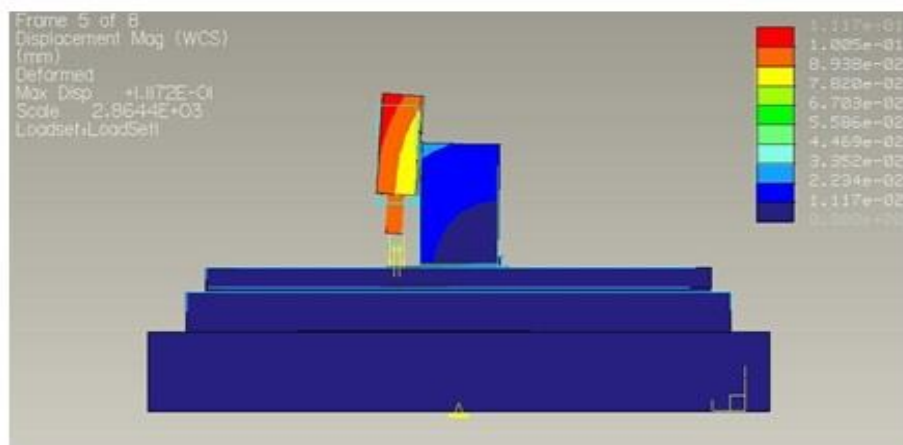Figure 5: Deflections of machine due to simulated machining forces.

Figure 6: Deflections of machine due to simulated machining forces.

Table 1: Overall deflections and structural loop stiffness

Load (N)	Direction (Vertical)	Deflection (micron)		Overall loop Stiffness (N/micron)	
		Ram	Work-plate	Predicted	Measured
10,000	Z	98	8	94	105

Table 2: Compliance of the machine between the ram and work-plate due to the various structural components

Structural Component	Vertical load (10,000N)		% Defl micron	% Compliance (micron/N) 10^{-4}
	Ram	Work-plate		
Subsoil	1	1	2	2
Concrete foundation	1	1	2	2
Foundation connectors	12	<1	11	11
Beds	1	<1	1	1
X axis linear bearings	6	<1	6	6
X axis gearbox	<1	<1	<1	<1
Gantry	35	<1	33	33
Y axis linear bearings	16	<1	15	15
Y axis ballscrew	<1	<1	<1	<1
Headstock	26	<1	24	24
Ram	1	<1	1	1
Work-plate found. conn.	<1	4	4	4
Work-plate	<1	1	1	1
Total	99	7	100	106

5.2 Deflections due to machine self weight

Figures 7 shows the basic FEM used to assess the effect on the foundation of the 30 Tonne weight of the moving gantry and Figures 8 shows the resulting distortion of when the gantry is at mid X axis traverse position.
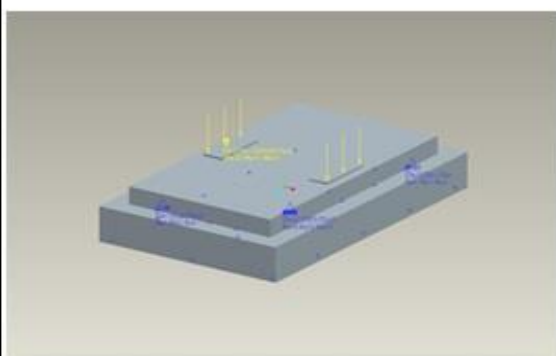
Figure 7: FEM of foundation with gantry loading
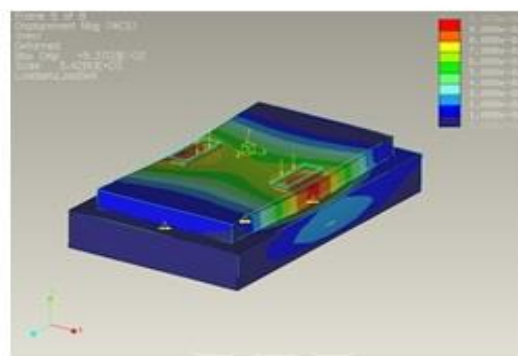
Figure 8: Distortion of foundation due to gantry weight

The resulting bending along the X axis is shown in Figures 9 and is 94 micron whereas the ISO straightness tolerance for a 10m X axis machine is 50micron.
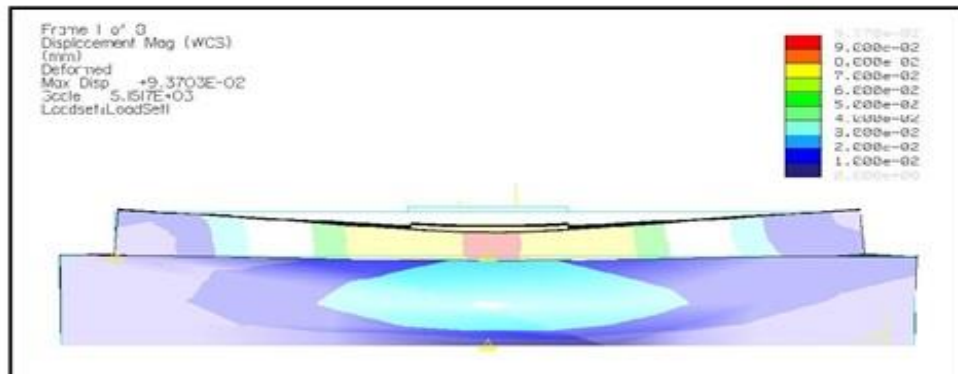
5.2 Contd

Figure 9: Deflection along X axis of the foundation due to gantry weight

5.3 Deflections due to work-piece weight

Figures 10 and 11 show the foundation distortion resulting from the heaviest component, equal to a uniformly distributed load of 30 Tonne.
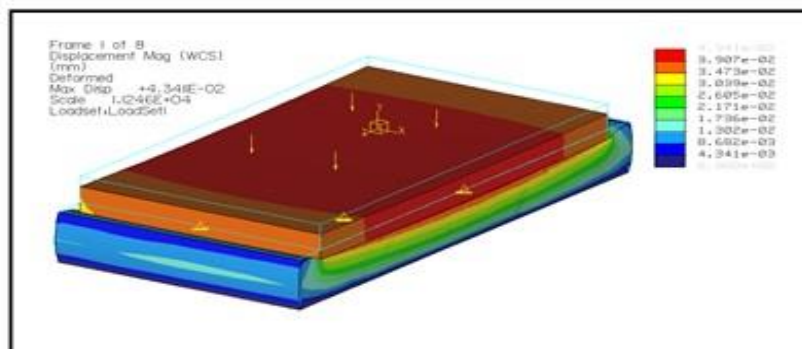

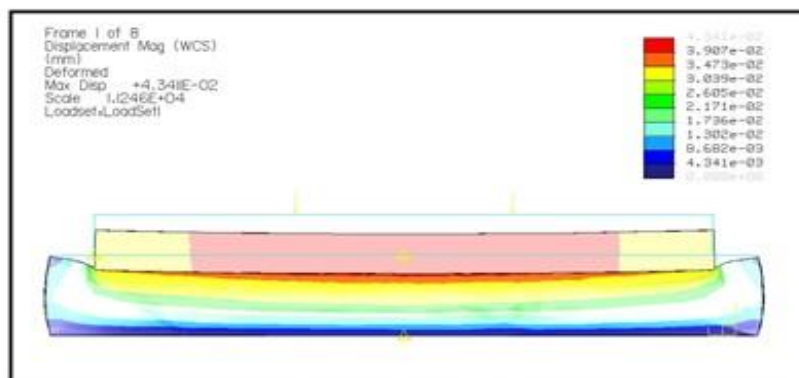Figure 10: Distortion of the foundation due to heaviest component

Figure 11: Deflection of the foundation along the X axis

The resultant absolute vertical deflection of the foundation is 43 micron with bending at its upper surface of 8 micron , measured along the X axis.

6 Conclusions

This paper clearly demonstrates it is now possible to comprehensively analyse the static characteristics of structures of large and complex machine tools and the need to include the concrete foundation and supporting subsoil in order to obtain a full understanding of their behaviour.

The use of modern Finite Element Analysis software packages and the associated hardware, as a tool for determining the static stiffness characteristics for a machine tool structure can be seen to have significant advantages in terms of time and accuracy of results over the traditional methods using classical theoretical calculation techniques.

The depth of analyses gives access to information that will allow the machine tool designer to optimise structures with respect to weight and size such that maximum stiffness and minimum mass can be achieved.

7 Acknowledgments

References

[1] Ford D.G., Postlethwaite S.R., Blake M.D., The identification of non-rigid errors in a vertical machining centre, *Proc Instn Mech Engrs Vol 213 Part B, 1999*

[2] Brogen, T.H.N. The stiffness of Machine Tool Foundations, *MTIRA, 1970 Research Report No. 33*

[3] Brogen, T.H.N. and Stansfield, F.M. The design of Machine Tool Foundations, *Proc 11th International MTDR Conference, 1970, pp 333-353*

[4] Pro/Mechanica-Using Structure with Pro/Engineer, Parametic Technology Corporation.

[5] Myers A, Ford D G, Barrans S M, *2005 Lamdamap Conference*, Finite element analysis of the static stiffness of a foundation for a large machine tool.

[6] Myers A, Ford D G, Barrans S M, *Journal of Physics: Conference Series Vol 13, 2005, pp 410-413*, Measurement techniques for determining the static stiffness of foundations for machine tools.

2009-04 Evaluation and Comparison of a Large Machine Tool Structure with ISO Standard Alignment tests.

Evaluation and comparison of a large machine tool structure with ISO standard alignment tests

A. Myers, S M Barrans, A P Longstaff, S Fletcher, D G Ford
Centre for Precision Technologies, University of Huddersfield, England

Abstract

In order to satisfactorily machine precision components it is necessary for machine tools to be able to achieve extremely high levels of geometric accuracy. This requires their structures to be extremely rigid such that deflections caused by self weight and traversing of the moving elements do not induce distortions that exceed the required tolerances of the components which are manufactured by the machines.

To aid this aspect of machine tool technology, a range of standards have been systematically created which specify in great detail a variety of geometric tests which can be applied to the various configurations of machine tools currently in use today. Certain machine tool companies will use national or ISO standards, others will create their own, often based upon the ISO but tailored to suit their specific machine configuration and characteristics.

However, achieving the required tolerances can be extremely difficult due to a number of reasons such as geometric errors, thermal distortions causing errors to change as temperatures change and load errors causing the errors to change due to the variation in load magnitude and the changes in positions of the loads.

One major source of load errors on large machine is caused by the machine's own weight and its re-distribution as the machine is traversed through its own working stroke, whereas another significant source is caused by the variety in component weights and their variation in position, either on static or moving table machines. In some cases the tolerances specified in standard tests can be tighter than grade "A" straightedge tolerances and achieving this accuracy under conditions which apply to large and heavy machine tool installations can cause significant problems and considerable unanticipated costs.

A review is made here of how these difficulties might be overcome by use of modern technology and adopting the outlined planned approach to the design and build procedure used of large and heavy machine tools.

1   Introduction

This paper investigates the effect of the static machine self weight and component load errors on a typical machine tool structure, including the concrete foundation and how the magnitude of these errors compare with the allowable tolerances as specified by typical official standards.

The paper discusses how the discrepancies between actual machine errors and the standard tolerances specified can be minimised and overcome on a typical machine tool configuration, by appropriate use of Finite Element Modelling at the design stage, sufficiently robust specification of foundation stiffness and improved measurement techniques.

2   Machine configurations and associated standards

Machines which are being addressed by this paper can typically have traverse dimensions of 20m for the "X" axis, 5m for "Y" axis and 1.5m for the "Z" axis.

2.1   Machine configurations and components

Two examples of types of machine tools are being considered in this paper, travelling gantries and moving column machines, both of which are prevalent in most large manufacturing facilities and are used to produce a vast range of components found in the general engineering industry, in particular in the rail, automotive, ship building and aerospace sectors.

Typical component examples are aircraft parts such as turbine engine casings, wing spars, stringers, ribs and skins, undercarriage parts, fuselage frames and skins or the engine bed plate for a nuclear submarine.

Figure 1 shows the machining of a general engineering fabrication and in Figure 2 the crankcase for a large marine diesel engine can be seen with the half cap bearing housings for the crankshaft being bored and faced.

Figure 1: Moving gantry machine   Figure 2: Moving column machine

A specific requirement is that these machines are constructed to tolerances which are very precise and in practice can be very difficult to achieve, particularly in normal factory conditions without air conditioning and which are susceptible to significant fluctuations of the environmental temperature.

To assist determination of the required tolerances there is now an increasingly large number of national and international standards available for the many different configurations of machine that recommend the tolerances to which the individual characteristics of the machine should be produce e.g. straightness of the "X" axis should be no greater than 5 microns per metre of traverse.

2.2   Associated ISO standards

The International Standards Organisation (ISO) corresponding alignment test standards for the specific configurations of machines shown in figure 3 and figure 4 are ISO 8636-2:2007 [1] and ISO 3070-2:2007 [2] respectively. The standards specify a wide range of tests (in excess of 20), some of which are influenced by the moving of the machines through their traverses or the placing of components on the work support areas (work-plates). It is these tests that are being considered in this paper. A more general standard, ISO 230-1:1996 [3] covers the generic method of testing for all machine tools.
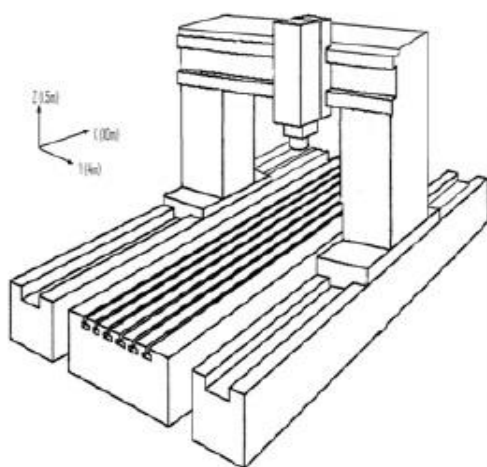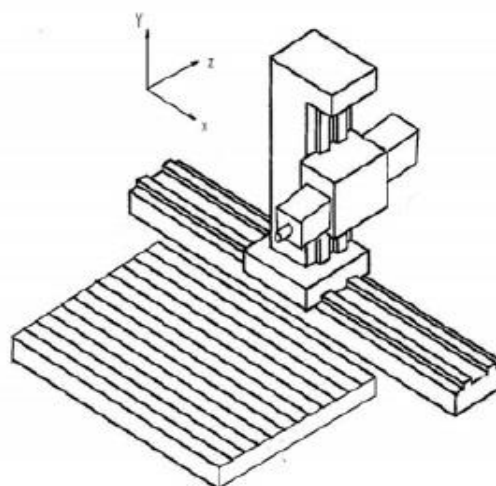

Figure 3: Moving gantry type mc   Figure 4: Moving column type mc

3   Critical alignment tests

3.1   Gantry type machine tests

Both the "X" axis "Y" axis straightness errors measured in the vertical plane are influenced by traversing of the main gantry beam, the head-slide and the component weight and its position.

3.2   Column type machine tests

The "X" axis straightness measured in the vertical plane is influenced by traversing of the moving column and the component weight and its position.

The "Y" axis verticality measured in the horizontal plane is influenced by traversing of the column, the head-slide, the ram and the component weight and position.

The "Y" and "Z" axes alignments are both influenced by traversing of the head-slide and the ram.

3.3   Tolerance values

Typical value for straightness tolerance is circa 10 micron per metre for each axis. These types of machine are generally installed to a gravitational reference initially though this is not a requirement of the standards since it is not necessary to ensure the component is machined correctly. It is done to establish a datum for subsequent reference to check whether or not subsidence might have subsequently occurred due to the foundation or the sub-soil beneath it.

3.4   Equipment used for measurement

A wide range of equipment is used for checking the large machines, such as water levels, electronic levels, taut wire and microscope, alignment telescopes, laser trackers, laser interferometers, dial test indicators, straightedges and squares.

4   Finite Element Modelling (FEM)

By use of Fininte Element Analysis it is possible to determine within a high confidence level whether or not traversing of the machine and or the weight and position of the workpiece will adversely affect the alignments mentioned in "3.1" and "3.2" to such an extent that the machine cannot be constructed within the allowable tolerances mentioned in "3.3".

4.1   Assumptions

By careful consideration of all relevant characteristics of the machine structure, including the foundation and sub-soil etc and assuming linear behaviour of all elments it is possible to accurately predict the static stiffness of all significant structural members.

From this information it can be determined whether or not deflections will take place such that the tolerances specified in the corresponding standard test sheets can be met.

If any aspect of the structure is determined to have a compliance value such that the tolerances cannot be met then subsequent redesign of the structure or foundation can be carried out.

4.3 Data required for FEM

To carry out succesful FEM structural information is needed on all major elements of the machine through from the sub-soil, concrete foundation, foundation connectors, grout material, casting material, guide-way linear bearing stiffness values, journal bearings stiffness for the main spindle etc.

However, this analyis is stiffness based and unlike stress analysis, in this case, certain details such as fillets and bolt holes etc can be ignored since they have a second order effect on the resulting deflections and distortions.

To achieve sufficient accuracy with the FEA it is not only necessary to have the manufacturing drawings of all major structural members in order to provide dimensional information as well as Young's Modulus etc but also such data as the Coefficient of Uniform Elastic Compression for the sub-soil and the "E" value for the concrete appropriate for the level of steel re-enforcement.

4.4 Finite Element Model of machine and component

A full model of a typical gantry machine, see figure 5, based upon work carried out [4] [5] [6], has been developed using Pro/e 3D CAD [7],to specifically analyse static distortions.
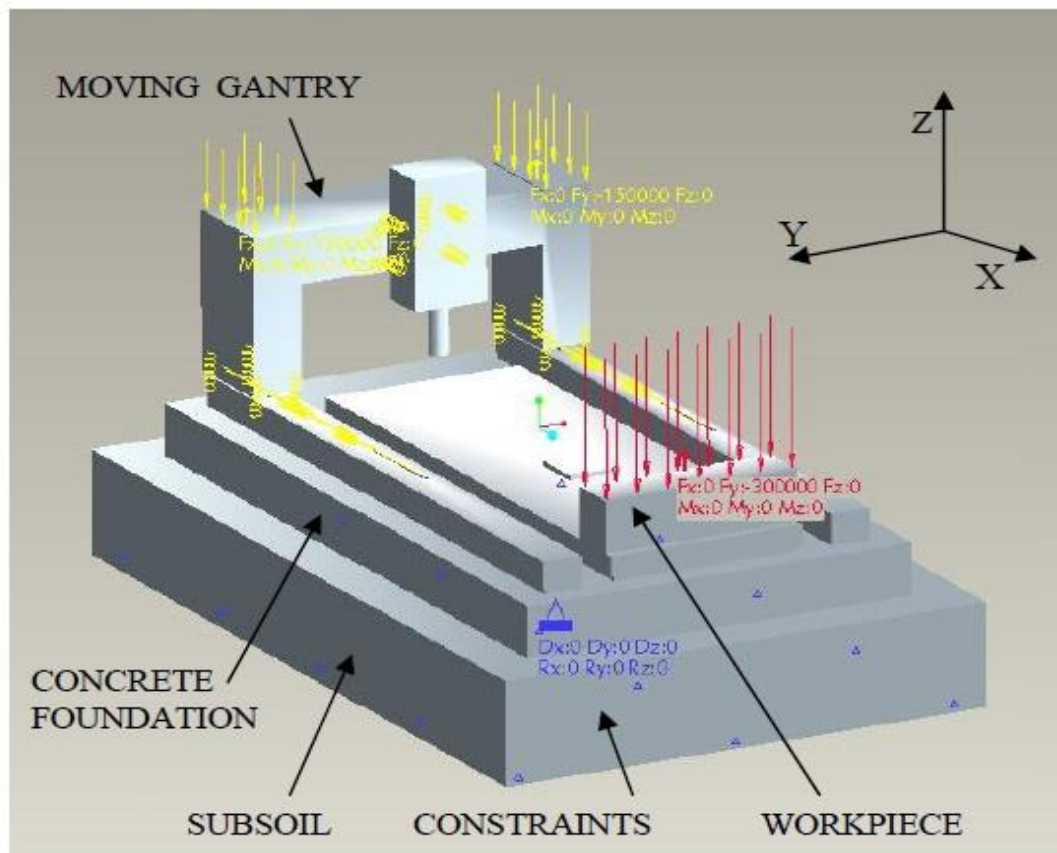

Figure 5: FEA model required for full analysis of static alignment conditions

Relevant dimensional detail taken from manufacturing drawings was used to construct the model which included all major structural members, sub-soil, concrete foundation, foundation connectors, beds, guide-way linear bearings, gantry beam, headstock, ram and spindle.

4.5   Finite Element Analysis of machine

Using Pro/e Mechanica [7] the model was analysed to evalutate the distortions and deflections which would occur due to the machine traversing through its full "X" axis travel and the loading of various simulated components onto a range of positions on the work-plates.

5   FEA Results

5.1   Deflections due to machine moving weight

Movement of the gantry (35 Tonnes) along the "X" axis was simulated and the deflected shape of the machine beds were computed to show the error in straightness that would result from the machine overall structural compliance, as shown in figures 6 and 7 below.

The machine gantry was moved in a number of discrete increments and the bed shape determined for each position. From this a resulting profile for the machine straightness of movment in the vertical planeent could be determined.
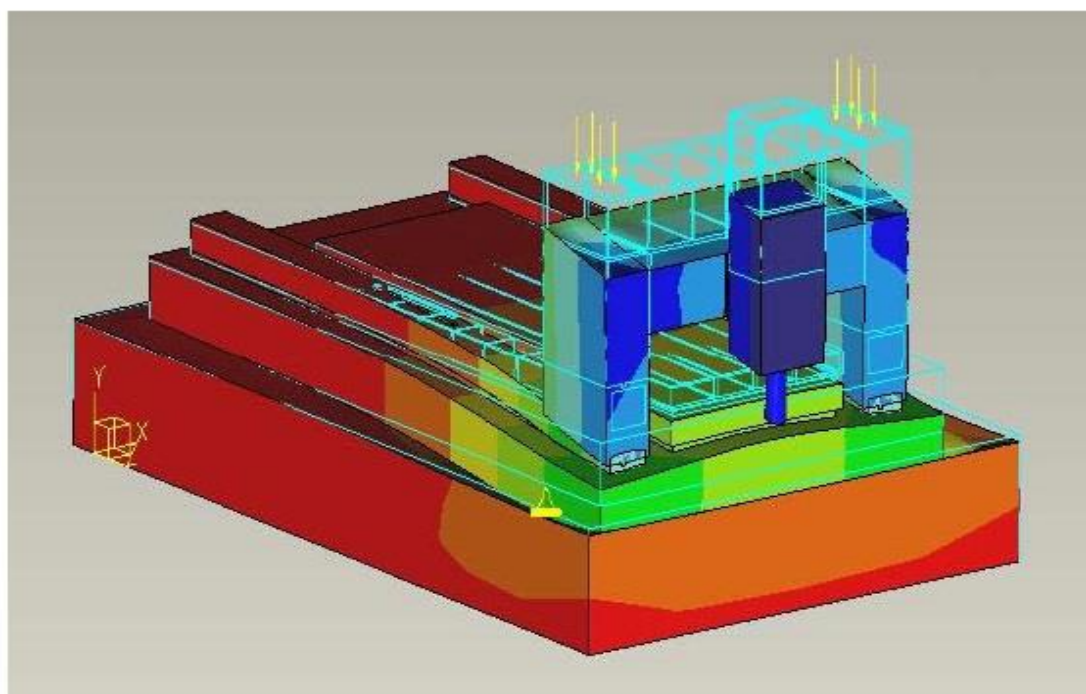

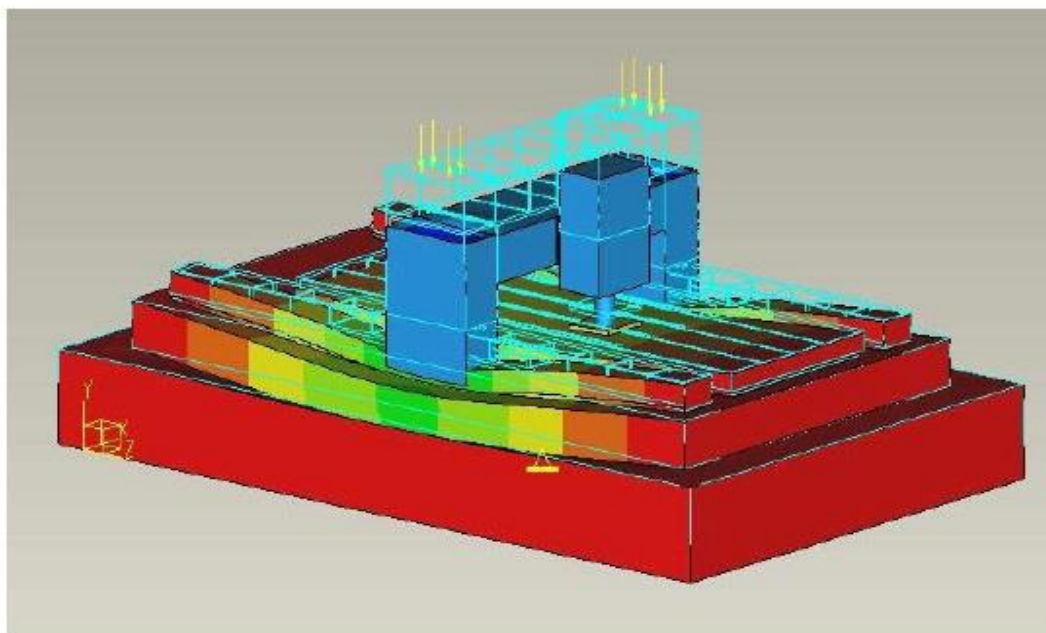Figure 6: Loading simulation of the machine as traversed along "X" axis

Figure 7: Deflection of the machine beds with gantry at mid X traverse

5.2 Deflections due to work-piece weight at various positions

5.2.1 Work-piece at minimum X traverse position

Figures 8, 9 and 10 show the workplate, foundation and subsoil distortion resulting from the heaviest component, equal to a uniformly distributed load of 30 Tonne over a 4m by 1m area of the workplate.
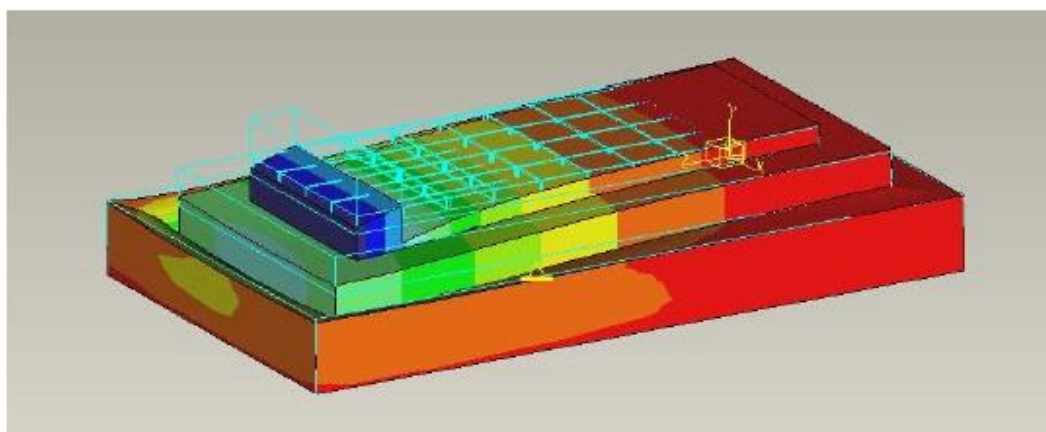

Figure 8: Deflection of the workplates due to workpiece at X minimum

The resultant absolute vertical deflection of the foundation was computed for a range of positions of the maximum anticipated component placed onto the workplates.

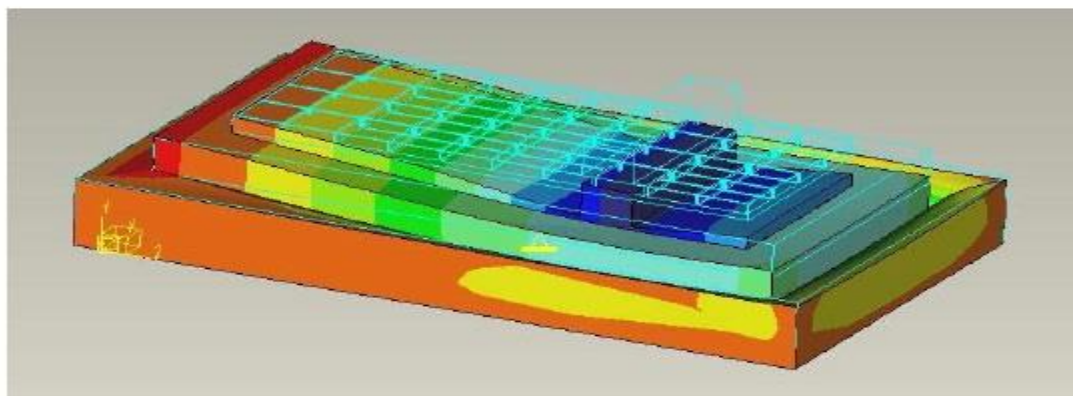## 5.2.2 Work-piece at quarter X traverse position

Figure 9: Deflection of workplates due to workpiece at quarter X axis

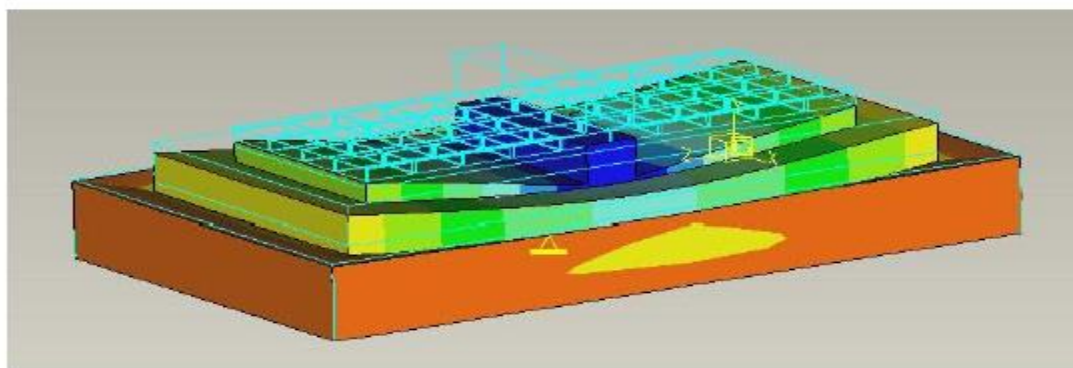## 5.2.3 Work-piece at middle of X traverse position

Figure 10: Deflection of workplates due to workpiece at quarter X axis

5.3   Comparison of tolerances

The most critical tolerances are for "X" axis straightness and pitch were compared with measured and predicted values for moving gantry and workpiece loadings as shown in tables 1 and 2.

Table1: Comparision of ISO, FEA and measured values

MOVING GANTRY MACHINE				
Test No.	Test type	ISO tests	FEA	Measured
		Tolerance (microns / metre)		
G2a	Pitch	100	140	130
Workplate	Pitch	N/A	60	70

Table2: Comparision of ISO, FEA and measured values

MOVING COLUMN MACHINE			
Test No.	Type	ISO tests	Measured
		Tolerance	
G3a	Straightness	50 microns	70 microns
G4a	Pitch	60 microns / metre	80 microns / metre

6   Discussion of Results

FEA and actual machine measurements confirm that the tolerances specified in official standards can be difficult to achieve under certain circumstances. When this is the case remedial work is almost always extremely expensive and not always successful. It was noted that no tests are specified for checking the adverse effect of the weight of heavy workpieces on the alignments.
Remedial actions can involve:-

1. Underpinning of the concrete foundation by use of ring beams.
2. Deliberate re-working of the relevant structural members to produce cambering effects to correct for non-rigid body distortions [8].
3. Compensation techniques [9] in the control circuits
4. All these solutions are generally costly additions to the original price

FEA shows that the main aspects of concern are:-

1. Sub-soil
2. Concrete foundation
3. Mc structural design
4. Foundation connectors
5. Traverse beds

Techniques available to prevent problems:-

1. FEM and analysis to predict non rigid behaviour and to modify the structural design appropriately prior to manufacture.
2. Specification of the concrete foundation:

FEM shows that the stiffness of a typical gantry machine bed can be less than 5% of that of the concrete foundation emphasising the fact that correct foundation design [10] [11] is absolutely critical.

Traditionally, machine tool builders apply limited attention to the detail of the foundation and often are restricted to specifying only the minimum depth of concrete to be used.

A much more successful method is to specify the necessary stiffness at the surface of the concrete based on analysis of the tolerances required by the appropriate standard.

Due to the unpredictable nature of subsoil, in order to achieve the correct specification it is necessary not only to take bore hole samples of the subsoil, but also to carry out soil surface plate tests to determine the coefficient of uniform elastic compression for the actual site conditions.

6 Conclusions

The paper has attempted to identify weaknesses associated with machine tool design and build which can cause considerable unanticipated costs due to difficulties in achieving the necessary high levels of alignment tolerances which are required for manufacturing high precision components.

These issues not only apply to the large machine tools described in detail in this paper but similarly to any other machine tools that are dependent upon a concrete foundation in order to function correctly in order to meet the ever more demanding accuracy tolerances found on modern engineering parts.

By adopting certain planned procedures as outlined above, it is now possible to take advantage of modern technology to avoid many alignment related issues that can be so costly when constructing and installing large machine tools. Future work will involve a full FEM analysis of the moving column machines.

References

[1]   ISO 8636-2:2007 – Machine Tools – Test conditions for bridge-type milling machines – Testing of the accuracy

[2]   ISO 3070-2:2007 – Machine Tools – Test conditions for testing the accuracy of boring and milling machines with horizontal spindle

[3]   ISO 230-1:1996 Test code for machine tools – Part 1: Geometric accuracy of machines operating under no-load or finishing conditions

[4]   Myers A, Ford D G, Barrans S M, *2005 Lamdamap Conference,* Finite element analysis of the static stiffness of a foundation for a large machine tool.

[5]   Myers A, Ford D G, Barrans S M, *Journal of Physics: Conference Series Vol 13, 2005, pp 410-413,* Measurement techniques for determining the static stiffness of foundations for machine tools.

[6]   Myers A, Ford D G, Barrans S M, 2007 Lamdamap Conference, Structural analysis of a large moving gantry milling machine including its work support system and foundation.

[7]   Pro/Mechanica-Using Structure with Pro/Engineer, Parametric Technology Corporation.

[8]   Ford D.G., Postlethwaite S.R., Blake M.D., The identification of non-rigid errors in a vertical machining centre, *Proc Instn Mech Engrs Vol 213 Part B, 1999*

[9]   Schwenke H, et al. (2008) "Geometric error measurement and compensation of machines–An update". CIRP AnnalsManufacturing Technology 57(2): 660-675

[10   Brogen, T.H.N. and Stansfield, F.M. The design of Machine Tool Foundations, *Proc 11th International MTDR Conference, 1970, pp 333-353*

[11]   Brogen, T.H.N. The stiffness of Machine Tool Foundations, *MTIRA, 1970 Research Report No. 33*

2013-09 New low cost sensing head and taut wire method for automated straightness measurement of machine tool axes.

New low cost sensing head and taut wire method for automated straightness measurement of machine tool axes.

O Borisov, S Fletcher, AP Longstaff and A Myers

Centre for Precision Technologies, School of Computing and Engineering, University of Huddersfield, Queensgate, Huddersfield, HD1 3DH, UK

o.borisov@hud.ac.uk

Abstract. This paper describes a novel method to measure straightness error of an axis of motion with a system utilizing taut wire, optical sensor and reference error cancellation technique. In contrast to commonly used taut wire, straightedge or laser-based methods it combines simplicity of setup and low cost with high levels of automation, accuracy and repeatability. An error cancellation technique based on two-point method is applied for the first time to a versatile reference object which can be mounted at any place of machine's working volume allowing direct measurement of motion straightness of a tool point. Experimental results on a typical machine tool validate performance of the proposed taut wire system with a commercial laser interferometer operating in the same conditions is used as a reference. The proposed method shows highly repeatable results of better than ±0.25μm over the range of 0.48m and measurement accuracy comparable to the interferometer of ±0.5μm.

Keywords. Straightness, error separation, two-point method, taut wire, slotted optical sensors, low cost measurement, motion error.

1. Introduction

The performance characterisation of machine tools is prevalent in modern manufacturing industry where component accuracy is crucial. Straightness in two orthogonal planes, along with positioning error and three angular deviations, often referred to as roll, pitch and yaw, represents six components of error of any nominally linear motion system [1]. On machine tools having multiple axes, those geometric errors combine and affect the accuracy of produced components. It is important, therefore, that all geometric errors including

1

straightness are known (measured) to understand capability and ideally reduced to a minimum to maintain highest accuracy of machining.

Unlike other geometric errors, straightness error measurement involves detection of lateral displacements along the direction of axis travel. Most direct straightness-measurement systems consist of a straightness reference and a displacement indicator [2]. There is always a great difference in values of straightness error compared to the distance along which they are measured. It is approximately 10^5 and so the straightness reference should be – long and flat at the same time. Here lies the main problem of straightness measurement in space – finding a suitable reference object. Measurement of straightness typically involves material artefacts (straightedges) or various optics (from telescopes to lasers) or even levels using earth gravitation as a horizontal reference for angular displacements to be converted to the lateral ones.

Because straightness measurement cannot be split over the distance along the axis, straightedges are limited by their own dimensions allowing measurements within their lengths only. An attempt to solve this issue by Pahk relies on multiple measurements with partial overlapping [3]. Increased range comes at a cost of reduction in accuracy which is highly dependent on the number of overlaps and overlapped length.

Telescopes and autocollimators, which have been the first optical methods [4], with time advanced to numerous laser-based techniques where a highly coherent laser beam was used as a straightness reference [5-7]. Conventional Helium-Neon laser interferometers manufactured by companies such as Agilent and Renishaw have set a high level of measurement accuracy (Agilent 55283A ±0.2% of measured value, Renishaw XL-80 ±0.5%) but did not put an end to research in the straightness area. Being relatively expensive, slow, complicated and susceptible to disturbances over longer ranges, laser interferometers gave way to numerous alternatives and advancements aiming to overcome those well-known disadvantages.

Fan and Zhao introduce a simple laser test for measuring straightness using a four-quadrant photo detector [8]. The method does not depend on expensive matched optics and uses a shorter laser beam to improve its stability, demonstrating 0.5µm repeatability on a 100mm range. This result is not validated against other methods; the system is only calibrated with a laser interferometer which can still leave systematic errors of the system unknown. To increase sensitivity of a conventional laser (HP5518A) using more sophisticated optics, Lin [9] shows a possible advancement in accuracy achieving repeatability of 1µm over 200mm.

A solution to avoid using more stable (and more expensive) dual-frequency lasers is described by Feng [10] and Kuang [11]. A single-mode fibre-coupled laser produces a beam which strikes into a corner reflector mounted on the moving spindle and reflects back to a photodetector. Like all laser-based methods, this one suffers from beam pointing stability issues which get worse with distance. Moreover, the method involves a laser interferometer for calibration and relies on quality of the beam which leads to further expense related to a powerful laser emitter. Internal setup of the measuring unit requires space, numerous adjustments and laboratory conditions.

Measuring angular displacements instead of linear ones using a different optic setup is presented by Zhu [12]. Similar to previous laser method in terms of setting up, this one claims to provide a higher accuracy once again taking advantage of improved and more complicated optics. The same time the system remains sensitive to measurement distance.

Chen et al [13] describe a dual-frequency laser with two Wollaston prisms to compensate air disturbances over a very long range of 16m. An experiment, carried out in laboratory conditions, claims to show high measurement stability of 3.6µm. This, however, not necessarily means the corresponding level of accuracy because only overall 230µm-high V-shape of the measured profile was reproduced when its details fell into the area of measuring system repeatability of 20µm.

All the improvements mentioned above might not be sufficient to solve the issue with lasers where accuracy is compromised over the measuring range as it is affected by the refraction index of air turbulence and, for some systems, beam pointing stability. Estler [14] in his comprehensive review of long range measurements, where he describes all the factors affecting a laser beam propagating in the air, shows that the beam actually bends and this happens rather randomly which can make modelling and compensation of such error a challenge.

To overcome the limitations of methods using a beam of light or solid artefacts a different physical reference object together with a different measurement setup is required. The first one needs to be flexible in length yet solid which mean range flexibility and low environmental susceptibility. The second one needs to be range-independent and non-contact to maintain high measurement accuracy over the range. A technique that would fit into those requirements is straightness measurement using a taut wire. It provides the overall desired physical setup but its accuracy and efficiency issues are yet to be addressed.

2

2. Method

The taut wire is a known reference for measuring straightness [1, 14, 15]. A length of the wire, stretched between two points, gives a straight line assuming catenary effects are negligible, eliminated or subtracted. The wire can have long lengths (The wire may begin to sway with lengths greater than 15m) and any orientation in space needed to make it nominally parallel to an axis of motion, such as on a machine tool. Step by step misalignment comparison of wire and axis nominal travel trajectory allows calculation of straightness of one relative to another. The main reasons why this method is not widely used at present are its low accuracy and inefficient data gathering methods. The accuracy is compromised by both variability of the wire reference and typical wire detection methods such as microscope or electrical contact. Even commercial non-contact implementation with the use of laser diode [16] has stated precision of ±5 µm. All of those methods require manual intervention leading to a time-consuming process and involve relatively high levels of measurement uncertainty. Figure 1 shows the proposed solution to overcome those issues:

Figure 1. Measurement principle.

Each of the key features of the method is described below:

1. Nylon fishing wire is readily available in any length; it is lightweight, portable and easily-mountable. Its diameter variation depends on wire quality, stretching force and settling time and normally lies within 2-20µm between the lowest and highest point. A wire made of steel, like string on a musical instrument is successfully used in fixed-length straightedges [15], but it is less suitable for long ranges because of its limited availability and poor dimensional quality. Thin wires provide low sensitivity when using an optical detector and require more effort when choosing the right stretching force (to get the wire as straight as possible while avoiding breakage).

2. Slotted optical sensors like those manufactured by Omron are primarily designed for automation applications to detect the presence of a non-transparent object between the fixed wavelength emitter and receiver. Bench testing has proved that they have sensitivity and stability enough for detection of objects even on a sub-micron level. For this work an Omron sensor, shown in figure 2, is used as it provides good balance between sensitivity and range and can be easily mounted. These are low cost, portable, and mass-manufactured so are readily available and have provided an excellent solution for measuring lateral displacements of a stretched wire passing through the sensing area.
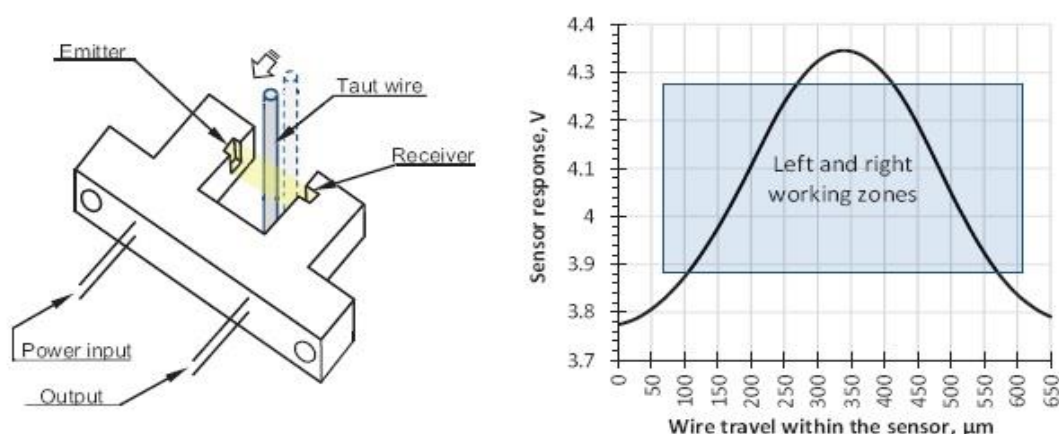

Figure 2. Omron photomicrosensor and its sensitivity graph.

3

3. Fine adjustment carriages are used for precise alignment of the wire with the measured axis within a travel range of several millimetres. Adjustment of the carriages can be checked very quickly using feedback from the sensors without the need of additional equipment. Removal of slope between the wire and 0.5m axis typically takes 5 minutes while alignment of the laser beam can take 7-10 minutes.

4. The technique of the reference error cancelation during step by step straightness measurements (also referred as "two-point method") was first published in 1979, applied to a machined steel plate [17-18]. Error in the reference was taken out of calculation by using data from an additional displacement sensor. If the distance between a pair of sensors is equal to the increment of axis travel, they both can be used together to measure relative displacement at every point. Adding each value to the sum of the previous reading, starting from zero, gives a separated lateral error of measured axis.

This approach was successfully tested on a 7m long boring machine, when the error was measured along 5m range with 100 or 200mm increments [15] showing its high potential. Gap sensors (sensitivity 5μm/mV) provided good correlation with a laser interferometer measuring an error of 40μm.

The improvements that followed [19-20] still rely on a solid 3-dimensional straightness reference, requiring consideration of its pitch error which had to be measured separately. Another issue is a large accumulated error – negligible on the first step, its amount soon exceed the measured value. To prevent that, a larger step size and calculation of intermediate values have been proposed [20]. More recent applications of two-point method (even expanded to three-point) are in topography and surface profile measurements [21-23] where the reference error of a moving stage is separated achieving sub-micron accuracy levels using capacitive sensors.

All those developed methods represent a good use of error cancellation principle applied to straightness measurement of machined parts whether it is a precision guide, cylinder or a flat surface. Application of those methods to machine tool's axes can be challenging because the straightness reference needs to be specially positioned and have a variable length if it is to be useful on a wide range of machines.

On the other side, straightness of an axis guide way can be very different from the straightness of motion of the tool or workpiece point due to the error magnification by other axes forming a kinematic chain between them. Therefore it is not sufficient to measure the guide or attached artefact (for example, using capacitive sensors), a direct measurement between the tool/workpiece interface is necessary to ensure high accuracy.

Here we introduce an alternative use of the error cancelation technique when the straightness reference is a stretched wire. Unlike a straightedge, the wire can be considered to be a 2-dimensional reference as its cross-section is round. This means only one wire error, its change in diameter, needs to be eliminated and the only measured lines are axis and wire surfaces belonging to the same plane. The wire is a simple object which can be easily placed at any part of machine's working volume to measure straightness of corresponding axes directly, without estimation which can be a source of measurement error like it is the case with laser interferometry.
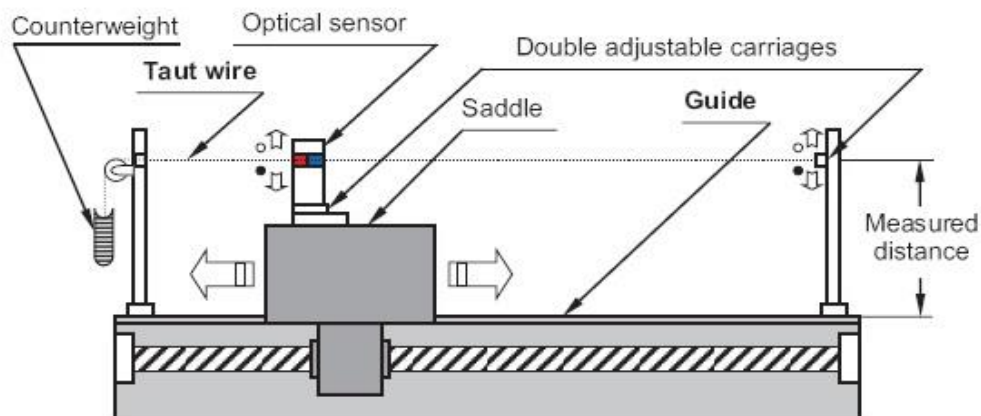

Figure 3. Taut wire measurement system mounted on a machine tool.

4

The taut wire setup shown in figure 3 consists of: two stands, the distance between which covers the full measured axis; the wire itself stretched between them; the new optical sensing head mounted on the moving component of the machine using a post having the same length as a typical tool so that systematic and random (vibrational) effects from linear and rotational error components will be representative of those in operation. Position of the wire can be adjusted using the aforementioned dual axis carriage. Measurement of the axis straightness is based on the following conditions:

1. Both the wire and the measured machine axis have time-invariant (at least for the duration of the test) surface profiles (straightness values over the range) i.e. repeatable systematic errors dominate over non-repeatable and random errors.
2. Straightness error of the first point of the measured surface has zero value. Upon completion of the measurement, least-squares fitting eliminates any residual slope while not changing its shape.
3. Measurement time is sufficiently short so that no change in straightness of the machine axis can occur.
These conditions enable separation of the wire surface profile from the profile of measured axis. In case of single sensor measurement they both combine and the total reading at every point represents the sum of both errors. If wire error greatly dominates the straightness error of the axis, measurement fails.
Along with wire error caused by deviation of its diameter, there are random errors caused by wire movement due to airflow, vibration and stretching force.
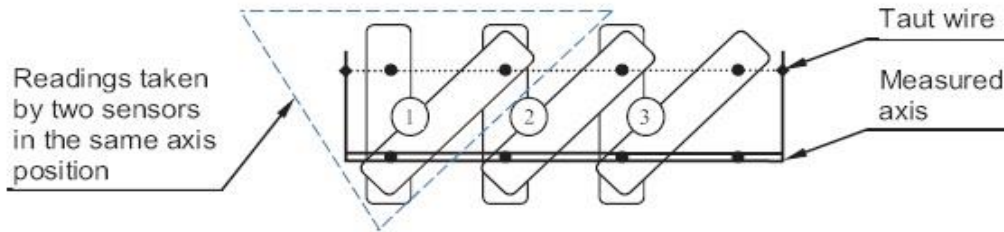

Figure 4. Dual sensor measurement.

Figure 4 shows the order of measuring: every time the machine stops, current axis error combined with error of the wire on current and the subsequent steps are measured. This way every time readings are taken from both sensors. Because the distance between the sensors matches the axial increment (the method to achieve that is described at the end of this section), the first sensor takes position of the second one on the previous step and measures the same error on the wire but combined with different error of the axis. On the figure it is shown by pairs of rectangles (pairs of readings): 1, 2, 3... The following subtraction of second reading of the first pair from the first reading of second pair (both have the same amount of wire error) gives the difference between axis errors which is between the first and the second steps. Accumulation of those numbers obtained from full number of steps (starting from 0) gives the straightness error of the axis on every step.
When two sensors are used simultaneously and readings are taken at every two adjacent points of the wire, and the distance between those points is the same as the machine movement increment, the following calculation [17] separates axis and wire errors (including some random ones) from each other:

$$x_i = x_{i-1} + s_i - c_{i-1} = \sum_{1}^{i}(s_i - c_{i-1}) \qquad (1)$$

Where x – axis error on step i,
         c – combined (measured) error from the first sensor,
         s – combined error from the second sensor.

According to the first condition $x_1 = 0$, all the other values of x are calculated using equation 1.
This equation confirms that the calculated axis error is not influenced by the wire error (including slope) at all as long as it and the machine positioning is repeatable. This error separation enhances the accuracy of straightness measurement regardless of the distance and error amount, though importance of the wire and machine repeatability increases with the length of measured axis and number of sampling points as the

5

positioning error accumulates. To control the accumulation, all tests were carried out as multiple bi-directional runs and the difference between corresponding results has proven to be very small, typically less than one tenth of a micron during all of the validation tests.

Error cancellation reduces only the systematic part of measurement error; random contributors like errors in the sensors themselves, including electrical fluctuations, remain. Because those measurement errors are cumulative, even such small effects could become problematic over longer axes. The method can therefore be expanded to a third sensor to provide averaging at each measurement point. Due to the cost and availability of the sensors, this does not degrade the practicality of the solution at all.

Separation of the sensors in the measuring head is determined once by using a piece of opaque tape attached to the wire. Detection of the edge of the tape while slowly moving the machine axis gives each sensor a clear change in readings taken and the difference in machine coordinates of both points gives the measured step size. Uncertainty using this simple method comes from accuracy of the axis, shape of the tape, speed of motion, etc. It is generally in order of 10μm which is sufficient because rate of change in diameter of the fishing wire is very small, typically stays within a tolerance of 0.1μm/1mm (i.e. just 0.001μm over 10μm).

3. Measurement error

The proposed combination of taut wire and multiple optical sensors used together cancelling the reference error, is subject to certain systematic errors limiting the method's accuracy. The two-point method itself, as a basic principle is perfect and the error appears on the stage of its practical implementation. In case of profile measurements with capacitive sensors, the main error factors reported are zero-difference [20] and pitch error [22] which need to be measured separately and the system calibrated accordingly.

This system uses multiple optical sensors which have different and non-linear outputs but this difference is relatively small and the output is fairly linear in the range of 200μm (figure 2). After simple calibration described in section 5 all outputs are linearized into one straight line with a permanent sensitivity value for all sensors.

Rotational components of a measured axis of motion have a negligible effect on the optical sensors because rotation of the wire within the sensing area does not change the amount of light blocked by the wire and consequently the sensor output is not affected:
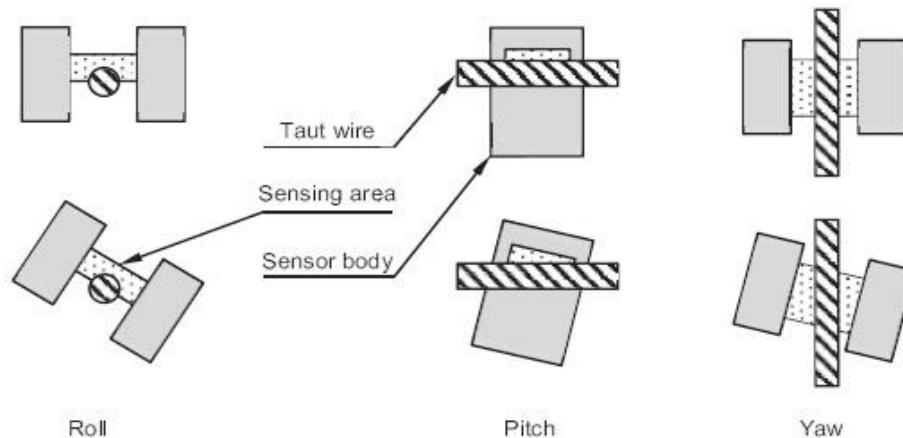
Figure 5. Rotational components of motion affecting the system.

The sensors are sensitive to linear displacements in one direction only, i.e. errors in the transverse directions resulting from the machine's kinematic chain and length of the post consisting of both linear and rotational components do not contaminate the reading. Similarly, change in the relative orientation of the sensor to the wire does not affect the reading because the result is negligible change in the amount of light blocked by the sensor.

6

4. Physical system

A system diagram and the new measurement device itself are shown on figure 6. Raw voltage from the optical sensors passes through low pass (≈3Hz) filters before undergoing analogue to digital conversion for calculation of the measured error using equation 1.

Figure 6. The system dataflow diagram and measurement device.

The device is assembled on a steel plate carrying optical sensors, stabilized power circuit and individual sensitivity controls for every sensor. Possible potentiometer drifting proved to have a negligible effect on the measurem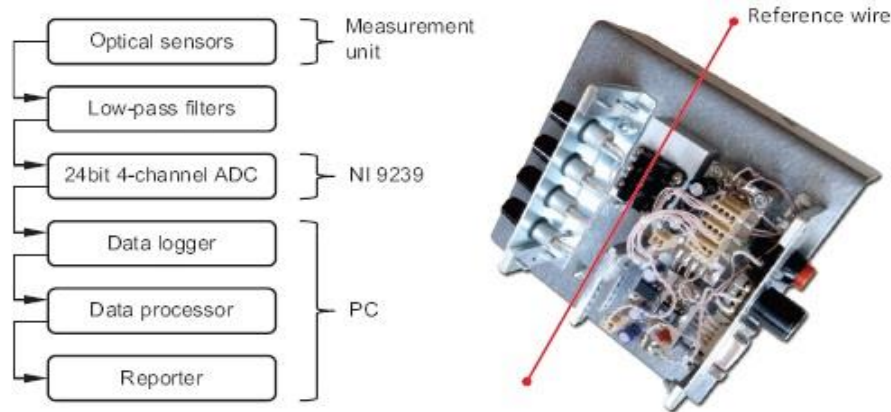ent accuracy because only power going to light emitting diodes can change and therefore does not change sensitivity of the sensors. Manual adjustment moves the working zone vertically within the sensing area (shown on figure 2) allowing better intersection between sensors to increase straightness measuring range.

The present design has three sensors mounted horizontally. This works in several different measurement schemes: using first and second sensors as a pair for error cancelation; using second and third in the same way; using both pairs simultaneously and taking the average of them to reduce the total uncertainty; take the first and third pair when longer step size is required (to reduce the time of long range measurements); use the first, second and third separately or all three separately (for single sensor measurement with averaging when the reference error is negligible compared to the axis error). Orientation of the device determines the straightness error to be measured. Spare space is available for a set of vertically mounted sensors for simultaneous straightness measurement in both perpendicular planes.

Dynamic data capture, when the machine moves continuously, is also possible with axis feed rate not exceeding 150mm/min (in the current implementation of the sensing head). This speed depends on the maximum speed of sensor power circuit and can be determined experimentally finding a maximum feed rate value which does not change the measured straightness value compared to the one obtained with a lower speed.

5. Validation

The system was validated on a machine tool axis that was 0.5m long and horizontally orientated. Straightness in the vertical plane was measured using a Renishaw XL-80 laser interferometer having stated straightness measuring accuracy of ±0.5µm over 0.48m. Shortly after, measurement was done using the proposed taut wire (DAIWA Sensor Monofil 0.26mm diameter) with minimal Abbe offset to eliminate effects of angular errors on the axis. In both cases the straightness profile was obtained with step size of 19.956mm, equal to the actual distance between two optical sensors. All data readings were taken with four second dwell interval to allow the long term averaging of the interferometer system to stabilise. For new system, the same dwell time was used during which averaging of 40 readings was used to reduce the amount of noise and small random errors. Every test run was bi-directional to ensure random error detection. Slope errors on both planes were eliminated prior to measurement using double adjustable carriages (figure 3).

7

Both optical sensors were calibrated using a high accuracy (<3μm over full 12mm range) digital dial test indicator so that the linear sensitivity was established with a magnitude of 1.6mV/μm.

In the case of the laser, an average of three sequential bi-directional tests was obtained for comparison with the wire. To include in the validation consideration for the fact that every piece of wire has its own unique surface profile, three different pieces were tested and on each of those three runs were also completed. Prior to measuring, the wire was left to settle for approximately five minutes. Normally such time period is enough for good quality fishing wire to stabilize: during that time it is continuously changing its diameter becoming thinner as it stretches. Stabilization time is individual for every wire material, thickness and stretching force. Finding the minimal period while the wire cannot be used for measurements is a simple procedure of logging measurement data while the machine is not moving, assuming relatively stable thermal conditions.

Figure 7 shows averaged (here and after – least square fitted to remove residual slope) results of measuring straightness using the same piece of wire. Three bidirectional tests performed one after another show repeatability within 0.2μm.
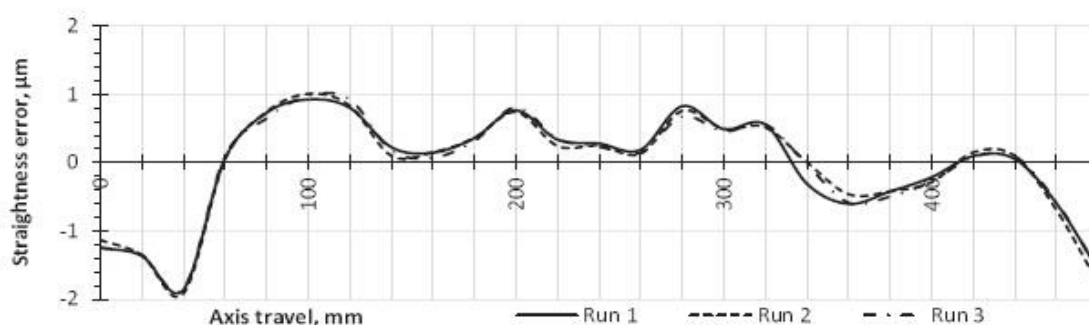
Figure 7. Repeatability within one piece of the wire.

After three tests were completed, the wire was replaced, a new wire piece left to settle and measured. Then again replaced, settled, measured. The results are shown in figure 8, with non-repeatability across all nine measurements never exceeding 0.5μm.
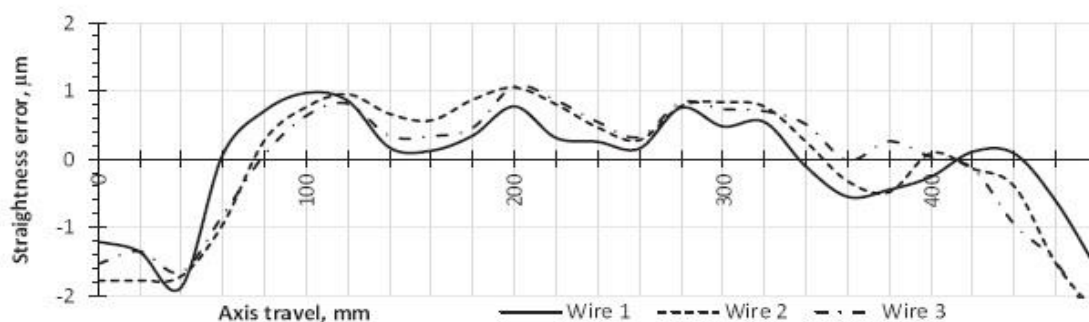
Figure 8. Wire repeatability within three pieces.

Figure 9 contains results of a single-sensor measurement of three wire pieces for comparison. It is clearly visible that without error cancellation the taut wire is poor as a straightness reference giving a non-repeatability of up to 4μm and no obvious common profile which can not be obtained by averaging.

8

Figure 9. Wire repeatability within three pieces (single-sensor test).

Figure 10 confirms a good correlation to within 1µm between averaged laser and average of three wires measurement results. Taking into account a very low value of measured error and fundamenal differences between measuring methods, certain output discrepancy should be considered normal.
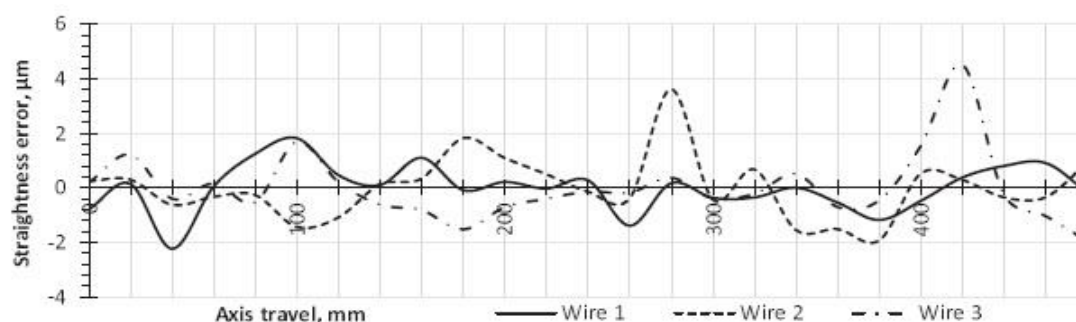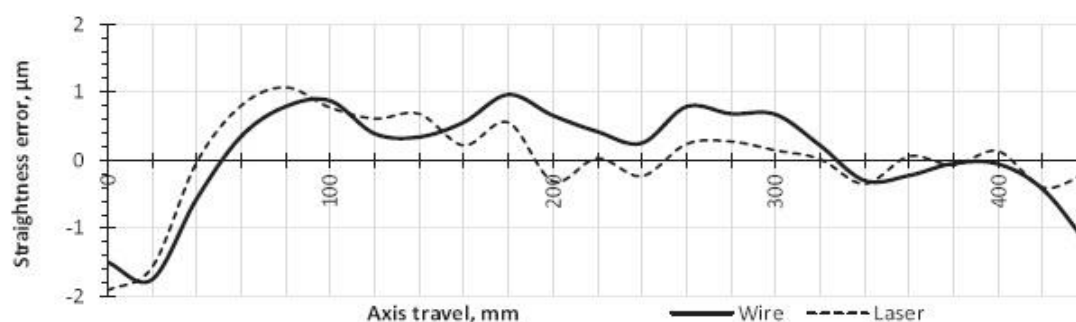

Figure 10. Wire against the laser.

To find out the actual measurement capability of both methods in terms of random error, idle mode (the machine is nominally stationary) tests were carried out. The laser was set to long term averaging mode, all tests were sequential, with a few minutes time between them, all in normal workshop conditions including airflow and vibrations. The results, shown in figures 11 and 12 demonstrate one order of magnitude difference. The stability of the wire setup output is significantly higher than that of laser at less than 0.1µm over the duration representing typical measurement tests. This is particularly important because the test was done under representative manufacturing conditions including working machinery in close proximity, airflow from people moving around, temperature gradients, vibration, dust and dirt. Two positions of the reader head were tested for stability; the middle of the wire and close to the end where the wire is mounted. No noticeable difference was detected.

Figure 11. Laser interferometer idle stability.

9

Figure 12. Wire idle stability.

It is important to note that figure 12 contains the accumulated error of almost a hundred sequential readings yet maintains excellent stability. Overall, the proposed system appears to be highly resistant to environmental effects, which gives reason to expect good results from measuring longer axes.
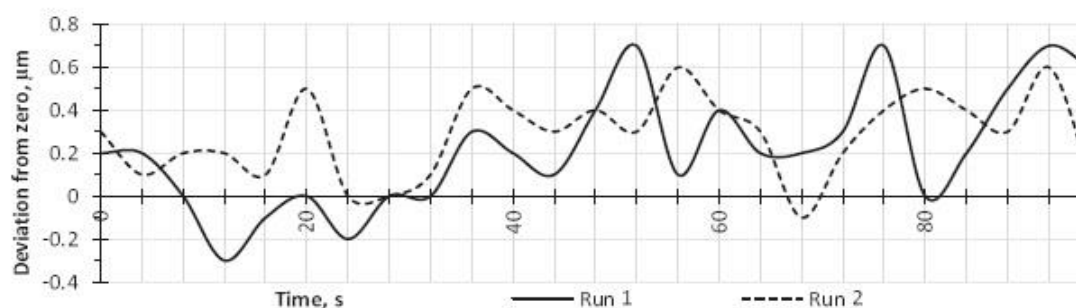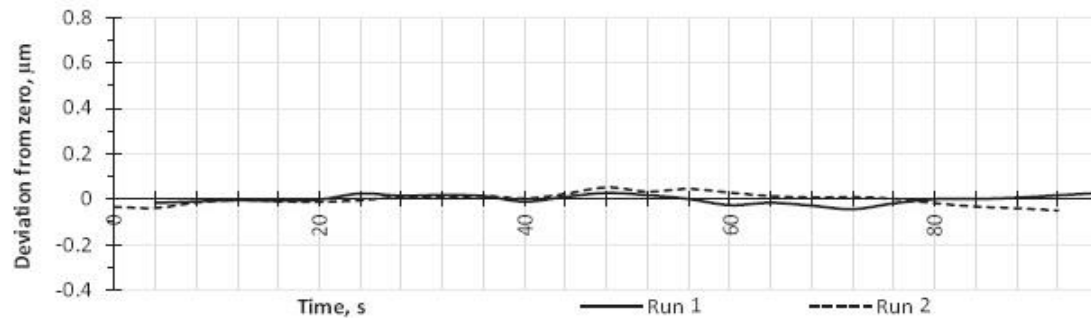
6. Conclusions

A novel straightness measuring system comprising ultra-low cost optical sensor unit, taut wire (with fine adjustment carriages) and error cancellation technique is proposed. The system is capable of eliminating the inherent random wire error and demonstrates similar accuracy level of ±0.25µm compared to a conventional laser interferometer and superior repeatability over a measuring range of 0.48m. A quick and simple wire setup allows measurement of an axis in any position and in principle, both coordinate planes at once. The method has been successfully tested over a 0.48m distance which validates the newly designed sensing unit and methodology. In contrast to the laser interferometry method, the wire setup does not become more difficult with the distance as sensitivity of reference adjustment does not change. Practically it can mean a considerable difference in set-up time increasing with the length of measured axis. In this case the system can be used as a supplement to laser interferometer, increasing the efficiency of its industrial application. Experimental results presented confirm that the output does not depend on actual wire superficial straightness or variation in diameter after its error is eliminated using the double sensor measurement method. Finally, the result is shown to be stable and accurate, providing an excellent opportunity of reducing the time and cost of straightness measurements.

The aforementioned low cost nature of the solution also makes it a candidate for permanent installation either as a live sensor on a structure or available locally for efficient normal or quick check axis measurement to feed into SPC. Further development will concentrate on longer axes measurement and on adding a second set of sensors for simultaneous capture of straightness profiles in two planes decreasing test time without any appreciable increase of associated costs.

7. Acknowledgements

8. References

[1] Schwenke H, Knapp W, Haitjema H, Weckenmann A, Schmitt R and Delbressine F 2008 Geometric error measurement and compensation of machines - An update *Ann. CIRP – Manuf. Technol.* **57** Issue 2 660-75.

[2] *ISO 230-1:1996, Test Code for Machine Tools. Part 1.* Geometric Accuracy of Machines Operating Under No-Load or Finishing Conditions *ISO Geneva*

[3] Pahk H J, Park J S and Yeo I 1997 Development of straightness measurement technique using the profile matching method, *Int. J. of Mach. Tools and Manuf.* **37** Issue 2 135-47.

[4] Greve J W and Wilson F W 1967 Handbook of Industrial Metrology, Printice-Hall, Inc, New York.

[5] Weck M M 1980 Geometric and kinematic errors, *Technol. Machine Tools* **5** 9–12.

[6] Hickman P A 1968 Optical tilting viewed in a new light, *Laser Focus* **4** (5) 22.

10

[7]   Hermannsfeldt A B et al. 1968 Precision alignment using a system of large rectangular Fresnel lenses, A□l. O□tics **7** 995.

[8]   Fan K C and Zhao Y 2000 A laser straightness measurement system using optical fiber and modulation techniques *Int. J. of Mach. Tools and Manuf.* **40** Issue 14 2073-81.

[9]   Lin S-T 2001 A laser interferometer for measuring straightness *O□t. □ Laser Technol.* **33** Issue 3 195-9.

[10]   Feng Q, Zhang B and Kuang C 2004 A straightness measurement system using a single-mode fiber-coupled laser module *O□t. □ Laser Technol.* **36** Issue 4 279-83.

[11]   Kuang C, Feng Q, Zhang B, Liu B, Chen S and Zhang Z 2005 A four-degree-of-freedom laser measurement system (FDMS) using a single-mode fiber-coupled laser module *Sensors and Actuators A□l. Ph□s.* **125** Issue 1 100-108.

[12]   Zhu L-J, Li L, Liu J-H and Zhang Z-H 2009 A method for measuring the guideway straightness error based on polarized interference principle *Int. J. of Mach. Tools and Manuf.* **49** Issues 3-4 285-90.

[13]   Chen Q, Lin D, Wu J, Yan J and Yin C 2005 Straightness/coaxiality measurement system with transverse Zeeman dual-frequency laser *Meas. Sci. Technol.* **16** 2030-37.

[14]   Estler W T, Edmundson K L, Peggs G N and Parker D H 2002 Large-Scale Metrology - An Update, *Ann. CIRP − Manuf. Technol.* **51** Issue 2 587-609.

[15]   Salsbury J G and Hocken R J 2002 Taut wire straightedge reversal artefact *Init. of Precision □n□ineerin□at the □e□Innin□of a Millenniu□* III 644-8.

[16]   Microplan   Group: Wire   laser   alignment   system.   http://www.microplan-group.com/mpg/ENG/laser.html Accessed 7 December 2012.

[17]   Tozawa K, Sato H, Komazaki M and O-Hori M 1979 Correlation of the Straightness of Machine Tool with Machined Accuracy *Pre□ JSM□*790-17.

[18]   Tanaka L, Tozawa K, Sato H, O-hori M, Sekiguchi H and Taniguchi N 1981 Application of a new straightness measurement method to large machine tool *Ann. CIRP* **30**(1) 455-9.

[19]   Tozawa K, Sato H and O-Hori M 1982 A new method for the measurement of the straightness of machine tools and machined work *J. Trans. ASM□Mech □esi□n* **104** 587-92.

[20]   Tanaka H and Sato H 1986 Extensive analysis and development of straightness measurement by sequential-two-points method *Trans ASM□J. □n□ Ind.* **108** 176-82.

[21]   Gao W, Yokoyama J, Kiyono K. Straightness measurement of cylinder by multi-probe method. *Precision □n□*2002; **28(3)**: 279-89.

[22]   Elster C,Weingartner I. Coupled distance sensor systems for high-accuracy topography measurement. *Precision □n□*2006; **30(1)**: 32-8.

[23]   Liu S, Watanabe K, Chen X, Takahashi S, Takamasu K. Profile measurement of a wide-area resist surface using a multi-ball cantilever system. *Precision □n□*2009; **33**: 50-5.

11

2014-06 Performance evaluation of a new taut wire system for straightness measurement of machine tools.

Performance evaluation of a new taut wire system for straightness measurement of machine tools

CrossMark

Oleg Borisov[*], Simon Fletcher[1], Andrew Longstaff[1], Alan Myers[2]

Centre for Precision Technologies, TC/10 CPT Research Office, University of Huddersfield, Queensgate, Huddersfield, West Yorkshire HD1 3DH, United Kingdom

ARTICLE INFO

ABSTRACT

This paper describes evaluation of a method of measuring the straightness of motion of machine tool axes using a taut wire and an optical sensor head mounted at the tool point location. In contrast to commonly used taut wire instruments, straightedges or laser-based methods, this solution combines low cost, simplicity of setup and automated data capture while achieving state of the art accuracy suitable for application on precision machine tools. A series of tests are discussed which examine the performance of the new sensing head and different wires which highlight the suitability of the taut wire properties as a straightness reference. Experimental results obtained on a production machine tool are provided with respect to the accuracy and repeatability of both the proposed taut wire system and a laser interferometer operated under the same conditions. The reference errors of wires made of different materials are compared and the wire catenary is separated from the measurement results. The uncertainty budget for taut wire and laser systems is presented and expanded uncertainty of 4 μm obtained for both. During the experiment, the method showed excellent repeatability with two standard deviations of 1.5 μm over a measuring range of 1.5 m; this performance matches that of a commercial laser interferometer-based straightness reference to within 0.1 μm.

1. Introduction

Straightness errors, along with positioning and angular errors, are present in every linear motion system [1]. According to the international standard ISO230 part 1 [2], the straightness of a moving stage can be determined by measuring lateral displacements of the stage while it moves. In order to do this, a straightness reference and a displacement indicator are required. In practice, this gives rise to a variety of straightness methods utilizing straightedges, taut wires or laser interferometers. Each method has its own advantages and disadvantages depending on such factors as required accuracy, measuring range, ease of use, speed and cost.

Straightness measuring methods using a straightness reference intrinsically depend on the straightness of the reference and how this changes under different measuring conditions. While the effects of support, temperature variation, vibration, etc. must all be taken into consideration, the effects are generally exacerbated by increase in axial range. This is particularly important since every

machine tool has moving axes and those machines with long axes, required to increase the machine tool's functional capability, are often susceptible to higher levels of errors. Thus, the error needs to be measured over longer distances where straightness-measuring solutions become less accurate.

The reason for such a dependency is the physical contradiction between different requirements of the straightness reference: it must be long, stable and straight, ideally two-dimensional and, which is particularly important, capable of being placed at any area of the machine's workspace to represent the desired tool point path. Finding such an artefact presents a significant challenge that ultimately leads to a compromise between the factors. At present, material artefacts like straightedges or optical devices (mostly lasers) are used to create a reference line from a solid structure or a light beam against which the axis straightness should be measured.

Being simple and easy to use straightedges are limited by their own dimensions, allowing measurements within their lengths only. Partial overlapping introduced by Pahk et al. [3] extends the potential measuring range but the speed of process, accuracy and uncertainty of measurement can be compromised by the size and quantity of overlaps.

Another approach utilizes laser-based techniques relying on a highly coherent light beam, having long axial ranges suitable for most machine tools and a high quoted level of accuracy. The Renishaw XL-80, a popular measurement instrument, has a stated

* Corresponding author. Tel.: +44 01484 472413.
  E-mail addresses: briarmains@gmail.com, o.borisov@hud.ac.uk (O. Borisov), s.fletcher@hud.ac.uk (S. Fletcher), a.p.longstaff@hud.ac.uk (A. Longstaff), a.myers@hud.ac.uk (A. Myers).
  [1] Tel.: +44 01484 472413.
  [2] Tel.: +44 01484 473660.

accuracy for measurement of straightness on short (up to 4 m) axes of ±0.5% ±0.5 ±0.15M^2 µm (where M= measured distance in metres). The accuracy decreases to ±2.5% ±5 ±0.015M^2 µm when using long range optics over lengths exceeding 4 m. This is because the angle of the reflecting optic, called a Wollaston prism, is smaller for the long-range kit, making the system more sensitive to inhomogeneity of the air. Estler et al. [4] in their review of long range measurements showed that the beam unpredictably bends while passing through the air. Magalini and Vetturi [5] carried out experiments which also demonstrated a high level of uncertainty due to the environment, using a Hewlett Packard laser interferometer. Measuring the straightness of a centre lathe axis, they calculated an uncertainty of 4 µm rising up to 16 µm (calculated on the basis of a 95% confidence interval) over 8.5 m when laboratory conditions are changed to a productive department. Comparing a precision level and taut wire microscope combination with an HP5519A laser interferometer, the authors concluded that laser interferometry did not enable lower uncertainties than that caused by the first two methods.

Other optical methods not employing interferometry have also been developed, aiming to address the issues of cost, speed and environmental effects. Most of them concentrate on consideration of cost and simplicity of setup. Fan and Zhao [6] used a different layout of the measurement system where the laser beam emitted at one end of the measured axis faces a four quadrant photo detector instead of a mirror. That principle halved the beam length compared to conventional interferometers and was found to have an accuracy of 0.3 µm within a ±100 µm measuring range and 0.5 µm repeatability on 100 mm axial range. While not setting a new level of accuracy, the method is potentially lower in cost since it does not require any matched optics (prisms, reflectors).

Lin [7] integrated a double straightness reflector, Wollaston prism and a traditional reflected layout to achieve repeatability of 1 µm over the range of 200 mm. The same reflected layout but with a single-mode fibre-coupled laser was tested by Feng et al. [8] and Kuang et al. [9]. In that case a longer axis of 1.35 m is measured against a dual frequency laser interferometer with the result of matching to within a few micrometres for a straightness error having a magnitude of 160 µm.

Chen et al. [10] combined a dual-frequency laser with two Wollaston prisms, aiming to compensate air disturbances on the range of 16 m in laboratory conditions. The system was stated to provide a high measurement stability of 3.6 µm while the actual comparison test result did not show a value lower than 20 µm. Also, it was admitted that the two alternative methods have very large uncertainty making it difficult to quantify the accuracy of the proposed system.

The aforementioned approaches successfully reduce the effect of environmental stability of the laser beam but do not eliminate it completely and in some cases require optical arrangements that may not be practical or economical. The stability remains proportional to the propagation distance as it has been proved by Magalini and Vetturi [5]. Alternative straightness references do exist and in particular physical references are successfully applied, using reversal techniques to improve accuracy, but these are generally limited in their measuring range.

In this paper, a taut wire and specially designed sensing head is proposed as an effective solution. The combination of the wire's availability, flexibility, lightweight and proximity to two-dimensional structure gives an excellent example of a physical straight line. As it will be shown, diameter inconsistency and gravitational sag of the wire, affecting its own straightness, do not significantly change its reference property because the former is shown not to be significant and does not increase with wire length, and the latter can be predicted and compensated at the calculation stage. The findings in this paper are considered novel because,
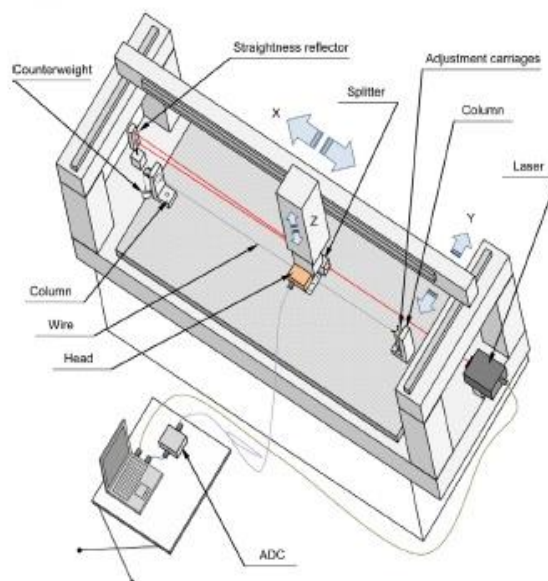

Fig. 1. Taut wire system and laser interferometer used for evaluation setup on the machine.

despite being a well-known reference for measuring straightness [1,4,11], a detailed analysis of the taut wire measurement for long-range measurement has not been the subject of published research.

2. Method

This paper describes performance evaluation of a sensor head [12] applied to the measurement of 1.5 m long machine tool axis. The main attention paid to the effects of measuring length, dynamics of the machine and overall uncertainty budgeting.

The system includes taut wire mounted on two vertical stands along the measured axis (Fig. 1). One end of the wire is fixed on the first column while the other end is passed through a hole on the second column, over a wheel and attached to a freely suspended counterweight which provides a constant stretching force. The moving stage has the measuring head attached to it so that the wire passes through its optical sensors capturing lateral displacements of the head at every point of axis travel. The signals from the sensors are fed into an analogue to digital converter where they are transformed into straightness measurement data.

The measuring head (Fig. 2) has four sensors, two each in the vertical and horizontal orientations. The vertical sensors provide data for the straightness measurement while one horizontal sensor enables fine positioning of the head relative to the wire for slope error removal. In case of measuring straightness in horizontal plane, signal from one of the vertical sensors provides positioning data and combined signal from horizontally orientated sensors – measured error.

Precise alignment of the wire and the axis can be achieved through manual operation of fine adjustment carriages attached to the right column. Adjustment is only required at one end of the wire, making the process very simple and efficient.

Apart from sensors, the head carries electronic circuits for powering the sensors and regulation unit with four potentiometers for fine adjustment of sensor sensitivity. Everything is mounted on an angled plate which can be attached to the moving carriage or a spindle either directly or using a magnetic base. The assembly plate holds a plastic cover with slotted holes to allow the wire to pass
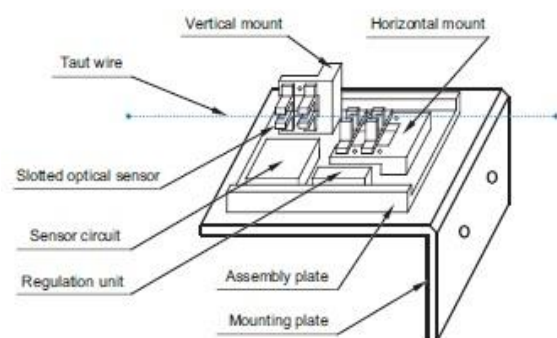
Fig. 2. Measuring head without cover.

through it. The cover is important because it protects the components and also blocks ambient light that can affect the sensors.

The basic principle of device operation consists of light beam emitted and received within each sensor. When the wire enters the working area of each, it reduces the amount of light received which changes electric output of the sensor. This change is monitored in real time, transformed into digital form and converted to micrometres of lateral displacement of the head relative to the wire fixed on the machine table.

3. Test setup

The system was set up on a 5-axis milling machine to measure the straightness of its longest horizontal axis in the vertical plane. Both wire support columns were mounted on the machine's table with a distance of 2.2 m between them. The counterweight was chosen so that the stretching force was as close to the maximum the wire could withstand according to its specification, ensuring the wire remained as stable and straight as possible. The sensor head was mounted on the spindle carrier together with optical splitter from Renishaw XL-80 laser interferometer kit, both representing desired tool point location. The laser itself was set up at a position to measure the same axis without any movement of the machine except along the measured axis. The separation between the laser beam and the wire was approximately 100 mm.

The catenary, or sagging of the wire, becomes significant on vertical measurements on horizontal axes when a distance between the wire mounting points is 1.5 m or greater, resulting in 1–2 μm of systematic error. This effect can be estimated as a parabolic [13] deflection depending on the tension, wire weight and length (Fig. 3). It was automatically subtracted from the measurement data. The associated uncertainty in is provided in Section 6.

4. Test conditions

The machine is located in a workshop having no special environmental control and is therefore susceptible to the usual airflow, temperature gradients, etc. caused by open workshop doors (the doors of the machine itself were shut), neighbouring working machinery, operators moving around, etc.

Both measurement systems were left idle for 20 min to complete the warm up stabilization stage. Bi-directional tests were performed at least three times to reduce the effects of random error sources. Axis movement speed was set to 5 mm s^{-1} for all measurement runs. Each measurement was taken with the machine nominally stationary at a discrete step of 20 mm. The laser was set to long term averaging mode (rolling average with 4 second window); the wire system output had a two sample rolling average applied.

The progressive slope, common to straightness measurements due to misalignment of the straightedge with the axis under test was always reduced to less than 3 μm and therefore did not affect the measurement. In the case of the taut wire, this slope was minimized in both planes. The wire chosen was DAIWA Sensor Monofil 0.26 mm diameter which is a high quality fishing wire and was found by experimentation to be most suitable for measurement purposes.

Fig. 4 shows some measurement results for different wire materials. Variation in the material used and the manufacturing process for metallic wires introduces different reference errors. However, the specified type of fishing wire was found to perform repeatably without strict limitation of size and quality.

5. Performance evaluation

The X-axis of the 5-axis machine tool used for evaluation had horizontal (EYX) and vertical (EZX) straightness errors of 4 μm and 5 μm respectively over a 1.5 m travel range, as measured using a Renishaw XL-80 laser system. The first test aimed to ensure the taut-wire system does not suffer from any "crosstalk" effect which could be the case when using the optical sensors. Two EYX measurements were completed with different misalignment (slope error) of 150 μm and 5 μm in the vertical direction. The result, presented in Fig. 5, shows a very low effect on measured straightness.

The next step was to measure the axis with the same laser interferometer and short range straightness optics to determine the repeatability in such strict conditions of low straightness error, low slope error (which could affect the interferometer) and 1.5 m axis. Six tests were performed sequentially (Fig. 6).

Analysis of the result obtained from the laser had a calculated spread of two standard deviations of better than 2 μm in optimal test conditions. In order to reduce the random influences,

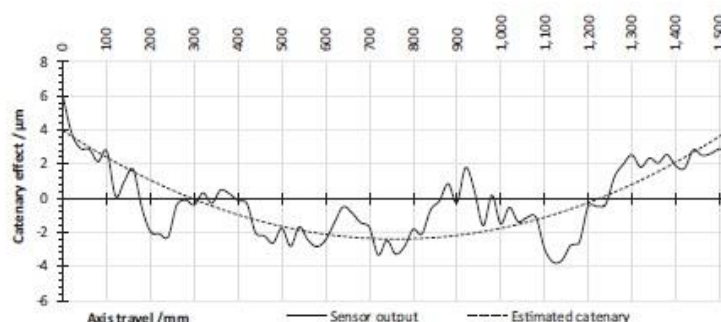Fig. 3. Estimated catenary effect caused by gravity.

495
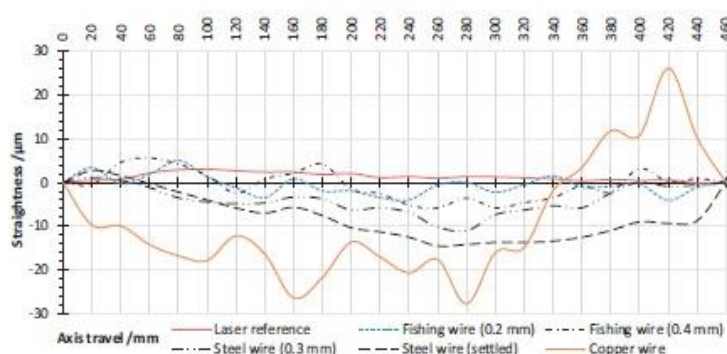
Fig. 4. Test of different wires.
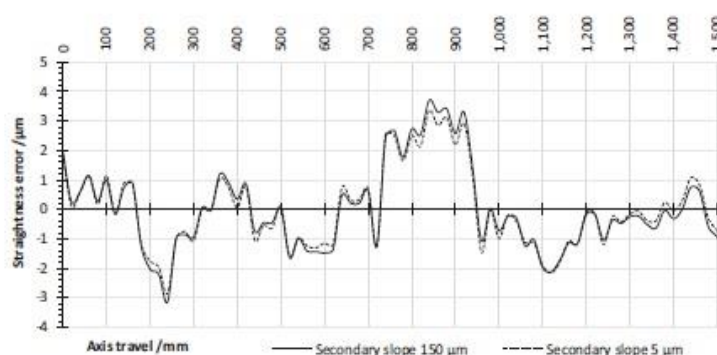
Fig. 5. Vertical straightness error dependency on horizontal error of the same axis using the wire.

averaging of multiple runs was required to get the best reference data against which the new sensor could be compared. This took additional time during which the thermal distortion of the machine could begin to have an effect. The machine's repeatability can be visually estimated from Fig. 7 (combined with the repeatability of the wire) and is considerably higher than the one of the laser setup.

Considering the taut wire system, the repeatability is affected by the systematic error of the reference (installed wire piece). Fig. 8 illustrates the difference between different pieces of the same type of wire. In this case straightness references are different but their results still close to each other. However, this is the largest contribution to measurement uncertainty for the system as described in Section 6. Due to the efficiency of the system, it is feasible to complete additional tests to enable averaging of the results from different wire pieces for wire error reduction.

As suggested, an average of these three different pieces of wire was used to provide the measurement shown in Fig. 9 for comparison with the average from the laser system. There is a good correlation in magnitude and shape, confirming that the systematic error of the wire is either significantly lower than the measured error or/and can be reduced by increasing the number of measurements.

In addition to standard measuring tests, static tests were also carried out to confirm the stability of both measurement methods independently of the machine. This eliminated any variability introduced by the machine's drives and axes to isolate the stability
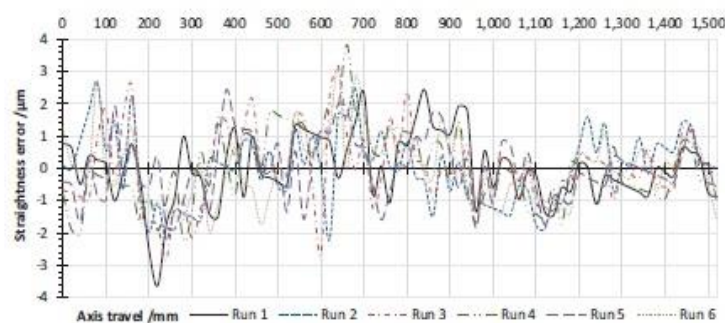
Fig. 6. Straightness error measured six times using the laser.
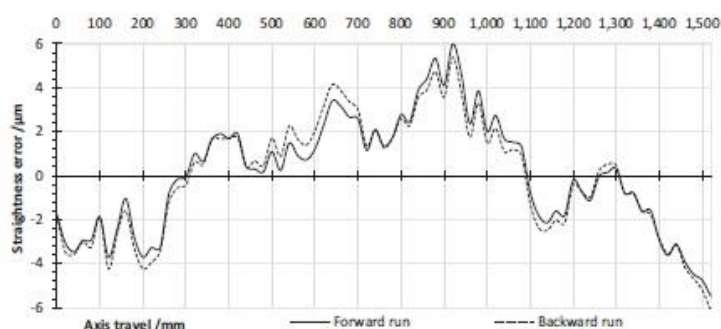
Fig. 7. Combined repeatability of the machine and the wire system.
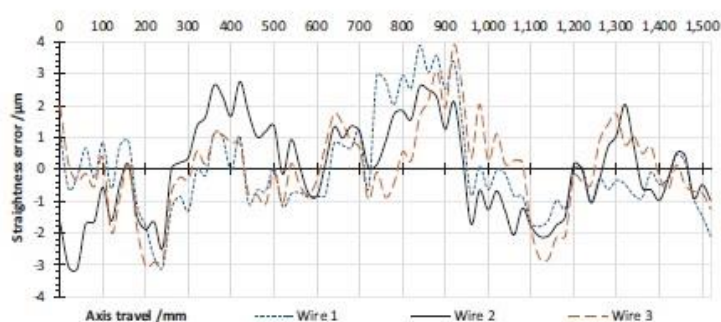
Fig. 8. Straightness error measured several times using different wire pieces.
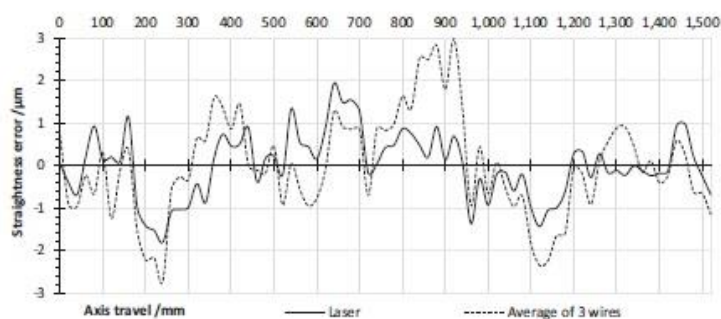
Fig. 9. Straightness error measured using the laser and the taut wire.

of each method in typical environmental conditions with respect to axial range. ISO230 part 1, section 6.3.3 [2] recommends that the sampled data should not exceed 10% of the tolerance of the specified test.

According to the same standard laser interferometer and optical sensor head were positioned in the middle of the normal axis travel range; this is theoretically the least stable position along the taut wire. Readings were taken every four seconds during a five-minute interval, similar to the capture pattern for the pseudo-static test described above. Each sample was subject to the averaging methods used for the other tests.

Fig. 10 shows more than one order of magnitude difference in output stability between both methods (standard deviations 0.43 μm and 0.04 μm, respectively). This suggests the combination of taut wire and non-contact optical measuring system is suitable for typical machine axis measurement.

6. Uncertainty analysis

Measurement uncertainty U was determined according to the method presented in the technical report ISO230 Part 9 [14], using basic equations applied to uncertainty budget contributors listed in Table 1. The conditions included a 1.5 m axis, measured for straightness in vertical plane over a 15-minute period using the wire specified earlier (Section 4). All contributors were deemed to be uncorrelated. Their distribution was assumed rectangular because no specific knowledge of them is available and therefore possible overestimation of corresponding uncertainties was considered reasonable. Standard uncertainty of each contributing component was given as:

$$u_i = \frac{a^+ - a^-}{2\sqrt{3}} \tag{1}$$

497
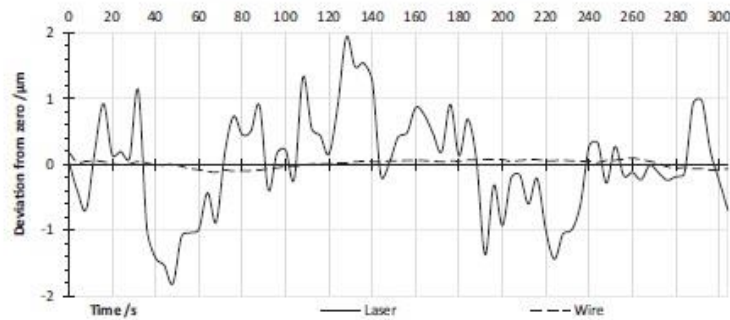
Fig. 10. Static stability of the laser and the taut wire.

where a^- and a^+ are lower and upper limits of distribution, respectively. Combined uncertainty u_c was derived as a sum of its contributors:

$$u_c = \sqrt{\sum u_i^2} \qquad (2)$$

And with coverage factor k, derived from total degrees of freedom, expanded measurement uncertainty U was calculated as:

$$U = k \cdot u_c \qquad (3)$$

The table above describes factors contributing towards measurement uncertainty. The first three represent angular deviations of the axis during its linear motion. These were measured by tilting the spindle and then separating the vertical lateral displacement from the measured value. It was necessary to quantify the sensitivity of the measuring system to the unwanted rotational movements of the axis during the test runs. All three effects change the position of the wire within the optical sensor slightly moving it forward/backwards (pitch and yaw) or left/right (roll). Horizontal alignment is the uncertainty due to slope in the corresponding plane (Fig. 5). The wire catenary estimation has an error due to wire length (2.2 m between stands) and weight measurement. Electronic noise together with drift as measured while the axis was stopped at its end, minimizing the effect of wire movement. The next two parameters characterize properties of the wire, measured during idle tests. The sensor calibration error represents sensor non-linearity approximation during system calibration when the axis moves known intervals incrementally in a vertical direction.

Sensitivity coefficients were obtained from the combined sensitivity value of the optical sensors, which was 16 mV/μm. Degrees of freedom were estimated as the number of repeated measurements (n–4) less one.

The total value of degrees of freedom was derived using a Welch–Satterthwaite equation:

$$\upsilon = \frac{\left(\sum u_i^2/n_i\right)^2}{\sum (1/(n_i-1))(u_i^2/n_i)^2} \qquad (4)$$

This gives $\upsilon = 3.41$ which corresponds to coverage factor $k = 3.31$. The resulting $U_{wire} = 4$ μm could not be compared directly with the accuracy specification of a Renishaw XL-80 laser interferometer, which is 0.86 μm. Knapp in his paper [15] provides an uncertainty budget for laser interferometer, the same contributors were calculated to obtain combined uncertainty for our laser system (Table 2).

This gives $U_{laser} = 4$ μm which is somewhat lower than the value quoted by Knapp (6 μm) and is similar to the wire system result mentioned above. The actual results obtained on the machine (Figs. 6 and 8) have two standard deviations of 1.5 μm for both the laser and taut wire systems. This confirms good performance correlation between both systems.

Table 1
Uncertainty budget for straightness measurement using taut wire system.

Contributor	Average value	Unit	Sensitivity coefficient	Effect, μm		Uncertainty, μm	Degrees of freedom
				a^-	a^+	u	
Axis pitch	–	mV/deg	0.063	0.01	0.02	0.003	3
Axis roll	–	mV/deg	0.063	0.10	0.50	0.115	3
Axis yaw	–	mV/deg	0.063	0.15	0.80	0.188	3
Horizontal alignment	30	μm/m	0.01	0.20	0.60	0.115	3
Catenary estimation error	0.15	μm/m	2.2	0.2	0.4	0.058	3
Electric noise	1.26	mV	0.063	0.07	0.10	0.009	3
Electronic drift	0.7	mV/h	0.063	0.10	0.20	0.029	3
Wire profile variation	–	μm	1	1.00	5.00	1.155	3
Wire profile drift	1.7	μm/h	0.25	0.25	0.45	0.058	3
Sensor calibration error	–	μm	1	0.02	0.50	0.139	3

Table 2
Uncertainty budget for straightness measurement using laser interferometer.

Contributor	Average value	Unit	Sensitivity coefficient	Effect, μm		Uncertainty, μm	Degrees of freedom
				a^-	a^+	u	
Laser device	2.5	μm	1	0.50	4.50	1.155	3
Thermal drift	1.2	μm	1	1.00	1.40	0.115	3
Air disturbance	0.6	μm	1	0.50	0.70	0.058	3
Δ surface temperature	2	°C	0.4	0.40	1.20	0.231	3

As can be seen from Figs. 4 and 8, the main contributor to the taut wire system uncertainty was the unique profile of each piece of wire installed. Consequently, the straightness value depends on the quality of the wire, which normally does not exceed 4 μm and does not depend on wire length being limited by its diameter inconsistency. This allows high stability of the system installed on longer axes to be assumed despite environmental effects normally having a pre-emptive contribution to the uncertainty of other methods. As shown before (Figs. 8 and 9), taut wire system uncertainty can be further decreased by the averaging of different wire results in the same conditions at the expense of additional time spent on wire reinstallation and repeated measurement runs.

7. Conclusions

The performance of a new measuring system has been evaluated for measurement of machine tool axis straightness. It is based on an existing taut wire reference, which has been implemented using new materials, precise optical sensors and new measurement methodology. The system was tested in real manufacturing workshop conditions and compared to a typical alternative commercial system, namely a laser interferometer system. The profile of the machine axis was reproduced by both systems with just 1 μm difference. A detailed analysis of factors affecting measurement uncertainty has been performed with an expanded uncertainty of 4 μm and good correlation between both systems. Additionally, statistical analysis on various data sets showed two standard deviations of 1.5 μm.

Stability and repeatability were tested with respect to the measured axis length. Experiments proved excellent stability of the taut wire and optical sensor head when compared to the interferometer system during typical measurement durations. This shows the high potential of the method in terms of stability.

The first practical advantage of the taut wire system is its suitability for long range measurements. Environmental effects have very little random influence with correct tension in the wire, while systematic error due to wire diameter inconsistency is not significant and was not found to depend on the length of the wire and therefore on the length of the axis being measured. According to six different wires tested, DAIWA Sensor fishing wire is considered to be the most suitable for straightness measurement. The catenary effects on the wire can be calculated and removed from the systematic error by subtraction of a parabolic curve.

From these results, the system developed is shown to provide an efficient solution for measuring axes up to 1.5 m. Due to the characteristics, it is anticipated that advantages in stability will benefit longer axes as well where the performance of alternative methods degrades substantially.

Acknowledgement

References

[1] Schwenke H, Knapp W, Haitjema H, Weckenmann A, Schmitt R, Delbressine F. Geometric error measurement and compensation of machines – an update. Ann CIRP – Manuf Technol 2008;57(2):660–75.
[2] ISO 230-1:1996, Test Code for Machine Tools. Part 1. Geometric Accuracy of Machines Operating Under No-Load or Finishing Conditions ISO Geneva.
[3] Pahk HJ, Park JS, Yeo I. Development of straightness measurement technique using the profile matching method. Int J Mach Tools Manuf 1997;37(2):135–47.
[4] Estler WT, Edmundson KL, Peggs GN, Parker DH. Large-scale metrology – an update. Ann CIRP – Manuf Technol 2002;51(2):587–609.
[5] Magalini A, Vetturi D. Laser interferometry for straightness measurements in a weakly controlled environment. In: XVIII IMEKO world congress, metrology for a sustainable development. 2006.
[6] Fan KC, Zhao Y. A laser straightness measurement system using optical fiber and modulation techniques. Int J Mach Tools Manuf 2000;40(14):2073–81.
[7] Lin S-T. A laser interferometer for measuring straightness. Opt Laser Technol 2001;33(3):195–9.
[8] Feng Q, Zhang B, Kuang C. A straightness measurement system using a single-mode fiber-coupled laser module. Opt Laser Technol 2004;36(4):279–83.
[9] Kuang C, Feng Q, Zhang B, Liu B, Chen S, Zhang Z. A four-degree-of-freedom laser measurement system (FDMS) using a single-mode fiber-coupled laser module. Sens Actuators Appl Phys 2005;125(1):100–8.
[10] Chen Q, Lin D, Wu J, Yan J, Yin C. Straightness/coaxiality measurement system with transverse Zeeman dual-frequency laser. Meas Sci Technol 2005;16:2030–7.
[11] Salsbury JG, Hocken RJ. Taut wire straightedge reversal artefact. In: Init. of Precision Engineering at the Beginning of a Millennium III. 2002. p. 644–8.
[12] Borisov O, Fletcher S, Longstaff AP, Myers A. New low cost sensing head and taut wire method for automated straightness measurement of machine tool axes. Opt Lasers Eng 2013;51(8):978–85.
[13] Lockwood EH. Chapter 13: the tractrix and catenary. In: A book of curves. Cambridge: Cambridge University Press; 1961. p. 122.
[14] ISO 230-9:2005, Test Code for Machine Tools. Part 9. Estimation of measurement uncertainty for machine tool tests according to series ISO 230, basic equations ISO Geneva.
[15] Knapp W. Measurement uncertainty and machine tool testing. Ann CIRP – Manuf Technol 2002;51(1):459–62.

THERMAL RELATED PAPERS

2005-07 Compensation of Thermal Errors on a Small Vertical Milling Machine

Compensation of thermal errors on a small vertical milling machine

S. Fletcher, A.P. Longstaff and A. Myers
Centre for Precision Technologies, University of Huddersfield, UK

Abstract

It is well known that thermal distortions are a significant contributor to machine tool inaccuracy and compensation of thermal errors on CNC machine tools is becoming more popular with some machine tool builders incorporating temperature sensors on the machine at the build stage. Significant research in the field has produced a number of sophisticated techniques for modelling thermal errors from FE techniques to Neural Networks.

In this paper, new development based on a previously published [1] modelling technique is described with emphasis on new measurement methods and compensation implementation methodology. New software has been created to run in a popular modern windows based open architecture controller enabling low cost and efficient implementation of compensation for geometric and thermal errors.

The software exists in two levels, the first being a real-time part in the NC enabling fast compensation of rapidly changing errors such as geometric errors and position dependent thermal error. The second level is an advanced graphical user interface integrated into the existing controller interface facilitating improved human - machine interface and increased functionality.

This paper will concentrate on the thermal compensation part of the software with results presented for air cutting tests and cutting trials. The results show accuracy improvements of greater than 70% for position independent and position dependent thermal errors including compensation for environmental fluctuations.

1 Introduction

The accuracy of CNC machine tools is important in modern manufacturing industries where tolerances continually tighten. It is well known thermal distortions are a significant contributor to machine tool inaccuracy and compensation of thermal errors on CNC machine tools is being implemented by some machine tool builders. These systems are invariably controller based utilizing a few discrete temperature sensors incorporated on the machine at the build stage. The systems are usually specific to a machine or range of machines within the company.

The last decade has seen significant research into highly sophisticated compensation systems that effectively model the thermal errors. Some examples are given from three different authors [2, 3, 4, 5, 6] that have done significant work in the field for a number of years. The majority of these systems employ advanced models such as neural networks or regression analyses that require training to effectively predict the machine behaviour under various operating conditions and determine optimum positions of the temperature sensors. These are serious limitations for a system that is to be industrially applicable. Ramesh [4, 5] provides results showing the wide ranging errors associated with varying operational conditions and overcomes some of the training by using on machine inspection to continually update and retrain a neural network. Although this improves the model robustness, it does not retract from the complex nature of most of these systems either in terms of implementation or testing. This makes many of the systems to date impractical for industrial application.

Research at the University of Huddersfield has produced a flexible thermal compensation system [1, 7] that has been implemented on many machine tools including machines within manufacturing industry. This paper describes the error measurement and modelling methodology which includes techniques implemented to facilitate model development and improve model accuracy offline and thermal imaging is an important part of this process. Hardware modification for permanent application of temperature sensors can then be implemented with confidence, requiring fewer machine tests for final model parameter modification and model validation. And as stated previously, such savings in downtime are of paramount importance in most industrial situations.

2 Measurement

The majority of CNC machine tools have high speed rotating components such as spindles and therefore many internal heat sources. A basic study of the machine highlights where the major heat sources are and thermal imaging is used to facilitate this process by efficiently scanning the entire machine in its operating state. On the small Vertical Milling Machine (VMC) used for most of this work, the spindle motor and spindle bearings are the main internal heat sources associated with cutting. In addition rapid Y-axis movement (parallel to the head) causes heating of the ballscrew axial support bearing causing a scale offset error. This internally generated heat and changes in the environrment can cause significant errors between the toll and the workpiece.

Most error measurements are based on the ISO standard 230 part 3 which specifies methods of test for most thermal errors. Measurement for compensation however has different requirements often requiring variations to the tests to maximise the information that can be obtained. A variety of results are reported by Longstaff [8].

2.1 Temperature

Acquiring as much temperature information from the machine during the initial testing phase is critical for making efficient use of the machine availability.

2.1.1 Spindle running

Thermal imaging is very simple and rapid to set-up and is used extensively to record temperature of large surface areas at regular intervals, usually every minute during a measurement test. Figure 3-1 shows one image taken from a sequence of the headslide during a spindle heating phase.

It is important to measure the temperature of as many of the other structural elements as possible that may contribute to the error being measured to avoid repeating tests. Low cost, accurate and compact digital temperature sensors are used to measure those parts of the structure that cannot easily be thermally imaged or that are expected/shown to have small thermal gradients. This is the case with the column on this machine. 3 discrete sensors were surface mounted on each side of the column spanning its height and equally spaced. Because the sensors are digital, any number of sensors can communicate down a single communications wire, significantly reducing the number of wires required. This advantage is emphasised in section 3.

2.1.2 Axis running

Sensors were placed near the Y axis ballscrew axial constraint bearing attached to the bed to measure heat conducted into the bed. The support bearing at the other end of the ballscrew was also measured but this bearing only provides radial support and as expected did not generate any significant heat.

The nut is mounted on the underside of the Y axis and does not contribute to Y-axis error. Experience has shown however that all the heat generating components associated with the same motion component, in this case the Y-axis, will generate the same temperature profile (providing no other direct influence such as artificial cooling). Although the nut profile will have a much higher magnitude than the bearings and the bed, it can be used to get high resolution information that is more immune to external influence such as ambient temperature change. Two sensors were therefore surface mounted on the nut.

3 Model development

The model flexibility comes from a novel programming language that comprises calculations and functions dedicated to typical machine tool structural element distortions. A model definition system uses this language and defines the temperature sensors to be used, structure, distortions and finally the compensation values. This system is reported in detail by White [1, 9]. New

techniques and software have been created to facilitate model development and these are discussed in this section.

The flexibility of the model is further enhanced by the high density of digital temperatures sensors used on the machine enabling reliable and accurate calculations of complex structural distortions.

3.1 Spindle movement

A heating and cooling cycle is run during which we measure movement of the spindle and temperature of the structure. Figure 3-1 (a) shows the movement of the spindle relative to the workpiece during a two hour spindle heating and cooling cycle. A detailed study of the temperature distribution within the identified elements is achieved using discreet digital temperature sensors and thermal imaging, as shown in figure 3-1 (b).
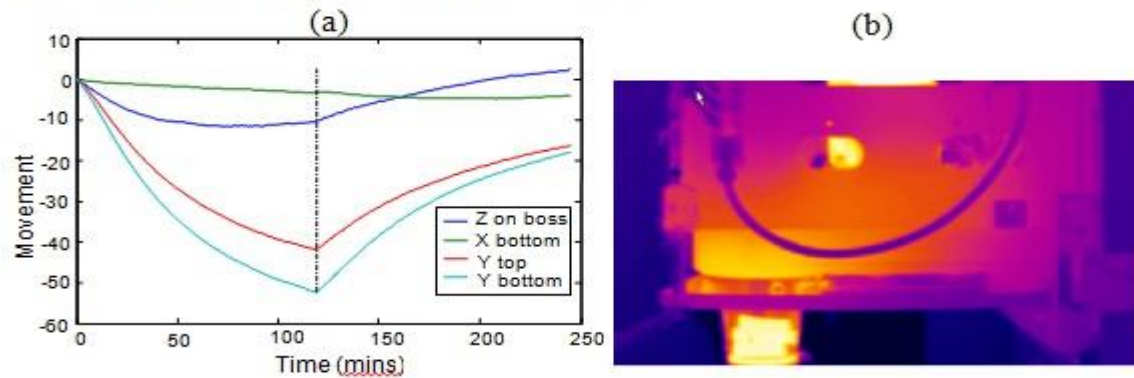
Figure 3-1. Spindle movement and thermal image of headslide

The thermal model is initially created using the basic mechanical design of the machine and the temperature gradients. At least two temperature sensing lines are required to determine the temperature gradients for calculation of distortion as well as expansion. Figure 3-2 shows the headslide errors.

Where:-

B_z, B_y = Z/Y error resulting from bending

E_f, E_x = Expansion of front and rear of the head

E_l = Expansion of the head

e_z, e_y = Z/Y error from head distortion

h_s = Sensor line distance

$e_z = E_f + B_z - E_r$

$e_y = E_l - B_y$

Figure 3-2. Headslide detail

Spacing between the lines needs to be sufficiently large to gain resolution in the calculation of angles and the lines need also to be located where the temperature gradients are prominent. Location of the lines may also be restricted by the physical design.

3.1.1 Model definition

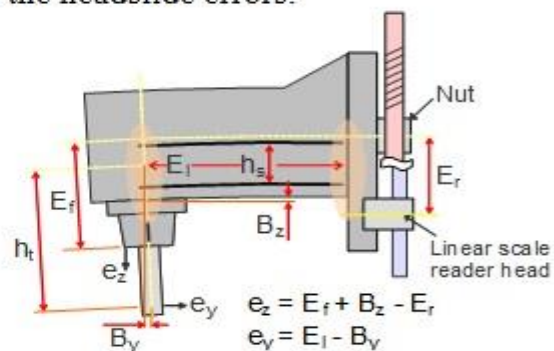Model definition is simplified through the use of a variety of functions that carry out specific calculations for typical structural element distortions. In this example we use the 'BEND' function to calculate the transverse distortion resulting from temperature gradients identified by the two lines of sensors [1].

$$B_z = BEND(999, \; l2\_s31, \; l1\_s31, \; 31, \; C_{L2}, \; C_{L1}, \; 15, \; h_s, \; E_{mat}, \; 0)$$

Where the 2nd, 3rd and 4th arguments specify the range of sensors previously defined in the model, C_{L2} and C_{L1} are correction parameters and E_{mat} is the expansion coefficient of the material. Correction values are applied to compensate for the inaccuracy of surface measurement so each sensor line or group of sensors will have one. The parameters should be within the bounds $1 =<$ $C_n <= 2$. Generally, if parameters are less than 1 or greater than two, it suggests that the fundamental model design or location of the temperature measurement is inadequate.

The final X, Y and Z compensation values are a combination expansions, distortions etc. For this Y axis model, which is the direction in which most thermal errors contribute, we get:

$$TotalY = headY + columnY - environmentY - offsetY - scaleY + workpieceY$$

This value is then used by VCS to modify the axis position. The workpiece entry is related to new work that is being undertaken to compensate for workpiece temperature variation with some initial results mentioned briefly in section 3.3.

3.1.2 Model simulation

Thermal image sequence information is used to produce virtual temperature sensing lines with, if required, high resolution. The software shown in Figure 3-3 extracts temperature from every image providing very detailed gradient information over time as shown in the graph on the right. This data is fed back into the thermal model which can be run in a Matlab based offline development environment. The environment simulates exactly the operation of the thermal model in VCS therefore the effectiveness of the initial model can be tested very easily and thoroughly using data similar to that which will be finally available on the machine. Different positions of the lines and even discrete sensors can be simulated and compensation results compared with the measured data.

The obvious advantage of the above methodology is that the temperature sensor placement can be optimised accurately through the use of very similar temperature data provided by the thermal image sequence. Thus the final hardware integration is more accurate. In addition, the virtual sensing lines can be tuned to a suitable resolution to indicate the sensor density of the strips being applied to the machine.
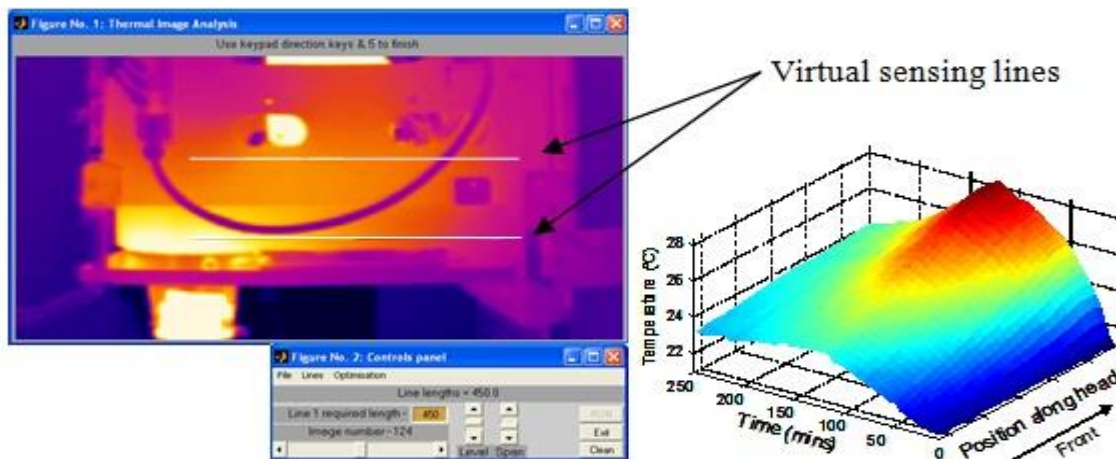
Figure 3-3. Temperature extraction from thermal imaging

3.1.3 Hardware installation

Permanent temperature measurement is usually achieved using unique temperature sensing strips as shown in Figure 3-4. The strips are physically flexible for modest surface undulations and have a low profile to fit under guarding or between structural elements etc. Strips can contain many sensors; in the case below each line has 30 individual sensors at 15mm intervals. As well as resolution, this provides redundancy, creating a more robust system for industrial applications. If a sensor reports a failure or a reading cannot be obtained, the specific sensor can be identified and the software then interpolates between the two adjacent sensors until a maximum failure limit is met. This density can be achieved because all the sensors communicate down the same wire.

If discrete or pairs of sensors are to be used then they are either surface mounted or embedded in the machine structure. The latter is preferred as the temperature readings are more accurate because they are less affected by the ambient temperature. The small size of the sensors also lends itself well to this type of application. Generally the sensors are very reliable and strips are designed such that they are protected from coolant, swarf etc.
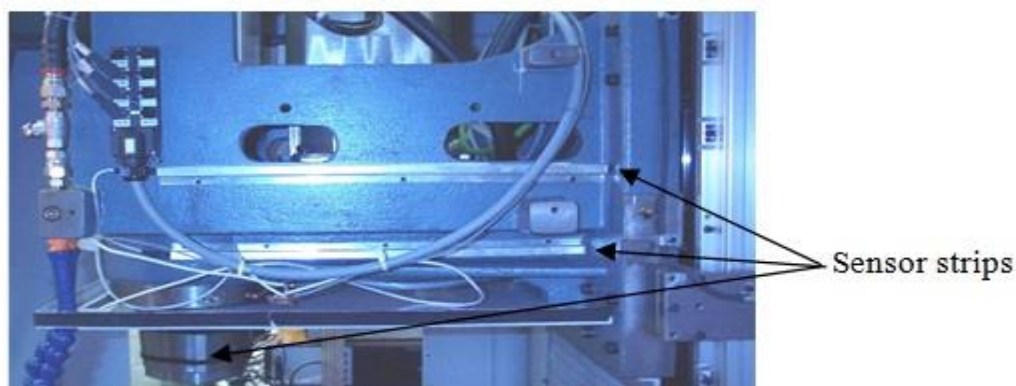

Figure 3-4. Application of sensor strips on the headslide

3.2 Axis heating

Figure 4-1 shows the PITE and PDTE associated with movement of the Y axis. The PDTE requires knowledge of the Y axis position and the temperature of the linear scale relative to a reference, usually 20°C. Special variables within the model are used to get the axis positions from the VCS system. The scale temperature is determined by measuring the air temperature close to the scale. The PITE results from internally generated heat as mentioned previously. The scale is fixed to the bed with a defined pinned position which is the thermal datum for the scale. The scale offset error is calculated using this position relative to the column, which is the reference for the head calculations in the same direction, and the temperature of the bed measured near the bearings.

3.3 Workpiece

Workpiece temperature compensation can only be achieved if its temperature and thermal datums are known. Controller based compensation as described in section 4 enables this information to be passed to the model. A predictable datum is determined by consideration of the clamping arrangement. The flexible model system allows a simple calculation to be performed using the available information similar to that shown below for the Y axis.

$$yWorkPos = PosnY/1000 - YWorkDatum$$
$$yWorkError = workTempAboveRef * yWorkPos * workCoeffExp$$

4 Software implementation

The VCS software can currently be applied either through a PC, through an Osai Series 10 controller and more recently through a Siemens 840D controller (SinVCS) and it is this version that has been used for applying the compensation shown in this paper. The controller based integrations have the important advantage of requiring no additional hardware except for temperature sensors. We can communicate with the sensors via a serial port which already exist on this, and most controllers. The simplified integration onto the machine significantly reduces machine downtime and improves robustness of the system.

4.1 SinVCS

The software exists in two levels, the first being a real-time part in the NC enabling fast compensation of rapidly changing errors such as geometric errors and position dependent thermal error. The second level is an advanced graphical user interface integrated into the existing controller interface facilitating improved human - machine interface and increased functionality. Longstaff [10] describes the system in more detail.

4.2 Thermal logging and model validation

Once the sensors are attached to the machine a random duty cycle is usually performed to show the effectiveness of the model under conditions different to

the initial testing. VCS enables logging of all the temperatures and any variables, specified in model for saving, to a file. The detailed model and real temperature information in the log file can be run through the offline simulation again and compared with new compensated error data. Results from manual tweaking (if required) of the model can be immediately tested offline. The software also enables automatic adjustment of correction factors using a least squares optimisation procedure using the difference between the model output and the measured data as the control element. Figure 4-1 shows the modelling results for the spindle heating (left graph) and the axis heating tests.
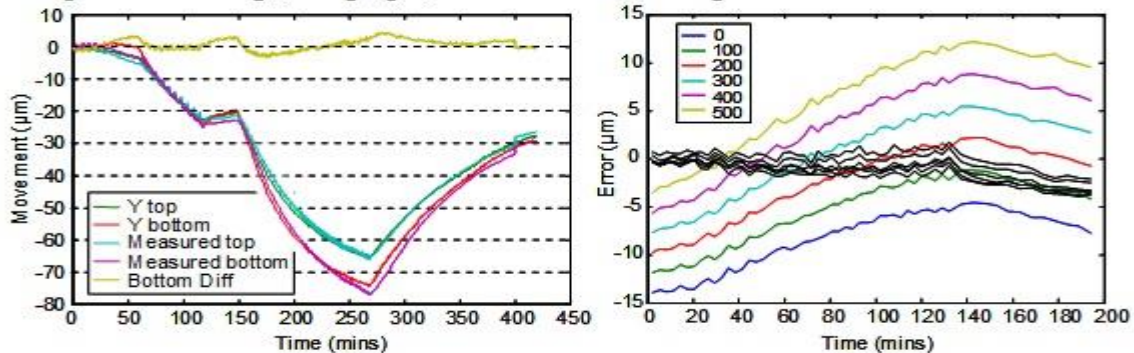

Figure 4-1. Y axis pre and post compensation results

5   Results

A number of additional validation tests extending the operating conditions of the machine and cutting trial were run with the results presented in this section.

5.1   Spindle movement

In order to further validate the compensation an extended random duty cycle spindle heating test was run which includes spindle speed variations and spindle stoppages. Figure 5-1 shows the uncompensated and compensated error in the Y and Z directions. Position independent thermal error in Y-axis direction reduced from $71\mu m$ to $7.5\mu m$ ($\approx 90\%$) and Z axis error reduced from 14 to 3.5 ($\approx 75\%$). This improvement would be seen in short-term machining operations or where the machine was in a temperature controlled environment.
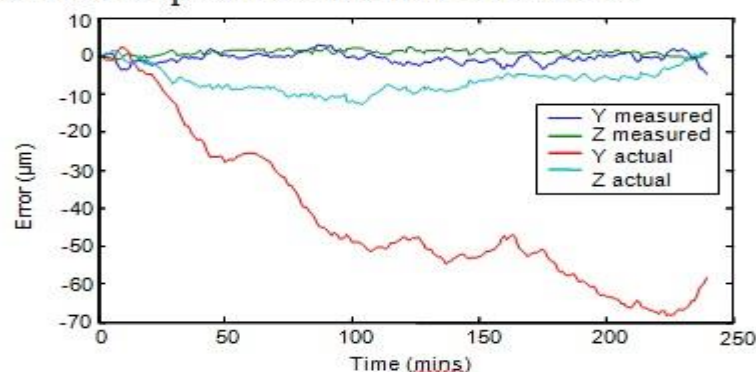

Figure 5-1. Compensation results for random spindle duty cycle

Monitoring the spindle movement over days rather than hours means that the daily cyclic environmental temperature fluctuations and associated errors will occur. Compensation results show a reduction in the magnitude of the errors by more than 50% to just ±7μm over a 65 hour test.

5.2 Axis heating

Two axis heating and cooling tests separated by an overnight cool-down were run without temperature control. Figure 5-2 shows Position Independent Thermal Error (PITE) reduction of approximately 60%. The span of the traces in the graph is the Position Dependent Thermal Error (PDTE) and this has been reduced by 65%. Variation in PDTE was reduced by approximately 75%.
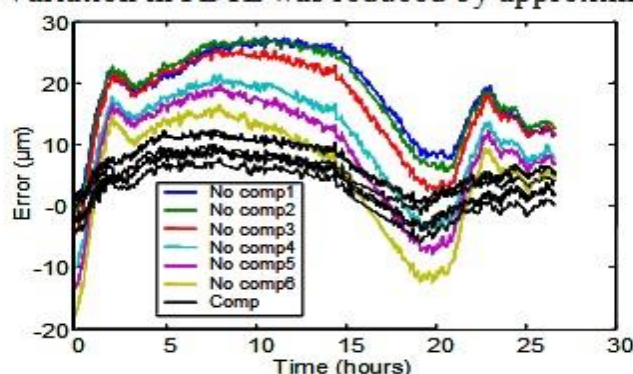

Figure 5-2. Y axis heating test compensation results

5.3 Workpiece cutting and results

In order to validate the performance of the compensation system under cutting conditions, three NAS 979 circle-diamond-square aluminium test pieces have been machined 1) Uncompensated, 2) Geometric compensation, and 3) Geometric and thermal compensation. After manufacture, the test pieces were measured on a CMM in a temperature controlled environment. The errors for some representative dimensions showed that compensation has been very successful. The average geometric improvement is approximately 30% and the average improvement resulting from thermal and geometric compensation is approximately 94%. These significant improvements in accuracy can be expected when machining occurs with the workpiece at a different temperature to that of the linear scale (or ballscrew if rotary encoder feedback is being used). This situation is often the case when a temperature controlled environment is not used and without strict control of the temperature of the coolant.

6 Conclusions

Temperature measurement using thermal imaging and offline model development techniques have been implemented to reduce machine downtime and improve model accuracy before application of hardware on the machine.

Compensation for the main sources of thermal error on a small vertical milling machine has been successfully implemented through a modern open architecture controller, namely a Siemens 840D controller. The main errors

include PITE in the Y and Z directions caused by both internally generated heat and environmental temperature change, and PDTE caused by column bending and temperature variation between the linear scale and workpiece.

The typical magnitude of error reduction can be seen in the bar chart shown in figure 6-1. The average percentage reduction is 70% and the greatest 90% for Y axis error caused by internal heat generated from a random duty heating and cooling cycle. The error was reduced from 71μm to 7.5μm over a 4 hour period.

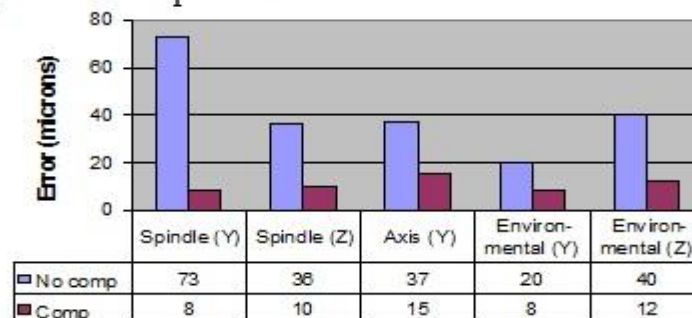A series of cutting trials were carried out that showed the effectiveness of workpiece temperature compensation.

	Spindle (Y)	Spindle (Z)	Axis (Y)	Environ-mental (Y)	Environ-mental (Z)
No comp	73	36	37	20	40
Comp	8	10	15	8	12

Figure 6-1. Bar chart of typical thermal compensation results

7 References

1. White AJ, Postlethwaite SR, Ford DG, 'A General Purpose Thermal Error Compensation System for CNC MachineTools', Fifth International Conference on Laser Metrology and Machine Performance - Lamdamap '01, University of Birmingham, pp3-13, 2001.

2. H. Yang, J. Ni, 'Adaptive model estimation of machine-tool thermal errors based on recursive dynamic modeling strategy', International Journal of Machine Tools and Manufacture, v45, Issue 1, 2005, pp1-11.

3. H. Yang, J. Ni, 'Dynamic neural network modeling for nonlinear, non-stationary machine tool thermally induced error', International Journal of Machine Tools and Manufacture, v45, Issues 4-5, 2005, pp455-465.

4. R. Ramesh, M. A. Mannan, A. N. Poo, 'Thermal error measurement and modeling in machine tools: Part I. Influence of varying operating conditions', Int. Journal of Machine Tools and Manuf., v43, Issue 4, 2003, pp391-404.

5. R. Ramesh, M. A. Mannan, A. N. Poo and S. S. Keerthi, 'Thermal error measurement and modeling in machine tools: Part II. Hybrid Bayesian Network-support vector machine model', International Journal of Machine Tools and Manufacture, v43, Issue 4, 2003, pp405-419.

6. Chen, J.S., Ling, C.C., (National Chung Cheng Uni.), "Improving the machine accuracy through machine tool metrology and error correction", Int. Journal of Advanced Manufacturing Technology, v11, 1996, pp198-205.

7. Fletcher S, Postlethwaite SR, Ford DG, 'Volumetric compensation through the machine controller', Fifth Int. Conference on Laser Metrology and Machine Performance - Lamdamap '01, pp321-330, 2001.

8. AP Longstaff, S Fletcher, DG Ford, "Practical Experience of Thermal Testing with Reference to ISO Part3" Proceedings of the Sixth LAMDAMAP Conference, pp.473- 482, July 2003.

9. White AJ, Postlethwaite SR, Ford DG, 'Measuring and Modelling Thermal Distortion on CNC Machine Tools', Fifth International Conference on Laser Metrology and Machine Performance - Lamdamap '01, pp69-79, 2001.

10. Longstaff P, Fletcher S, Myers A, 'Volumetric compensation through a Siemens controller', Submitted for publication in Laser Metrology and Machine Performance VII, 2005.

2005-10 Flexible Modelling and Compensation of Machine Tool Thermal Errors

FLEXIBLE MODELLING AND COMPENSATION OF MACHINE TOOL THERMAL ERRORS

Simon Fletcher, Andrew P. Longstaff, Alan Myers
Centre for Precision Technologies, University of Huddersfield, Queensgate, HD1 3DH, England

1 Introduction

Geometric errors on CNC machine tools have reduced significantly over the past few decades and compensation either through the controller or with retrofit systems have helped improve accuracy even further. This move is driven by a trend of ever tightening tolerances on components manufactured on these machines, especially where simplified assembly is required such as the Aerospace industries. Thermal errors have affected the accuracy of production machines for a long time but now for many industries with large machines and small error budgets, they are the dominant source of inaccuracy and are often the most difficult to reduce. Many solutions exist for the machine tool builder to reduce the errors that can be applied at the design stage including symmetric structures, low coefficient materials, liquid cooling systems etc. Design effort and cooling systems can add significant cost and usually cannot eliminate the errors but only help reduce them. Active and pre-calibrated compensation can be an important and effective alternative with some machine tool builders incorporating temperature sensors on the machine at the build stage. These systems are invariably controller-based using a simple model to estimate error at the tool and they are usually specific to a machine or range of machines within the company. These systems can produce good results for linear repeatable thermal errors and they work best in conjunction with good design [1].

Generally most thermal errors measured between the tool and workpiece are caused by a complex interaction of structural distortions having different heat sources, thermal time constants and expansion coefficients. Because of these causes the errors are time-varying and non-linear and are therefore difficult to model accurately. Significant research in the field of thermal error compensation has produced a number of sophisticated retrofit techniques for modelling thermal errors that employ techniques such as Neural Networks and multiple linear regression analyses [2, 3, 4, 5]. These systems can produce excellent results but often require complicated hardware and software systems and testing regimes to train the models or optimise temperature sensor positions for the particular machine or application.

This paper discusses new compensation capabilities and model development techniques that build on work by White [6, 7] to enhance the efficiency of application and machine accuracy. The philosophy relies on comprehensive measurement of temperature and a flexible compensation system that uses a novel programming language dedicated to modelling non-rigid behaviour of machine structural elements. The system practicality has been proven through industrial application.

Machine downtime, although undesirable, is required for completion of most phases of a thermal compensation system particularly the measurement of machine thermal behaviour, hardware implementation of temperatures sensors and compensation system and finally validation testing. It has already been mentioned that many successful modelling techniques require long testing regimes to provide sufficient information for robust model creation. The techniques described in this paper are designed to minimise this requirement in all areas.

2 Machine measurement

Acquiring as much temperature information from the machine during the initial testing phase is critical for making efficient use of the machine availability. Most machine heat sources are easily identified but thermal imaging can be used to enhance this process or determine the magnitude of heat generation during normal production. Once the main heat sources are identified a detailed study of the temperature distribution is required during a strategic test while measuring error. A thermal imaging system is set-up to capture images on a time basis while the heat sources are excited. This information is ideal for efficient determination of the correct compensation methodology, particularly temperature sensor density and placement. It is important to measure all other structural elements and environment that may contribute to the measured error. Low cost, accurate and compact digital temperature sensors are used extensively for this purpose.

Error between the tool and workpiece is measured using a spindle analyser or laser similar to that described by the ISO Standard 230 part 3. Most methods are based on this standard, however, measurement for compensation has

different requirements often resulting in variations to the tests to maximise the information that can be obtained. A variety of results are reported by Longstaff [8].

3   Model development

Detail about the modelling methodology is described by White [6]. Generally, the machine elements are analysed in there simplest form as far as possible. This enables reliable calculations of distortion such as bending and expansion using knowledge of the relevant structural dimensions and detailed temperature data. Small models of structures affected by running the spindle, the axes and changes in the environment or workpiece are combined to produce a comprehensive model with final compensation values for each axis direction.

3.1   Temperature

Figure 1 shows a saddle structure from a gantry machine that has a ballnut mounted at the rear. The image is part of sequence that can be analysed using the MatLab software shown. Virtual sensors and sensor strips are placed on the image from which detailed temperature gradient information can then be extracted and used in the development model as shown by the graph in figure 1. This simulation of the individual temperature sensors and sensor strips that will finally be applied to the machine enables accurate determination of the hardware requirements.

The developed thermal model can be run in another MatLab environment to acquire compensation results for comparison with the measured data captured during the initial testing phase. Manual or automatic adjustment of the model including trying different positions and resolutions for the temperature sensors can be tested offline easily. Through offline model optimization, a high level of confidence can be realized for the location of the temperature sensors for permanent installation. This minimizes the machine downtime and labor involved with sensor application, many of which may be embedded in the machine structure to enhance material temperature measurement accuracy.
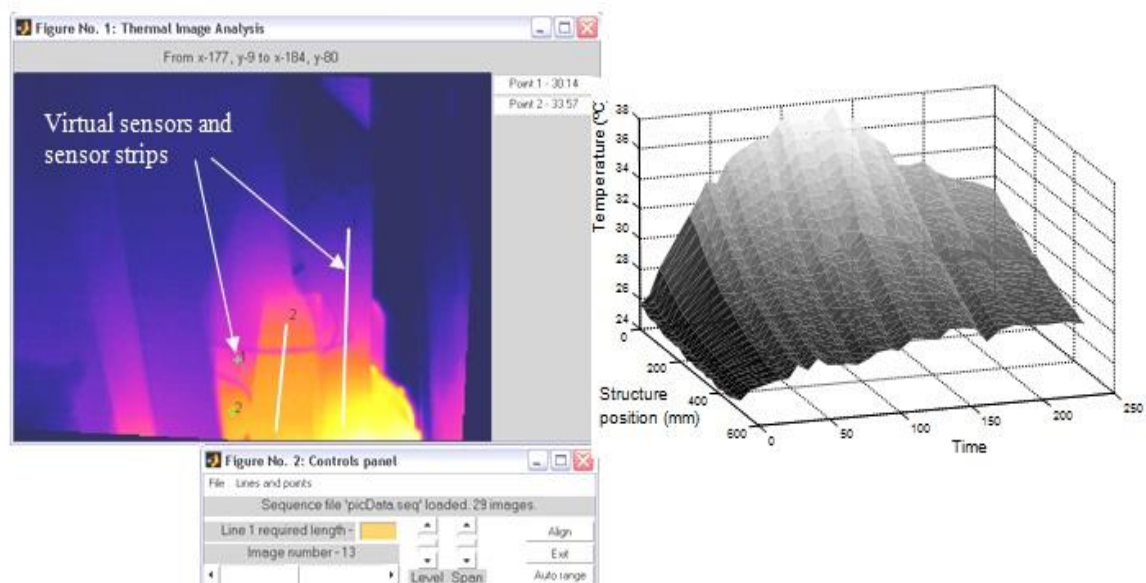

Figure 1. Virtual temperature sensor placement for model and hardware optimisation

4   Software implementation

The latest version of the University of Huddersfield compensation software VCS runs in the popular Siemens open architecture 840D controller. Many advantages are obtained by integrating into the controller both for geometric [9] and thermal compensation. Significant advantages include low cost and efficient implementation of compensation for geometric and thermal errors and having access to information about the current machining process such as workpiece offsets, materials, tool offsets and much more. This information enables compensation for differential expansion caused by inevitable variations in temperature of the feedback system and the workpiece.

5 Results sample

This section contains a sample of the results obtained from compensation on a small vertical milling machine.

5.1 Spindle movement

Model validation usually involves a random duty cycle. In this example a random duty spindle running cycle was used. Figure 2 shows the uncompensated and compensated error in the Y and Z directions. Position independent thermal error in Y-axis direction reduced from 71µm to 7.5µm (≈90%) and Z axis error reduced from 14 to 3.5 (≈75%). This improvement would be seen in short-term machining operations or where the machine was in a temperature controlled environment.
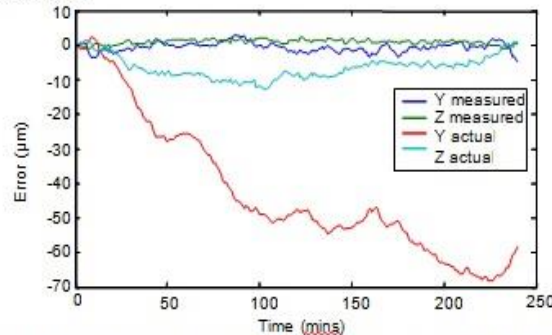

Figure 2. Compensation results for random spindle duty cycle

Monitoring the spindle movement over days rather than hours enables daily cyclic environmental temperature fluctuations and associated errors to be measured. Compensation results show a reduction in the magnitude of the environmental errors by more than 50% to just ±7µm over a 65 hour test. This is obviously time consuming and would therefore be carried out only if significant errors were being experienced, for example if machining times are long combined with environmental fluctuations [8].

5.2 Position dependent thermal error (PDTE)

PDTE can become dominant where cycle times for finishing cuts are small compared to the often slow changing Position Independent Thermal Errors (PITE), especially on large workpieces or where the workpiece coefficient of thermal expansion does not match that of the machine feedback system. For scale and workpiece errors we need the respective expansion coefficients, temperatures and a thermal datum. Most of these parameters change depending on workpiece so the flexible thermal modelling system can obtain this information from the NC as on offset such as G54 or as a parameter in the part program. With this information the workpiece error can be calculated using:

$$xWorkError = workTempAboveRef * (PosnX/1000 - XWorkDatum) * workCoeffExp$$

Combined with similar calculations for scale error and using a reference temperature such as 20°C, the error in the scale and workpiece can be compensated. Figure 3 (a) shows position error before and after compensation using a laser interferometer measuring with reference to 20°C. Both the PITE (scale offset) and PDTE (scale expansion) constituents are significantly reduced.
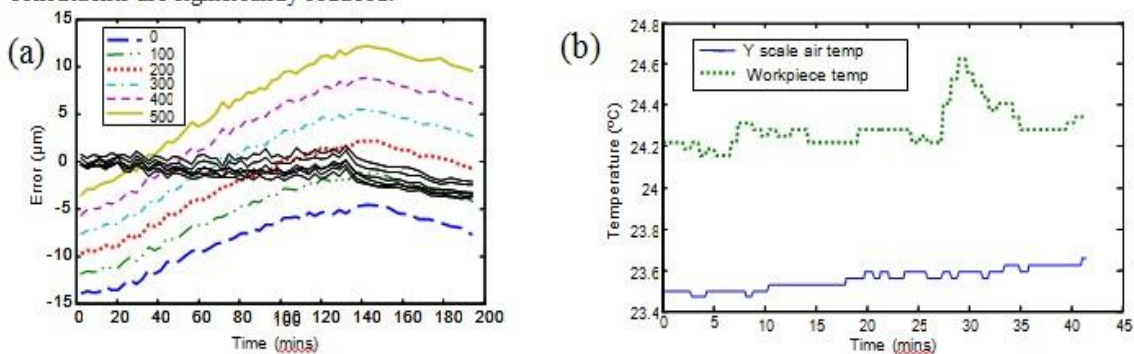

Figure 3. PDTE compensation and temperature of workpiece and scale during finishing operations

Further PITE validation was achieved during cutting trials using NAS979 test pieces machined in a non-temperature controlled environment. Temperature of the scale and workpiece as shown in Figure 3 (b) were used. Pre thermal compensation, the mean error from 5 representative dimensions of approximately 200mm was 27µm. With thermal compensation active, the mean error is 2µm which is a reduction of 91%. These significant improvements in accuracy can be expected when machining occurs with the workpiece at a different temperature to that of the position feedback system.

6   Conclusions

A flexible thermal compensation system has been devised that can compensate for all significant thermal errors on machine tools including many non-thermally related non-rigid errors. The system has been implemented on a PC and in two standard controllers [9, 10] for improved efficiency of application and reduced cost.

An error measurement and modelling methodology is briefly described which includes techniques implemented to facilitate model development and improve model accuracy offline and thermal imaging is an important part of this process. Hardware modification for permanent application of temperature sensors can then be implemented with confidence, requiring fewer validation tests and saving downtime. This is important for industrial applications.

A sample of results is presented for tests similar to those found in the ISO 230-3 standard and cutting trials. Typical accuracy improvements of greater than 70% are achieved for position independent and position dependent thermal errors including compensation for errors caused by environmental fluctuations.

Acknowledgements

References

1. Ramesh R, Mannan MA, Poo AN, 'Error compensation in machine tools — a review: Part II: thermal errors', International Journal of Machine Tools and Manufacture, v40, Issue 9, 2000, pp1257-1284.
2. Ramesh R, Mannan MA, Poo AN, and Keerthi SS, 'Thermal error measurement and modelling in machine tools: Part II. Hybrid Bayesian Network-support vector machine model', International Journal of Machine Tools and Manufacture, v43, Issue 4, 2003, pp405-419.
3. Yang H and Ni J, 'Dynamic neural network modeling for nonlinear, nonstationary machine tool thermally induced error', International Journal of Machine Tools and Manufacture, v45, Issues 4-5, 2005, pp455-465.
4. Chen JS, Ling CC, (National Chung Cheng Uni.), "Improving the machine accuracy through machine tool metrology and error correction", International Journal of Advanced Manufacturing Technology, v11, 1996, pp198-205.
5. Yang H, Ni J, 'Adaptive model estimation of machine-tool thermal errors based on recursive dynamic modelling strategy', International Journal of Machine Tools and Manufacture, v45, Issue 1, 2005, pp1-11.
6. White AJ, Postlethwaite SR, Ford DG, 'A general purpose thermal error compensation system for CNC machine tools', Laser Metrology and Machine Performance V, pp3-13, 2001.
7. White AJ, Postlethwaite SR, Ford DG, 'Measuring and Modelling Thermal Distortion on CNC Machine Tools', Laser Metrology and Machine Performance V, pp69-79, 2001.
8. Longstaff AP, Fletcher S, Ford DG, "Practical Experience of Thermal Testing with Reference to ISO Part3" Laser Metrology and Machine Performance VI, pp473- 482, 2003.
9. Longstaff AP, Fletcher S, Myers A, 'Volumetric error compensation through a Siemens controller', Laser Metrology and Machine Performance VII, 2005, pp422-431.
10. Fletcher S, Postlethwaite SR, Ford DG, 'Volumetric compensation through the machine controller', Laser Metrology and Machine Performance V, pp321-330, 2001.

2005-12 Practical Compensation of All Significant Thermal Errors in Machine Tools

PRACTICAL COMPENSATION OF ALL SIGNIFICANT THERMAL ERRORS IN MACHINE TOOLS

S. Fletcher, A.P. Longstaff, A. Myers and D.G. Ford
Centre for Precision Technologies
School of Computing and Engineering
University of Huddersfield, HD1 3DH, United Kingdom

Abstract: Thermal errors continue to be a major source of machine tool inaccuracy within the precision manufacturing industry. This paper describes a generally applicable, practical and flexible thermal error compensation system for the reduction of most systematic thermal errors. A new implementation of the system in a modern open architecture controller minimises hardware requirements and provides access to information such as workpiece offsets enabling compensation for differential expansion between the feedback system and workpiece. Results from standard metrology tests show an average reduction of 70% for position independent and position dependent thermal errors. Cutting results in a non-temperature controlled environment show 90% error reduction.

Keywords: Thermal error compensation, machine tool accuracy

1 INTRODUCTION

Tolerances within the precision manufacturing industry continue to challenge machine tool builders and often require costly design effort to overcome the errors within the machine. The ability to compensate for many geometric errors using modern controllers or for all errors using the UoH Volumetric Compensation System (VCS) ([1], [2]) provides a proven and cost effective solution for the reduction of geometric errors. The contribution of thermal errors to the machine inaccuracy is significant especially in precision machining and on large fast machines. Significant effort is required, usually at the design stage, to reduce these errors resulting in a difficult non-linear relationship between accuracy and cost particularly where environmental temperature control is required.

Compensation of thermal errors on CNC machine tools can be an effective solution with some machine tool builders incorporating temperature sensors on the machine at the build stage. These systems are usually specific to a machine or group of similar machines and can produce good results for linear repeatable thermal errors and they work best in conjunction with good design [3]. Generally applicable compensation is difficult due to the complexity of thermal errors and those systems that have been developed invariably involve complicated modelling techniques such as Neural Networks ([4],[5],[6]) or Regression analyses [7]. Such systems require training but suffer in accuracy if conditions change from those tested. Ramesh [8] incorporates machining parameters during the Neural Network training to improve accuracy. Although good results are often presented, most systems require significant testing and therefore machine downtime to ensure a robust model.

This paper describes a generally applicable thermal error compensation system that uses a unique flexible thermal modelling technique enabling reduction of most systematic thermal errors. This is combined with a measurement and model development strategy that is practical and has been applied to industrial applications. Model flexibility comes from a novel programming language that comprises calculations and functions dedicated to typical machine tool structural element distortions. A new implementation of the system in a modern open architecture controller is described which provides the significant advantage of having access to information about the current machining process such as workpiece offsets. This information enables compensation for differential expansion caused by inevitable variations in temperature of the feedback system and the workpiece.

Minimising machine downtime is important for an industrial retrofit system and this paper describes a machine measurement and modelling methodology to facilitate model development and improve model accuracy offline before permanent application of temperature sensors. This increases confidence and requires fewer machine tests for final model parameter modification and model validation.

Significant thermal errors include the wide range of errors found on a wide variety of machines tested [9], ranging from cam grinders to 30m long gantry systems.

1.1 Position dependent thermal errors (PDTE)

PDTEs can be the most significant thermal errors depending on the operating conditions and design of the machine. For a geometrically accurate and fairly short machining times, errors caused by differential expansion can be an order of magnitude larger than the other errors. The following list describes these significant errors.

1. Variation in environmental temperature causing differential expansion between the position feedback device and the workpiece.
   - Variation in coefficient of thermal expansion of the position feedback device and workpiece.
   - Variation in thermal time constant of the position feedback device and workpiece.
   - Vertical temperature gradients resulting in temperature variation of feedback device high above the floor and workpiece near the floor.
2. Variation in workpiece temperature causing differential expansion
   - Swarf build up conducting heat into the workpiece and fixture.
   - Temperature controlled flood cooling maintaining workpiece temperature stability while the machine and feedback device changes
   - Non-temperature controlled flood cooling changing the workpiece temperature.
3. Distortion of machine guideways causing changes in angular and straightness errors
   - Bending of a column causing change in position error with position of an axis on the column.

1.2 Position independent thermal errors

Some PITE can occur fast such as those caused by rapid changes in spindle speeds, while others may change gradually throughout the day caused by structure distortion resulting from environmental fluctuations.

1. Structural deformation causing movement of the tool relative to the workpiece
   - Internally generated heat particularly from spindles and spindle bearings.
   - Environmental temperature fluctuations and absorption of radiated heat.
2. Internally generated heat affects the structural loop between the scale thermal datum and the tool or workpiece.
   - High feedrates from tool changing or high speed machining etc induces heat in ballscrews and support bearings.
   - Hydrostatic guideways generate heat through internal fluid friction.

2 SYSTEM IMPLEMENTATION

Generally, the procedure for implementing the thermal compensation system is as shown in Figure 1. The methodologies developed are designed to maximise the retrieval of temperature and error information to enable more offline work thereby reducing machine downtime.
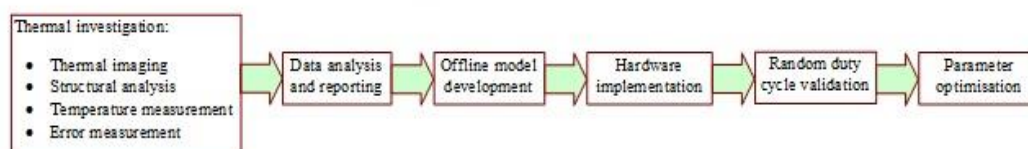

Figure 1. Flow diagram of system implementation

2.1 Thermal investigation

Typically, this is a series of tests designed to capture thermal error while monitoring temperature. To maximise this information, thermal imaging is used extensively from full structure scans while the machine is in normal operations to detailed sequences of images of a particular structure such as a headslide or bed

section similar to that shown in figure 2. Error between tool and workpiece is usually measured using a nest of Non-contact displacement transducers (PITE) or a laser interferometer (PDTE).

2.2 Offline model development

Figure 2 shows thermal analysis of a sequence of images of a headslide from a small vertical machining centre (VMC1). Virtual sensors and sensor strips are placed on the image from which detailed temperature gradient information can then be extracted and used in the development model as shown by the 3D graph. This simulation of the individual temperature sensors and sensor strips that will finally be applied to the machine enables accurate determination of the hardware requirements.
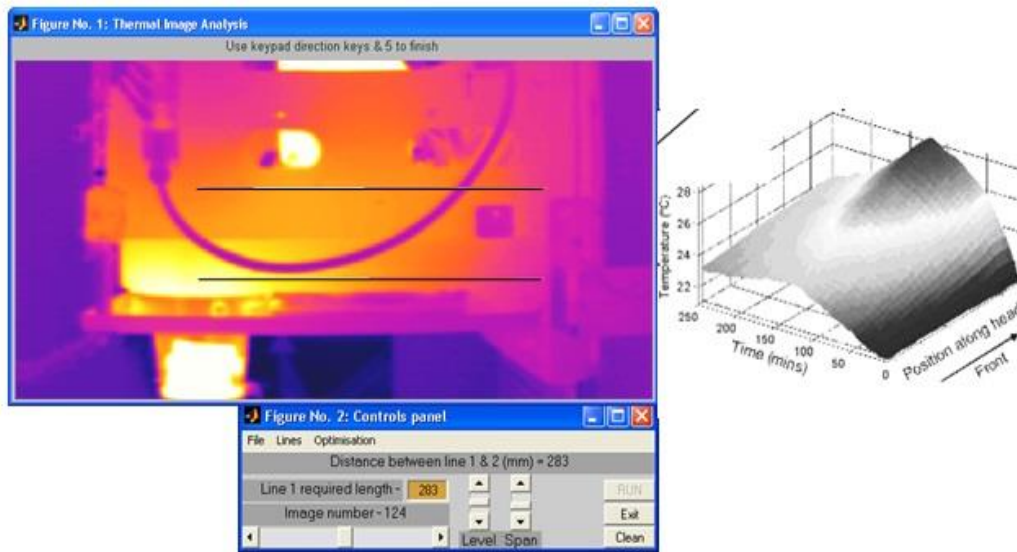

Figure 2. Example of temperature extraction from thermal image sequence

Ramesh [10] discusses variation in error even with similar structure temperature depending on the operating parameters. In this case, model accuracy is maintained through measurement of gradients across a structure not just single point or low resolution measurements.

A thermal model is created using the basic mechanical design of the machine and the temperature gradients. In this example two temperature sensing lines are required to determine the temperature gradients for calculation of distortion as well as expansion. Figure 3 shows the headslide errors.

Where:-
B_z, B_y = Z/Y error resulting from bending
E_f, E_r = Expansion of front and rear of the head
E_l = Expansion of the head
e_z, e_y = Z/Y error from head distortion
h_s = Sensor line distance

$e_z = E_f + B_z - E_r$
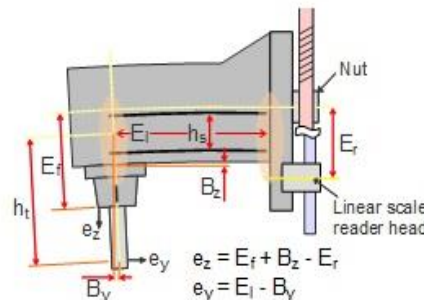$e_y = E_l - B_y$

Figure 3. Headslide detail

Model definition is simplified through the use of a variety of functions that carry out specialist calculations for typical structural element distortions. For example, the 'BEND' function [[11]] is used to calculate the transverse distortion resulting from temperature gradients identified by the two sensor lines.

B_z = BEND(SensorLine1, SensorLine2, LineDisplacement, E_{mat}, CorrectionFactors)

Where E_{mat} is the expansion coefficient of the material. The correction values are applied to compensate for the inaccuracy of surface measurement. Embedding the sensors into the structure where possible can improve the accuracy significantly. Generally, if correction factors are less than one or greater than two, it suggests that the fundamental model design or location of temperature measurement is inadequate. The final X, Y and Z compensation values are a combination of such expansions, distortions etc. For the Y axis model of VMC1, which is the direction in which most thermal errors manifest, we get:

$$TotalY = f(Head(Expansion, Bending), Column(Expansion, Bending), Y(Offset, Scale), WorkpieceEffect)$$

This value is then used by VCS to modify the axis position. White [11] describes in more detail the modelling language and structure.

2.3 Hardware implementation

A combination of unique sensor strips and discrete sensors are attached to/embedded into the structure at those positions identified from the offline modelling work or through experience. The strips are physically flexible for modest surface undulations and have a low profile to fit under guarding or between structural elements etc. Figure 4 shows a series of strips held to the surface using aluminium brackets. The strips can contain many sensors with the smallest interval being 15mm. As well as resolution, this provides redundancy, creating a more robust system for industrial applications. If a sensor reports a failure or a reading cannot be obtained, the specific sensor can be identified and the software then interpolates between the two adjacent sensors until a maximum failure limit is met. This density can be achieved because all the sensors communicate down the same wire. Figure 5 shows heat flow from the spindle and motor to the guideway via the friction pads. This flow is dependent on the location of the spindle axis and causes non-uniform distortion or bulging of the guideway resulting in both PDTE and PITE.
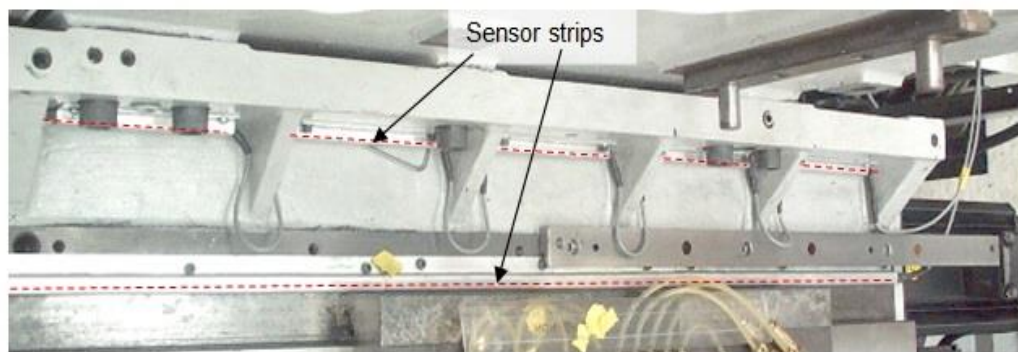

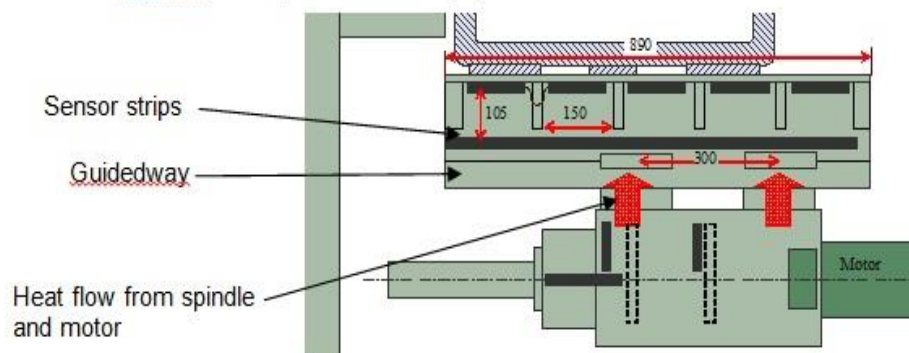Figure 4. Example of sensor strip placement on a machine

Figure 5. Sensor and machine layout

The latest version of the University of Huddersfield compensation software VCS runs in the popular Siemens open architecture 840D controller. Many advantages are obtained by integrating into the controller both for geometric [2] and thermal compensation. Significant advantages include low cost and efficient

implementation of compensation for geometric and thermal errors and having access to information about the current machining process such as workpiece offsets, materials, tool offsets and much more. This information enables compensation for differential expansion caused by inevitable variations in temperature of the feedback system and the workpiece (section 3).

2.4   Validation and optimisation

Random duty cycle tests are used to validate the created model. The thermal model has a section for specifying temperatures and variables for recording to file. This information can be applied through the offline model development software to compare the results with the remaining error measuring during the tests. Final optimisation can then be applied easily if required with the results of the changes simulated instantly for the entire test. Typically, correction factors are applied to the temperature readings as it is here where differences can occur between actual machine temperatures and that measured on the structure surface. Figure 6 shows the compensation result for the machine shown in section 2.3. The Z and Y errors have been reduced by 75% and 50% respectively.
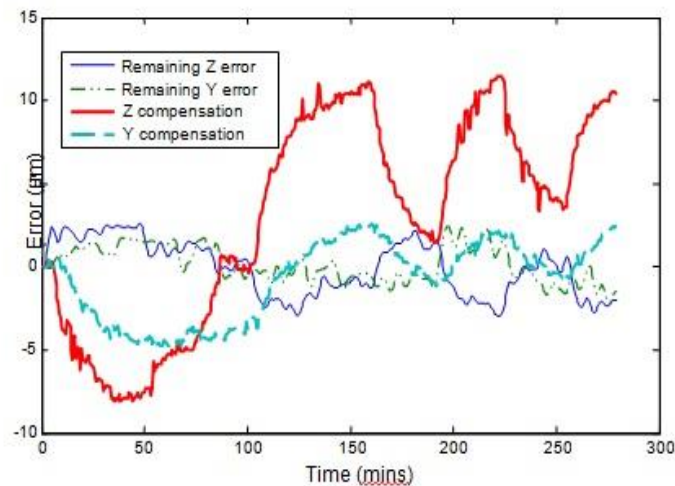

Figure 6. Validation test data

3   COMPENSATION RESULTS

These results are for recent work on the small vertical machining centre VMC1 using VCS incorporated into the Siemens 840D controller.

3.1   Axis PDTE and PITE

The PDTE and PITE described in section 2.3 and compensation in section 2.4 are caused by heat generated through running the spindle. The PITE error in figure 7 is caused by heat in the axis support bearing generated from running the axis. Heat in the bearing conducts into the bed causing expansion producing a scale offset as the position of the scale attached to the bed is changing relative to the tool. The PDTE is caused by change in scale temperature. The central cluster of traces in the graph show the errors after compensation are significantly reduced. The temperature of the scale is estimated from air temperature measurement very close to the scale and has, therefore, some inaccuracy which accounts for the residual variation.
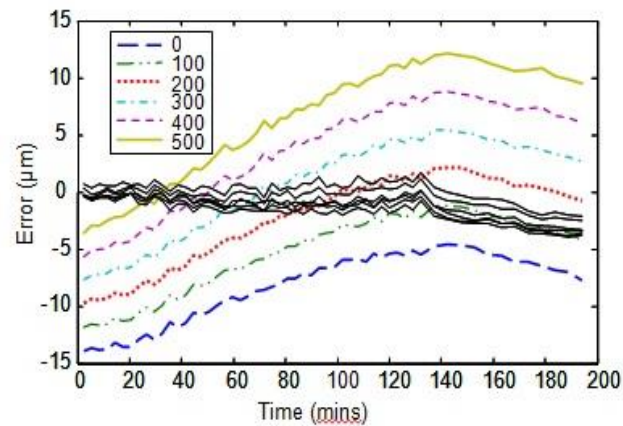
Figure 7. PDTE and PITE compensation result.

3.2 Workpiece expansion

Compensation for PDTE of the feedback device can create more error if the part temperature is varying. For scale and workpiece error compensation we need the respective expansion coefficients, temperatures and a thermal datum. In this case the expansion coefficients were approximately 10.7μm/m/°C and 23μm/m/°C for the glass scales and aluminium test piece respectively. Parameters that change depending on workpiece such as thermal datum can be obtained from the NC as on offset such as G54 or as a parameter in the part program. The temperature of the workpiece was measured using two sensors embedded into the underside of the workpiece. With this information the workpiece error can be calculated using:

$$xWorkError = workTempAboveRef * (PosnX/1000 - XWorkDatum) * workCoeffExp$$

This workpiece and scale are both compensated with reference to 20°C removing the need for a differential calculation.

Validation of the workpiece compensation was achieved with cutting trials using NAS979 test pieces machined in a non-temperature controlled environment. Figure 8 (a) and (b) show the scale and workpiece temperature during roughing and finishing respectively. Without thermal compensation, the mean error from 5 representative dimensions of approximately 200mm was 27μm. With thermal compensation active, the mean error is 3μm which is a reduction of 89%. These significant improvements in accuracy can be expected when machining occurs with the workpiece at a different temperature to that of the position feedback system.
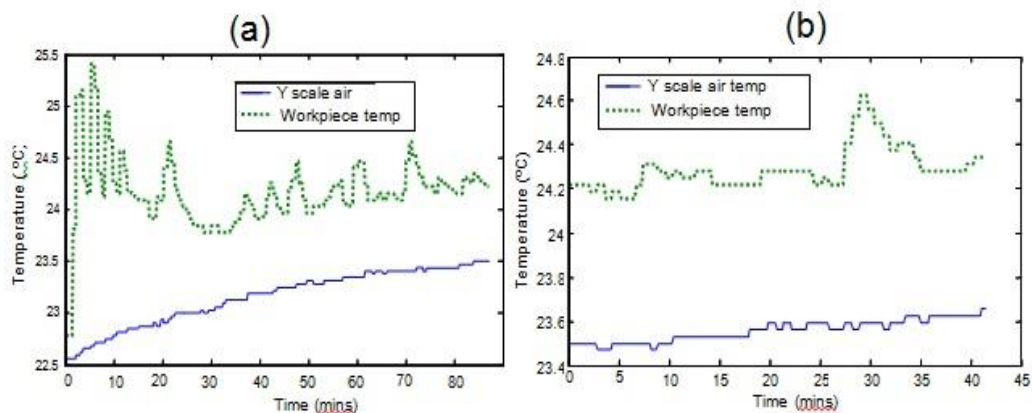

Figure 8. PDTE compensation and temperature of workpiece and scale during finishing operations

3.3 Environmental error

The time taken to measure environmental effects can be prohibitive within industry. However, if compensation is necessary then an extended test period is required to include the daily cyclic environmental temperature fluctuations. Figure 9 shows environmental error reduced to just ±7µm over a 65 hour test. The residual errors are due to air temperature affecting the surface measurement of the material temperature. Embedding the sensors into the structure will improve the results especially where the air temperature changes rapidly, in this case towards the end of the test when the factory heating started on a Monday morning.
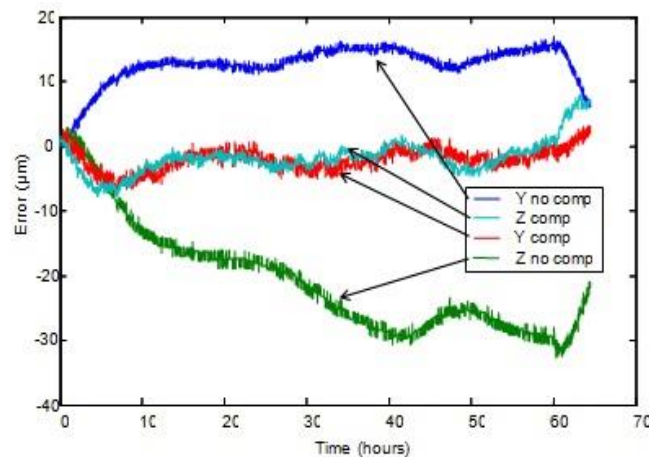

Figure 9. Compensation results for extended environmental test

3.4 Spindle heating

This usually involves a random duty cycle spindle heating test including spindle speed variations and spindle stoppages. Figure 9 shows the uncompensated and compensated error in the Y and Z directions. Position independent thermal error is reduced from 71µm to 7.5µm (≈90%) and from 14 to 3.5 (≈75%) respectively. This improvement would be seen in short-term machining operations or where the machine was in a temperature controlled environment.
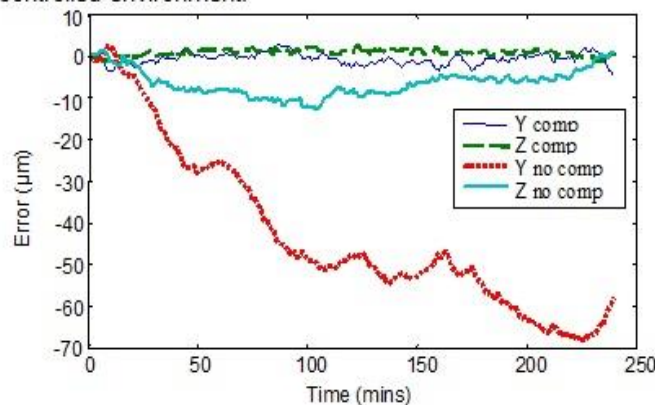

Figure 10. Compensation result for spindle induced PITE

4 CONCLUSIONS

A thermal compensation system and compensation methodology is shown that is practical and can compensate for all significant thermal errors on machine tools.

Results from standard metrology tests show an average reduction of 70% for position independent and position dependent thermal errors.

NAS 979 components machined under a non-temperature controlled environment show a remaining error of less than 5μm with compensation, proving the effectiveness of the system for reduction of differential expansion.

ACKNOWLEDGEMENTS

REFERENCES

[1]. S.R. Postlethwaite, D.G. Ford, "A practical system for 5 axis volumetric compensation" Laser Metrology and Machine Performance IV, pp379-388, 1999.

[2]. A.P. Longstaff, S. Fletcher, A. Myers, 'Volumetric error compensation through a Siemens controller', Laser Metrology and Machine Performance VII, 2005, pp422-431.

[3]. R. Ramesh, M.A. Mannan, A.N. Poo, 'Error compensation in machine tools — a review: Part II: thermal errors', International Journal of Machine Tools and Manufacture, v40, Issue 9, 2000, pp1257-1284.

[4]. C.D. Mize, J.C. Ziegert, 'Neural network thermal error compensation of a machining center', Precision Engineering, v24, Issue 4, 2000, pp338-346.

[5]. H. Yang, J. Ni, 'Dynamic neural network modeling for nonlinear, nonstationary machine tool thermally induced error', International Journal of Machine Tools and Manufacture, v45, Issues 4-5, 2005, pp455-465.

[6]. J.S. Chen, CC. Ling, (National Chung Cheng Uni.), "Improving the machine accuracy through machine tool metrology and error correction", International Journal of Advanced Manufacturing Technology, v11, 1996, pp198-205.

[7]. J.H. Lee, S.H. Yang, 'Statistical optimization and assessment of a thermal error model for CNC machine tools', Int. Journal of Machine Tools and Manufacture, v42, Issue 1, 2002, pp147-155.

[8]. R. Ramesh, M.A. Mannan, A.N. Poo, S.S. Keerthi, 'Thermal error measurement and modelling in machine tools: Part II. Hybrid Bayesian Network-support vector machine model', International Journal of Machine Tools and Manufacture, v43, Issue 4, 2003, pp405-419.

[9]. A.P. Longstaff, S. Fletcher, D.G. Ford, 'Practical Experience of Thermal Testing with Reference to ISO Part3', Laser Metrology and Machine Performance VI, pp473- 482, 2003.

[10]. R. Ramesh, M.A. Mannan, A.N. Poo, 'Thermal error measurement and modelling in machine tools: Part I. Influence of varying operating conditions', International Journal of Machine Tools and Manufacture, v43, Issue 4, 2003, pp391-404.

[11]. A.J. White, S.R. Postlethwaite, D.G. Ford, 'A general purpose thermal error compensation system for CNC machine tools', Laser Metrology and Machine Performance V, pp3-13, 2001.

AUTHORS: Dr Simon Fletcher, Dr Andrew P Longstaff, Alan Myers, Prof Derek G Ford, Centre for Precision Technologies, School of Computing and Engineering, University of Huddersfield, Queensgate, Huddersfield, United Kingdom, HD1 3DH, Phone +44 1 484 472596. E-mail: a.p.longstaff@hud.ac.uk

2007-04 Measurement Methods for Efficient Thermal Assessment and Error Compensation

Measurement methods for efficient thermal assessment and error compensation

S. Fletcher[1], A.P. Longstaff[1], A. Myers[1]

[1]University of Huddersfield, United Kingdom

s.fletcher@hud.ac.uk

Abstract

Radically improving the accuracy of modern precision machine tools through design and build practices is generally considered cost ineffective compared with electronic compensation. For the geometric errors in a machine tool, compensation is becoming standard practice and most modern controllers provide this ability albeit at varying levels of sophistication. Thermal compensation features, either within controllers or builder specific systems, are generally much more limited and consider only linear problems such as spindle growth on high speed spindles or scale length. Various sophisticated systems based on learning algorithms such as regression or Neural network techniques have been shown to be very effective for modelling much more of the machine non-linear thermal behaviour. Despite this capability, the systems can remain out of reach of general industrial application due to their complexity and requirement for significant on-machine testing to train the models. This paper discusses methods for obtaining the temperature information required for offline model development and on-line compensation associated with a novel, extremely flexible modelling technique.

Thermal imaging has been shown to be an important temperature assessment tool but radiative measurement accuracy is usually in the order of +/-2℃. This paper shows test results with cross image relative accuracy and linearly optimised absolute accuracy of within +/-0.15℃. The comprehensive temperature information is used for model development, optimisation and simulated hardware location compatible with discreet sensor placement and unique, low cost, temperature sensing strips. These provide high spatial resolution for detailed on-line measurement of any significant thermal gradients for compensation of complex distortions. Significant reductions have been achieved using the modelling technique, typically between 70 and 90% of machine tool position-independent and position-dependent thermal errors under various validation conditions. The methodology does not use training methods thus machine downtime is reduced while flexibility and accuracy are retained for compensating all systematic thermal errors. The on-line software is incorporated into a complete compensation system both PC based and incorporated into a modern open-architecture controller.

1   Introduction

The method of modelling based on temperature measurement is often the most practical for compensating the thermal errors of precision machine tools, particularly for a generic system designed to be applicable to a wide variety of machine types and configurations. Efficiency and practicality means that there are different requirements for the measurement tasks associated with thermal assessment and on-line compensation. These tasks have been addressed using thermal imaging, temperature sensing strips and embedded workpiece sensors. This paper concentrates on using thermal imaging and describing the sensor strips for efficient and robust model development and on-line compensation applied using a flexible modelling technique and advanced thermal compensation system [1].

2   Thermal imaging

Non-contact temperature measurement using thermal imaging solves many practical problems associated with rotating parts, non-interference on workpieces and coverage of large surface areas as well as providing much greater detail of thermal gradients. This section looks at obtaining improved accuracy beyond the usual specifications for portable imaging systems (Flir ThermaCAM S65 in this case).

A small aluminium component was used into which a 100mm long thermister with 0.002℃ accuracy was embedded with complete interference ensured using thermally conductive paste. During a natural cooling cycle, image sequences at 50Hz for 2s were taken periodically.

Figure 1 shows an analysis on the noise level of the camera which showed between 0.3°C and 0.7°C variation across pixels.
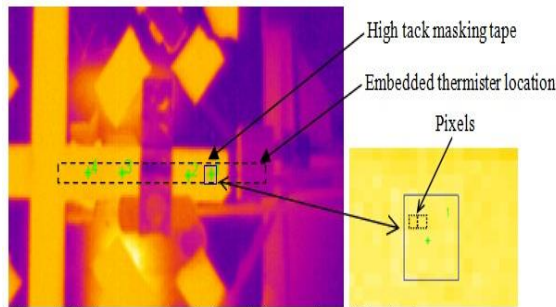

Figure 1. Test component analysis and close up view of pixel noise

Averaging of 400 images was used to create one low noise image per measurement cycle. The variation in temperature between the thermal images and the reference thermister is shown in figure 2. The underestimation equates to just 0.04°C/°C using an emissivity of 0.92 and is highly linear. A simple least square correction produces an extremely accurate measurement within +/-0.15°C over a 30°C range and variable environment of more than 2°C. This was repeatable to within 1% of the reading.
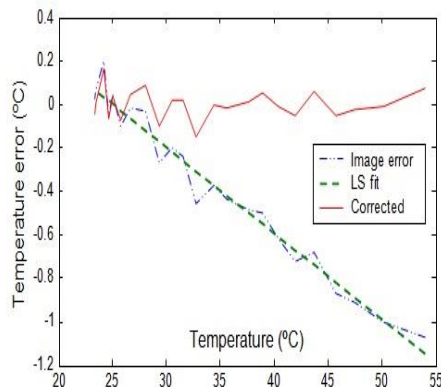

Figure 2. Thermal imaging accuracy result

2   Surface measurement

Thermal imaging is seldom a practical solution for on-line measurement for compensation and can even be impractical during the testing phase because of the requirement for an unobstructed view of the structure. Accurate elongated platinum resistance thermometers can obtain an average temperature over a large area but they do not provide information about gradients and therefore complex distortions. Many structural elements on machine tools have rough surfaces or surfaces that exhibit changes in level and angle to meet the requirements of the designer. Attaching temperature sensors to such surfaces requires great flexibility. A unique sensing strip that employs a special flexible circuit board allows convenient application of many sensors at a spatial resolution of 15mm while handling surface irregularities with bend radii as little as 1mm. Figure 3 shows the sensor strip and example mounting arrangement using the mounting holes provided in the strip.
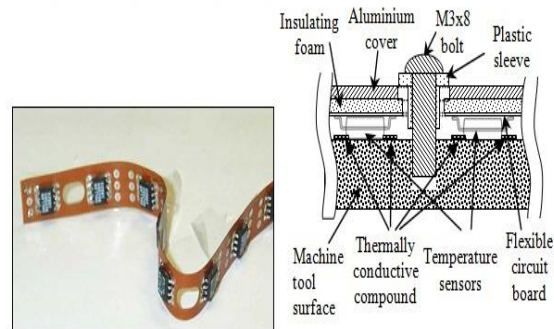

Figure 3. Sensor strip and mounting example on machine surface

Any number of digital temperature sensors can be mounted in a line on the surface of a machine tool with only a single 3-core cable between all devices and to the computer or controller for compensation. This system eliminates the need for large numbers of wires and junction boxes, leading to a relatively simple and rapid application. For protection, a silicon based conformal coating spray or thin-walled heat shrink tubing can be used, both if which have proven long term resistance to coolant ingress.

3   Modelling

Thermal gradients can cause distortions such as bending that can produce fast moving errors amplified by the large structural elements [2]. Tests on several vertical machining centres have shown rapid bending of the headslide causing error in two directions whose magnitudes are dependent on tool length. Robust and efficient

Proceedings of the Topical Meeting: Thermal Effects in Precision Systems – Maastricht- December 2007

modelling is achieved using the detail from thermal imaging to simulate and optimise the location of the sensing strips. Temperature data is extracted and loaded directly into the modelling functions, the basics of which are described in more detail by White [3]. The images also enable rapid determination of simple correlations between structural temperatures and measured error from limited machine assessment time. Discrete sensors are placed where imaging is not possible such as inside structures.

4   Application example

Figure 4 shows an application, using aluminium brackets for mounting and protection, of the sensors on a vertical machining centre headslide. In this example, tests were run with and without spindle cooling which, as expected, showed significant variation in error magnitude and profile caused by changes in the thermal gradients as shown by the images in Figure 5.

Figure 4. Application of sensor strips onto irregular VMC head.
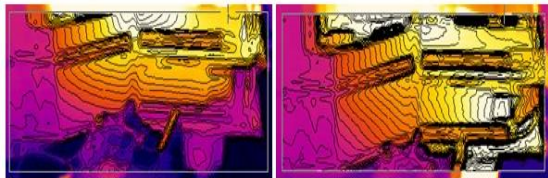

Figure 5. Variation in thermal gradients with spindle chiller unit on and off

The strips enable the same model to predict both errors to better than 85% highlighting the robust nature of the model. Figure 6 shows the error reduction in the Y axis direction from 18µm to just 4µm during a random duty validation cycle. Similar results were obtained in the Z direction with negligible error in X due to structural symmetry.
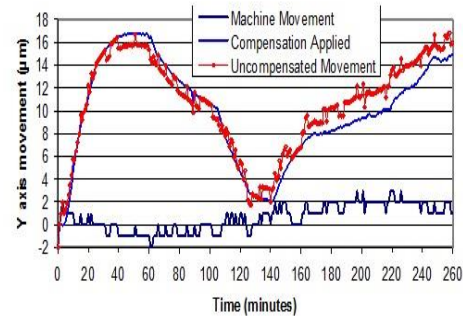

Figure 6. Result of compensation in Y direction for random duty cycle

For complete compensation of the position dependent thermal errors, the differential expansion between the linear scale feedback and workpiece is modelled using embedded workpiece sensors. Machining results show 80% reduction in error in an uncontrolled environment of 25ºC.

5   References

[1] Fletcher S, Longstaff AP, Myers A, Ford DG 'Practical compensation of all significant thermal errors in machine tools', 3rd International Congress on Precision Machining, Vienna, pp109-117, 2005.

[2] White AJ, Postlethwaite SR, Ford DG, 'Measuring and modelling thermal distortion on CNC machine tools', LAMDAMAP V, pp 69-79, 2001.

[3] White AJ, Postlethwaite SR, Ford DG, 'A general purpose thermal error compensation system for CNC machine tools', LAMDAMAP V, pp3-13, 2001.

2007-05 Flexible Compensation of Thermal Errors

Flexible compensation of thermal errors

A.P. Longstaff [1], S. Fletcher[1], A. Myers[1]

[1] University of Huddersfield, United Kingdom

a.p.longstaff@hud.ac.uk

Abstract

As thermal error modelling methods becomes more sophisticated, so the models they generate become more complex. Once the basic elements such as linear expansion and element bending have been addressed, more complex features related to the machine-component interface begin to dominate. The thermal model therefore includes a greater number of variables which can be not only machine, but also process specific.

A single piece of software has been created that is able to compensate the rigid-body geometric errors for any three-axis machine tool, or machine with a fork head. It is possible to generate such a system because the geometric models remain constant over all machine configurations, with only the error profile changing on each machine.

To be able to include a universal compensation package for thermal error correction requires a more flexible approach. This paper describes a unique compensation language that has been created that runs as a visual basic script in the machine controller. The software reads temperatures, axis positions and other parameters and passes calculated compensation values to the main compensating routines which run at a much lower level in the system.

The advantage of this system is that the compensation model can be modified on the CNC during the integration period without requiring a software rebuild. Automatic error checking is built into the scripting language, which picks up syntax errors, mistyped variable names, etc. before the algorithm is run.

Important machine parameters such as tool length, coolant flow status, part program information, etc. can be read directly from the machine data tables and used in the compensation model.

This paper describes some of the issues involved in the design of the system and discusses the results of applying the software on a small production machine, where it has yielded an average improvement of 80%.

1 Introduction

Compensation for the errors in precision systems can broadly be achieved in two ways. The first, largely adopted for compensation produced by machine manufacturers, employ specific hard-coded algorithms for each machine design that they produce, optimised to the level they perceive to be suitable for their target industry. The second strategy provides a single compensation system that can be flexibly configured during the integration process to run for many different machine types. This approach has direct benefits for end-users who have machines from different manufacturers, since a single "compensation system" can be supported across all machines, thus reducing training costs. This paper discusses such a system that describes the machine-specific compensation model using a visual basic scripting language.

2 Description of the compensation system

The compensation system described in this paper has been integrated into a Siemens 840D controller. Figure 1 shows the interaction of the various parts of the compensation system.
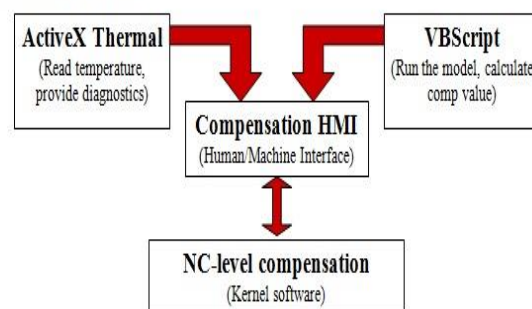

Figure 1: Schematic of compensation system

The human machine interface, or "**Compensation HMI**", is used for specifying and editing the compensation script file during integration and acts as a supervisory process during normal operation. In this package geometric and other compensations are

handled in addition to thermal compensation. The HMI is empowered to take action if any part of the system is not correctly operating. The HMI can prohibit compensation, produce operator warnings or instigate machine alarms, feedhold, emergency stop, etc.

The temperatures are read cyclically with a visual basic "**ActiveX Thermal**" component. The sample rate is dictated by the compensation script, reducing overheads on parts of the system where thermal changes are slower, or have less significance. The ActiveX also provides diagnostics for the sensors. Sensor redundancy should be provided in harsh environments - diagnostics can be used to predict sensor failure.

The **VBScript** part of the package is run as a component within the HMI. It executes the user script with system constants being loaded once at start-up and the remainder of the code being processed cyclically line-by-line. The user-defined script, based on that by Fletcher [1], uses standard VB function calls, arithmetic operations, memory mapping, etc. It has been expanded upon to permit user-defined functions for calculations such as sensor averaging, thermal bending, bulging, etc.

Figure 2: Variable monitoring window

VBScript was chosen to run the thermal compensation for a number of reasons. Some of the main advantages arise from the need for a robust system that is sufficiently flexible that can be built up on-line during installation. For example, the use of the VB "Option Explicit" syntax forces variable declaration, helping to avoid run-time errors.

Syntax checking is also handled by the windows software, removing the need for large amounts of pre-compiler code within the compensation software.

The accessibility of the scripting also allows useful functions such as the ability to check values of the thermal model while a test is running. Figure 2 shows a model debugging window, in which the value of any model constants or variables or any valid expression can be displayed at each iteration of the model.

Once compensation has been calculated and validated it is passed to the "**NC-level compensation**", which issues compensation commands to each axis.

2.1 Process-specific information

Because of the system design, important operation-specific information can be transferred from the machine operator to the compensation system. A link to a dynamic data exchange (DDE) server can be used to monitor, in real time, many system variables such as workpiece offset (G54), coolant flow, etc.

Other information can be transferred through implementation of a novel scheme where the parameters are framed in compensation-system specific syntax and incorporated in the part program. The compensation system can intercept the part program block being executed and optimise performance by interpreting the process-specific information. Table 1 shows the relevant syntax, where:

- the comment label prevents the controller from attempting to process the line,
- the SoftwareID is used by the HMI interpreter to direct the instruction to the correct part of the package. In this case "T" indicates thermal,
- the VariableID can be any recognised variable within the compensation script,
- the value is that which should be assigned to the designated variable.

The first example in the table tells the software the coefficient of expansion of the workpiece, while Example 2 indicates the thermal datum of the workpiece in X.

Table 1: Example Part Program code used for process-specific compensation

Syntax	Comment label	SoftwareID	VairableID	Value
Example 1	%	VCST	WorkPieceEC	24.000
Example 2	%	VCST	WorkTDatumX	294.111

3   System validation

The compensation system has been validated by metrology and by machining test pieces based upon the NAS-979 test piece. Three 300mm aluminium pieces were manufactured on a test machine; one on the uncompensated machine; with geometric compensation [2]; and with geometric and thermal compensation. After manufacture, the test pieces were measured on a CMM, with some dimensions shown in figure 3.
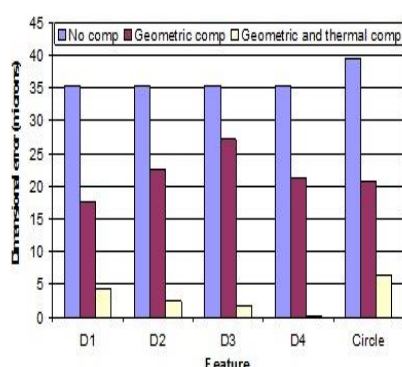

Figure 3: Compensation results

All pieces were machined in similar conditions at around 25°C. The effectiveness of the compensation system can be clearly seen, with the average accuracy of the features being improved by 80% by thermal compensation, and 92% overall.

Acknowledgements

References

[1]   Fletcher S, Longstaff AP, Myers A, "Flexible modelling and compensation of machine tool thermal errors", 20th Annual Meeting of the American Society for Precision Engineering, 2005

[2]   Longstaff AP, Fletcher S, Myers A, Ford DG "Volumetric compensation of machine tools makes geometric errors negligible", 3rd International Congress on Precision Machining, pp209-216, 2005

2011-05 Efficient thermal error prediction in a machine tool using finite element analysis.

Efficient thermal error prediction in a machine tool using finite element analysis

Naeem S Mian, Simon Fletcher, Andrew P Longstaff and Alan Myers

University of Huddersfield, Queensgate, Huddersfield HD1 3DH, UK

E-mail: nshaukat80@hotmail.com

Abstract

Thermally induced errors have a major significance on the positional accuracy of a machine tool. Heat generated during the machining process produces thermal gradients that flow through the machine structure causing linear and nonlinear thermal expansions and distortions of associated complex discrete structures, producing deformations that adversely affect structural stability. The heat passes through structural linkages and mechanical joints where interfacial parameters such as the roughness and form of the contacting surfaces affect the thermal resistance and thus the heat transfer coefficients. This paper presents a novel offline technique using finite element analysis (FEA) to simulate the effects of the major internal heat sources such as bearings, motors and belt drives of a small vertical milling machine (VMC) and the effects of ambient temperature pockets that build up during the machine operation. Simplified models of the machine have been created offline using FEA software and evaluated experimental results applied for offline thermal behaviour simulation of the full machine structure. The FEA simulated results are in close agreement with the experimental results ranging from 65% to 90% for a variety of testing regimes and revealed a maximum error range of 70 μm reduced to less than 10 μm.

Keywords: thermal error, finite element analysis, FEA, thermal compensation, offline thermal error prediction, ambient air pockets

(Some figures in this article are in colour only in the electronic version)

1. Introduction

Thermal deformations of machine tool structural elements have been a major problem for precision engineering industries. It has been reported that thermal errors can represent 70% of the total volumetric error [1]. Complex interaction of structural components having different heat sources, thermal time constants and thermal expansions is generally the cause of nonlinear structural deformations, hence the thermal errors [2]. This has driven extensive industrial and research effort to compensate thermally induced errors which lead to dimensional inaccuracies in parts. Significant research methods and retrofit techniques such as the linear/multiple regression technique [3–5], neural networks and sensor systems [6–9] have proved their capabilities with excellent thermal prediction and compensation results but they are subjected to their own constraints for complexity, robustness, cost and time consumption. Thermal machine testing is a

major obstacle for the implementation of many such methods for industries where production machine availability cannot be compromised. Numerical techniques for model training, data collection and computation methods to predict thermal errors generate uncertainties in terms of time requirements, complicated hardware and associated costs. In some cases, finite element analysis (FEA) has been used as part of the research as a validation tool on discrete structural elements, but not on a full CNC machine for thermal compensation. However, it has proved its significance in predicting thermal errors and reduced time scales which in turn leads to reduced machine downtime [10, 11]. The FEA method is also widely used on systems other than CNC machines. Kim *et al* [12] have proved a well-matched comparison between FEA and other experiments for temperature distributions in the warm hydroforming process for aluminium alloy. On the CNC side, Jedrzejewski *et al* [13] and Zhou *et al* [14] have proved the FEA method's great potential to investigate specific structures and

N S Mian *et al*

the behaviour of CNC machines to achieve desired optimal high accuracy of the workpiece by means of compensating dimensional errors. Haitao *et al* [15] investigated the thermal behaviour of machine tool spindle using FEA and suggested that experiments could be replaced by the FEA simulations. Ratchev *et al* [16] showed useful results for compensating cutting forced induced error using FEA simulation techniques. These set good examples of using the FEA method towards predicting thermal behaviour of a full CNC machine tool.

This paper will present the offline FEA simulations of the full machine by first using the data extracted from short-term internal heat/cool testing with its validations and then the procedure repeated in reverse order where the simulation was run for an extended complex duty cycle and later validated on the machine. For offline simulations, Abaqus CAE 6.7–1 [17] FEA software was used.

2. Thermal contact resistance

Thermal contact resistance (TCR) [18, 19] is the resistance to heat flowing through structural joints (thermal contact conductance). This results in nonlinear thermal behaviour which adversely produces nonlinear thermal deformations across mechanical joints and other complex discrete structures within the machine. For accuracy of results, experiments were conducted to obtain thermal contact conductance values experimentally for their use at joining surfaces in the ABAQUS machine assembly model. The experiments were conducted on two rectangular steel plates of similar dimensions with average surface finish of 2 μm. Surface flatness was measured at 14 μm which is easily eliminated with standard clamping force and therefore has negligible effect on the heat flow. Four digital thermal sensors in sets of two were embedded into the plates to ensure high accuracy measurement of the core temperatures.

Prior to the thermal contact conductance experiments, the influence of convective heat transfer on the surface of the body was calculated by heating up one of the steel plates and suspended horizontally to cool to room temperature of 20 °C in a free convection mode. The convection coefficient value obtained was 6 W m^{-2} °C^{-1}. Thermal contact conductance experiments were carried out in two phases, first with cleaned dry plates and then with oiled plates. In the first phase, plate-1 was heated to approximately 52 °C and plate-2 clamped immediately onto the heated plate-1 using four M14 bolts. Contact pressure at the joint was varied by using torque values ranging from 35 to 85 N m, typical for machine tool joints, applied to the fastening bolts to evaluate the effect of increasing contact pressure or clamping force on the thermal contact conductance value across the joint. Since both rectangular plates were of similar material and dimensions, the thermal contact conductance was calculated using equation (1) [20]:

$$hc = \frac{Q'k}{Ak\Delta T - 2Q'\Delta L} \quad (1)$$

where h_c is the thermal contact conductance and k is the thermal conductivity of steel. Clamping forces were calculated using equation (2) [21]:
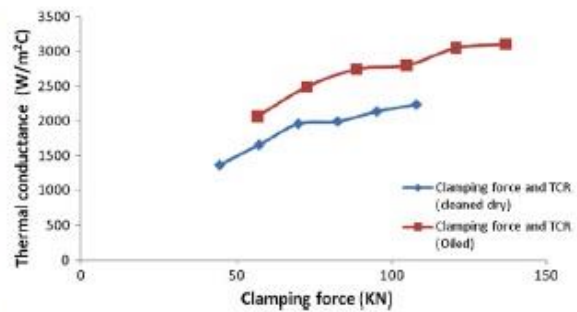
$$Pi = T/KD \quad (2)$$

Figure 1. Clamping force and thermal contact conductance values in cleaned dry and oiled conditions.

where *Pi* is the clamping force, *T* is the torque applied, *K* is the torque coefficient and *D* is the bolt nominal diameter. Here, *K* can be calculated using equation (3) [21]:

$$K = \{[0.5p/\pi] + [0.5\mu t(D - 0.75p\sin\alpha)/\sin\alpha] + [0.625\mu cD]\}/D, \quad (3)$$

where

D	is the bolt nominal shank diameter,
p	is the thread pitch (bolt longitudinal distance per thread),
α	is the thread profile angle $= 60°/2$,
μt	is the thread coefficient of friction and
μc	is the collar coefficient of friction.

In phase 2, the same test was repeated with oil applied to the plate's contacting surfaces and bolt threads to change the condition from dry to wet or from clean to contaminated. As expected, an increased trend of thermal contact conductance was observed with increasing torque and from dry to oiled conditions. The values were applied to the FEA models to predict the structural thermal behaviour. Figure 1 shows the clamping force and thermal contact conductance profiles in dry cleaned and oiled conditions.

From machine manufacturer data the spindle is clamped to the carrier using six bolts tightened to 70 N m in dry conditions. A thermal contact conductance value of 2520 W m^{-2} °C^{-1} was extrapolated using the exponential curve fitting technique on the above data and used at the carrier/spindle interface.

3. Machine FEA modelling setup

For quick and optimized analyses, idealized models of small VMC CNC machine structural elements such as spindle, carrier, tool (test mandrel), bearings, column, base, saddle and table were created and assembled in Abaqus 6.7–1. The model is further simplified by the symmetrical design of the machine. Small details such as fillets and chamfers were neglected. The bearings, belt drive and motor supporting structures were represented as major heat generation sources. Figure 2 shows the created model of the assembly.
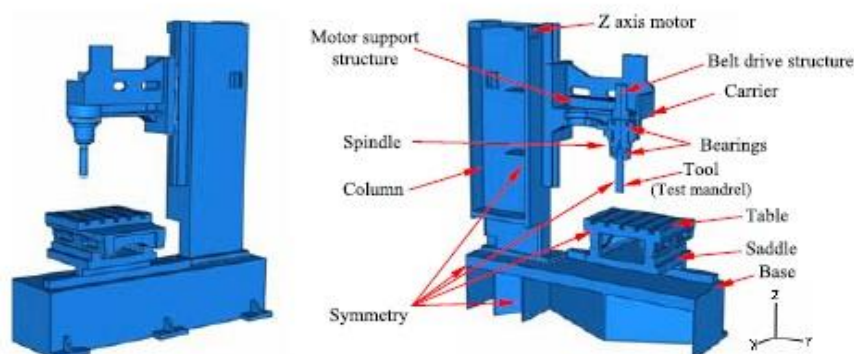
2

N S Mian *et al*

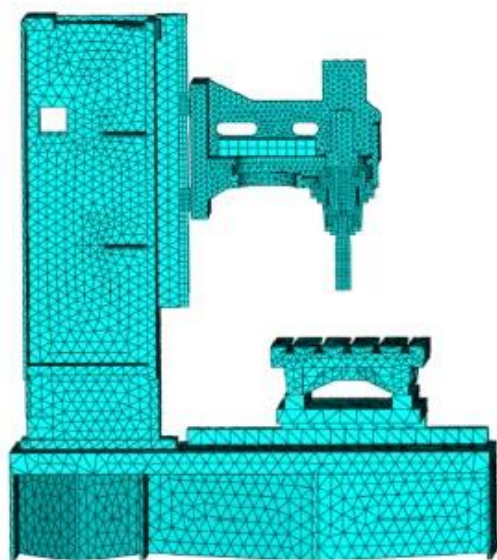**Figure 2.** Generated CAD model of the machine assembly.

Figure 3. Meshed model of the machine.

3.1. Boundary conditions applied to the machine model

3.1.1. Meshing and applied constraints. The model was meshed using tetrahedral, hexahedron and hexahedron dominated (hexahedron/wedge) elements where applicable using Abaqus default meshing technique. A higher density mesh was chosen for the structures neighbouring the heat sources compared to the rest of the structure to ensure sufficient nodes for accuracy and data extractions. Meshing revealed the total of 49 919 elements and 20 418 nodes. Figure 3 shows the meshed assembly of the machine.

The machine model was applied with the symmetry constraint at surfaces from where the machine was halved. The base was fixed from the bottom of the supports using displacement constraint. Boundary conditions were applied with the measured initial and ambient temperatures explained in section 5. Figures 4 and 5 show the information about the applied symmetry and displacement constraint position respectively.

Material properties The machine under research has three major materials, i.e. steel, cast iron and an invar test mandrel. These material properties were assigned to their respective structures in the FEA software. Cast iron was applied to the Carrier head; steel was applied to the spindle, bearings, column, guide ways, carriages, base, saddle and table; and invar was applied to the test mandrel. The material properties of steel, cast iron and invar are presented in table 1.

All simulations were performed as transient thermal simulations.

4. Machine testing

For determining the accuracy of the results, it was necessary to devise an efficient strategy to calculate the convective heat transfer coefficient (h) due to airflow across test mandrels or generic tooling. A thermal imaging camera was set up to view the heat sources and temperature variation around the spindle housing and test mandrel.

4.1. Determination of the convective heat transfer coefficient (h)

4.1.1. Testing procedure. The Flir Thermacam S65 thermal imaging camera was placed at a position where the test mandrel, spindle housing and carrier head were visible. A temperature sensor was positioned adjacent to the test mandrel to measure ambient temperature change during the heating and cooling phases. The spindle was rotated at 8000 rpm (see section 5 for speed selection) for 1 h and stopped for a cool-down period. The heating and cooling cycle data were recorded with thermal imaging (1 Hz).

Figure 6 shows the temperature obtained from the surface of the test mandrel. The plot shows that when the spindle started, the heat was continuously being convected during the tool rotation which causes the test mandrel temperature increase with slow progression; however, the temperature started to increase after spindle stop.
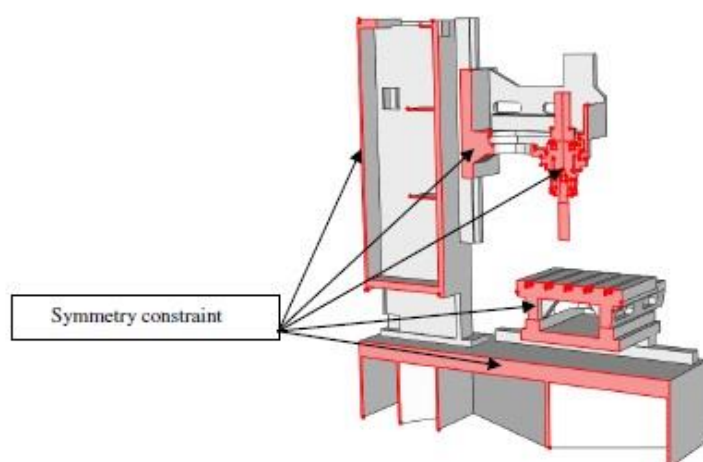
3

N S Mian *et al*

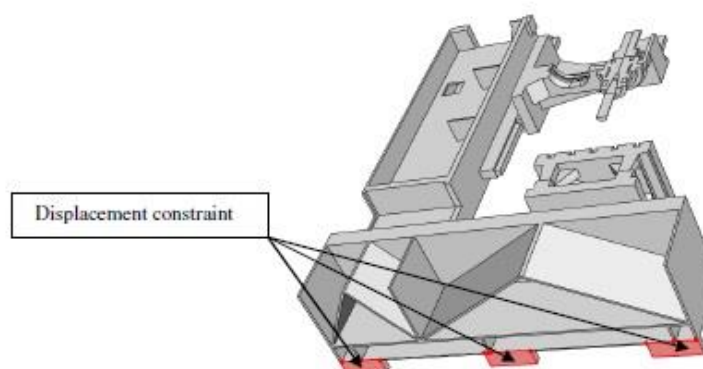**Figure 4.** Location of the applied symmetry constraint.

Figure 5. Location of the applied displacement constraint.

Table 1. Properties of steel, cast iron and invar.

	Steel	Cast iron	Invar	Units (mm)
Conductivity (k)	51.9	52.329	15	mJ (mm °C)$^{-1}$
Density	7.805×10^{-9}	7.2×10^{-9}	8.20×10^{-9}	tonne mm^{-3}
Specific heat capacity (C_p)	$473 \times 10^{+6}$	$506 \times 10^{+6}$	$525 \times 10^{+6}$	mJ (tonne °C)$^{-1}$
Modulus of elasticity	205 000	124 000	145 000	N mm^{-2}
Coefficient of linear expansion	11.7×10^{-6}	9×10^{-6}	1.2×10^{-6}	m (m °C)$^{-1}$
Poisson's ratio	0.3	0.24	0.3	

This explains that the cooling effect present during the tool rotation was stopped and the energy from the spindle started to flow inside the mandrel causing its temperature to rise. The convection coefficient h was calculated as 92 W m^{-2} °C^{-1}. This value was applied to the test mandrel during the heating cycle simulations. Similarly, the convection values for the spindle (9 W m^{-2} °C^{-1}), carrier head (2 W m^{-2} °C^{-1}), table (12 W m^{-2} °C^{-1}), base (0.1 W m^{-2} °C^{-1}) and column (5.7 W m^{-2} °C^{-1}) were obtained and a rounded average of 6 W m^{-2} °C^{-1} was used in simulations.

5. Machine testing at 8000 rpm (online test)

5.1. Thermal testing

Initially, 3 h testing was conducted; the first hour was monitored to determine the thermal behaviour for the machine structure after deactivating the E-Stop. Deactivating the E-Stop causes some motors and drives to activate which are used to hold structural parts in place. The activation of the drives causes some motors to heat up. For example, the Z-axis motor holds the Z-axis in position causing heat flow into the column. This procedure was performed in order to
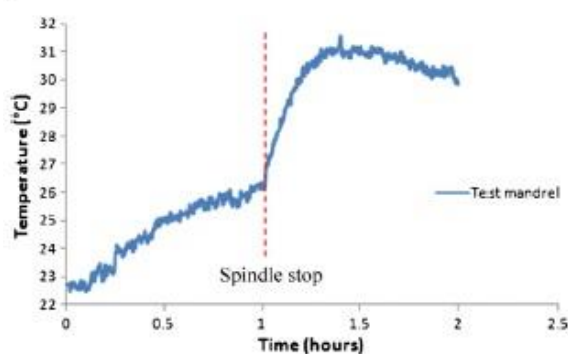
4

N S Mian *et al*

Figure 6. Temperature measured at the test mandrel upper surface.

achieve stabilized initial conditions before the actual testing to reduce uncertainties. The 1 h machine stabilization period was followed by a 1 h heating and 1 h cooling cycle. The machine spindle was tested at its highest spindle speed of 8000 rpm to assure maximum thermal behaviour. The thermal data were recorded using 65 temperature sensors located in unique strips [22] at the surface of the carrier and spindle boss considered as thermal key points, explained by White *et al* [23] along with six other temperature sensors positioned around the machine to measure ambient temperatures. Figure 7 shows the positions of surface sensor strips and ambient sensors around the machine. Thermal imaging was also used to capture data every 10 s to observe the spatial and temporal temperature distribution and location of the heat sources.

Heat drawn from the machine often creates air pockets which reduce the cooling rate of the machine. The heat that stays within air pockets causes the temperature magnitude to remain relatively higher than the normal ambient which effectively causes associated structures to respond often significantly after spindle stops when cooling takes place. The observation of the machine revealed that one side of the column was very close to the fitted electrical cabinet, the front of the column was close to the carrier head and the gap between the column and the carrier head serves to be a potential air pocket.

The column itself is a hollow structure used to route machine cables which also generate a localized heat source. Therefore, three out of six ambient sensors were placed in proximity to the air pockets.

5.2. Displacement testing

Five non-contact displacement transducers (NCDTs) were placed around a test mandrel to monitor the displacements of the tool in the X, Y and Z axes due to the thermal effect produced during the 1 h spindle heating and cooling test. The stabilization period revealed the machine displacement error range of approximately 3 μm in Z and 1 μm in Y (figures 9 and 10) which is suspected to be caused by the column bending due to the Z-axis motor-generated heat. During the heating and cooling test, the machine was observed to exhibit a displacement error of approximately 70 μm in Y and approximately 23 μm in Z (results in section 8). The errors in the X-axis are considered negligible because of the symmetry of the machine.

6. Offline simulations and assessments

Thermal data obtained from 1 h heating were analysed and applied to the FEA simulation model for offline thermal assessment. The data obtained from experiments was converted into thermal loads and applied as body heat fluxes generated by the heat sources in the simulation. This methodology was validated through benchmark tests to simulate heat distribution originating from those complex or rotating structures where thermal sensors are hard to install. For example, the temperature from the bearings housed in the spindle could not be measured directly therefore the data were obtained from the spindle surface. Since bearings are the main heat sources in the rotating spindle, surface temperature was converted into thermal load and applied to the bearing by calculating the energy required for the temperature change provided with the specific heat capacity of the associated material. To accurately calculate the heat flux, the temperature
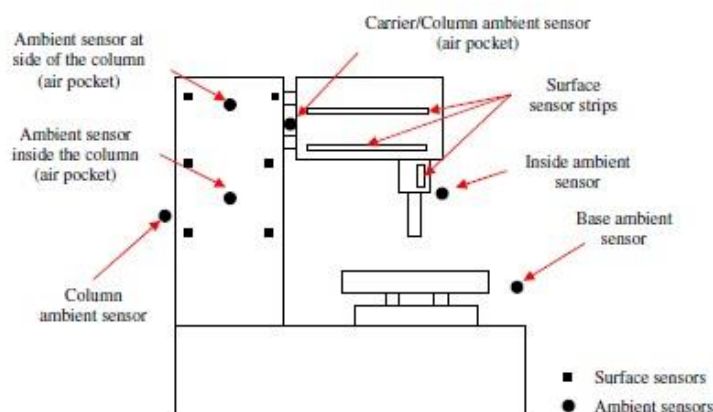

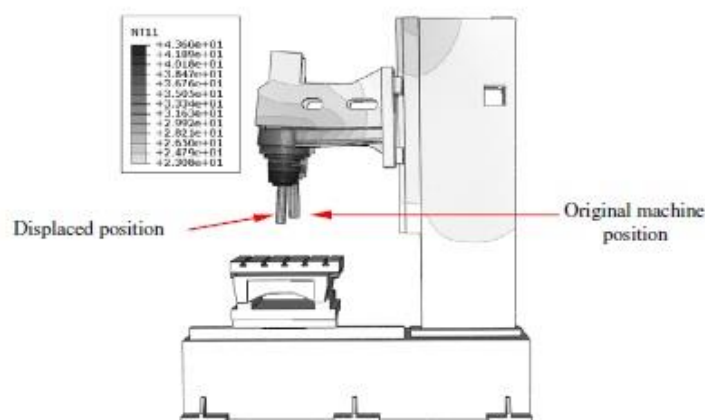**Figure 7.** Position of the ambient sensors around the machine.

5

Figure 8. Deformations in the machine due to temperature distribution (NT11 = temperature (°C)).
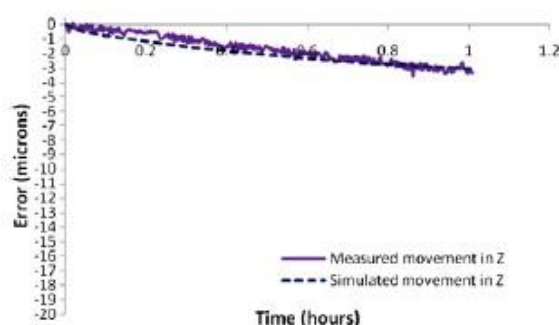

Figure 9. Z-axis movement during the stabilization period.
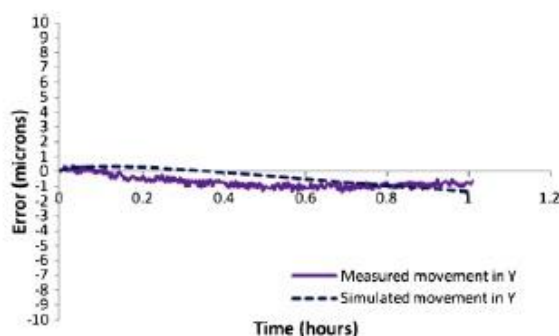

Figure 10. Y-axis movement during the stabilization period.

rise of the top of the test mandrel was also measured using thermal imaging. This temperature rise is due to the heat energy entering into the test mandrel, i.e. the energy loss from the spindle. This energy was accounted for when obtaining the heat flux value and added to the obtained heat flux value for the lower bearing. Similarly, the surface temperature data from thermal image and carrier mounted sensors were analysed and converted into body heat fluxes for the belt drive and spindle motor housing area. Ambient conditions were applied as sink temperatures in the software. Those areas of the machine which were considered as air pockets were separately selected within the machine CAD model and applied with the ambient temperatures measured by the temperature sensors placed in the air pockets (figure 7).

6.1. Calculations

Equation (4) was used to obtain the total energy (Q'), i.e. the energy generated by the heat source and the energy loss from the body housing that heat source. The Q' was then divided by the volume of concerned heat source to obtain the body heat flux value to be applied in the simulations. Short test periods of up to 1 h should be sufficient to obtain a measurable

Table 2. The calculated body heat flux values for 4000 and 8000 rpm spindle speeds.

	Body heat flux (mW mm^{-3})	
	4000 rpm	8000 rpm
Lower bearings	0.06	0.34
Upper bearing	0.11	0.49
Carrier belt drive	0.37	1
Spindle belt	0.33	0.56
Z-axis motor	0.23	0.23
Spindle motor mounts	0.08	0.137

increase in surface temperature for the calculations. Radiation is negligible due to the low working temperatures:

$$Q' = mCp\Delta T/t + hA\Delta T. \qquad (4)$$

Body heat flux values obtained at 8000 rpm and are shown in table 2. The values shown for the 4000 rpm spindle speed will be discussed in section 9.

These heat flux values were applied to the respective heat sources and the simulation was set for 3 h; 1 h stabilization, 1 h heating followed by 1 h cooling.

Figure 8 shows the simulated temperature gradient distribution in the column, spindle, carrier and test mandrel
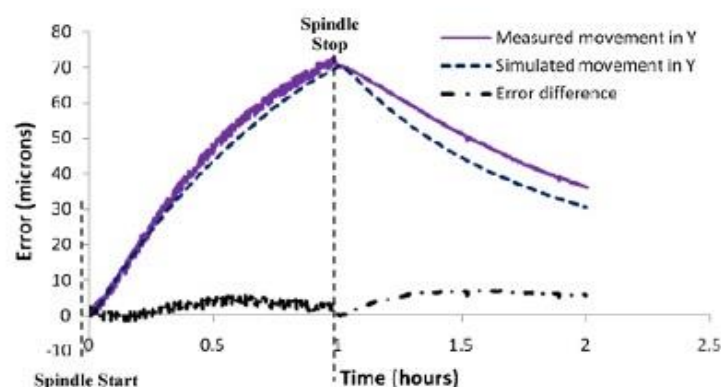
6

N S Mian *et al*

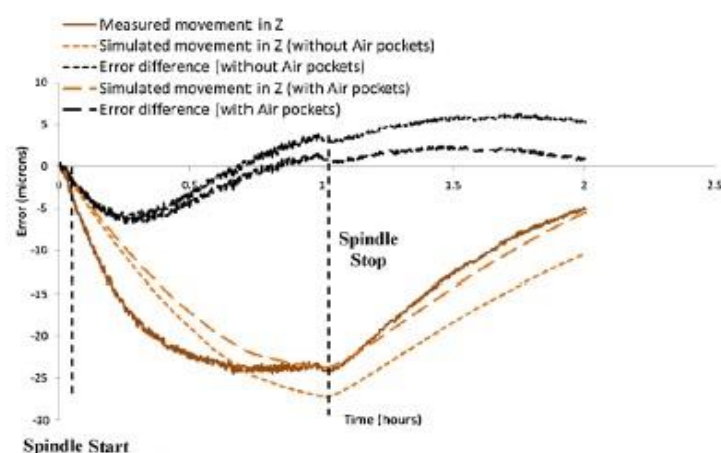**Figure 11.** *Y*-displacement profiles agreement (high spindle speed test).

Figure 12. Z-displacement profiles agreement (high spindle speed test).

after a 1 h heating cycle; and the thermal deformation of the machine.

7. Temperature and displacement simulation results (offline assessment)

7.1. Result agreements (1 h heating/1 h cooling)

The first step was to check the agreement of the simulated stabilization period result and the experimental stabilization period result. The simulated data were extracted from the nodes located at the actual displacement sensor locations used to monitor *Y* and *Z* axes. The error difference range between the measured and the simulated profiles in figures 9 and 10 was observed to be less than a micron and therefore considered negligible. The axis scale was increased to observe the profile shape.

The agreements of heating and cooling cycles are shown in figures 11 and 12. The black profile in the plot shows the magnitude of the difference between measured and simulated profiles.

Very good agreement was found between the measured and simulated displacement profiles of 87% for the *Y*-axis and 63% for the *Z*-axis. The Z-axis plot also shows the comparison of profiles with and without air pockets revealing improved agreement after their consideration. The simulation took approximately 30 min (the computer used to perform the simulation had an AMD Phenom 9950 Quadcore 2.60 GHz processor, 4 GB of RAM, NVIDIA GeForce 9400 GT graphics card and Windows XP 32 bit operating system). The residual error in the agreement remained under 10 μm for both axes. The drift of the simulated *Y*-axis error from the measured error is suspected to be due to the slow rate of change of the structural temperature due to local environmental changes. The heat convected during the heating cycle is confined within structural pockets which effectively increases local associated ambient temperatures and therefore reduce the cooling rate. The measured ambient temperatures were applied as single values to each structure and those values were kept constant during both heating and cooling cycle simulations and therefore underestimated the slow rate of change of the actual ambient temperature around local structure vicinities and resulted in
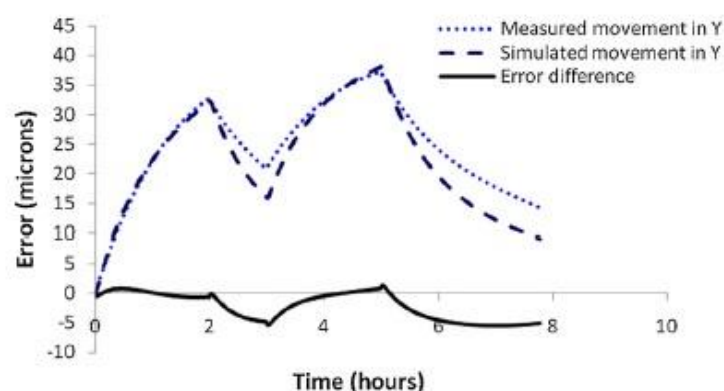
7

Figure 13. *Y*-displacement profiles agreement (step heat and cool cycle).

Table 3. Agreement ranges obtained for more tests conducted at 4000 rpm.

4000 rpm	Agreement ranges (%)		Agreement ranges (%)	
	Short term test (1 h heating/1 h cooling)	Residual errors (μm)	Long term test (3 h heating/2 h cooling)	Residual errors (μm)
Y-axis	83%	6 μm	81%	6 μm
Z-axis	71%	2 μm	71%	4 μm

a higher simulated cooling rate compared with the measured result. This elaborates the importance of considering the rate of change of ambient temperatures during and after machining operations.

8. Machine testing at 4000 rpm

The technique of calculating heat fluxes from the surface temperatures and predicting the thermal displacement behaviour offline was further validated at a different spindle speed of 4000 rpm for the VMC used. The 3 h test was repeated. Thermal data from the heat sources were collected to calculate the new values for the heat fluxes at this speed listed in table 2 and a new convection value h of 58 W m^{-2} $^\circ$C^{-1} for the rotating test mandrel. The calculated information is used in the next section.

8.1. Step heating and cooling test (4000 rpm)

Extended thermal trials on production machine tools necessitate expensive or impractical machine downtime; therefore, one of the greatest advantages of improving offline simulation capability is to enable characterization of the machine to a reasonable accuracy over such medium- and long-term periods. This section is specifically targeted towards obtaining good agreements for a long-term complex duty cycle. This time, the task was to use the established coefficients in an FEA simulation and validate on the experimental results from a complex duty cycle. The duty cycle was composed of 9 h with 1 h stabilization, two 2 h heating cycles with 1 h cooling gap and 3 h cooling in the end. The simulation used the same body heat flux values listed in table 2. After simulations,

the machine was then tested for the same duty cycle at the spindle speed of 4000 rpm.

8.1.1. Profile agreements. Figure 13 shows the results and again very good agreement of 82% was obtained for the displacement error profiles in the *Y*-axis direction; whereas, the *Z*-axis was 70%. The residual error remained under 7 μm for both *Y* and *Z* axes.

More tests conducted at 4000 rpm with short- and long-term duty cycles also revealed very good agreement. Table 3 summarizes the results.

9. Discussion

The simulated results were revealed to be in good agreement with the measured results; however, further improvements may be possible to reduce the drifting of the simulated profiles from the measured. Since a single value of the ambient temperature was used during simulations, defining ambient temperatures as a transient function in the software may increase the agreement percentage especially during the cooling cycle. Also, vertical temperature gradients around the machine are suspected to have a contribution on the overall thermal behaviour of the machine especially during long-term simulations. It is proposed to increase the number of temperature sensors and place them vertically on and around the machine to measure the vertical temperature gradients (surface and ambient); and sectioning the CAD model vertically for applying the measured initial temperature conditions and long-term ambient conditions accordingly to the sectioned structural elements (figure 14). Detailed
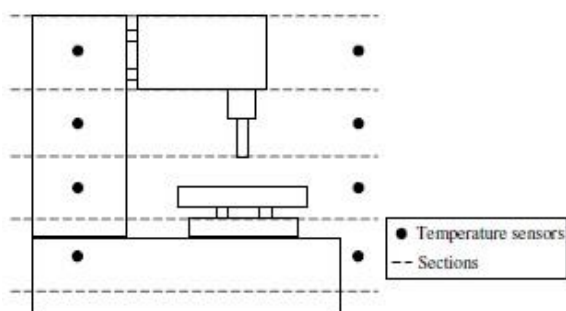
8

N S Mian *et al*

Figure 14. Proposed temperature measurement and simulation technique.

assessments of isotherms in the machine structural elements neighbouring heat sources could improve the calculated body heat flux values and therefore the simulated results.

10. Conclusion

Thermal distribution and its associated error in a small VMC CNC machine tool were studied and analysed experimentally and predicted offline using FEA. Heat transfer experiments between contacting surfaces in assemblies and structural linkages were given high importance to obtain accuracy in FEA results. In-depth experimental work has been carried out to obtain the thermal behaviour in the machine structure by running the machine, extracting detailed temperature and displacement data to calculate relevant heat fluxes for offline analyses. The machine was tested for its thermal characteristics at 8000 rpm spindle operating speed. The temperature data obtained from the testing were used to simulate the behaviour of the machine and the results were well correlated. The technique was further validated by operating the machine at 4000 rpm spindle speed for a variety of duty cycles. All simulated results (4000 rpm and 8000 rpm) obtained were in close agreement ranging between 65% and 90% when compared with the measured movements. The residual error remained under just 10 μm. The body heat flux methodology and FEA simulation enable quick and efficient offline assessments of temperature distribution and displacement in machine tool structures; this results in a significant reduction in machine non-productive downtime and can provide significantly more thermal data for the creation and validation of robust long-term error compensation models or design changes

Since machine downtime is a dominant issue within manufacturing industries, the technique discussed provides a method where the machine downtime can be reduced using offline simulation techniques for extended and complex real-world machine operations. Rapid CAD model development, testing of the machine for a relatively small time period, the use of the calculated heat loads at a particular spindle speed for extended simulations without testing the machine, and FEA, which itself is a quick computational technique in terms of computer resource usage, are well-achieved advantages of this work.

References

[1] Fletcher S 2001 Computer aided system for intelligent implementation of machine tool error reduction methodologies *PhD Thesis* University of Huddersfield

[2] Bryan J 1990 International status of thermal error research *Ann. CIRP* **39** 645–56

[3] Pahk H J and Lee S W 2002 Thermal error measurement and real time compensation system for the CNC machine tools incorporating the spindle thermal error and the feed axis thermal error *Int. J. Adv. Manuf. Technol.* **20** 487–94

[4] Du Z C, Yang J G, Yao Z Q and Xue B Y 2002 Modelling approach of regression orthogonal experiment design for the thermal error compensation of a CNC turning centre *J. Mater. Process. Technol.* **129** 619–23

[5] Wu C-H and Kung Y-T 2006 Thermal analysis and compensation of a double column machining centre *Proc. Inst. Mech. Eng.* B **220** 109–17

[6] Ramesh R, Mannan M A, Poo A N and Keerthi S S 2003 Thermal error measurement and modelling in machine tools: II. Hybrid Bayesian network-support vector machine model *Int. J. Mach. Tools Manuf.* **43** 405–19

[7] Yang H and Ni J 2005 Dynamic neural network modelling for nonlinear, nonstationary machine tool thermally induced error *Int. J. Mach. Tools Manuf.* **45** 455–65

[8] Chen J-S 1997 Fast calibration and modelling of thermally-induced machine tool errors in real machining *Int. J. Mach. Tools Manuf.* **37** 159–69

[9] Yuan J and Ni J 1998 The real-time error compensation technique for CNC machining systems *Mechatronics* **8** 359–80

[10] Kang Y, Chang C-W, Huang Y, Hsu C-L and Nieh I-F 2007 Modification of a neural network utilizing hybrid filters for the compensation of thermal deformation in machine tools *Int. J. Mach. Tools Manuf.* **45** 376–87

[11] Wu C-H and Kung Y T 2003 Thermal analysis for the feed drive system of a CNC machine centre *Int. J. Mach. Tools Manuf.* **43** 1521–8

[12] Kim B J, Van Tyne C J, Lee M Y and Moon Y H 2007 Finite element analysis and experimental confirmation of warm hydroforming process for aluminium alloy *J. Mater. Process. Technol.* **187–188** 296–9

[13] Jedrzejewski J, Kowal Z, Kwasny W and Modrzycki W 2005 High-speed precise machine tools spindle units improving *J. Mater. Process. Technol.* **162–163** 615–21

[14] Zhou J M, Andresson M and Stahl J E 2004 Identification of cutting errors in precision hard turning process *J. Mater. Process. Technol.* **153–154** 746–50

[15] Haitao Z, Jianguo Y and Jinhua S 2007 Simulation of thermal behaviour of a CNC machine tool spindle *Int. J. Mach. Tools Manuf.* **47** 1003–10

[16] Ratchev S, Liu S, Huang W and Becker A A 2006 An advance FEA based force induced error compensation strategy in milling *Int. J. Mach. Tools Manuf.* **46** 542–51

[17] Hibbitt, Karlsson and Sorensen, Inc 2000 *ABAQUS/CAE User's Manual 6.1.* Pawtucket, RI, USA

[18] Ramesh R, Mannan M A and Poo A N 2000 Error compensation in machine tools—a review: II. Thermal error *Int. J. Mach. Tools Manuf.* **40** 1257–84

[19] Attia M H and Kops L 1979 Nonlinear thermoelastic behaviour of structural joints—solution to a missing link for prediction of thermal deformation of machine tools *ASME Trans., J. Eng. Ind.* **101** 348–54

[20] Hagen K D 1999 *Heat Transfer with Applications* (Upper Saddle River, NJ: Prentice-Hall) ISBN: 0-13-520941-2

[21] Euler G D 2010 Bolt preload calculation [Online]. Available at http://euler9.tripod.com/fasteners/preload.html (accessed 15 December 2010)

9

[22] Fletcher S, Longstaff A P and Myers A 2007 Measurement methods for efficient thermal assessment and error compensation *EUSPEN Topical Meeting 'Thermal Effects in Precision Engineering' (3–4 December 2007, Maastricht, The Netherlands)* pp 48–50

[23] White A J, Postlethwaite S R and Ford D 2001 Measuring and modelling thermal distortion on CNC machine tools *5th Int. Conf. on Laser Metrology and Machine Performance—Lamdamap (University of Birmingham)* pp 69–79

10

2012-06 An efficient offline method for determining the thermally sensitive points of a machine tool structure.

An efficient offline method for determining the thermally sensitive points of a machine tool structure

N.S. Mian, S. Fletcher, A.P. Longstaff and A. Myers
University of Huddersfield, Queensgate, HD1 3DH, UK

Abstract. Whether from internal sources or arising from environmental sources, thermal error in most machine tools is inexorable. Out of several thermal error control methods, electronic compensation can be an easy-to-implement and cost effective solution. However, analytically locating the optimal thermally sensitive points within the machine structure for compensation has been a challenging task. This is especially true when complex structural deformations arising from the heat generated internally as well as long term environmental temperature fluctuations can only be controlled with a limited number of temperature inputs. This paper presents some case study results confirming the sensitivity to sensor location and a new efficient offline method for determining localized thermally sensitive points within the machine structure using finite element method (FEA) and Matlab software. Compared to the empirical and complex analytical methods, this software based method allows efficient and rapid optimization for detecting the most effective location(s) including practicality of installation. These sensitive points will contribute to the development and enhancement of new and existing thermal error compensation models respectively by updating them with the location information. The method is shown to provide significant benefits in the correlation of a simple thermal control model and comments are made on the efficiency with which this method could be practically applied.

Keywords: Finite element analysis, FEA, Matlab, Thermal error, Thermal error compensation, Thermally sensitive locations

1.1 Introduction

Thermal errors have been identified as a major contributor to the overall volumetric error of a machine tool, in many cases up to 70% [1]. Several techniques based on analytical, empirical and numerical methods have been established to control the effect of thermal errors. These techniques are widely used and applied with a basic ideology to establish a thermal model based on relationships between the measured temperature of the machine from various locations, used as temperature inputs and the displacement at the tool [2]. The temperature inputs however in some cases may be difficult to identify if propagation of the temperature gradients is complex due to the combined effect of internal and external heat sources and perhaps due to the complexity of the machine structure. These ambiguities therefore add complexities to identify sensitive locations within the structure and stands out to be a challenging task with a limited number of temperature inputs. It has been observed that the performance of the conventional empirical and statistical approaches such as Artificial Neural Network (ANN) and Linear Regression [3, 4] heavily rely on the data from sensitive location within the machine structure for effective and robust thermal compensation such as varying environmental conditions. Kang et al [5] used a hybrid model consisting of regression and NN techniques to estimate thermal deformation in a machine tool. The total of 28 temperature sensors were placed on (18) and around (10) the machine to acquire internal heating and environmental data. The training time for the model was 3 hours. Yang et al [6] tested a INDEX-G200 turning centre to model thermal errors. Temperature variables were selected using engineering judgement as temperature sensors were placed on or near the possible heat sources and Multiple Linear Regression technique was used to model thermal errors. Training time for the thermal model however was not mentioned. Krulewich [7] used the Gaussian integration method using polynomial fit to identify the optimum thermal points on the machine spindle. The spindle was put through heating and cooling cycles providing 3.5 hours of training data to locate three optimum measurement points where the results correlated to 96%. The author compared this method with a statistical technique and found that the Gaussian integration method requires significantly less training data.

It has been observed that a significant amount of data is generally required to identify sensor locations and train models which inevitably requires machine downtime therefore such methodologies can be impractical for general application. It is also the fact that machine structures are sensitive to environmental changes which means that the training data acquired in the first instance may not respond well to the new conditions and therefore

2   N.S. Mian, S. Fletcher, A.P. Longstaff and A.Myers

a new set of training data may be required [7]. This paper presents an offline technique based on FEA. The technique provides the ability to identify optimised sensitive locations within the machine structure offline for any set of data either from internal heating or external environmental conditions. Being software based, using the Graphical User Interface (GUI) of the FEA software, this technique integrates the visual aspect to aid reviewing the location of the sensitive areas and the practicality for sensor installations. The application of this technique requires minimal machine downtime as any set of the measured thermal conditions can be assessed offline to obtain the thermal behaviour of the machine. This means that new sensitive areas inside the machine structure may be located according to the new thermal conditions. Satisfactory correlations between the measured and the FEA simulated results are a pre-requisite to the application of this technique. In this paper, this technique is applied on the results from simulation case study previously conducted.

1.2   Case Study

This study was conducted on a 3 axis Vertical Machining Centre (VMC) located on the shop floor with uncontrolled environmental temperature. The machine FEA model was created in Abaqus/Standard 6.7-1 FEA software [10] using manufacturer provided engineering drawings. Fig 1.1 shows the generated CAD model of the machine. The model of the machine was simplified by cutting into half because of the symmetry in the X axis direction and complex structures such as fillets and chamfers were simplified and represented using simple corners to avoid complexity of meshing and nodes.
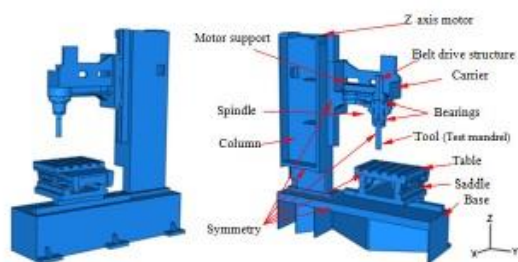

Fig 1.1 Generated CAD model of the machine assembly

Mian et al [8, 9] conducted tests to exploit the thermal behaviour of the VMC when subjected to the spindle heating and varying environmental conditions. Mian [8, 9] proposed a technique in which only one short term data set obtained during one hour internal heating is required to obtain thermal parameters and simulate the heat transfer within structures. This short term data set is used to create the FEA thermal model to simulate the machine for a variety of real world testing regimes. The results showed good correlation between the experimental results and the FEA simulated results typically between 70% and 80%. Mian [9] also conducted environmental tests where

the machine was tested for three continuous days in two seasons (winter and summer). The aim was to achieve good correlation in results from one season test and validate the methodology with good correlation results in different environmental conditions i.e. in a different season. Both tests successfully validated the FEA environmental thermal model with good correlations typically above 60%. This technique in effect can remarkably reduce the machine downtime by creating the CAD model of the machine in the FEA software and simulate it to create an environmental thermal model that is able to simulate the effect of any set of varying environmental conditions.

This method therefore provides a platform to use FEA modelling as an offline tool to determine not only machine behaviour, but also help with the development of compensation models by determining the location of sensitive nodes/areas. The case study by Mian [8, 9] was therefore used for differentiating between areas sensitive to internal heating and environmental temperature fluctuations.

The remainder of the paper details a method and the developed software for the offline assessment of the FEA data and help determine the temperature-displacement sensitive nodes based on search parameters and their physical locations within the FEA model. The information can be used to retrofit sensors for compensation; however there can be practical limitations to their attachment.

1.3   Nodal data extraction

The Abaqus simulation software provides the facility to extract surface and sub-surface nodal data within the FEA model. Since the model has to be meshed for FEA analysis, the nodes from the mesh can be used to represent individual points on the structure. Therefore using this facility, the nodal data was extracted to find nodes of interest. The predicted error is obtained as the difference in displacement between a node on the table and a node on the tool. In this case the dependant parameters are slope and hysteresis.

The slope is simply the magnitude of displacement for any given change in temperature ($°C/\mu m$). Hysteresis is caused by the time lag involved with typical surface temperature measurement which is related to the distance between the temperature sensor and the true effective temperature which is causing the distortion. A node location with high slope sensitivity will require lower resolution in the measurement of temperature and induce less noise when applied in models as described later. The lowest hysteresis will represent that area that relates well to thermal displacement and responds in a linear fashion whether the machine is being heated or cooled. The nodal date is extracted from Abaqus and the files are converted

and imported into Matlab software. Matlab functions were written to calculate the slope and hysteresis for each node and return the best ones with respect to an axis.

1.3.1   Matlab program routines

The function imports the nodal data from the FEA software and extracts the error between the tool and workpiece in each direction, and the temperature of all the nodes. Then it calculates the slope (°C/μm) using a linear least square fit and hysteresis (μm), using deviation from the straight line, for all nodes. These are compared against a predefined set of ranges to filter out the best nodes. The range may be set based on the resolution of the temperature sensors and required accuracy for compensation. There can be thousands of nodes depending on the mesh density of the machine model. If no nodes are found then the range must be widened. The nodes are filtered for slope and hysteresis separately to maintain flexibility so that different nodes can be used for different jobs, not always both. The final node numbers satisfying both filters are then used to locate their positions in the CAD model of the relevant structure. Fig 1.2 shows the function calls where comparison takes place using a specified range, in this case the range for the slope sensitivity is from 0.17 °C/μm (min) to 0.20 °C/μm (max) and 5.44 μm (min) to 8 μm (max) for the hysteresis. The first and second lines filter out node numbers for the slope sensitivity and hysteresis respectively using the range. The third line is then used to match node numbers in both arrays and obtain the matched nodes numbers. Fig 1.3 shows the Matlab array editor displaying 8 nodes filtered out from the total of 4113 from the carrier (Fig 1.6) structure mesh. The first column shows node number, the second column shows slope sensitivities and the third column shows the hysteresis values. These 8 nodes have shown to have the highest slope sensitivities (Fig 1.4) and the lowest hysteresis values and will effectively be used to place permanent temperature sensors for use in error compensation systems. It can also be observed that nodes 738 and 739 possess the highest slope sensitivity among the other filtered nodes and a slightly higher hysteresis values relative to other filtered nodes, however an agreement can be obtained to prioritize the selection of nodes that were located at the surface for practical installation of temperature sensors. This priority may not be the case if slope sensitivities and hysteresis values are significant at node positions inside the structure.

Fig 1.2 Part of Matlab program code for assigning range

Fig 1.3 Filtered nodes
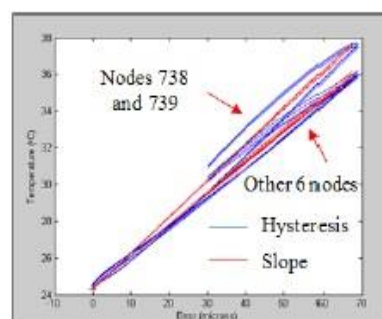
Fig 1.4 Slope and hysteresis plot

1.4   Internal heating test – Carrier sensitivity against the Y axis and Z axis displacement

Since the carrier holds the spindle in place, it is the most affected structure as the heat from the spindle flows directly into it. Therefore this structure was analysed to locate the temperature-displacement sensitive nodes for internal heating. Fig 1.5 shows the visual representation of the simulated deformation of the machine.
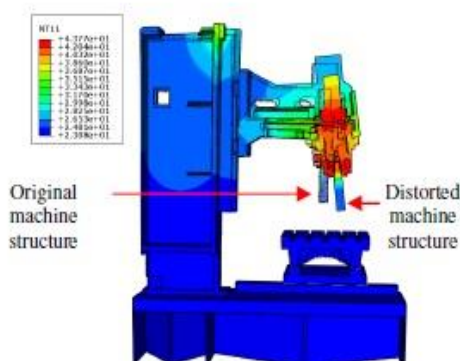
Fig 1.5 Simulated visual representation of deformation of the machine due to internal heating

4   N.S. Mian, S. Fletcher, A.P. Longstaff and A.Myers

Fig 1.6 shows the best surface nodes found using the Matlab search routine. Other visible nodes are inside the structure.
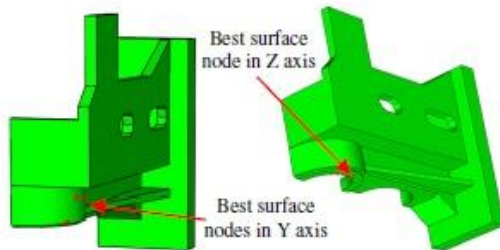
Fig 1.6 Nodes sensitive to spindle heating on the carrier

Fig 1.8 Environmental sensitive nodes within the full machine

1.5   Validations

Using the similar approach shown in section 1.3.1, the best identified surface node (Fig 1.6) was checked which give the sensitivity of 0.20°C / μm and hysteresis of 7μm. This linear fit gives a simple model for the Y axis of $5\Delta t_{int}$ - 106.5. This was applied to measured temperature data from a sensor fitted to the machine surface close to the identified node position, with correlation to measured displacement of 84% as shown in Fig 1.7.

Fig 1.7 Validation of the FEA model against measured error due to internal heating

1.5.1   Environmental sensitive nodes inside the full machine structure

Using the similar procedure the nodes sensitive to the varying environmental conditions, including different seasons, were found in the machine structure. During this preliminary work, each structure was a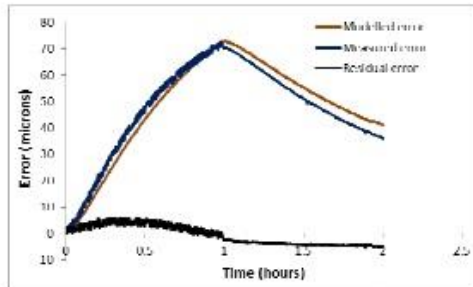nalysed individually for efficiency to locate sensitive nodes with the higher slope and lowest hysteresis approach. Future to consider the full machine structure as one component to locate the set of sensitive nodes. Fig 1.8 shows the full machine FEA model with highlighted environmental sensitive nodes individually located on components.

1.6   Conclusions

It has been observed that the simulation of thermal behaviour of complex machine structures using FEA can provide a solid platform for offline assessment of the machine error and model identification. FEA results from previously conducted case studies were used to locate nodes in the structural elements of a 3 axis VMC that were sensitive to temperature change and movement of the machine structure in Y and Z axes. Matlab functions were used to manipulate the extracted data from the FEA software, calculate the hysteresis and slope for any given node and filter out the best node locations by using a range of highest slope sensitivity and lowest hysteresis value. The location of the filtered nodes were analysed using the Abaqus GUI. The priority is given to surface nodes rather than the internal nodes for practical temperature sensor installation on the machine. The validation result showed the predicted sensitive nodal location correlated to better than 84%. By determining the best linear relationships, simple models are available and compatible with the common thermal compensation methods available in most modern NC controllers.

1.7   References

[1]   Bryan, J., International Status of Thermal Error Research (1990). CIRP Annals - Manufacturing Technology, 1990. 39(2): p. 645-656.

[2]   Chen, J.S. and G. Chiou, Quick testing and modeling of thermally-induced errors of CNC machine tools. International Journal of Machine Tools and Manufacture, 1995. 35(7): p. 1063-1074.

[3]   Tseng, P.C., A real-time thermal inaccuracy compensation method on a machining centre. International Journal of Advanced Manufacturing Technology, 1997. 13(3): p. 182-190.

[4]   Yang, S., J. Yuan, and J. Ni, The improvement of thermal error modeling and compensation on machine tools by CMAC neural network. International Journal of Machine Tools and Manufacture, 1996. 36(4): p. 527-537.

[5]   J Yang, J.G., et al., Testing, variable selecting and modeling of thermal errors on an INDEX-G200 turning center. International Journal of Advanced Manufacturing Technology, 2005. 26(7-8): p. 814-818.

[6]   Kang, Y., et al., Estimation of thermal deformation in machine tools using the hybrid autoregressive moving-average - Neural network model. Proceedings of the Institution of Mechanical Engineers, Part B: Journal of Engineering Manufacture, 2006. 220(8): p. 1317-1323

[7]   Debra A, Krulewich., Temperature integration model and measurement point selection for thermally induced machine tool errors. Mechatronics, 1998. 8(4): p. 395-412.

[8]   Mian, N.S., et al., Efficient thermal error prediction in a machine tool using finite element analysis. Measurement Science and Technology, 2011. 22(8): p. 085107.

[9]   Mian, N, Fletcher, S, Longstaff, A.P., Myers, A and Pislaru, C, Efficient offline thermal error modelling strategy for accurate thermal behaviour assessment of the machine tool. In: Proceedings of Computing and Engineering Annual Researchers' Conference 2009: CEARC'09. University of Huddersfield, Huddersfield, pp. 26-32. ISBN 9781862180857.

[10]   ABAQUS/CAE: Hibbitt, Karlsson and Sorensen, Inc., Pawtucket, RI 02860-4847, USA.

2013-02 The significance of air pockets for modelling thermal errors of machine tools.

The significance of air pockets for modelling thermal errors of machine tools

N. S. Mian, S. Fletcher, A. P. Longstaff, A. Myers
University of Huddersfield, Queensgate, Huddersfield HD1 3DH, UK
Email: n.mian@hud.ac.uk

Abstract

It is well known, especially with the prevalence of compensation for geometric errors, that thermal error represents the most significant proportion of the total volumetric error of the machine tool. Thermal error in machine tools originates from changes to internal and external heat sources that vary the structural temperature of the machine tool resulting in the non-linear deformation of the machine structure. The ambient conditions inside and around the machine vicinity are varied not only by the external heat sources but, equally importantly but less well understood, by the machine itself when local air pockets are warmed inside the voids of the machine during the machining process. Air pockets are areas within the machine structure where the localized heat convection rate is reduced by the heat confined within them causing the temperature to vary slowly relative to the other places of the machine. This results in a relatively slower response of the associated structure. Consideration for this effect is an important, yet often ignored element of thermal modelling which deteriorates the prediction capability of many thermal models.

This paper presents a case study where FEA (Finite Element Analysis) is used for the thermal modelling of a machine tool and the issue of air pockets is addressed by measuring and considering the temperature in voids. It was found that the consideration of the most significant air pockets improved the prediction capability of the FEA thermal model in the Z-axis direction from 50% to 62% when compared with the experimental results Z-axis. This paper highlights the significance of air pockets with regard to the thermal modelling and it is believed that the consideration of the temperature measurement inside voids of the machine structure and inclusion of their effect may significantly improve the performance of any thermal model.

1   Introduction

Thermal errors in machine tools are caused by temperature changes in the structure, which arise from internal and external heat sources. Non-uniform distribution of the temperature gradients leads to non-linear thermal expansion of structural elements, deteriorating the relation between the tool and workpiece positioning. There has been significant focus towards the development of error compensation models for thermal errors due to internal heat sources but relatively little on compensating for the effect of environmental temperature variations, although these are known to be significant, perhaps due in part to the associated machine downtime to measure the machine response. Predictive methods, such as finite element modelling (FEM) can be used to simulate such effects, but inaccuracy occurs with simplifications and uncertainties in the boundary conditions. This paper focuses on the effect of the localised heat confinement inside non-continuum solid areas i.e. structural voids within the machine tool containing pockets of air where the flow of heat to the surrounding environment is restricted. The surrounding structure typically responds slower to natural cooling relative to other assembly structures exacerbating the complexity of the machine distortion.

Several methods have been introduced to control thermal errors in machine tools from which the electronic compensation method can be considered as a cost effective and simple-to-implement solution which uses analytical, empirical and numerical approaches to create a relationship between the induced overall displacement between the tool and workpiece and the temperature change in order to compensate the error. Thermal error due to internally generated heat in machine tools has been the major focus among researchers. Hao [1] used a genetic algorithm-based back propagation neural network (GA-BPN) method using 16 thermistors placed at various location of a turning machine tool. The spindle, headstock, axis leadscrew and the bed were selected for temperature measurement to compensate dynamic and highly nonlinear thermal error, but only one ambient temperature sensor was used. The reported thermal error compensation improvement was 63% Du et al [2] applied an orthogonal regression technique to more than 100 turning centres of the same type and specifications. It was found that the technique was able to reduce the cutting diameter thermal error from 35μm to 12μm. The technique was stated as robust due to its year-round repeatable improvement in accuracy. The accuracy is expected to increase if long term shop floor environmental temperatures fluctuations were considered. Kim et al [3] analysed a ballscrew system for two dimensional temperature distributions both in real time and steady state using FEM. The proposed FEM model was based on the assumption that the screw shaft and the nut are solid and hollow cylinders respectively. The convective coefficient was also assumed to be constant. Huo et al [4] carried out an FEM analysis on a grinding machine aimed to integrate the effects of thermal deformation of the machine structure and the heat produced by the machining process. At first, the temperature distribution was simulated followed by validations by the on-machine measurements. The temperature information was

then used to estimate the thermal deformation. The machining process was also simulated to obtain the temperature distribution within the cutting zone and its effect on the machine. This temperature information was used as an input heat source to the FEM. The preliminary results for simulated temperature distribution and displacements in the Z-axis direction are shown for 3.6 minutes and quoted as, "promising". Environmental effects around the machine were not considered. A review conducted by Mayr et al [5] details the importance of measuring the effect of thermal errors in machine tools where, besides other important thermal error contributors such as coefficients of thermal expansions and conductivity of associated materials, attention is drawn towards the importance of taking into account the varying ambient conditions. Similarly, research from Longstaff et al [6] and Fletcher et al [7] also drew attention towards the effect of environmental fluctuations by conducting case studies on a variety of machines. In an attempt to monitor the environmental thermal error on machine tools, Mian et al [8] conducted research on a small 3 axis Vertical Machining Centre (VMC) production machine tool in order to model thermal errors using FEA. Two environmental thermal error tests, conducted in summer and winter, were reported to show variable overall temperature fluctuations. In summer the overall temperature fluctuated by 4°C, resulting in a deflection of 12μm in the Y axis and 28μm in the Z-axis whereas 5°C fluctuation in winter revealed 18μm in the Y axis and 35μm in the Z axis. The correlation between the measured and simulated results was shown to be better than 60% for both tests. Mian et al [9] analysed the machine deformation due to the effect of internal heat sources during spindle heating tests while the ambient conditions were measured. Comparison with simulated results using FEA showed that the correlations had an improvement from 50% to 62% by considering the effect of a few observed air pockets inside the machine structure.

FEA has therefore been shown to be an important tool for model development and error compensation. However, improvement in accuracy can be gained by reducing assumptions and including in the model important aspects. This paper seeks to include in the model, with justification, consideration of the thermal behaviour of air pockets, which may be categorized as internal ambient sources. Air pockets are common due to the many structural voids required to make the structure both rigid and lightweight. The size and location of these air pockets may result in a varying influence producing asymmetry and non-linearity in the overall thermal behaviour of the machine tool.

This paper provides a case study which highlights the significance of air pockets with regard to their nature of existence and their contribution towards the overall performance of the machine. The paper is structured in two stages. The first stage provides the modelling and experimental methods required to include the thermal behaviour of air pockets in the thermal model and cites the accuracy improvement achievable presented by Mian [9] of the Z-axis displacement with when considering air pockets in the thermal model. In the second stage, these air pockets are simulated and analysed individually and compared with the measured results in essence to relate their nature of existence

such as their geometry, location and size with their significance on the overall thermal performance of the machine. All simulations include the analysis of the full machine and the improvements in the correlation with the vertical Z direction, being the most significant [9] are presented.

2 Case Study

Mian et al [9] showed a method of using FEA for the thermal modelling of machine tools. The work revealed that consideration of air pockets is required to improve accuracy. The test comprised of 1 hour stabilization period, to attempt to provide a stable initial condition, followed by one hour heating and one hour cooling phases.

2.1 Air pockets

Air pockets are voids and gaps either inside the structure or in the immediate vicinity of the machine where the heat from either the machining process or external sources is confined due to restricted air flow, which consequently reduce the natural cooling rate of the associated structure. The location, size and geometry of an air pocket can be critical to the overall thermal performance of the machine. In this case study, three air pockets were analysed individually to observe their significance on the overall thermal performance of the machine:

- One side of the column was very close to the attached electrical cabinet (termed as column/elect) and is an "open" air pocket
- The front of the column was close to the carrier head (termed as column/carrier)
- The column itself is a hollow structure used to route machine cables which also generate a localized heat source (termed as column/hollow).

Each air pocket analysed had a different nature and geometry such as the column/elect air pocket which is outside the machine i.e. it is a gap between the electrical cabinet and the column with the size of 140mm x 461mm x 1537mm. This gap behaves, thermally, as an air pocket due to restricted airflow, which traps the radiation from the electrical cabinet and from the heat of electrical cables passing from the cabinet into the column. The column/hollow air pocket is a tall hollow geometrical air pocket inside the column with the size of 236mm x 418mm x 1198mm having a relatively small aperture size of 236mm x 210mm which restricts the air flow. The column/carrier air pocket is a gap between the carrier head of the machine and the column to house the ball screw with the size of 289mm x 125mm x 960mm. The exterior ballscrew guard is a flexible, hinged metal plate, whose nature and therefore effect on the airflow, changes with axis position.

2.1.1 Application of ambient temperatures to the FEA model

Figure 1 show the temperature measured by the base ambient sensor, column ambient sensor, and internal ambient sensor. These three sensors were originally placed on the machine prior to the experimentation with air pockets. The result shows that the internal sensor is affected by being inside the enclosed machine guarding.
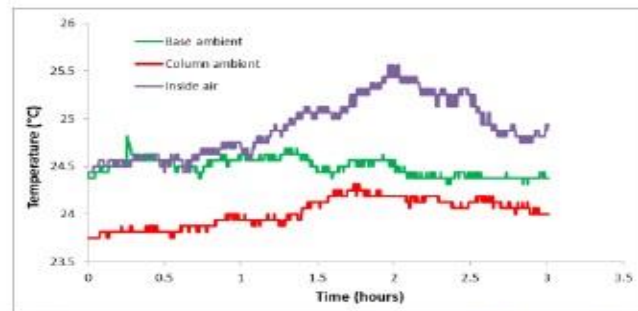
Figure 1: Ambient temperature measured around the machine (8000rpm – By originally placed sensors)

In the first stage simulation, ambient temperatures from the three temperature sensors were applied in the FEA model. Since the variations in the ambient temperatures measured were not significant, it was decided to use single averaged values to define sink temperatures (Abaqus film condition) in the software. This simplifies simulation setup and helps reduce simulation times. The temperature data from the inside ambient sensor was applied to the column/carrier face with 25.5°C. The temperature data from the column ambient sensor was applied to the column with 24.25°C. The temperature data from the base ambient sensor was applied to the base/table face with 24.5°C. The obtained convection value of $6W/m^2/°C$ was applied to the full machine structure during simulations apart from the test mandrel which was applied with $92W/m^2/°C$ during the 8000rpm heating cycle and $6W/m^2/°C$ during the cooling cycle [9].

The correlation between FEA and experimental testing, shown in Figure 7 (where a comparison can be made between the profiles with and without considerations to air pockets), Z-axis was be around 45%. The low correlation and lack of profile convergence in the Z-axis direction was examined. The experimental results show a faster Z-axis response, especially in the cooling phase, which could be a result of additional carrier and column bending caused by non-uniform ambient temperatures due to the aforementioned air pockets.

2.1.2 Re-testing the machine

The number of ambient temperature sensors was increased and placed in proximity to the main identified air pockets. Figure 2 shows the positions of six temperature sensors placed around the machine, three ambient sensors (**in bold**) placed originally and the additional three ambient sensors which were placed

later inside the suspected air pockets (*in italics*). Figure 3, Figure 4 and Figure 5 show, in blue, the local ambient changes detected by these new temperature sensors. The original measured column ambient temperature is also plotted, in red, to show the differences between ambient temperatures.
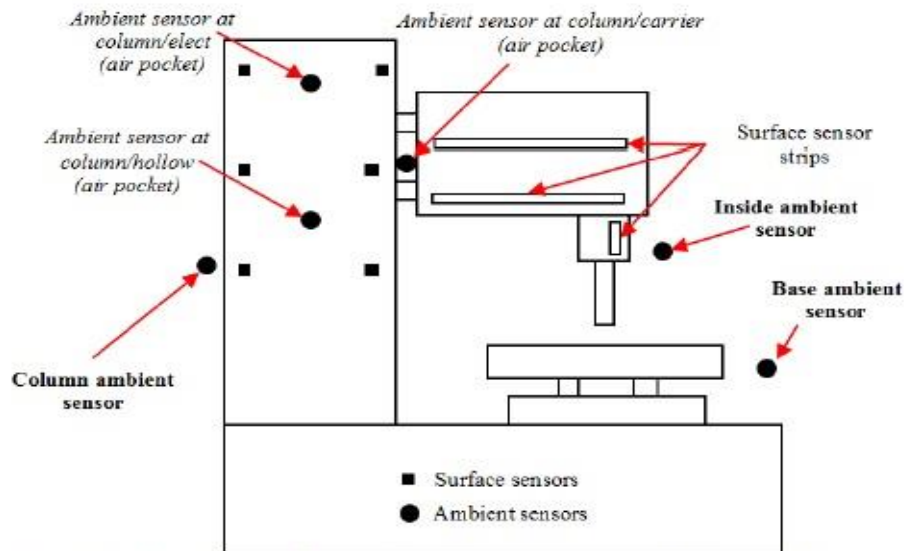
Figure 2: Position of the ambient sensors around the machine
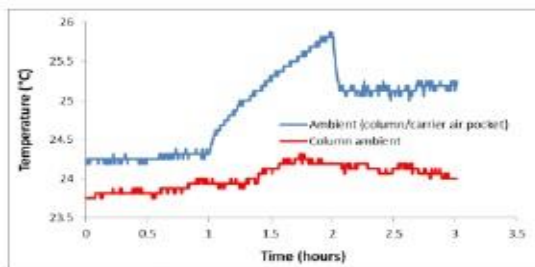
Figure 3: Ambient temperature inside column/carrier air pocket
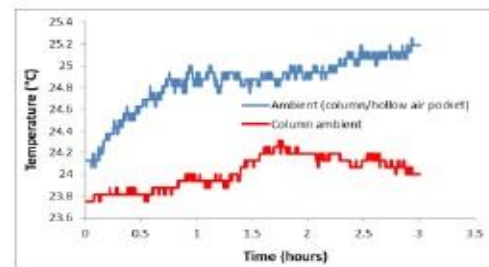
Figure 4: Ambient temperature inside column/hollow air pocket
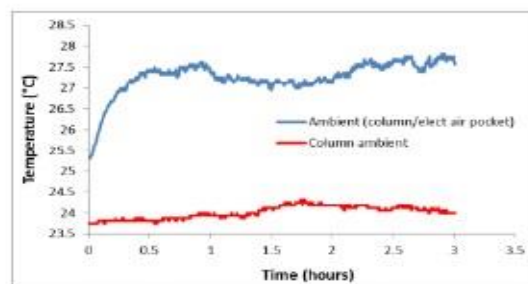
Figure 5: Ambient temperature inside column/elect air pocket

The column/carrier air pocket showed a linear temperature increase during the heating cycle whereas the column/hollow air pocket showed a gradual temperature increase throughout the test span which is suspected to be due to the heating of cabling inside. Relatively, a rapid and significant temperature

increase can be observed inside the column/elect air pocket during the stabilization period which is suspected to be the heat from the electrical cabinet and the cables being confined when the drives were energised during the machine stabilization phase (first hour). It can also be observed that the initial temperature had a large magnitude difference compared to the initial temperatures of other air pockets and the outside column environment.

Previously the whole column was simulated with a constant ambient (sink) temperature in Abaqus. However, the above plots confirm that ambient temperature around the column is not constant. The local temperature change was selected from each plot and applied to the respective column sides as sink temperature. The column/carrier face was simulated with a temperature of 25.35°C considering that approximately 1.6°C temperature change occurred at that face from the start of the test (23.75°C surface temperature measured at the column). Similarly the inside face of the column was simulated with 25.25°C considering approximately 1.5°C temperature change and the column/Electrical cabinet face was applied with 27.25°C considering approximately 3.5°C temperature change. Figure 6 show the column faces where ambient magnitudes obtained from the new test were applied.

| column/carrier interface air pocket | column/hollow air pocket | column/elect cabinet air pocket | Column back face (column ambient) |

ΔT 1.6°C   ΔT 1.5°C   ΔT 3.5°C   ΔT 0.5°C
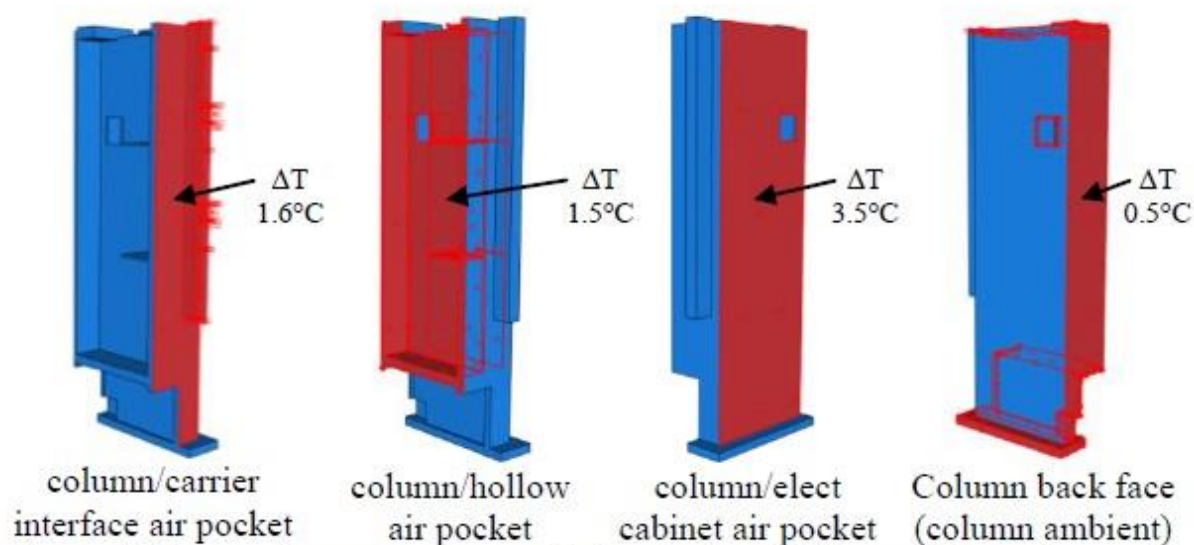
Figure 6: Measured temperatures applied to the faces of the machine column to represent potential air pockets in Abaqus

The simulation was repeated and Figure 7 show the correlation results for the Z-axis where a comparison can be made between the profiles with and without considerations to air pockets. Importantly, in the Z -axis direction an improved correlation of 62% was achieved compared to around 45% for the simpler model. The residual error remained is less than 10μm in magnitude. Figure 8 is the visual representation of the simulated deformation of the machine.
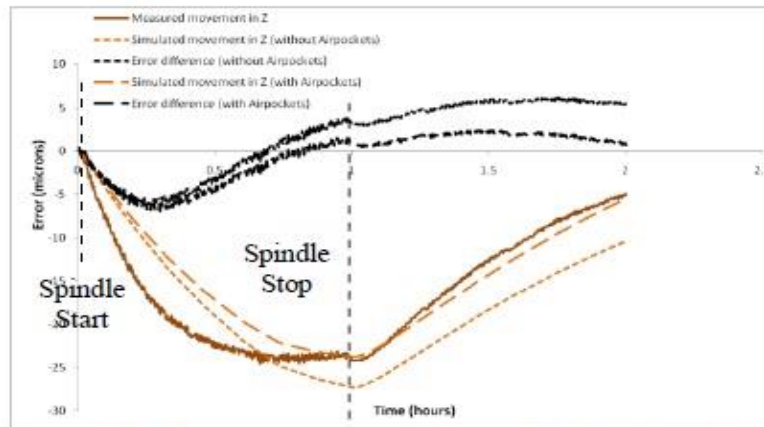
Figure 7: Z-Displacement profiles correlation (8000rpm)
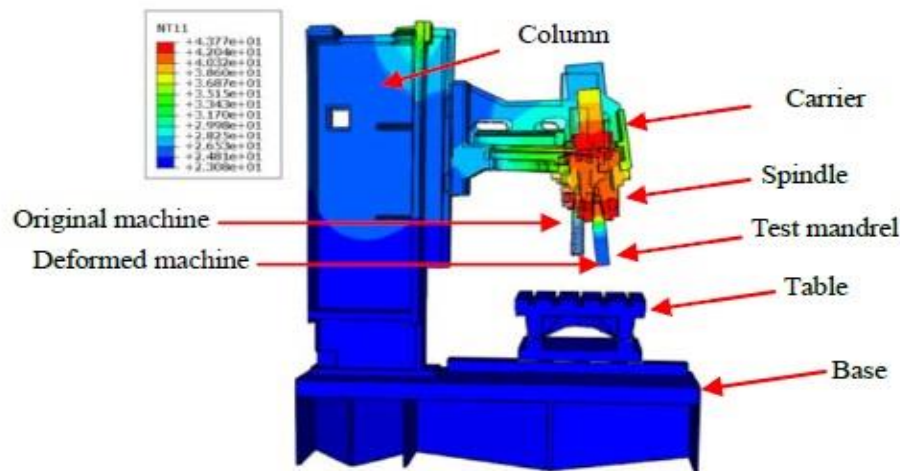
Figure 8: Simulated visual representation of deformation of the machine due to internal heating

2.2 Analysis of individual air pockets

This section details simulation-based analysis for each air pocket. The aim is to distinguish between the nature of the existence of air pockets with respect to their significance toward affecting the overall thermal performance of the machine. In this case study, all air pockets were considered as rectangular areas, although this is a justifiable simplification. Since the consideration of all air pockets in the FEA model improved the correlations of the Z-axis [9], at this stage it is important to note the distinction of each air pocket towards overall improvement of results for which each air pocket is now individually analysed. This is important analysis when undertaking error avoidance, to design out the cause of the error, or during development of thermal compensation to ensure the correct locations are monitored. Simple methods, such as improving ventilation, can be inherently more stable than implementing sophisticated and specialized compensation.
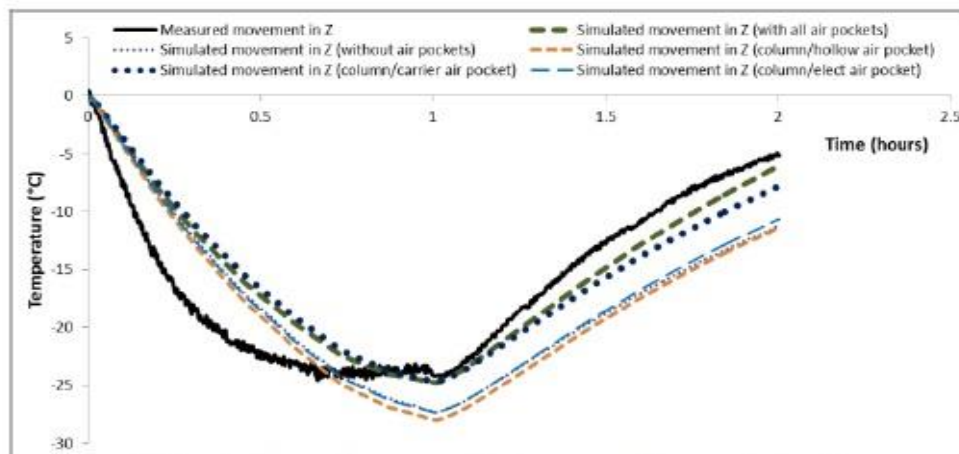
Figure 9: Individual air pocket towards the overall correlation improvement

The results shows that without the consideration of air pockets in the FEA, the model results showed excessive displacements during the heating cycle compared to the measured results. To a lesser extent, the cooling cycle results in the FEA also show deviation in amplitude. It is obvious from results that the column/carrier air pocket had the most effect and caused excessive bending in the column, which in effect created an angle, or out-of-squareness of the whole spindle-carrier structure. This effect better matched the measured cooling cycle profile but also brought the overall magnitude of the Z displacement closer to the measured. In comparison, the rest of air pockets individually improved the overall performance to a lesser extent. Table 1 shows the correlation improvement from inclusion of air pockets.

Table 1: Correlation improvements

Air pocket	Correlation improvement
No air pocket	45%
column/elect	47%
column/hollow	46%
column/carrier	54%
All pockets	62%

It can be observed that the most significant air pocket is the gap between the column and the carrier, which is not a structural void, and which apparently experiences the most heat build-up during the heating cycle and fails to release it during the cooling cycle. The resultant heat inside the gap is suspected to be the combination of heat radiation from the carrier structure and the ball screw motor; and from the air flow around the spindle and test mandrel consequently turning that gap into a virtual heat source. Careful investigation of this area revealed that the lack of ventilation was due to the ballscrew motor restricting the airflow by effectively sealing the top of the void. The effects from air pockets may be reduced by improving the ventilation system by considering the size of apertures and creating airflow by installing small fans.

3 Conclusions

This paper explains the behaviour of air pockets inside the structure of a machine tool and their effect on the overall machine thermal performance. An improvement in the correlation of results between the measured and the FEA simulated results was achieved by including the effect of air pockets in the FEA model. Correlation result from a spindle heating test was improved from less than 45% to 62% in the Z-axis with spindle running at 8000rpm. Later, each air pocket was analysed individually to understand their significance on the overall correlation improvement. Perhaps counter intuitively, the most significant pocket was between the column and the carrier.

It can be stated that error avoidance by good design to counter the effect of air pockets is recommended where convenient. However, in cases where avoidance is not possible, air pocket behaviour must be considered during the development of any thermal compensation model to improve their predictability.

4 References

1. Hao, W., Z. Hongtao, G. Qianjian, W. Xiushan, Y. Jianguo, *Thermal error optimization modeling and real-time compensation on a CNC turning center*. Journal of Materials Processing Technology, 2008. **207**(1-3): p. 172-179.
2. Du, Z.C., et al., *Modeling approach of regression orthogonal experiment design for the thermal error compensation of a CNC turning center*. Journal of Materials Processing Technology, 2002. **129**(1-3): p. 619-623.
3. Kim, S.K. and D.W. Cho, *Real-time estimation of temperature distribution in a ball-screw system*. International Journal of Machine Tools and Manufacture, 1997. **37**(4): p. 451-464.
4. Huo, D., et al., *A Novel FEA Model for the Integral Analysis of a Machine Tool and Machining Processes*. 2004. p. 45-50.
5. Mayr, J., et al., *Thermal issues in machine tools*. CIRP Annals - Manufacturing Technology, 2012. **61**(2): p. 771-791.
6. Longstaff, A.P., S. Fletcher, and D.G. Ford, *Practical experience of thermal testing with reference to ISO 230 Part 3*, in *Laser Metrology and Machine Performance VI*, D.G. Ford, Editor. 2003, WIT Press: Southampton. p. 473-483.
7. Fletcher, S., A.P. Longstaff, and A. Myers, *Flexible modelling and compensation of machine tool thermal errors*, in *20th Annual Meeting of American Society for Precision Engineering*. 2005: Norfolk, VA.
8. Mian, N.S., et al., *Efficient estimation by FEA of machine tool distortion due to environmental temperature perturbations*. Precision Engineering, (in press).
9. Mian, N.S., et al., *Efficient thermal error prediction in a machine tool using finite element analysis*. Measurement Science and Technology, 2011. **22**(8): p. 0851

2013-05 Comparative study of ANN and ANFIS prediction models for thermal error compensation of CNC machine tools

Comparative study of ANN and ANFIS prediction models for thermal error compensation on CNC machine tools

A Abdulshahed, A Longstaff, S Fletcher, A Myers.
Centre for Precision Technologies, University of Huddersfield, Queensgate, HD1 3DH, England. Email: u0953276@hud.ac.uk

Abstract

Thermal errors can have significant effects on CNC machine tool accuracy. The errors usually come from thermal deformations of the machine elements created by heat sources within the machine structure or from ambient change. The performance of a thermal error compensation system inherently depends on the accuracy and robustness of the thermal error model. In this paper, Adaptive Neuro Fuzzy Inference System (ANFIS), Artificial Neural Network (ANN) and Particle Swarm Optimization (PSO) techniques were employed to design four thermal prediction models: ANFIS by dividing the data space into rule patches (ANFIS-Scatter partition model); ANFIS by dividing the data space into rectangular sub-spaces (ANFIS-Grid partition model); ANN with a back-propagation algorithm (ANN-BP model) and ANN with a PSO algorithm (ANN-PSO model). Grey system theory was also used to obtain the influence ranking of the input sensors on the thermal drift of the machine structure. Four different models were designed, based on the higher-ranked sensors on thermal drift of the spindle. According to the results, the ANFIS models are superior in terms of the accuracy of their predictive ability; the results also show ANN-BP to have a relatively good level of accuracy. In all the models used in this study, the accuracy of the results produced by the ANFIS models was higher than that produced by the ANN models.

1. Introduction

Errors due to the changes in the temperature of the machine tool elements create relative movement between the tool and the workpiece during the machining process, which affects the accuracy of the part being produced, these are known as the thermal errors [1]. According to various publications [2-4], thermal errors represent approximately 70% of the total positioning error of the

CNC machine tool. With improvements of machine tool positioning accuracy, tooling, and enhanced machining performance improved, thermal errors have become more significant. As a result, a reduction of thermal errors is needed for high-precision manufacturing systems [5].

Two different ways have been used to reduce the thermal errors of machine tools: Thermal error avoidance and thermal error compensation [1]. In thermal error avoidance, heat-source isolation, structural improvement and materials that have a low thermal expansion coefficient are used to reduce the thermal errors. Although, this can improve basic machine accuracy, it is neither cost-effective nor applicable to the renewal of existing machine tools [1]. Thermal error compensation attempts to forecast the thermal errors and then compensate for them with software. Extensive research has been carried out in the area of thermal error compensation [2]. There are two main research areas in relation to this: Numerical analysis techniques such as the finite-element method [6] and the Newton-Raphson method [7] are utilized for thermal error compensation. These methods are restricted to qualitative analysis because of the complexity of machine tool structures, such as geometrical dimensions and machine joints. The second area uses empirical modelling, which is based on the measurement of temperature changes and thermal drift of the machine tools. Examples include multiple regression analysis [8], types of Artificial Neural Networks [9], fuzzy logic [10], adaptive network fuzzy inference system [11] and a combination of several different modelling methods [2].

Among these error compensation methods, the Adaptive Neuro-Fuzzy Inference System and Artificial Neural Network models were the most promising methods: They showed satisfactory predictive accuracy in many real-world applications. These models have their own advantages, and disadvantages. Experiments show that neither of them needs a proper selection of thermal sensors and their locations, in order to ensure the prediction accuracy and robustness of these models. Further exploration regarding the selection of thermal sensors for thermal error compensation models is needed.

The motivations behind this paper are to develop a method competent in determining the key temperature sensors for modelling using grey system theory and also to determine the empirical relationships for the estimation of thermal errors. Adaptive Neuro Fuzzy Inference System (ANFIS) and traditional Artificial Neural Network (ANN) techniques were used to design four thermal prediction models: ANFIS by dividing the data space into rule patches (ANFIS-Scatter partition model); ANFIS by dividing the data space into rectangular sub-spaces (ANFIS-Grid partition model); ANN with a back-propagation algorithm (ANN-BP model) and ANN with a PSO algorithm (ANN-PSO model), and compare the versatility, the robustness and their prediction accuracy.

2.   Material and methods

An artificial intelligence system is a system that can make decisions which would be considered intelligent if they were made by a human being. They adjust themselves using some conditions (input data), and they improve decisions automatically for future conditions. Artificial Neural Networks, fuzzy

logic systems, particle swarm optimisation, and neuro-fuzzy systems are the most common artificial intelligence system types. In this part of the paper, the theory behind and structures for artificial intelligence systems will be described. Furthermore, proper selection of thermal sensors and their locations will be introduced using the grey system theory.

2.1   Artificial Neural Networks (ANNs)

Artificial Neural Networks, especially the Multi-Layer Perceptron networks (MLP) are an extension of perceptron neural networks, which have one or more hidden layers. A group of the neurons which are connected with each other through the environment form the whole ANN. Figure 1 shows the basic structure of the ANN. The learning algorithm is defined as a mathematical tool that sketches the methodology and the speed for the network, to obtain the steady state of network parameters successfully. There are many optimization methods which can be used to train the ANN, such as the back-propagation algorithm (BP) and particle swarm optimization (PSO). The choice of the error function and the optimization techniques are significant, because they may increase the stability of the ANN. The back-propagation algorithm is the basic learning mechanism: In this algorithm, the ANN output on presentation of input data is matched with the desired output to obtain the error. The error is used to incrementally adjust appropriate weights in the connection matrices to reduce it. Following many presentations of training data, the error value of the ANN is expected to be decreased to a satisfactory level, and the ANN will have then learned how to resolve the task modelled by training data. Particle swarm optimization (proposed by Eberhart and Kennedy [12]) is also an optimization technique. Researchers have applied it to train ANN and have found that ANN with PSO has a good training performance, a faster convergence rate and a better predicting ability than ANN with BP [13]. In this paper, in order to enhance the ability of ANN to make predictions it is adjusted with the PSO technique.
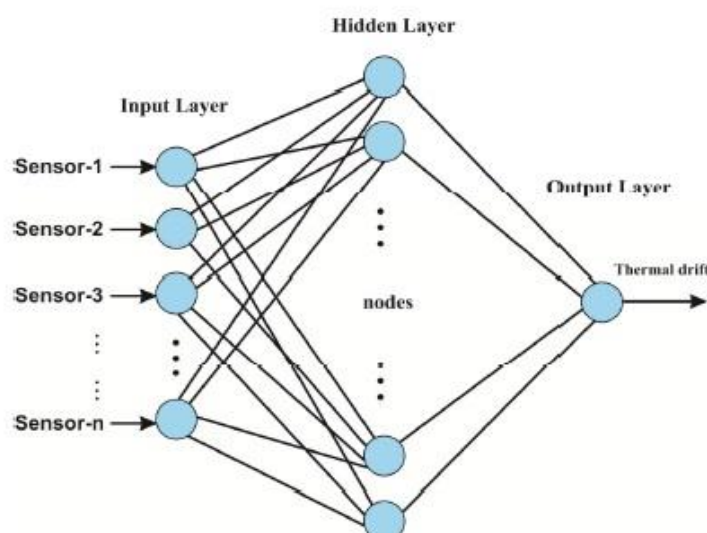
Figure 1: Basic structure of ANN model.

2.2 The Adaptive Neuro-Fuzzy System (ANFIS)

The architecture and learning procedure of the Adaptive Neuro-Fuzzy System (ANFIS), have both been described by Jang [14]. According to Jang, the ANFIS is a neural network that is functionally the same as a Takagi-Sugeno type inference model. The ANFIS is a hybrid intelligent system that takes the advantages of ANN and the fuzzy logic theory into a single system. By employing the ANN technique to update the parameters of the Takagi-Sugeno type inference model, the ANFIS is given the ability to learn from given training data, the same as ANN. The solutions mapped out onto the Takagi-Sugeno type inference model can therefore be described in linguistic terms.

The efficiency of any ANFIS model depends on the success in partitioning the input and output variables space correctly. This can be achieved by using a number of methods such as grid partitioning (ANFIS-Grid partition model), the subtractive clustering method (ANFIS-Scatter partition model) and fuzzy c-means clustering [15]. The equivalent ANFIS network with two variables is shown in Figure 2:The first layer implements a fuzzification, the second layer executes the T-norm of the antecedent part of the fuzzy rules, the third layer normalizes the membership functions (MF), the fourth layer computes the consequent parameters, and finally the last layer calculates the overall output as the summation of all incoming signals [14].
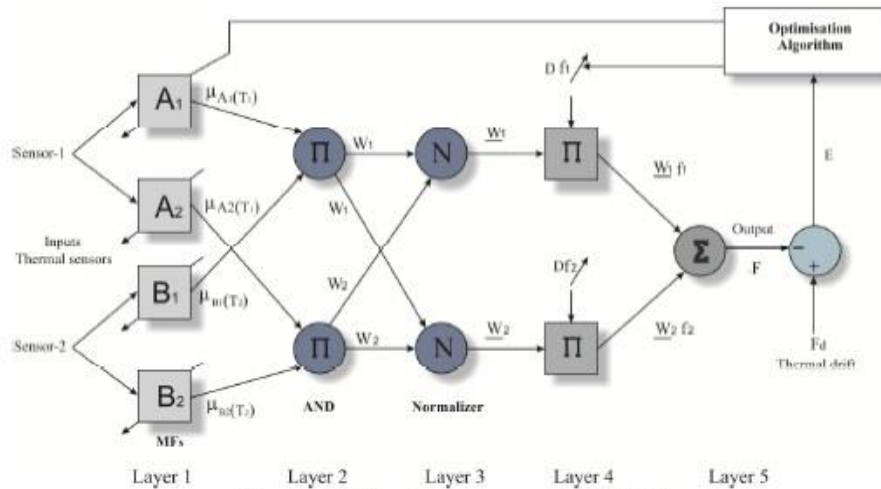
Figure 2: Basic structure of ANFIS.

2.3 GM (h, N) Model

In grey system theory, the main function of the GM (h, N) model is a way to acquire a calculation of the measurement between the discrete sequences and to compensate the shortcomings in the traditional methodology [16]. Assume that the original data with a number of samples (N) is described in sequences $x_i^{(0)}(k)$, $i = 1,2, \ldots, N$.

$x_1^{(0)}(k)$, and sequences $x_2^{(0)}(k), x_3^{(0)}(k), x_4^{(0)}(k), \ldots x_N^{(0)}(k)$ are the influential factors of the system, then the GM (h, N) model is described as [16]:

$$\sum_{i=0}^{h} a_i \frac{d^{(i)} x_1^{(1)}}{dt^{(i)}} = \sum_{j=2}^{N} b_j x_1^{(1)}(k) \tag{1}$$

Where, (i) a: Is the developing coefficient. (ii) b: Is defined as the grey input. (iii) $x_1^{(1)}(k)$: The major sequence. (iv) The accumulation generating operation AGO $x^{(0)} = x^{(1)}$

$$= [\sum_{k=1}^{1} x^{(0)}(k), \sum_{k=1}^{2} x^{(0)}(k), \sum_{k=1}^{3} x^{(0)}(k), \dots \sum_{k=1}^{n} x^{(0)}(k)]$$

According to the previous definition of GM (h, N), the GM (0, N) is a zero order grey system, which can be described as follows:

$$az_1^{(1)}(k) = \sum_{j=2}^{N} b_j x_j^{(1)}(k) = b_2 x_2^{(1)}(k) + b_3 x_3^{(1)}(k) + \dots + b_N x_N^{(1)}(k) \tag{2}$$

Where, $z_1^{(1)}(k) = 0.5 x_1^{(1)}(k-1) + 0.5 x_1^{(1)}(k) k = 2,3,4,\dots,n$.
The analytical steps are shown below.

1- Substituting the AGO value, we can write.

$$az_1^{(1)}(2) = b_2 x_2^{(1)}(2) + \dots + b_N x_N^{(1)}(2)$$
$$az_1^{(1)}(3) = b_2 x_2^{(1)}(3) + \dots + b_N x_N^{(1)}(3)$$
$$\dots \dots \dots \dots \dots \dots \dots \dots \dots \dots \dots \dots$$
$$az_1^{(1)}(n) = b_2 x_2^{(1)}(n) + \dots + b_N x_N^{(1)}(n) \tag{3}$$

2- Dividing a_1 in both sides, then the equations (3) can be written as

$$\begin{bmatrix} 0.5x_1^{(1)}(1) + 0.5x_1^{(1)}(2) \\ 0.5x_1^{(1)}(2) + 0.5x_1^{(1)}(3) \\ \vdots \\ 0.5x_1^{(1)}(n-1) + 0.5x_1^{(1)}(n) \end{bmatrix} = \begin{bmatrix} x_2^{(1)}(2) & \cdots & x_N^{(1)}(2) \\ x_2^{(1)}(3) & \cdots & x_N^{(1)}(3) \\ \vdots & \cdots & \vdots \\ x_2^{(1)}(n) & \cdots & x_N^{(1)}(n) \end{bmatrix} \begin{bmatrix} \frac{b_2}{a_1} \\ \frac{b_3}{a_1} \\ \vdots \\ \frac{b_N}{a_1} \end{bmatrix} \tag{4}$$

Assume $\theta_m = \frac{b_j}{a_1}$, where $m=2,3,\dots,N$, then equation(4) can be rearranged into:

$$\begin{bmatrix} 0.5x_1^{(1)}(1) + 0.5x_1^{(1)}(2) \\ 0.5x_1^{(1)}(2) + 0.5x_1^{(1)}(3) \\ \vdots \\ 0.5x_1^{(1)}(n-1) + 0.5x_1^{(1)}(n) \end{bmatrix} = \begin{bmatrix} x_2^{(1)}(2) & \cdots & x_N^{(1)}(2) \\ x_2^{(1)}(3) & \cdots & x_N^{(1)}(3) \\ \vdots & \cdots & \vdots \\ x_2^{(1)}(n) & \cdots & x_N^{(1)}(n) \end{bmatrix} \begin{bmatrix} \theta_2 \\ \theta_3 \\ \vdots \\ \theta_N \end{bmatrix} \tag{5}$$

3- The coefficients of the model can be obtained by solving this equation:

$$\hat{\theta} = (B^T B)^{-1} B^T Y \tag{6}$$

Where,

$$Y = \begin{bmatrix} 0.5x_1^{(1)}(1) + 0.5x_1^{(1)}(2) \\ 0.5x_1^{(1)}(2) + 0.5x_1^{(1)}(3) \\ \vdots \\ 0.5x_1^{(1)}(n-1) + 0.5x_1^{(1)}(n) \end{bmatrix}, \quad B = \begin{bmatrix} x_2^{(1)}(2) & \cdots & x_N^{(1)}(2) \\ x_2^{(1)}(3) & \cdots & x_N^{(1)}(3) \\ \vdots & \cdots & \vdots \\ x_2^{(1)}(n) & \cdots & x_N^{(1)}(n) \end{bmatrix} \quad \hat{\theta} = \begin{bmatrix} \theta_2 \\ \theta_3 \\ \vdots \\ \theta_N \end{bmatrix}$$

Therefore, the influence ranking of the major sequences (thermal sensors) on the output sequences (thermal drift) can be known by comparing the model values of ($\theta_2 \sim \theta_N$).

3.   Experimental work

In this study, experiments were performed on a small vertical milling centre (VMC). Three non-contact displacement transducers (NCDTs) were used to measure the drift of the tool in the X, Y and Z axes. The thermal data was measured using 58 temperature sensors placed in strips at the carrier and spindle boss surfaces as explained by White et al [3], other eleven ambient temperature sensors were placed around the machine to pick up the ambient temperature [6]. A general overview of the experimental setup is shown in Figure 3.
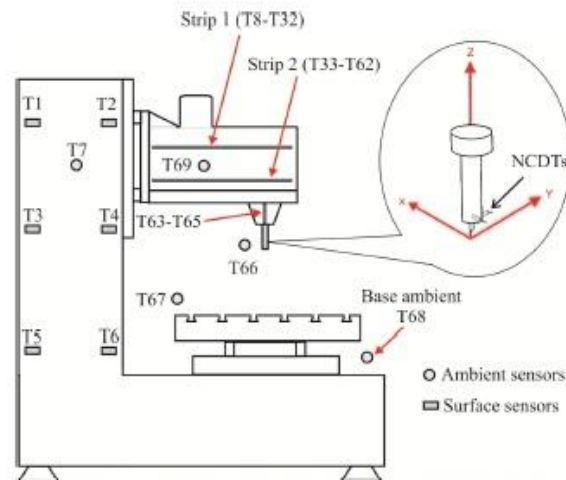
Figure 3: A general overview of the experimental setup.

The machine was examined by running the spindle at its highest speed of 8000 rpm for 60 minutes to excite the largest thermal behaviour. It was then stopped for 60 minutes for cooling. The temperature sensors at the selected points on the machine tool and the thermal drift of the spindle were measured simultaneously; the thermal drift of the machine is shown in Figure 4. The maximum drift of the X-axis is 2 μm, the Y-axis is 60 μm, and the Z-axis is 22 μm. In this paper, the X-axis thermal drift is much smaller than that of Y-axis and Z-axis due to mechanical symmetry and therefore can be ignored [3]: Only the Y-axis and Z-axis are considered.
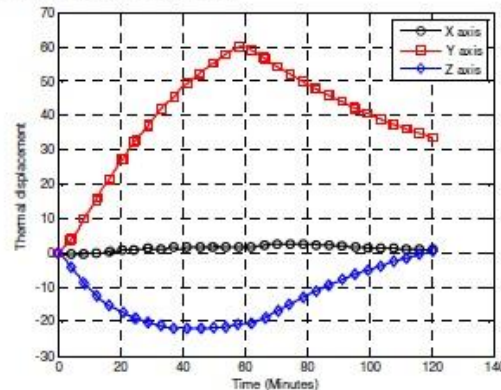
Figure 4: Thermal drift of the machine spindle.

The influence coefficient between the thermal error in the Y direction and the temperature sensors are calculated using the GM (0, N) model. The representative temperature sensors for modelling are selected from each group (Surface sensors and ambient sensors) according to their influence coefficient value. The representative thermal sensors T2, T16, T29, T55, T63 and T71 (which are located on the column, carrier, spindle boss, and base) are used as the thermal key sensors for modelling.

3.1 ANN Models

Six temperature sensors (T2, T16, T29, T55, T63 and T71) were selected as input for models, and the thermal drift in Y direction was chosen as a target variable. Usually ANN models have three layers: Input, hidden and output layers. Although, for common engineering problems, one hidden layer is sufficient for model training, two or more hidden layers may be needed for very complex phenomena. An ANN models with three layers was used in this study. According to ANN models, the input layer has six sensors and the output layer has one sensor (the thermal drift in Y direction). The test (60 minutes heating and 60 minutes cooling) was used for training the models.

In order to examine the performance of the ANN models on non-training data, another test was carried out on the same machine in an operational cycle as follows: It was allowed to run at spindle speed 4000 rpm for 120 minutes, and then paused for 60 minutes before running for another 120 minutes; and then stopped for 180 minutes. During the experiment, the thermal errors were measured by the NCDTs, and the predicted displacements were obtained using ANN models. A validation test on the ANN-PB model and ANN-PSO model for thermal error prediction have shown satisfactory results (see Figure 5).
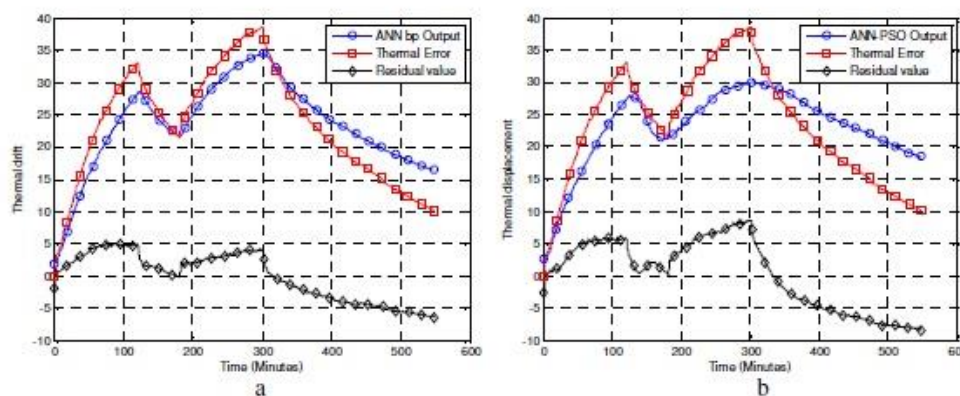
Figure 5: (a) ANN-BP model output vs. the actual thermal drift. (b) ANN-PSO model output vs. the actual thermal drift.

3.2 ANFIS Models

Similar procedures (ANN models) were carried out on the ANFIS models. The construction of two models (ANFIS-Grid and ANFIS-Scatter) is described as

follows: The number of the membership function is ($2\times3\times2\times2\times3\times2$ and $5\times5\times5\times5\times5\times5$) and in total (144 and 5) rules can be obtained to define their relationship with thermal displacement. The same test (60 minutes heating and 60 minutes cooling) was used for training the models. The Gaussian functions were used to describe the membership degree of these variables. After setting the initial parameter values in the ANFIS models, the input membership functions were adjusted using a hybrid learning scheme. The error between the output and expected values can be computed.

Simulation results show that the ANFIS models can provide a good prediction result with the validation data. Figure 6 presents the comparison between thermal drift from the actual measured data and the output of the models.
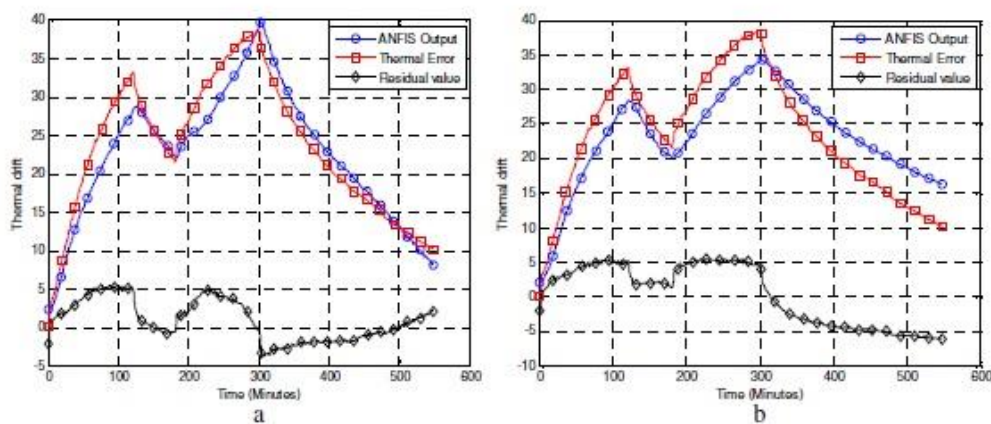
Figure 6: (a) ANFIS-Grid model output vs. the actual thermal drift. (b) ANFIS-Scatter model output vs. the actual thermal drift.

3.3 Results

The results of the GM (0, N) model can determine which sensors on the machine structure contribute most significantly to the total thermal drift. The models of ANFIS and ANN for the prediction of thermal drift were then constructed using six selected inputs and one output.

The results of this paper are as follows:

- The ANFIS models for the prediction of thermal drift revealed a more reliable prediction when compared with ANN models.
- The model prediction of thermal drift showed that the ANFIS-Grid partition model has a high prediction performance. The residual value of the model is smaller than ± 5 μm.

Three performance criteria including root mean square error (RMSE), Nash-Sutcliffe efficiency coefficient (E) and correlation coefficient (R) were used to judge the most optimum model. From the Table 1 (as a result of the comparison of RMSE, E and R indices for predicting thermal drift) it was revealed that the prediction performance of the ANFIS-Grid model is higher than those of ANFIS-Scatter, ANN-BP and ANN-PSO models, respectively. Thus, the accuracy of outputs decreases gradually from the ANFIS to the ANN models.

Table 1: Performance calculation of the used models.

Model	Training stage		Validation stage		
	E	RMSE	E	RMSE	R
ANFIS-Grid partition	0.990	0.225	0.89	2.8125	0.9530
ANFIS-Scatter partition	0.990	0.213	0.86	3.2057	0.9343
ANN-BP	0.990	0.3578	0.8098	3.7684	0.9287
ANN-PSO	0.980	0.4207	0.6158	5.3557	0.7567

4.　Conclusions

In this paper, various traditional ANN and hybrid ANFIS models were proposed for the prediction of the thermal errors on a CNC machine tool, and the following conclusions can be drawn:

- The new technique GM (0, N) model is able to find the optimal temperature sensors for thermal error modelling. The advantage of using key temperature sensors is greater economic efficiency and reduces modelling time. In addition, the robustness of the models can be increased and the predicting precision of the models using the optimal combination of the temperature sensors are enhanced.
- Experimental results show that the thermal error in the Y direction can be significantly reduced to less than ±5 μm using ANFIS models with validation data (different conditions of rotational speeds on the machine tool). The results also show that the ANN models can reduce the thermal error to less than ±10 μm. However, BP algorithms are limited during the training procedure, in that they are sensitive to the weight's initial values. If the weights are not correctly chosen, the training process might be cornered in a local minimum or maximum. In contrast, while a PSO algorithm gives unsatisfying results, further investigation is necessary in order to overcome some of the limitations of BP. A PSO algorithm also gives fast convergence during the training stage.

5.　References

1. Ni, J., *CNC machine accuracy enhancement through real-time error compensation.* Transactions, American Society of Mechanical Engineers, Journal of Manufacturing Science and Engineering, 1997. **119**: p. 717-725.
2. Li, J., et al., *Thermal-error modeling for complex physical systems: the-state-of-arts review.* The International Journal of Advanced Manufacturing Technology, 2009. **42**(1): p. 168-179.

3. White, A., S. Postlethwaite, and D.G. Ford. *Measuring and modelling thermal distortion on CNC machine tools*. in *5th International LAMDAMAP Conference*. 2001. University of Birmingham, UK.

4. Ramesh, R., Mannan, M, A., Poo, A, N., *Error compensation in machine tools-a review:Part II: thermal errors*. International Journal of Machine Tools and Manufacture, 2000. **40**(9): p. 1257-1284.

5. Yan, J. and J. Yang, *Application of synthetic grey correlation theory on thermal point optimization for machine tool thermal error compensation*. The International Journal of Advanced Manufacturing Technology, 2009. **43**(11): p. 1124-1132.

6. Mian, N.S., et al., *Efficient thermal error prediction in a machine tool using finite element analysis*. Measurement Science and Technology, 2011. **22**: p. 085107.

7. Harris, T.A. and M.N. Kotzalas, *Rolling bearing analysis*. Vol. 3. 2001: Wiley New York, NY.

8. Chen, J., J. Yuan, and J. Ni, *Thermal error modelling for real-time error compensation*. The International Journal of Advanced Manufacturing Technology, 1996. **12**(4): p. 266-275.

9. Chen, J. and G. Chiou, *Quick testing and modeling of thermally-induced errors of CNC machine tools*. International Journal of Machine Tools and Manufacture, 1995. **35**(7): p. 1063-1074.

10. Srinivasa, N. and J.C. Ziegert, *Automated measurement and compensation of thermally induced error maps in machine tools*. Precision engineering, 1996. **19**(2): p. 112-132.

11. Wang, K.C. *Thermal error modeling of a machining center using grey system theory and adaptive network-based fuzzy inference system*. 2006. IEEE.

12. Geethanjali, M., S.M. Raja Slochanal, and R. Bhavani, *PSO trained ANN-based differential protection scheme for power transformers*. Neurocomputing, 2008. **71**(4-6): p. 904-918.

13. Da, Y. and G. Xiurun, *An improved PSO-based ANN with simulated annealing technique*. Neurocomputing, 2005. **63**: p. 527-533.

14. Jang, R., *ANFIS: Adaptive-network-based fuzzy inference system*. IEEE transactions on systems, man, and cybernetics, 1993. **23**(3): p. 665-685.

15. Karahoca, A. and D. Karahoca, *GSM churn management by using fuzzy c-means clustering and adaptive neuro fuzzy inference system*. Expert Systems with Applications, 2011. **38**(3): p. 1814-1822.

16. Wei, M.C., et al. *Apply GM (0, N) to analyze the weighting of influence factor in the feminization of poverty-an example in Taiwan*. 2011. IEEE.

2013-06 Efficient estimation by FEA of machine tool distortion due to environmental temperature perturbations.

Efficient estimation by FEA of machine tool distortion due to environmental temperature perturbations

Naeem S. Mian*, S. Fletcher, A.P. Longstaff, A. Myers

Centre for Precision Technologies, University of Huddersfield, Queensgate, Huddersfield HD1 3DH, UK

ABSTRACT

Machine tools are susceptible to exogenous influences, which mainly derive from varying environmental conditions such as the day and night or seasonal transitions during which large temperature swings can occur. Thermal gradients cause heat to flow through the machine structure and results in non-linear structural deformation whether the machine is in operation or in a static mode. These environmentally stimulated deformations combine with the effects of any internally generated heat and can result in significant error increase if a machine tool is operated for long term regimes. In most engineering industries, environmental testing is often avoided due to the associated extensive machine downtime required to map empirically the thermal relationship and the associated cost to production. This paper presents a novel offline thermal error modelling methodology using finite element analysis (FEA) which significantly reduces the machine downtime required to establish the thermal response. It also describes the strategies required to calibrate the model using efficient on-machine measurement strategies. The technique is to create an FEA model of the machine followed by in application of the proposed methodology in which initial thermal states of the real machine and the simulated machine model are matched. An added benefit is that the method determines the minimum experimental testing time required on a machine; production management is then fully informed of the cost-to-production of establishing this important accuracy parameter. The most significant contribution of this work is presented in a typical case study; thermal model calibration is reduced from a fortnight to a few hours. The validation work has been carried out over a period of over a year to establish robustness to overall seasonal changes and the distinctly different daily changes at varying times of year. Samples of this data are presented that show that the FEA-based method correlated well with the experimental results resulting in the residual errors of less than 12 μm.

1. Introduction

The shop floor environment where a CNC machine is located can be of paramount importance for accuracy of manufacturing. Temperature controlled environments require high capital investments and running costs, which are undesirable and sometimes impractical. In environments where the temperature is not controlled, the changing day and night cyclic transitions and myriad other sources [1,2] can cause ambient temperatures to vary significantly both in magnitude and rate-of-change. These temporal fluctuations can cause spatial thermal gradients in a machine tool; the heat flow through the structure over time causes non-linear thermal deformations. Several research projects have been conducted to identify, predict and compensate the overall effect of the thermal distribution in a machine tool but with main emphasis on solving the effect of internally generated heat, particularly from the main spindle and during the machining processes. For example, Hao [3] used a genetic algorithm-based back propagation neural network (GA-BPN) method using 16 thermistors placed at the spindle, headstock, axis leadscrew and on the bed of a turning machine to compensate dynamic and highly nonlinear thermal error. Only one ambient temperature sensor was used which may not be sufficient to capture detailed environmental behaviour around the machine vicinity. The author reported the thermal error compensation improvement of 63%. Further reduction could be possible if detailed external environmental temperature swings were considered. Similarly, research from Yang et al. [4] tested an INDEX-G200 turning centre and used MRA technique to predict its thermal accuracy. The analysis result showed that the thermal error range for radius direction on that machine was approximately 18 μm, higher than expected. 14 thermal sensors were installed in groups and only one ambient sensor was used. While modelling, six temperature groups with variables were constructed and the model was assumed to be a linear function for the environmental temperature

* Corresponding author.
  E-mail address: nshaukat80@hotmail.com (N.S. Mian).

rise. The predicted thermal error between the spindle and the cutter revealed a residual error of 5 μm from a maximum error of approximately 18 μm for a test length of 4 h. Modelling time was not mentioned. Tseng and Chen [5] proposed a thermal error prediction model derived from the neural-fuzzy theory. IC-type temperature sensors and a Renishaw MP4 probe system were used to measure the temperature changes and thermal deformations respectively. Sensors were attached to the spindle motor, spindle sleeve side with one sensor measuring environmental variations. The prediction model improved the machining accuracy from 80 μm to 3 μm. The prediction model was further compared with MRA revealing accuracy improvements of ±10 μm to ±3 μm. However, the model training times and machine downtime are accountable issues with this research. One of the regression techniques known as orthogonal regression technique was employed by Du et al. [6]. This technique was applied to more than 100 turning centres of the same type and specifications. It was found that the technique was able to reduce the cutting diameter thermal error from 35 μm to 12 μm. The technique was stated as robust due to its year round repeatable improvement in accuracy. The accuracy is expected to increase if long term shop floor environmental temperatures fluctuations were considered.

Many researchers drew attention towards the environmental thermal drifts in machine tools which arise from a variety of sources while they emphasised the machine downtime required for detailed environmental testing as well as analysing the modelling methods and modelling time. Rakuff and Beaudet [7] drew attention to the importance and effect of the environmental temperature variation error (ETVE) while conducting a cutting test of 24 h on a diamond turning machine. The research suggested the provision of temperature controlled enclosures for the machine to avoid external thermal drifts to improve the accuracy of the process control. Fletcher et al. [8] provided useful information about cyclic environmental fluctuations and drifts with 50% reduction in error over a 65 h test, but drew attention to the detrimental amount of machine downtime for the thermal characterisation tests. Longstaff et al. [2] showed several tests conducted for the thermal error measurements produced by the environmental fluctuations combined with long term machining. The authors also highlighted some unexpected, rapid fluctuations of the environment with its effect on the accuracy of the machine. They also highlighted the machine downtime issues related with the measurements. Jedrzejewski et al. [9] discusses the complexities involved with improving the design of a machine tool when considerations of reducing thermal error are in focus. A highly accurate thermal model of the machine is presented and consideration of various parameters contributing to the thermal behaviour. For example, the design criteria considered the effects of environmental variations for 2.5 days, thermal effects arose due to the presence of guarding and bearing sets of high speed spindles. Quartz straight edges were modelled for environmental effect after mounting on the machine centre support beam. It was found that the straight edge fixed on the left side produced the lowest error of the other three locations tested. The information related to the FEA such as the modelling time was not clear and the operating conditions were not clearly stated. A concern shown by Bringmann and Knapp [10] about the effect of thermal drift while showing how increasing the number of measurement points (from 4 to 60) can lead to reduced uncertainties and higher accuracy for identified location errors of the rotary C-axis. The author reported that the further increase in the measurement points only leads to limited improvements as it can lead to extra time for measurement which increases the uncertainty of the thermal effect arising from environmental or ambient temperature changes until the measurement is complete.

It is apparent from the discussion that a great emphasis has been given to control the thermal effects mainly arising due to internal heating. As a result, most existing commercial error compensation systems deal with axis growth and spindle heating while neglecting ambient effects on the remainder of the structure. It is also apparent that a significant amount of machine downtime is associated with environmental testing particularly when the dominant cycles are daily or even weekly; Longstaff et al. [2] reported a significant issue for machines that experience a weekend shutdown. In most cases environmental testing to establish a relationship between temperature and response is avoided due to the cost to production associated with machine downtime. However, this omission can be critical when striving for the best possible accuracy of the machine tool. The problem is exacerbated since the scope of conditions during which test data can be acquired is very limited compared to true variation over facility operations and natural seasons.

This paper presents a novel offline environmental thermal error modelling method based on FEA that significantly reduces the machine downtime required for effective thermal characterisation. The proposed modelling method was tested and successfully validated on a production machine tool over a year period and found to be very robust (in this paper, samples of data measured during two seasons are presented). The validation confirmed the potential of this method to reduce the machine downtime normally required for the environmental testing from a fortnight to a few hours. The paper also highlights the effects of seasonal environmental temperature changes in a machine tool and the presence of vertical temperature gradients within a shop floor environment. The paper also describes on-machine measurement methods to acquire the required data efficiently using strategically placed temperature sensors during any convenient maintenance schedule period.

2. Proposed method

In general, environmental temperature changes are not as rapid as those from internally generated sources such as spindles. Additionally, there can be several different structural responses which require different metrology equipment to measure that cannot be used concurrently. Therefore, environmental testing normally takes from two days to several weeks to acquire sufficient data to establish the various relationships between varying temperature profiles and the response of the machine. To overcome the machine downtime issue, a novel modelling methodology based on a two-stage FEA is proposed in this paper where a Computer Aided Drawing (CAD) model of the machine is created in the FEA software (in this study Abaqus 6.7-1/Standard was used) [11]. This is followed by a determination of the initial thermal state for the FEA model, a key method developed in this research, which will establish a close match of the real initial thermal condition of the machine before conducting environmental simulations.

2.1. FEA modelling

A machine tool is, in practice, rarely at thermal equilibrium. Consequently, establishing the initial conditions for the FEA simulation of environmental change presents a significant problem as it adversely affects the comparison of the FEA and experimental results. To represent the realistic initial thermal state of the machine structure is a challenging task if the real temperature gradients are to be measured and applied to the model. Experimentally, the application of the individual temperature sensors at locations within the machine structural loop is laborious and prone to uncertainty in locating sensitive areas. In contrast to thermal error from running the machine where the heat sources are easy to identify for application of the sensors, environmental changes affect the whole structure. However, even if this is achieved, modelling the initial thermal state of the machine in the FEA software
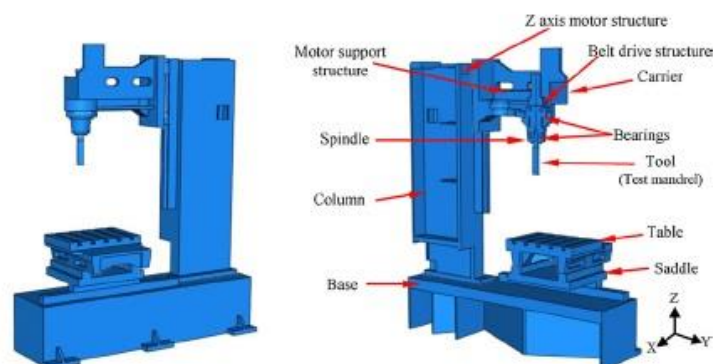
Fig. 1. Generated CAD model of the machine assembly with Z axis head moved up compared to [1] in essence to present a newer model corresponding to new test conditions.

remains challenging. Sectioning the modelled parts in the software and applying individual temperatures to them may represent the initial thermal state but it is a strenuous task and may cause incorrect temperature gradients due to section joints. This problem is solved by the proposed novel method which determines the initial thermal state for the machine model and also provides an estimate of the minimum time required for an environmental test on a machine (Section 2.3).

2.1.1. Machine model

A model of the machine is required. For the case study machine, a model described by the authors [1] with respect to internally generated heat was used to estimate the long-term environmental response. The machine was a precision 3-axis Vertical Machining Centre (VMC) with accuracy up to 3 μm; tested by manufacturing a NAS-979 component [12]. Simplified models of the machine were used to carry out offline simulations of the environmental behaviour of the machine, details of which are shown in Fig. 1.

The model was meshed using tetrahedral, hexahedron and hexahedron dominated (hexahedron/wedge) elements where applicable using Abaqus default meshing technique which revealed the total of 49,919 elements and 20,418 nodes. Fig. 2 shows the meshed assembly of the machine. All simulations are performed as transient thermal simulations where changing data from the temperatures sensors is applied in the software using the tabular amplitude technique.

2.2. Estimation of initial thermal state of the machine

Generally, prior to the start of any test, the machine elements exhibit variations in temperature due to the existence of temporal and spatial thermal gradients. In particular, vertical temperature gradients have been found to be significant [2,13]. As a result, it is unfeasible to accurately set initial temperatures of the components in the FEA software to match reality. A new technique of a two-stage simulation in Abaqus has been devised and applied to solve this problem. The first stage simulation in effect will estimate the time span required by a machine FEA model to 'absorb' the globally applied temperature for a temperature change representing the maximum variation likely to occur on the machine structure. This time span is termed as the 'settling time' and represents the temperature rise time for the steady state machine model when 'absorbing' the applied temperatures. The settling time is also representative of the minimum time required for on-machine testing which is explained in Section 2.3. This is followed by the second stage of normal environmental simulation that can be used for error modelling and compared with experiment for validation.

To set up the simulation, a standard shop floor temperature of 20 °C was applied as a uniform parameter to the full model of the machine as a 'Predefined Field' in the Abaqus software. Since this paper focuses on an attempt to prove the methodology and maintain relative simplicity in the FEA process, the entire model was applied with the convective heat transfer coefficient of $6\,W\,m^{-2}\,^\circ C^{-1}$ [1] which is an averaged value of the various heat transfer coefficients calculated experimentally [1]. It is acknowledged that more detailed application of surface specific coefficients could improve simulation accuracy (see Section 4.2). To estimate the time, the model was simulated until it achieved a temperature change indicative of the variation between the global assumed 20 °C and the applied temperature. A simulation was carried out with 1 °C temperature change to estimate the temperature rise time.
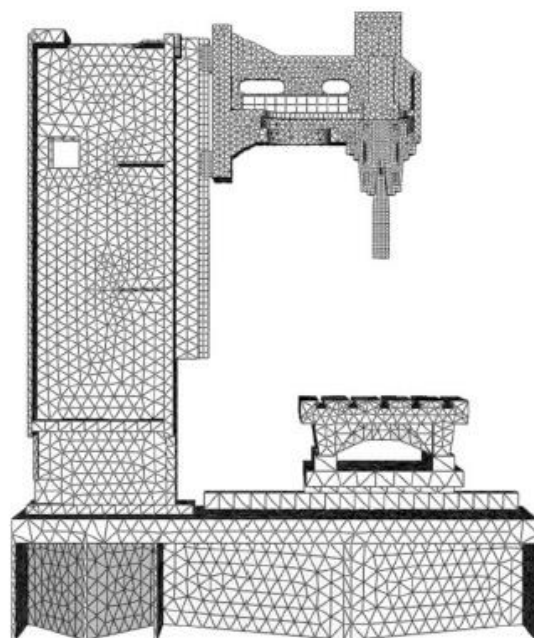

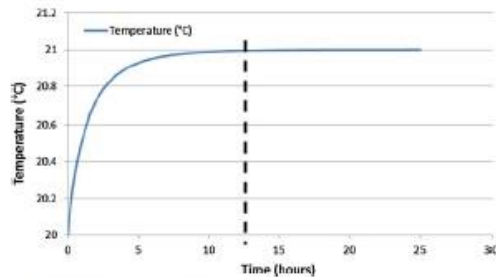**Fig. 2.** Meshed model of the machine.

Fig. 3. Settling time of 12.5 h was revealed for this machine's FEA model.

At the end of the simulation the temperature throughout the machine model was uniform; this ensured the selection of a random node to plot the settling time. The simulated result revealed that the machine model achieved 99.99% of the 1 °C temperature change from its initial temperature of 20 °C in 12.5 h as shown in Fig. 3. This settling time suggests that because the machine initial thermal state is unknown at the start of the simulation, this machine FEA model requires this settling time to absorb the applied recorded environmental temperature data at the end of which the temperature distribution should be synchronised with the real machine thermal state.

2.3. Model calibration

The model calibration sequences with the determination of the settling time at the first place. The settling time suggests the minimum environmental testing time required for this machine tool which is an important parameter for both; the production management to estimate the cost-to-production and for the accuracy of FEA results especially when achieving the initial thermal state of the machine FEA model before conducting environmental simulations. Therefore the environmental test to be conducted on the machine must ensure that the settling time is covered. The test then must be continued over a long period such as two or three days to establish the relationship between the machine thermal behaviour and environmental fluctuations occurring within the shop floor during the second stage simulation. The ambient sensors used to record data must be left situated in order to record continuously while the machine is in or off production. Since the determination of the settling time is an offline process therefore practically no machine downtime is required during the model calibration and for the application of this modelling methodology. The temperature sensors can be situated on the machine during any convenient maintenance schedule.

3. Validation of the method

The case study machine, described in 2.1.1, was modelled and calibrated as described. Standard environmental temperature variation error (ETVE) [14] tests were conducted on the 3-axis VMC over a period of a full year not only to validate but to confirm the robustness of the proposed methodology; however samples of data from two seasons (summer and winter) are presented. Three-day (consecutive) testing period was selected to ensure the setting time (12.5 h) data recording as well as to highlight thermal behaviour during normal 24 h periods on a nominally static machine tool. This means that the machine drives were inactive to avoid feedback correction from the position encoders; in essence to obtain the true deformation of machine structure. The model of the machine was not modified in any way during this validation phase.

3.1. Temperature and displacement sensor locations

The machine was already equipped with 65 temperature surface sensors in unique strips [15] for measuring detailed thermal gradients caused by the internal heat sources. Additionally seven surface sensors were placed on the column to track the environmental temperature gradients distribution in this tall structure and one surface sensor on the base. Three ambient sensors were placed inside the machine, at the machine column and adjacent to the base to measure environmental temperature variations. Five non-contact displacement transducers (NCDTs) were placed around a test mandrel to monitor the displacements and tilt of the test mandrel in the X, Y and Z axis directions. A 400 mm post made of invar was used to support the NCDTs. Invar is a steel alloy with a very low coefficient of thermal expansion ($1.2\,\mu\mathrm{m\,m^{-1}\,K^{-1}}$) which reduces the effects of changing environmental temperature. Sensor placements are shown in Fig. 4. With reference to the Base sensor, the inside ambient sensor was displaced by approximately 1 m vertically and 0.5 m horizontally while the column sensor was approximately 1.2 m vertically and 2 m horizontally apart.
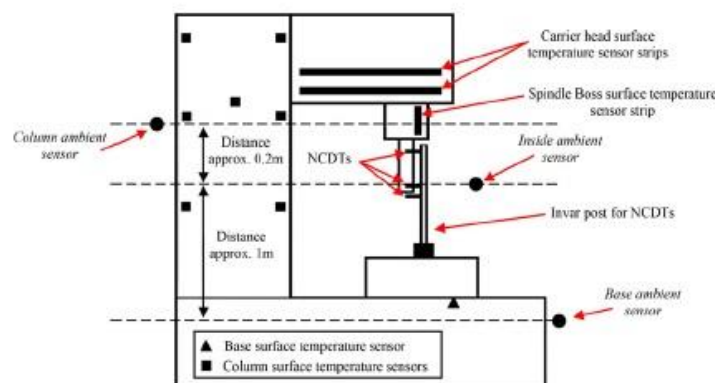

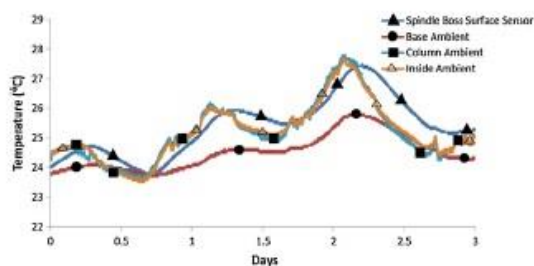**Fig. 4.** Temperature and displacement measurement locations.

Fig. 5. Temperature profiles obtained over 3 days period (summer test).

Fig. 7. Temperature gradients across the structure after the first stage (12.5 h) that represent the actual initial thermal state (summer test) – (NT11 – nodal temperatures – °C).

3.2. Summer test

The temperature information obtained from the surface sensor on the Spindle Boss and the ambient sensors for a 3 day period are shown in the Fig. 5. At the start of the test, the existence of a vertical temperature gradient around the machine of 1 °C was measured between the base ambient sensor and the column ambient sensor which creates the aforementioned complex initial state. It may also be of interest that the vertical temperature difference between the column ambient sensor and the base ambient sensor fluctuated to approximately 2.5 °C range over the test span which is further evidence of temperature instability within the shop floor environmental temperature arising from various sources such as the day and night transitions. Temperature fluctuations also occur when opening and closing workshop doors.

Fig. 6 shows the measured inside air temperature and the displacement of the mandrel in the Y-axis and Z-axis. The Y-axis displacement followed the temperature variation quite closely whereas the Z-axis displacement lagged the temperature by up to 3.6 h at some places. The analysis on the Y axis results (using the top and bottom NCDTs) revealed a 30 μm/m tilt present which is likely to have been caused by non-uniform distortions in the complex geometry of the structure resulting in the rapid response to the temperature variation; compared with the slow response of the Z-axis which is possibly contributed from pure expansion. The overall displacement range was approximately 12 μm for the Y-axis and approx. 28 μm for the Z-axis with the overall temperature swing of approximately 4 °C over 3 days. The X-axis results were negligible, due to the symmetry of the machine in this direction, and therefore not presented.

This test validates the hypothesis that environmental fluctuation causes thermal distortions in machine structure and proves the deterioration in the accuracy of a machine tool. It was also identified that vertical temperature gradients in a shop floor vary with height which can be critical to large and/or tall machines.
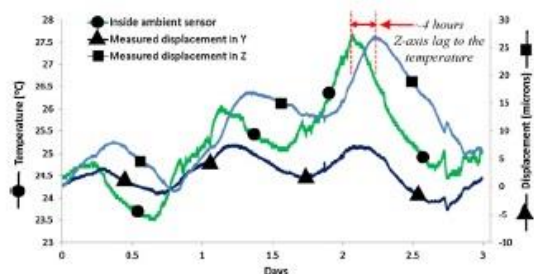
3.3. Validating settling time methodology

The settling time for this machine model was determined to be 12.5 h therefore data covering this time span was selected from the measured ambient data and used in the first stage simulation. As mentioned previously, the temperature data was applied as a transient function in the software using tabular amplitude technique for both simulation stages. Temperature data from the base sensor was applied to the base, information from the inside environmental sensor was applied to the carrier/spindle/tool and the table and temperature information obtained from the column ambient sensor was applied to the column. The result from the first stage simulation must provide not only the correct temperature profile but also the correct thermal memory to match the starting condition of the real machine. It must be noted that the simulations were carried out using only the ambient data which can be captured without machine downtime, the surface sensors are only used to compare and correlate the simulated results. Fig. 7 shows the simulated temperature gradients across the structure after the settling time which should represent the real surface temperature gradients after the 12.5 h span was lapsed. The predicted initial thermal state was revealed to be within ±0.2 °C range measured at points where surface sensors were placed and shown in Table 1

After the settling time simulation, a normal environmental simulation is then run in the second stage using the remainder of the recorded environmental temperature data. The measured and simulated profile results were plotted for the main second stage simulation. The simulated error is obtained as the difference in displacement between the table and the tool (test mandrel). Compared

Fig. 6. Y and Z axes displacements and the environmental temperature measured inside the machine (summer test).

Table 1
Comparison of measured and simulated surface temperatures after 12.5 h (summer test).

Structure	Measured temperature (°C)	Simulated temperature (°C)
Spindle boss surface	24.1	24
Column surface	24	23.9
Carrier head surface	24.2	24.0
Base surface	23.9	24

377
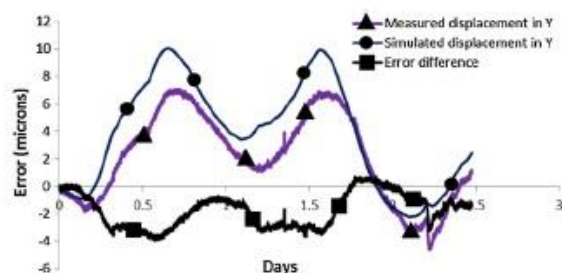
Fig. 8. Correlation between the measured and simulated Y axis displacement with settling time removed.
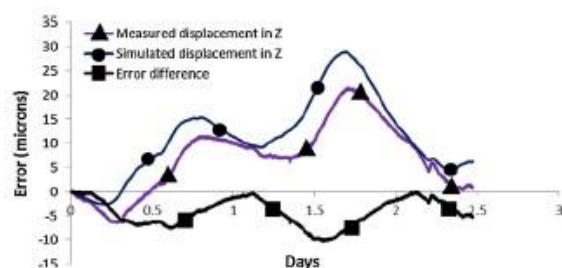
Fig. 9. Correlation between the measured and simulated Z axis displacement with settling time removed.

to the measured results, the correlations were 60% for the Y displacement profiles (Fig. 8) and 63% for the Z displacement profiles (Fig. 9). The residual errors were less than 5 μm for the Y axis and less than 11 μm for the Z axis. Including the settling time, separate simulations for temperature and displacement took approximately 30 and 40 min respectively (70 min in total). The computer used had typical PC specifications: AMD Phenom 9950 Quadcore 2.60 GHz processor, 4 GB RAM, NVIDIA GeForce 9400 GT graphics card and Windows XP 32bit operating system

4. Winter test

To further validate the robustness of this modelling methodology, another three-day test was carried out to observe the machine behaviour in the winter season. The workshop experienced typical single shift workshop heating patterns often encountered to maintain comfortable environmental temperature for the machine operators. The machine and measurement test conditions were the same as for the summer environment test.

The temperature information obtained from the ambient sensors and the spindle boss surface sensor are shown in Fig. 10. This time the vertical temperature difference between the column ambient sensor and the base ambient sensor fluctuated to
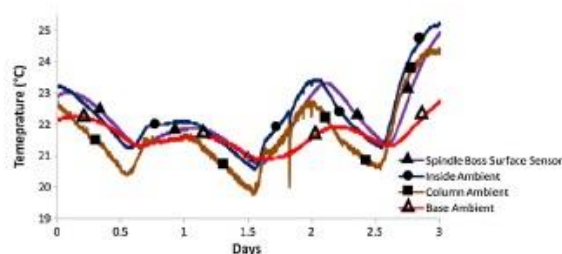
Fig. 10. Temperature data obtained over 3 days period (winter test).
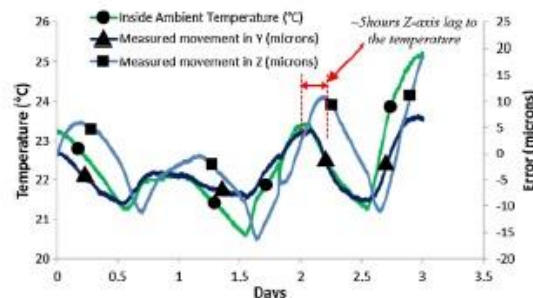
Fig. 11. Y and Z axes displacements and the environmental temperature measured inside the machine.

approximately 3 °C range over the test span which elaborates that even vertical temperature difference changes within similar vertical distances in different seasons. The spikes are suspected to be from the short periods for opening of workshop doors for deliveries which caused the shop floor environmental temperature to decrease.

Fig. 11 shows the measured inside air temperature and deformation of the machine in the Y axis and Z axis directions. The movement of both axes followed the temperature variation while the Z axis displacement followed but with approximately 5 h lag this time. The overall movement is 18 μm in the Y axis and 35 μm in the Z axis for an overall temperature swing of approximately 5 °C over the 3 days. This increase was expected because of the exaggerated day and nights heating transitions.

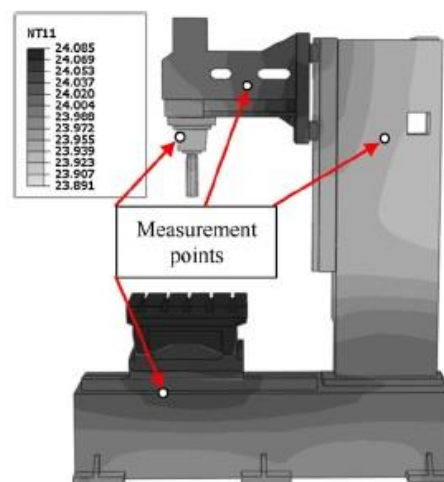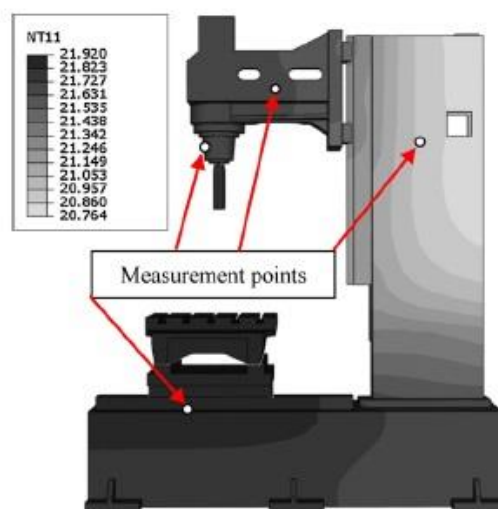**Fig. 12.** Temperature gradients across the structure after the first stage (12.5 h) that represent the actual initial thermal state (winter test).

Table 2
Comparison of measured and simulated surface temperatures after 12.5 h (winter test).

Structure	Measured temperature (°C)	Simulated temperature (°C)
Spindle boss surface	21.7	21.7
Column surface	21	20.9
Carrier head surface	21.6	21.6
Base surface	21.9	21.9

Table 3
Summary of the results.

	Y drift (μm)	Y model error (μm)	Y improvement (%)	Z drift (μm)	Z model error (μm)	Z improvement (%)
Summer	12	4.6	60	28	10	63
Winter	18	6.3	63	35	11.7	67
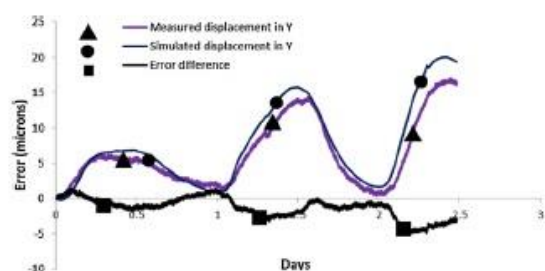
Fig. 13. Correlation between the measured and simulated Y axis displacement with settling time removed.

4.1. FEA simulations (offline assessments – winter test)

A similar procedure was followed for simulating the model. For the first stage, 12.5 h of the recorded data was used for the settling time as before, followed by the environmental simulation in the second stage. Fig. 12 shows the simulated temperature gradients across the structure after the settling time which represents the real surface temperature gradients after the 12.5 h span was lapsed. The predicted initial thermal state was revealed to be within ±0.2 °C range measured at points where surface sensors were placed and shown in Table 2.

4.1.1. Winter test correlations

The simulated results correlate well with the measured profile being 63% for the Y movement profiles (Fig. 13) and 67% for the Z movement profiles (Fig. 14). The residual errors were less than 7 μm in Y and less than 12 μm in Z.

The winter test not only validated the capability of the modelling methodology but also confirmed its robustness. Development of the CAD model, obtaining the settling time and FEA environmental simulations are conducted offline. The temperature sensors can be installed in any convenient maintenance schedule and environmental temperature data can be recorded while the machine in production therefore is non-invasive to production and cost effective as generally no machine downtime is involved. It is also highlighted that 12.5 h of settling time can be representative of a minimum time required for temperature data acquisition which can be recorded while the machine is in production.
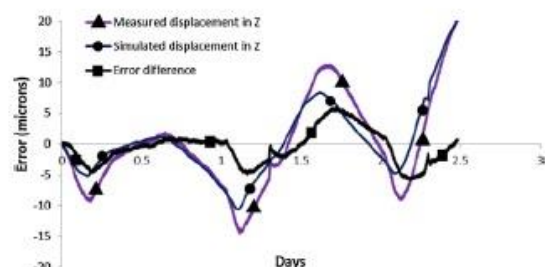
Fig. 14. Correlation between the measured and simulated Z axis displacement with settling time removed.

4.2. Summary of results

An FEA-derived thermal model of the machine was created in the summer using a 12.5 h settling time methodology. This methodology has been validated over a year period, with results from two Three-day tests (summer and winter) presented here. Table 3 summarises the results.

It can be observed that compared to good temperature correlations (>90%), the predicted positioning of the machine matched within 60–67% range with the measured movement. This is suspected to be due to the averaged heat transfer coefficient values used in this case study for the FEA model. It is anticipated that the positioning results can correlate better when the FEA model is applied with surface specific heat transfer coefficients that vary around enclosed voids creating air pockets that will vary in temperature independent to the bulk ambient temperature [1].

5. Conclusions

Environmental thermal testing is often avoided in industries due to the costs and inconvenience associated with machine downtime. This paper presented a novel offline environmental thermal error modelling method based on FEA that successfully deals with the machine downtime issue using a two-stage simulation method, short on-line testing period and non-disruptive offline temperature monitoring. The sequence of the method is to create a CAD model of the machine, determine the settling time of that machine model and create initial conditions in the first stage followed by the environmental simulation in the second stage. The settling time ensures the minimum time is spent on data acquisition. Temperature sensors can be installed on the machine during any convenient scheduled machine maintenance and the simulations can be done within an hour or two, so it is highly efficient. The methodology was successfully validated on a 3 axis vertical milling machine tool over a year period; samples of data from two ETVE tests during two seasons (summer and winter) are presented where the critical nature of the fluctuating shop floor environment and its effect on machine tool precision were also highlighted. The results revealed good correlations between the experimental and FEA simulated results typically between 60% and 70%. The modelling methodology has significantly reduced the machine downtime required for a typical environmental testing from a fortnight to only hours. Practically no machine downtime is associated with the application of this modelling methodology except for short validations (if required). Additional useful information can be obtained for predicting the effects of speculative conditions.

References

[1] Mian NS, Fletcher S, Longstaff AP, Myers A. Efficient thermal error prediction in a machine tool using finite element analysis. Measurement Science and Technology 2011;22(8):085107.

[2] Longstaff AP, Fletcher S, Ford DG. Practical experience of thermal testing with reference to ISO 230 Part 3. In: Ford DG, editor. Laser metrology and machine performance VI. Southampton: WIT Press; 2003. p. 473–83.

[3] Hao W, Hongtao Z, Qianjian G, Xiushan W, Jianguo Y. Thermal error optimization modeling and real-time compensation on a CNC turning center. Journal of Materials Processing Technology 2008;207(1–3):172–9.

[4] Yang JG, et al. Testing, variable selecting and modeling of thermal errors on an INDEX-G200 turning center. International Journal of Advanced Manufacturing Technology 2005;26(7–8):814–8.

[5] Tseng P-C, Chen S-L. The neural-fuzzy thermal error compensation controller on CNC machining center. JSME International Journal Series C Mechanical Systems, Machine Elements and Manufacturing 2002;45(2):470–8.

[6] Du ZC, Yang JG, Yao ZQ, Xue BY. Modeling approach of regression orthogonal experiment design for the thermal error compensation of a CNC turning center. Journal of Materials Processing Technology 2002;129(1–3):619–23.

[7] Rakuff S, Beaudet P. Thermal and structural deformations during diamond turning of rotationally symmetric structured surfaces. Journal of Manufacturing Science and Engineering 2008;130(4):041004–41009.

[8] Fletcher S, Longstaff AP, Myers A. Flexible modelling and compensation of machine tool thermal errors. In: 20th annual meeting of American society for precision engineering. 2005.

[9] Jedrzejewski J, Modrzycki W, Kowal Z, Kwaśny W, Winiarski Z. Precise modelling of HSC machine tool thermal behaviour. Journal of Achievements in Materials and Manufacturing Engineering 2007;24(1):245–52.

[10] Bringmann B, Knapp W. Machine tool calibration: geometric test uncertainty depends on machine tool performance. Precision Engineering 2009;33(4):524–9.

[11] ABAQUS/CAE User's Manual 6.1. Pawtucket, RI 02860-4847, USA: Hibbitt, Karlsson and Sorensen, Inc.; 2000.

[12] Mian, N.S. Efficient machine tool thermal error modelling strategy for accurate offline assessment; 2010. Available from: http://eprints.hud.ac.uk/11054/

[13] Weck M, McKeown P, Bonse R, Herbst U. Reduction and compensation of thermal errors in machine tools. CIRP Annals – Manufacturing Technology 1995;44(2):589–98.

[14] ISO 230-3:2007 test code for machine tools – Part 3: determination of thermal effects. International Organization for Standardization; 2007.

[15] Fletcher S, Longstaff AP, Myers A. Measurement methods for efficient thermal assessment and error-compensation. In: Proceedings of the topical meeting: thermal effects in precision systems. 2007.

2013-13 Application of GNNMCI (1, N) to environmental thermal modelling of CNC machine tools.

International Conference on Advanced Manufacturing Engineering and Technologies

Application of GNNMCI(1, N) to environmental thermal error modelling of CNC machine tools

Ali M Abdulshahed, Andrew P Longstaff, Simon Fletcher, Alan Myers

Centre for Precision Technologies, University of Huddersfield, UK, HD1 3DH
Email: Ali.Abdulshahed@hud.ac.uk

ABSTRACT

Thermal errors are often quoted as being the largest contributor to inaccuracy of CNC machine tools, but they can be effectively reduced using error compensation. Success in obtaining a reliable and robust model depends heavily on the choice of system variables involved as well as the available input-output data pairs and the domain used for training purposes. In this paper, a new prediction model "Grey Neural Network model with Convolution Integral (GNNMCI(1, N))" is proposed, which makes full use of the similarities and complementarity between Grey system models and Artificial Neural Networks (ANNs) to overcome the disadvantage of applying a Grey model and an artificial neural network individually. A Particle Swarm Optimization (PSO) algorithm is also employed to optimize the Grey neural network. The proposed model is able to extract realistic governing laws of the system using only limited data pairs, in order to design the thermal compensation model, thereby reducing the complexity and duration of the testing regime. This makes the proposed method more practical, cost-effective and so more attractive to CNC machine tool manufacturers and especially end-users.

KEYWORDS: Machine tool, Thermal error, Modelling, Grey neural network.

1. INTRODUCTION

Thermal errors of machine tools, caused by external and internal heat sources, are one of the main factors affecting CNC machine tool accuracy. A significant amount of research work has been devoted to the effects of internally generated heat from, for example, spindle motors, friction in bearings, etc. [1]. External heat sources are attributed to the environment in which the machine is located, such as neighbouring machines, opening/closing of machine shop doors, variation of the environmental temperature during the day and night cycle and differing behaviour between seasons. The complex thermal behaviour of a machine is created by interaction between these different heat sources. Ambient effects are arguably one of the most important, but most neglected in thermal error compensation systems [2]. An integrated model can be used in machine tool error compensation, taking into account the different heat sources [1]. An example of such a model for a CNC machine tool is given by White *et al.* [3].

Longstaff *et al.* [2] presented several Environmental Temperature Variation Error (ETVE) tests conducted on a wide range of machine tools and discussed the implications for produced parts. The authors also described a number of interesting phenomena when the machines were subjected to a wide variety of environmental conditions. Attention was also drawn to the prohibitive downtime required to conduct the ETVE test. Modification of the machine shop conditions is possible and can effectively reduce thermal errors on a number of machines at once, but may be difficult and costly to achieve. Fletcher *et al.* [4] provided useful information about daily cyclic environmental temperature fluctuations and associated drifts. Experimental results indicated, through error compensation, a reduction of the environmental errors by more than 50% to just $\pm 7\mu m$ over a 65 hour test, but also drew attention to the detrimental amount of machine downtime for the thermal characterisation tests. Rakuff and Beaudet [5] measured and modelled the ETVE of a machine tool over 23 h with no traffic in the workshop. They show how certain process variables, such as opening and closing of doors around the machine, affect the ETVE. Mian *et al.* [6] proposed a novel offline environmental thermal error modelling approach based on a finite element analysis (FEA) model that reduces the machine downtime usually needed for the ETVE test from a fortnight to 12.5 hours. Their modelling approach was tested and validated on a production machine tool over a one-year period and found to be very robust. However, building a numerical model can be a great challenge due to problems of establishing the boundary conditions and accurately obtaining the characteristic of heat transfer.

Research on thermal error compensation for machine tools by both academic institutions and industry has been rapidly accelerated recently in response to the growing demand of product quality. Effective compensation depends on the accuracy of the prediction model. Thermal error modelling and compensation techniques introduced to date have been found to suffer from a number of drawbacks that make their application in practical machining environments time consuming. Different structures of empirical models have been used to predict thermal errors in machine tools such as multiple regression analysis [7], artificial neural networks [7], adaptive neuro-fuzzy inference system [8, 9], Grey system theory [10] and a combination of several different modelling methods [11].

Whilst empirical models can be good at predicting thermal errors, they require a large amount of data with different working conditions to determine the governing laws of the original data. However, a realistic governing law may not exist even when a large amount of data has been measured. Furthermore, the process of obtaining such data can take several hours for internal heating tests and several days or more for the environmental test.

This paper aims to develop an effective and simple method to predict the Environmental Temperature Variation Error (ETVE) of machine tools. The work proposes a novel Grey Neural Network model with Convolution Integral GNNMCI(1,N), combining the Grey prediction model with convolution integral GMC(1,N) and PSO neural network model, and also adopting the GMC(1,N) model when selecting the inputs. The proposed model is a type of dynamic model described by a PSO neural network to extract realistic governing laws of the system using only a limited number of data pairs. The dynamic characteristic of the GNNMCI(1,N) model results from introducing the Grey accumulated generating operation (AGO) into the neural network. The benefits and novelty of this work are that a thermal model can be efficiently built with the minimum amount of temperature data in a very short time scale.

2. MODELLING THE THERMAL ERROR USING A GREY NEURAL NETWORK

The Grey systems theory, established by Deng in 1982 [12], is a methodology that focuses on solving problems involving incomplete information or small samples. The technique works on uncertain systems with partially known information by generating, mining, and extracting useful information from available data. So, system behaviours and their hidden laws of evolution can be accurately described. GM(1, N) is the most widely used implementation in literature [13], which can establish a first-order differential equation featured by comprehensive and dynamic analysis of the relationship between system parameters. The accumulated generating operation (AGO) is the most important characteristic of the Grey system theory, and its benefit is to increase the linear characters and reduce the randomness of the samples. Based on the existing GM(1,N) model, Tzu-Li Ties [14] proposed a GMC(1,N) model, which is an improved grey prediction model. The modelling values by GM(1,n) are corrected by including a convolution integral. However, Grey models lack the ability to self-learn, self-adapt or otherwise considering a feedback value.

Compared with other empirical models, artificial neural networks (ANNs) have a strong capacity for processing information, parallel processing, and self-learning. However, they have some disadvantages such as the need for a large number of learning samples, thus needing a long training computation time, and the non-interpretable problem of such "black box" systems. In addition, the working conditions of machine tools are in general complex and susceptible to unexpected noises. Therefore, ANN models in isolation have significant drawbacks as a modelling approach for thermal error compensation [3].

Because the way of presenting information for neural network and Grey models have some commonality in format, the two methods can be fused. Two levels can be added; an initial Grey level will process the input information and a whitening level after to process the output information to obtain good results [15]. Therefore, the Grey meaning is contained in the neural network. The advantages of both can be used to build a high-performance neural network model with a minimum amount of training data.

2.1. GNNMCI(1, N) Prediction Model

The fusion model of Grey system and neural network is employed in the modelling of the ETVE of machine tools. The model can reveal the long-term trend of data and, by driving the model by the AGO, rather than raw data, can minimize the effect of some of the random occurrences. Therefore, the first step for building GNNMCI(1,N) is to carry out 1-AGO (first-order Accumulated Generating Operation) to the data, so as to increase the linear characteristics and reduce the randomness from the measuring samples. Then the GNNMCI(1,N) model is trained with a PSO algorithm to generate the desired GNNMCI(1,N) model. Finally an IAGO (inverse Accumulated Generating Operation) is performed to predict the ETVE and generate the final compensation values. The model fully takes the advantages of neural networks and Grey models, and overcomes the disadvantages of them, achieving the goal of effective, efficient and accurate modelling. The modelling details are described as follows:

The Grey prediction model with convolution integral GMC(1, n) [14] is:

$$\frac{dX_1^{(1)}}{dt} + b_1 X_1^{(1)} = b_2 X_2^{(1)} + b_3 X_3^{(1)} + \cdots + b_N X_N^{(1)} + u \tag{1}$$

where b_1 is the development coefficient, $b_i (i = 2,3, \dots, N)$ the driving coefficient, and u is the Grey control parameter. Therefore, time response sequences can be obtained.

$$\hat{x}_1^{(1)}(k+1) = x_1^{(1)}(1)e^{-b_1 k} + u(t-1) \times \sum_{\tau=1}^{k} \left\{ e^{-b_1(k-\tau+\frac{1}{2})} \cdot \frac{1}{2}[f(\tau) + f(\tau-1)] \right\} \qquad (2)$$

Where $u(t-1)$ is the unit step function [14]; $f(\tau) = \sum_{j=2}^{N} b_j X_j^{(1)}(\tau) + u$ k=1,2,....,n.

To calculate the coefficients b_j and u, the neural network method can be used to map equation (2) to a forward neural network. Then, the neural network model is trained until the performance is satisfactory. Finally, the optimal corresponding weights are used as the Grey neural network weights to predict ETVE.

We can process equation (2) more. Let

$$G = u(t-1) \times \sum_{\tau=1}^{k} \left\{ e^{-b_1(k-\tau+\frac{1}{2})} \cdot \frac{1}{2}[f(\tau) + f(\tau-1)] \right\} \qquad (3)$$

We can rewrite equation (2) as:

$$\hat{x}_1^{(1)}(k+1) = \left(x_1^{(1)}(1) \right) e^{-b_1 k} + G \qquad (4)$$

Then equation (4) can be converted into equation (5) as follows:

$$\hat{x}_1^{(1)}(k+1) = \left[x_1^{(1)}(1) \frac{e^{-b_1 k}}{1 + e^{-b_1 k}} + G \frac{1}{1 + e^{-ak}} \right] (1 + e^{-b_1 k})$$

$$\hat{x}_1^{(1)}(k+1) = \left[x_1^{(1)}(1) \left(1 - \frac{1}{1 + e^{-b_1 k}} \right) + G \frac{1}{1 + e^{-b_1 k}} \right] (1 + e^{-b_1 k})$$

$$= \left[x_1^{(1)}(1) - x_1^{(1)}(1) \frac{1}{1 + e^{-b_1 k}} + G \frac{1}{1 + e^{-b_1 k}} \right] (1 + e^{-b_1 k}) \qquad (5)$$

Map equation (5) into a neural network, and the mapping structure is shown in Fig. 1.
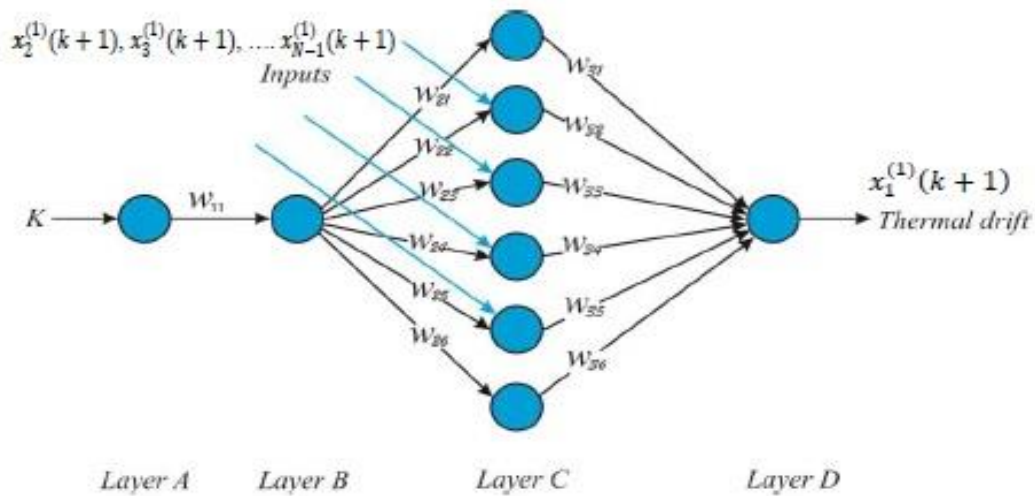
Fig. 1. The mapping structure of GNNMCI(1, N).

Where k is the serial number of input parameters;

In this study, $x_1^{(1)}(k + 1)$ is chosen as the thermal displacement data series (network output) and $x_2^{(1)}(k + 1)$, $x_3^{(1)}(k + 1)$, ... $x_{N-1}^{(1)}(k + 1)$, as a data seies of temprature sensores (N is the number of network inputs);

$w_{11}, w_{21}, w_{22}, ... w_{2n}, w_{31}, w_{32} ... w_{3n}$ are the weights of the network;

Layer A, layer B, layer C, and layer D are the four layers of the network, respectively.

Where, the corresponding neural network weights can be assigned as follows:

Let us assume that $d_1 = f(b_2)$, $\quad d_2 = f(b_2), ... \quad d_{N-2} = f(b_{2-N})$, $\quad d_{N-1} = f(u)$

$w_{11} = b_1$, $w_{21} = -x_1^{(1)}(1)$, $\quad w_{22} = d_1$, $\quad w_{23} = d_2, ..., w_{2N-1} = d_{N-2}$, $\quad\quad w_{2N} = d_{N-1}$

$w_{31} = w_{32} = w_{33} = \cdots = w_{3N} = 1 + e^{-b_1 k}$

The bias Θ value of $x_1^{(1)}(k + 1)$ is:

$$\Theta = \left(-x_1^{(1)}(k + 1)\right)\left(1 + e^{-b_1 k}\right) \tag{6}$$

The transfer function of Layer B is a sigmoid function $f(x) = \frac{1}{1 + e^{-x}}$, the transfer functions of other layer's neuron are adopted as a linear function $f(x) = x$.

2.2. GNNMCI(1, N) learning algorithm

The learning algorithm of GNNMCI(1, N) can be summarised as follows:

Step 1: For each input series, $(k, X_j^{(1)}(k))$, $(k = 2,3,...N)$, the output of each layer is calculated.

Layer A: $a = w_{11}k$;

Layer B: $b = f(w_{11}t) = \frac{1}{1 + e^{-w_{11}k}}$;

Layer C: $c_1 = bw_{21}$, $c_2 = x_2(k)bw_{22}$, $c_3 = x_3(k)bw_{23}, ... c_{n-1} = x_n(k)bw_{2n-1}, c_n = bw_{2n}$;

Layer D: $d = w_{31}c_1 + w_{32}c_2 + ... w_{3n-1}c_{n-1} + w_{3n}c_n - \Theta$

Step 2: A PSO algorithm [16] is adopted to train the GNNMCI(1, N) model. Each weight of model is encoded to each component of particle position, which means that each particle represents a specific group of weights. In the course of training, the model is repeatedly presented with training pairs. The model parameters are then adjusted until the errors between the predicted output and real output meet a tolerance criterion, or a pre-determined number of epochs has passed (in this work, ten training epochs are determined as the stopping criteria).

Step 3: export the optimal solution. $(w_{11}, w_{21}, w_{22}, w_{2N}, ... , w_{31}, w_{32}, ... , w_{3N})$.

3. EXPERIMENTS

In this study, an ETVE test was performed on a small vertical milling centre (VMC). This test was conducted to reveal the effects of ambient temperature changes on the machine and to predict the thermal displacement during other performance measurements [2]. In order to obtain the temperature data of the machine tool, a total of 27 temperature sensors were placed on the machine. Thirteen temperature sensors were attached on the spindle carrier, six on the column, and one on each axis ballscrew nut. Another six temperature sensors were

placed around the machine to detect the ambient temperature. Four non-contact displacement transducers (NCDTs) were used to measure the displacement of a test bar (used to represent the tool) while the spindle remained stationary. Three were used to measure displacement of the test bar in each axis direction. A fourth directly monitored displacement of the casting next to the spindle in the Z-axis direction to differentiate expansion of the tool from the machine. A general overview of the experimental setup is shown in Fig. 2.
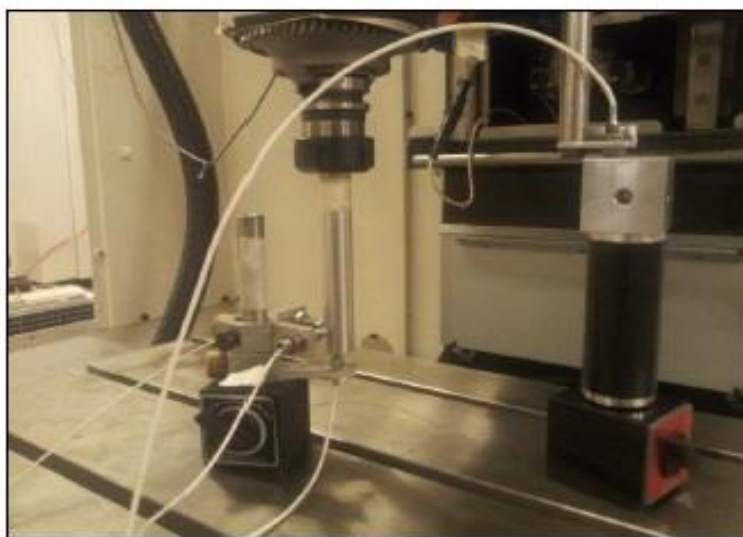
Fig. 2. A general overview of the experimental setup.

Results of an ETVE test are shown in Fig. 3. This test was carried out over a five-day period during spring bank holiday, with no significant activity in the workshop, followed by approximately three normal working days (160 hours). This data was sampled once every minute. The environmental temperature conditions for machine shop change due to the day /night cycle, where the temperature fluctuates by about 5 ˚C throughout the day, with lower temperatures in the morning and higher temperatures in the late afternoon and evening. The strongest response to the ambient change from the machine is in the Z-axis direction. There is a clear relation between the fluctuation in the environmental temperature and the resulting displacement. For example, the anomaly at the beginning of the test can be attributed to a short period (30 minutes) of the workshop door being opened. Externally, the conditions were snowy, which caused a drop in workshop temperature to below 11˚C. The overall movement caused by this phenomenon is 35 μm in the Z-axis and 25 μm in the Y- axis for an overall temperature swing of approximately 9 ˚C over the 30 minutes. Two similar events can be seen between 120 and 140 minutes. The magnitude of the environmental error can be compared to that from two hours spindle-heating test conducted according to ISO-230:3 which only produced 30μm of error in the Z-axis.

To demonstrate the modelling of ETVE using the Grey neural network approach, four temperature sensors were selected based on our work in [9]. Temperature sensors T1, T2, T5, and T9, which are located on the carrier, column, ambient near spindle, and ambient near the column, were selected according to their influence coefficient value using the GMC(1, N) model. They were used as the input variables for the GNNMCI(1, 5) model and the thermal drift in Z direction was used as a target variable.

International Conference on Advanced Manufacturing Engineering and Technologies

Fig. 3. Temperature measurements and machine movement due to environment.

For this study, a GNNMCI(1, 5) with a structure of 1-1-6-1was chosen. The details are: layer A has one node, the input time series k; layer B has one node; layer C has six nodes, the input variables nodes are from two to five, respectively; T1, T2, T5, and T9 are the input variable data. Layer D has an output variable node, which is the thermal displacement in Z-axis direction. The GNNMCI(1, 5) structure is shown in Fig. 1. The MATLAB software was used to realize the model.

Two compensation methods can be used to predict ETVE. The first is an off-line, pre-calibrated method. This means to obtain the GNNMCI(1, 5) model according to the thermal displacement and the temperature change during a short test, and then to use this model to predict the thermal displacement of other processes. The second method is to obtain the GNNMCI(1, N) model at the first stage of the manufacturing process, and then to use this model to predict the machine movement during the rest of the process. This uses additional measurement effort before the process begins.

To apply the first method, another test was carried out for 80 minutes on the same machine during a normal working day. During the experiment, the thermal errors were measured by the NCDTs and the temperature data was measured using the same selected sensors, sampling every ten seconds. The training samples were obtained from the first 5 readings (less than one minute) after the test had been started. All raw data was converted to AGO series, as discussed in section 2.1. Ten training epochs are adapted as the stopping criteria. In the PSO neural network, the number of population was set to be 90 whilst the maximum and minimum velocity values were 1.5 and -1.5, respectively. These values were obtained by optimization.

After finishing the training of the model, there were two ways to obtain the prediction values: directly obtaining the prediction values from the trained model; or taking out the Grey differential equation parameters from the trained model to equation (2) and then solving the equation to obtain the prediction values. Although both methods are similar theoretically, a large number of experiments have found that the first method needs less computation. Fig. 4 shows simulation results for 80 minutes.

Fig. 4: Simulation results for 80 minutes.

The process was repeated to create a GNNMCI (1, 5) model for the Y-axis direction. To validate the robustness of these proposed models on non-training data, a normal environmental simulation was run using the temperature data presented in Fig. 3. The measured and simulated profile results were plotted for the Z-axis and Y-axis. Compared to the measured results, the correlations were 97% for the Z displacement profiles Fig. 5, and 98% for the Y displacement profiles Fig. 6. The residual errors were less than ± 10 μm for the Z axis and less than ± 6 μm for the Y axis even when considering the rapid changes due to the opened workshop door. Under more predictable conditions, which could be achieved by better management of the environment, ±3μm would be achieved in each axis. Thus, the proposed GNNMCI (1, 5) model can predict the normal daily cyclic error accurately and also can track sudden changes of thermal error from a relatively small training sample.

Fig. 5.Correlation between the measured and simulated Z-axis displacement.

Fig. 6. Correlation between the measured and simulated Y-axis displacement.

2. CONCLUSIONS

Temperature-induced effects on machine tools are a significant part of the error budget. Changes in ambient conditions are an often overlooked effect that can be difficult to model, especially in unpredictable environments.

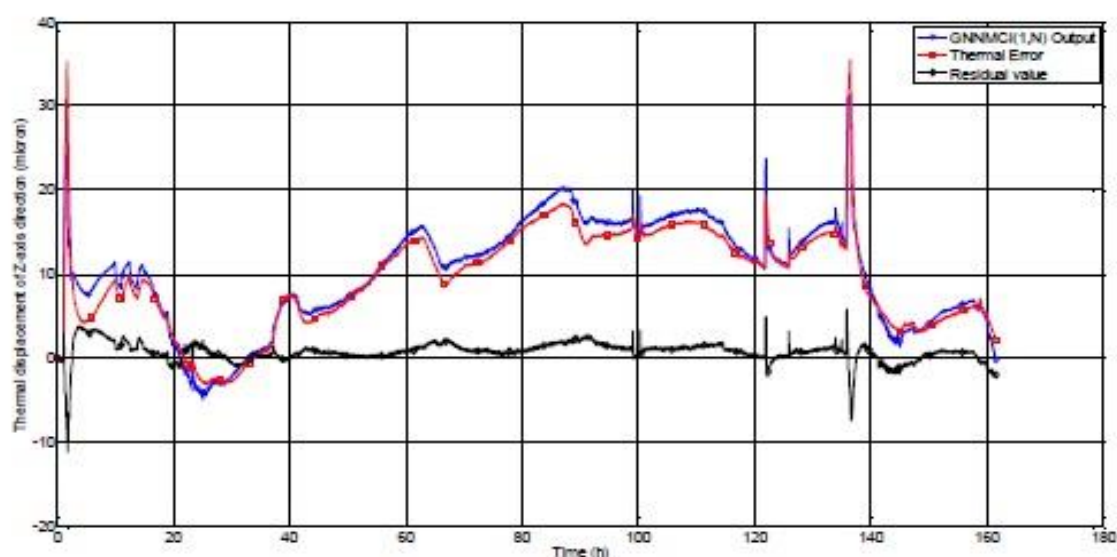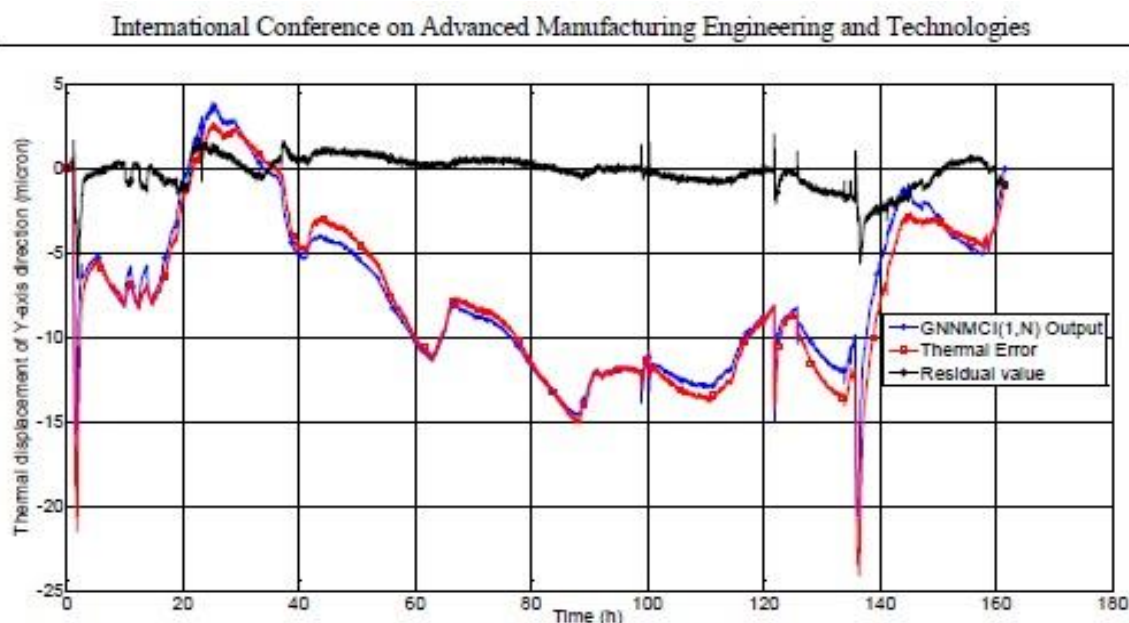In this paper, a novel thermal error modelling method based on Grey system theory and neural networks was developed to predict the environmental temperature variation error (ETVE) of a machine tool. The proposed model has been found to be flexible, simple to design and rapid to train.

The model is trained using data obtained from a short test of less than ninety minutes, which is desirable for minimising machine downtime. The accuracy of the model has not been compromised by restricting the training data. ETVE results in the Z-axis direction over a 160 hour test showed a reduction in error from over 20µm to better than ±3µm considering the normal daily cycles. When also considering unexpected phenomena, such as the rapid change in temperature when a workshop door was opened, the model still performs well, with an improvement from 40µm to less than ±10µm.

Similar results were achieved in the Y-axis direction, with this study not considering the X-axis direction due to symmetry of the machine.

It is anticipated that further improvement in correlation could be achieved by including rapid changes as part of the training data. However, this would compromise the aim of this work which is to train the model with "normal" data, but validate across a range of conditions.

The proposed method is a significant advantage over other models based on a single technique that have been used by many previous scholars where the data used to build the models is obtained from very long tests. The proposed model has significantly reduced the machine downtime required for a typical environmental testing from hours to only few minutes. According to experimental work, little machine downtime is needed to apply this modelling approach except to re-establish the model if needed.

The thermal error compensation model using GNNMCI(1, N) introduced in this study can be applied to any CNC machine tool because the model does not rely on a parametric model of the thermal error behaviour. In addition, this method is open to extension of other

different physical inputs meaning that alternative sensors can be deployed with minimal retraining required.

ACKNOWLEDGEMENTS

REFERENCES

[1] J. Mayr, et al., "Thermal issues in machine tools," *CIRP Annals - Manufacturing Technology*, vol. 61, pp. 771-791, 2012.

[2] A. P. Longstaff, et al., "Practical experience of thermal testing with reference to ISO 230 Part 3," in *Laser metrology and machine performance VI*, Southampton, 2003, pp. 473-483.

[3] A. White, et al., "A general purpose thermal error compensation system for CNC machine tools," in *Laser Metrology and Machine Performance V*, Southampton, 2001, pp. 3-13.

[4] S. Fletcher, et al., "Flexible modelling and compensation of machine tool thermal errors," in *20th Annual Meeting of American Society for Precision Engineering, Norfolk, VA*, 2005.

[5] S. Rakuff and P. Beaudet, "Thermally induced errors in diamond turning of optical structured surfaces," *Optical Engineering*, vol. 46, pp. 103401-103409, 2007.

[6] N. S. Mian, et al., "Efficient estimation by FEA of machine tool distortion due to environmental temperature perturbations," *Precision engineering*, vol. 37, pp. 372-379, 2013.

[7] J. Chen, et al., "Thermal error modelling for real-time error compensation," *The International Journal of Advanced Manufacturing Technology*, vol. 12, pp. 266-275, 1996.

[8] K. C. Wang, "Thermal error modeling of a machining center using grey system theory and adaptive network-based fuzzy inference system," in *Cybernetics and Intelligent Systems*, Bangkok, 2006, pp. 1-6.

[9] A. Abdulshahed, et al., "Comparative study of ANN and ANFIS prediction models for thermal error compensation on CNC machine tools," in *Laser Metrology and Machine Performance X*, Buckinghamshire, 2013, pp. 79-88.

[10] Y. Wang, et al., "Compensation for the thermal error of a multi-axis machining center," *Journal of materials processing technology*, vol. 75, pp. 45-53, 1998.

[11] K. C. Wang, "Thermal error modeling of a machining center using grey system theory and HGA-trained neural network," in *Cybernetics and Intelligent Systems*, Bangkok, 2006, pp. 1-7.

[12] D. Ju-Long, "Control problems of grey systems," *Systems & Control Letters*, vol. 1, pp. 288-294, 1982.

[13] L. Sifeng, et al., "A brief introduction to grey systems theory," in *Proceeding of IEEE International Conference on Grey Systems and Intelligent Services 2011*, Nanjing, 2011, pp. 1-9.

[14] T.-L. Tien, "A research on the grey prediction model GM (1, n)," *Applied Mathematics and Computation*, vol. 218, pp. 4903-4916, 2012.

[15] J. Yuan, et al., "Modeling of Grey Neural Network and Its Applications," in *Advances in Computation and Intelligence*. vol. 5370, L. Kang, et al., Eds., ed: Springer Berlin Heidelberg, 2008, pp. 297-305.

[16] V. G. Gudise and G. K. Venayagamoorthy, "Comparison of particle swarm optimization and backpropagation as training algorithms for neural networks," in *Swarm Intelligence Symposium, 2003. SIS'03. Proceedings of the 2003 IEEE*, 2003, pp. 110-117.

2015-03 Thermal error modelling on machine tools based on ANFIS with fuzzy c-means clustering using a thermal imaging camera.

Thermal error modelling of machine tools based on ANFIS with fuzzy c-means clustering using a thermal imaging camera

CrossMark

Ali M. Abdulshahed *, Andrew P. Longstaff, Simon Fletcher, Alan Myers

Centre for Precision Technologies, School of Computing and Engineering, University of Huddersfield, Queensgate, Huddersfield HD1 3DH, UK

ARTICLE INFO

ABSTRACT

Thermal errors are often quoted as being the largest contributor to CNC machine tool errors, but they can be effectively reduced using error compensation. The performance of a thermal error compensation system depends on the accuracy and robustness of the thermal error model and the quality of the inputs to the model. The location of temperature measurement must provide a representative measurement of the change in temperature that will affect the machine structure. The number of sensors and their locations are not always intuitive and the time required to identify the optimal locations is often prohibitive, resulting in compromise and poor results.

In this paper, a new intelligent compensation system for reducing thermal errors of machine tools using data obtained from a thermal imaging camera is introduced. Different groups of key temperature points were identified from thermal images using a novel schema based on a Grey model GM (0,N) and fuzzy c-means (FCM) clustering method. An Adaptive Neuro-Fuzzy Inference System with fuzzy c-means clustering (FCM-ANFIS) was employed to design the thermal prediction model. In order to optimise the approach, a parametric study was carried out by changing the number of inputs and number of membership functions to the FCM-ANFIS model, and comparing the relative robustness of the designs. According to the results, the FCM-ANFIS model with four inputs and six membership functions achieves the best performance in terms of the accuracy of its predictive ability. The residual value of the model is smaller than ± 2 µm, which represents a 95% reduction in the thermally-induced error on the machine. Finally, the proposed method is shown to compare favourably against an Artificial Neural Network (ANN) model.

© 2014 The Authors. Published by Elsevier Inc. This is an open access article under the CC BY license (http://creativecommons.org/licenses/by/3.0/).

1. Introduction

Thermal errors can have significant effects on CNC machine tool accuracy. They arise from thermal deformations of the machine elements created by external heat/cooling sources or those that exist within the structure (i.e. bearings, motors, belt drives, the flow of coolant and the environment temperature). According to various publications [1,2], thermal errors represent approximately 70% of the total positioning error of the CNC machine tool. Spindle drift is often considered to be the major error component among them [1]. Thermal errors can be reduced by amending a machine tool's structure using advanced design and manufacture procedures, such as structural symmetry or cooling jackets. However, an error compensation system is often considered to be a less restrictive and more economical method of decreasing thermal errors. An extensive study has been carried out in the area of thermal error compensation [3]. There are two general schools of thought

---

* Corresponding author.

related to thermal error compensation. The first uses numerical analysis techniques such as the finite-element method [4] and finite-difference method [5]. These methods are limited to qualitative analysis because of the problems of establishing the boundary conditions and accurately obtaining the characteristics of heat transfer. The second approach uses empirical modelling, which is based on correlation between the measured temperature changes and the resultant displacement of the functional point of the machine tool, which is the change in relative location between the tool and workpiece. Although this method can provide reasonable results for some tests, the thermal displacement usually changes with variation in the machining process. An accurate, robust thermal error prediction model is the most significant part of any thermal compensation system. In recent years, it has been shown that thermal errors can be successfully predicted by empirical modelling techniques such as multiple regression analysis [6], types of Artificial Neural Networks [7], fuzzy logic [8], an Adaptive Neuro-Fuzzy Inference System [9,10], Grey system theory [11] and a combination of several different modelling methods [12,13].

Chen et al. [6] used a multiple regression analysis (MRA) model for thermal error compensation of a horizontal machining centre. With their experimental results, the thermal error was reduced from 196 to 8 μm. Yang et al. [14] also used the MRA model to form an error synthesis model which merges both the thermal and geometric errors of a lathe. With their experimental results, the error could be reduced from 60 to 14 μm. However, the thermal displacement usually changes with variation in the machining process and the environment; it is difficult to apply MRA to a multiple output variable model. In order to overcome the drawbacks of MRA models, more attention has subsequently been given to the Artificial Intelligence (AI) techniques such as Artificial Neural Networks (ANNs). Chen et al. [7] proposed an ANN model structured with 15 nodes in the input layer, 15 nodes in the hidden layer, and six nodes in the output layer in order to drive a thermal error compensation of the spindle and lead-screws of a vertical machining centre. The ANN model was trained with 540 training data pairs and tested with a new cutting condition, which was not included within the training pairs. Test results showed that the thermal errors could be reduced from 40 to 5 μm after applying the compensation model, but no justification for the number of nodes or length of training data was provided. Wang [13] used a neural network trained by a hierarchy-genetic-algorithm (HGA) in order to map the temperature variation against the thermal drift of the machine tool. Wang [10] also proposed a thermal model merging Grey system theory GM(1,m) and an Adaptive Neuro-Fuzzy Inference System (ANFIS). A hybrid learning method, which is a combination of both steepest descent and least-squares estimator methods, was used in the learning algorithms. Experimental results indicated that the thermal error compensation model could reduce the thermal error to less than 9.2 μm under real cutting conditions. He used six inputs with three fuzzy sets per input, producing a complete rule set of $729 (3^6)$ rules in order to build an ANFIS model. Clearly, Wang's model is practically limited to low dimensional modelling. Eskandari et al. [15] presented a method to compensate for positional, geometric, and thermally induced errors of three-axis CNC milling machine using an offline technique. Thermal errors were modelled by three empirical methods: MRA, ANN, and ANFIS. To build their models, the experimental data was collected every 10 min while the machine was running for 120 min. The experimental data was divided into training and checking sets. They found that ANFIS was a more accurate modelling method in comparison with ANN and MRA. Their test results on a free form shape show average improvement of 41% of the uncompensated errors. A common omission in the published research is discussion or scientific rigour regarding the selection of the number and location of thermal sensors.

Other researchers have shown that a precise selection of thermal sensors and their position is needed to ensure the prediction accuracy and robustness of compensation models. Poor location and a small number of thermal sensors will lead to poor prediction accuracy. However, a large number of thermal sensors may have a negative influence on a model's robustness because each thermal sensor may bring noise to the model as well as bringing useful information. Additionally, issues of sensor reliability are commercially sensitive; the fewer sensors installed the fewer potential failures. Engineering judgment, thermal mode analysis, stepwise regression and correlation coefficient have been used to select the location of temperature sensors for thermal error compensation models [3]. Yan et al. [14] proposed an MRA model combing two methods, namely the direct criterion method and indirect grouping method; both methods are based on the synthetic Grey correlation. Using this method, the number of temperature sensors was reduced from sixteen to four sensors and the best combination of temperature sensors was selected. Jan Han et al. [16] proposed a correlation coefficient analysis and fuzzy c-means clustering for selecting temperature sensors both in their robust regression thermal error model and ANN model [17]; the number of thermal sensors was reduced from thirty-two to five. However, these methods suffer from the following drawbacks: a large amount of data is needed in order to select proper sensors; and the available data must satisfy a typical distribution such as normal (or Gaussian) distribution. Therefore, a systematic approach is still needed to minimise the number of temperature sensors and select their locations so that the downtime and resources can be reduced while robustness is increased. It is notable that most publications deal only with the reduction in sensors, but not the means by which the original set were determined. As a result the system is only shown for situations where the possible solutions are a subset of all potential locations, which requires non-trivial preconditioning of the problem. This is a situation where some aspects of the machine spatial temperature gradients might already have been missed and is typical when a machine model is being adapted, rather than evaluated from a new perspective.

In order to overcome the drawbacks of traditional Artificial Intelligence techniques such as ANNs and fuzzy logic, more attention has been focussed on hybrid models. For instance, in the fuzzy system's applications, the membership functions (MFs) typically have to be manually adjusted by trial and error. The fuzzy model performs like a white box, meaning that the model designers can explicitly understand how the model achieved its goal. However, such models that are based only on expert knowledge may suffer from a loss of accuracy due to engineering assumptions [8]. Conversely, ANNs can learn

from the data provided without preconceptions and assumptions. However, they perform as a "black box," which means that there is no information regarding the method by which the goal is achieved and so the achieved optimal solution can exhibit unrealistic physical characteristics that do not extrapolate to other situations. Applying the ANN technique to optimise the parameters of a fuzzy model allows the model to learn from a given set of training samples. At the same time, the solution is mapped out into a Fuzzy Inference System (FIS) that can be evaluated by the model designer as to produce a realistic representation of the physical system. The Adaptive Neuro Fuzzy Inference System (ANFIS) is such a neuro-fuzzy technique. It combines fuzzy logic and neural network techniques in a single system.

Construction of the ANFIS model using a data-driven approach usually requires division of the input/output data into rule patches. This can be achieved by using a number of methods such as grid partitioning or the subtractive clustering method [18]. However, one limitation of standard ANFIS is that the number of rules rises rapidly as the number of inputs increases (number of input sensors). For instance, if the number of input variables is n, and M is the partitioned fuzzy subset for each input variable, then the number of possible fuzzy rules is M^n. As the number of variables rises, so the number of fuzzy rules increases exponentially, increasing the load on the computer processor and increasing memory requirements. Thus, a reliable and reproducible procedure to be applied in a practical manner in ordinary workshop conditions was not proposed. It is important to note that an effective partition of the input space can decrease the number of rules and thus increase the speed in both learning and application phases. A fuzzy rule generation technique that integrates ANFIS with FCM clustering is applied in order to minimise the number of fuzzy rules. The FCM is used to systematically create the fuzzy MFs and fuzzy rule base for ANFIS.

In this paper, a thermal imaging camera was used to record temperature distributions across the machine structure during the experiments. The thermal images were saved as a matrix of temperatures with a specific resolution of one pixel, each of which can be considered as a possible temperature measurement point. The size of a temperature sensor means that, in a practical compensation system, sensing could not be physically applied at that spatial resolution. However, the locations can be centred on the optimal position and it is possible to use localised averaging of pixels to reduce any noise across the image. The Grey system theory and fuzzy c-means clustering are applied to minimise the number of temperature points and select the most suitable ones for a given target accuracy. ANFIS using FCM was implemented to derive a thermal prediction model. Temperature measurement points were chosen as inputs and thermal drift data was synchronously measured by non-contact displacement transducers (NCDTs) as the output. The ANFIS with FCM uses these input/output pairs to create a fuzzy inference system whose membership functions (MFs) are tuned using either the back-propagation (BP) or least-squares estimator learning algorithm. Using the rule base of FCM can increase the speed of the learning process and improve results. Finally, the performance of the proposed ANFIS model was compared with a traditional ANN model.

2. Thermal imaging camera

A thermal imaging camera provides a visible image of otherwise invisible infrared light that is emitted by all bodies due to their thermal state. The thermal imaging camera has become a powerful tool for researchers and has applications in various fields such as medicine, biometrics, computer vision, building maintenance and so on. In this paper, a high-specification thermal imaging camera, namely a FLIR ThermaCAM®S65, was used to record a sequence of thermal images of temperature distributions across the spindle carrier structure. This camera provides a sensitivity of 0.08 °C, and an absolute accuracy of ± 2%. Full camera specifications are provided in Table 1. The thermal imaging camera offers a continuous picture of the temperature distribution in the image field-of-view. This is important as it provides the distribution of heat during heating and cooling cycles across the whole machine structure. This allows the machine's structural elements to be measured online during the test. As well as the camera providing live continuous thermal images, they can also be recorded for further

Table 1
Thermal imaging camera specification (Source: FLIR Systems-2004).

Field of view/min focus distance	24° × 18° / 0.3 m	Thermal imaging camera
Spatial resolution (IFOV)	1.5 mrad	
Thermal sensitivity @ 50/60 Hz	0.08 °C at 30 °C	
Electronic zoom function	2,4,8, interpolating	
Focus	Automatic or manual	
Digital image enhancement	Normal and enhanced	
Detector type	Focal plane array (FPA) uncooled microbolometer; 320 × 240 pixels	
Spectral range	3.5–13 μm	

analysis. The thermal images are saved as a matrix of temperatures with a specific resolution of one pixel (equivalent to $2.25 mm^2$), which equates to over 76,000 temperature measurement points for this 320×240 resolution camera. These thermal images can be transferred to a personal computer for analysis.

In this work, the data has been analysed using MATLAB. One disadvantage of thermal imaging is it can have low absolute accuracy, usually in the order of ± 2 °C. A number of MATLAB functions have been developed to enhance this accuracy, including averaging the images to reduce pixel noise, alignment of images and extraction from the temperature data by averaging groups of pixels at a specific point [19].

The radiation measured by the thermal camera depends on the temperature of the machine tool structure, but is also affected by the emissivity of the machine surfaces. Additionally, radiation reflects from shiny surfaces (ball screw, test mandrel, etc.), and is directly captured by the thermal camera and appearing as very hot areas. In order to measure the temperature of the machine structure precisely it is therefore necessary to know the emissivity accurately, for which the application of masking tape with a known emissivity (0.95) is a common and effective solution. The camera parameters are then set according to the measurement conditions considering the emissivity of the machine tool material, the distance between the machine and the camera, the relative humidity and the ambient temperature, as shown in Table 2.

3. Adaptive Neuro-Fuzzy Inference System (ANFIS)

The Adaptive Neuro Fuzzy Inference System (ANFIS), was first introduced by Jang, in 1993 [20]. According to Jang, the ANFIS is a neural network that is functionally the same as a Takagi–Sugeno type inference model. The ANFIS is a hybrid intelligent system that takes advantages of both ANN and fuzzy logic theory in a single system. By employing the ANN technique to update the parameters of the Takagi–Sugeno type inference model, the ANFIS is given the ability to learn from training data, the same as ANN. The solutions mapped out onto a Fuzzy Inference System (FIS) can therefore be described in linguistic terms. In order to explain the concept of ANFIS structure, five distinct layers are used to describe the structure of an ANFIS model. The first layer in the ANFIS structure is the fuzzification layer; the second layer performs the rule base layer; the third layer performs the normalisation of membership functions (MFs); the fourth and fifth layers are the defuzzification and summation layers, respectively. More information about the ANFIS network structure is given in [20].

ANFIS model design consists of two sections: constructing and training. In the construction section, the number and type of MFs are defined. Construction of the ANFIS model requires the division of the input/output data into rule patches. This can be achieved by using a number of methods such as grid partitioning, subtractive clustering method and fuzzy c-means (FCM) [18]. In order to obtain a small number of fuzzy rules, a fuzzy rule generation technique that integrates ANFIS with FCM clustering will be applied in this paper, where the FCM is used to systematically create the fuzzy MFs and fuzzy rule base for ANFIS. Fig. 1 shows basic structure of the ANFIS with FCM clustering.

In the training section, training data pairs should first be generated to train an ANFIS model. These data pairs consist of the ANFIS model inputs and the corresponding output. The membership function parameters are able to change through the learning process. The adjustment of these parameters is assisted by a supervised learning of the input/output dataset that are given to the model as training data. Different learning techniques can be used, such as a hybrid-learning algorithm combining the least squares method and the gradient descent method is adopted to solve this training problem.

3.1. Fuzzy c-means clustering

Fuzzy c-means (FCM) is a data clustering method in which each data point belongs to a cluster, with a degree specified by a membership grade. Dunn introduced this algorithm in 1973 [21] and it was improved by Bezdek in 1981 [22]. FCM partitions a collection of n vectors $x_i, i = 1, 2, \ldots, n$ into fuzzy groups, and determines a cluster centre for each group such that the objective function of dissimilarity measure is reduced.

$i = 1, 2, \ldots, c$ are arbitrarily selected from the n points. The steps of the FCM method are, explained in brief: Firstly, the centres of each cluster $c_i, i = 1, 2, \ldots, c$ are randomly selected from the n data patterns $\{x_1, x_2, x_3, \ldots, x_n\}$. Secondly, the membership matrix (μ) is computed with the following equation:

$$\mu_{ij} = \frac{1}{\sum_{k=1}^{c} \left(\frac{d_{ij}}{d_{kj}}\right)^{2/m-1}}, \tag{1}$$

where, μ_{ij}: The degree of membership of object j in cluster i; m: is the degree of fuzziness ($m > 1$); and $d_{ij} = \|c_i - x_j\|$: The Euclidean distance between c_i and x_j.

Table 2
Thermal imaging camera parameters.

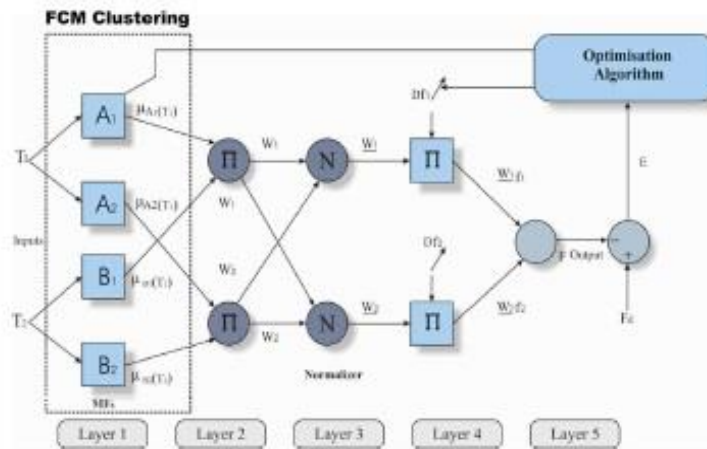|	
Distance	1.5 m
Emissivity	0.95
Ambient temperature	23 °C
Relative humidity:	30%

Fig. 1. Basic structure of ANFIS with FCM clustering.

Thirdly, the objective function is calculated with the following equation:

$$J(U, c_1, c_2, \ldots, c_c) = \sum_{i=1}^{c} J_i = \sum_{i=1}^{c} \cdot \sum_{j=1}^{n} \mu_{ij}^m d_{ij}^2. \tag{2}$$

The process is stopped if it falls below a certain threshold.

Finally, the new c fuzzy cluster centres $c_i, i = 1, 2, \ldots, c$ are calculated using the following equation:

$$c_i = \frac{\sum_{j=1}^{n} \mu_{ij}^m x_j}{\sum_{j=1}^{n} \mu_{ij}^m}. \tag{3}$$

In this paper, the FCM algorithm will be used to separate whole training data pairs into several subsets (membership functions) with different centres. Each subset will be trained by the ANFIS, as proposed by Park et al. [23]. Furthermore, the FCM algorithm will be used to find the optimal temperature data clusters for thermal error compensation models.

4. Grey model GM (0,N)

The interaction between different temperature sources and sinks creates a complex non-linear thermal behaviour for a machine tool. The model designers often want to know which sources have a dominant effect and which exert less influence on thermal response of the machine tool. The Grey systems theory, introduced by Deng in 1982 [24], is a methodology that focuses on studying the Grey systems by using mathematical methods with a only few data sets and poor information. The technique works on uncertain systems that have partial known and partial unknown information. It is most significant advantage is that it needs a small amount of experimental data for accurate prediction, and the requirement for the data distribution is also low [25]. The Grey model GM (h, N) is based on the Grey system theory, where h is the order of the difference equation and N is the number of variables [26]. The GM (h, N) model is defined as follows:

If in sequences $x_i^{(0)}(k), i = 1, 2, \ldots, N. x_1^{(0)}(k)$, is the main factor in the system, and sequences $x_2^{(0)}(k), x_3^{(0)}(k), x_4^{(0)}(k), \ldots x_N^{(0)}(k)$ are the influence factors of the same system, then the GM (h, N) model is described as [26,25]:

$$\sum_{i=0}^{h} a_i \frac{d^{(i)} x_1^{(1)}}{dt^{(i)}} = \sum_{j=2}^{N} b_j x_1^{(1)}(k), \tag{4}$$

where, a_1 and b_j are determined coefficients; b is defined as the Grey input; $x_1^{(1)}(k)$: The major sequence; $x_j^{(1)}(k)$: The influence sequences; and

The accumulation generating operation (AGO) $x^{(0)} = x^{(1)}$

$$= \left[\sum_{k=1}^{1} x^{(0)}(k), \sum_{k=1}^{2} x^{(0)}(k), \sum_{k=1}^{3} x^{(0)}(k), \ldots \sum_{k=1}^{n} x^{(0)}(k) \right]. \tag{5}$$

According to the previous definition of GM (h,N), the GM (0,N) is a zero-order Grey system, which can be described as follows:

$$z_1^{(1)}(k) = \sum_{j=2}^{N} b_j x_j^{(1)}(k) = b_2 x_2^{(1)}(k) + b_3 x_3^{(1)}(k) + \cdots + b_N x_N^{(1)}(k), \tag{6}$$

where,

$$z_1^{(1)}(k) = 0.5 x_1^{(1)}(k-1) + 0.5 x_1^{(1)}(k), \quad k = 2, 3, 4, \ldots, n.$$

From Eq. (4), we can write:

$$a_1 z_1^{(1)}(2) = b_2 x_2^{(1)}(2) + \ldots + b_N x_N^{(1)}(2),$$
$$a_1 z_1^{(1)}(3) = b_2 x_2^{(1)}(3) + \ldots + b_N x_N^{(1)}(3),$$
$$\ldots\ldots\ldots$$
$$a_1 z_1^{(1)}(n) = b_2 x_2^{(1)}(n) + \ldots + b_N x_N^{(1)}(n). \tag{7}$$

Dividing Eq. (5) by a_1 in both sides, then transfer into matrix form as follows:

$$\begin{bmatrix} 0.5 x_1^{(1)}(1) + 0.5 x_1^{(1)}(2) \\ 0.5 x_1^{(1)}(2) + 0.5 x_1^{(1)}(3) \\ \vdots \\ 0.5 x_1^{(1)}(n-1) + 0.5 x_1^{(1)}(n) \end{bmatrix} = \begin{bmatrix} x_2^{(1)}(2) & \cdots & x_N^{(1)}(2) \\ x_2^{(1)}(3) & \cdots & x_N^{(1)}(3) \\ \vdots & \cdots & \vdots \\ x_2^{(1)}(n) & \cdots & x_N^{(1)}(n) \end{bmatrix} \begin{bmatrix} \frac{b_2}{a_1} \\ \frac{b_3}{a_1} \\ \vdots \\ \frac{b_N}{a_1} \end{bmatrix}. \tag{8}$$

Assume $\frac{b_m}{a_1} = \theta_m$, where $m = 2, 3, \ldots, N$, then Eq. (6) can be simplified as follows:

$$\begin{bmatrix} 0.5 x_1^{(1)}(1) + 0.5 x_1^{(1)}(2) \\ 0.5 x_1^{(1)}(2) + 0.5 x_1^{(1)}(3) \\ \vdots \\ 0.5 x_1^{(1)}(n-1) + 0.5 x_1^{(1)}(n) \end{bmatrix} = \begin{bmatrix} x_2^{(1)}(2) & \cdots & x_N^{(1)}(2) \\ x_2^{(1)}(3) & \cdots & x_N^{(1)}(3) \\ \vdots & \cdots & \vdots \\ x_2^{(1)}(n) & \cdots & x_N^{(1)}(n) \end{bmatrix} \begin{bmatrix} \theta_2 \\ \theta_3 \\ \vdots \\ \theta_N \end{bmatrix}. \tag{9}$$

The coefficients of the model can then be estimated from the following equation:

$$\hat{\theta} = (B^T B)^{-1} B^T Y, \tag{10}$$

where,

$$Y = \begin{bmatrix} 0.5 x_1^{(1)}(1) + 0.5 x_1^{(1)}(2) \\ 0.5 x_1^{(1)}(2) + 0.5 x_1^{(1)}(3) \\ \vdots \\ 0.5 x_1^{(1)}(n-1) + 0.5 x_1^{(1)}(n) \end{bmatrix}, \quad B = \begin{bmatrix} x_2^{(1)}(2) & \cdots & x_N^{(1)}(2) \\ x_2^{(1)}(3) & \cdots & x_N^{(1)}(3) \\ \vdots & \cdots & \vdots \\ x_2^{(1)}(n) & \cdots & x_N^{(1)}(n) \end{bmatrix}, \quad \hat{\theta} = \begin{bmatrix} \theta_2 \\ \theta_3 \\ \vdots \\ \theta_N \end{bmatrix}.$$

Therefore, the influence ranking of the major sequences (input sensors) on the influencing sequence (thermal drift) can be known by comparing the model values of $(\theta_2 \sim \theta_N)$.

The whole block diagram of the proposed system is shown in Fig. 2, where spots 1 to N represent the virtual temperature sensor data captured from the thermal imaging camera, and the thermal drift obtained from non-contact displacement transducers (NCDTs).

5. Experimental setup

In this study, experiments were performed on a small vertical milling centre (VMC). The thermal imaging camera was used to record a sequence of temperature distributions across the spindle-carrier structure of the machine tool. Three NCDTs were used to measure the resultant displacement of a solid test bar, used to represent the tool. Two sensors, vertically displaced by 100 mm, measure both displacement and tilt in the Y-axis direction and a third measures displacement in the Z-axis direction (see Fig. 3). Distortions in the X-axis direction were not measured during this study, since experience has shown that the symmetry of the machine structure renders this effect negligible. A general overview of the experimental setup is shown in Fig. 4.

The use of masking tape on the machine provides areas of known emissivity. In particular, in some locations such as on the rotating test bar, the tape is required to provide a temperature measurement, which would be difficult to achieve by other means.

The VMC was examined by running the spindle at its highest speed of 9000 rpm for 120 min to excite the thermal behaviour. The spindle was then stopped for approximately 50 min for cooling. The thermal imaging camera was positioned approximately 1500 mm from the spindle carrier to ensure that the parts of the machine of interest were within the field
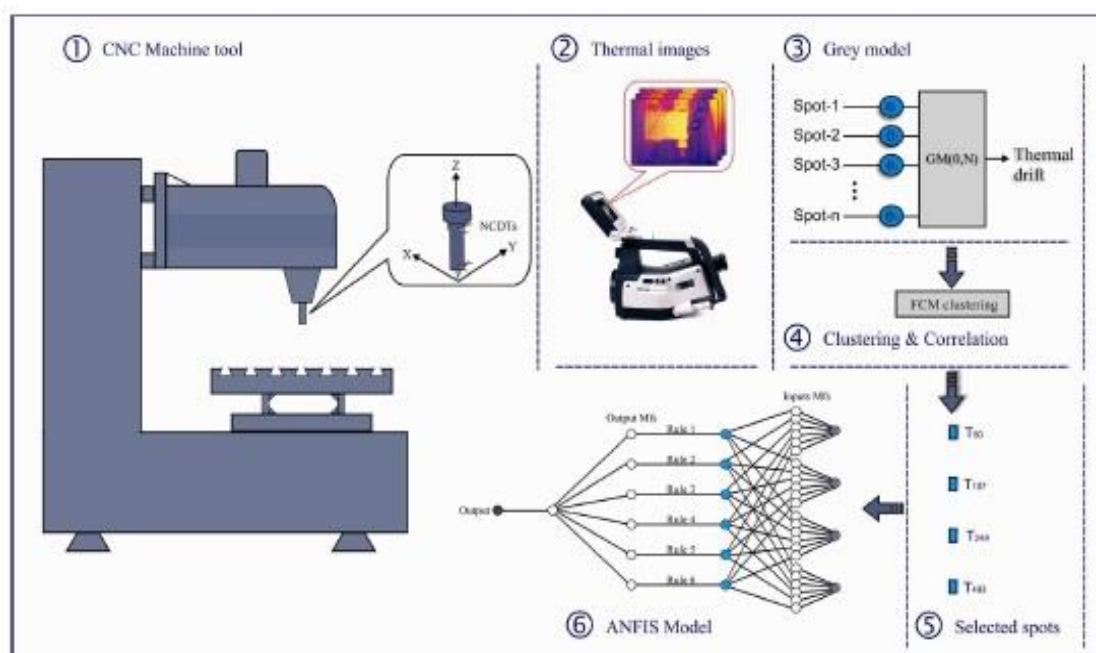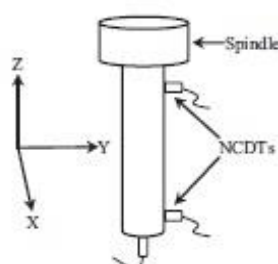
Fig. 2. Block diagram of the proposed system.

Fig. 3. Measurement of the thermal effect using a test bar and NCDTs.

of view. Images were captured and stored to the camera's memory card during the experiment at 10 s intervals. The thermal displacement at the spindle was measured simultaneously and is shown in Fig. 5. The maximum displacement for the Y top-axis is 20 μm, the Y bottom-axis is 23 μm, and the Z-axis is 35 μm.

MATLAB functions were developed to enhance and analyse the temperature data [19]. These functions include image averaging (to reduce noise from individual pixels), image alignment and the ability to extract a discrete point precisely by averaging groups of pixels. In addition, efficient methods of creating virtual sensors were created, including the ability to draw "lines" of temperature sensor spots representing strips [19]. This is important in order to obtain sufficient temperature data readings across the carrier structure. A Grey model was applied to the measured temperature data to quantify the influence of each spot across the carrier structure. Fig. 6 shows thermal images with 525 discrete spots on the carrier and Fig. 7 shows some extracted readings from these spots taken over the duration of the whole test.

5.1. Application of GM (0, N) model

The machine was run through a test-cycle of 120 min heating and approximately 70 min cooling. The temperature change and displacement of the spindle relative to the table in the Z-axis was captured throughout the test. This was used in the GM (0, N) model to determine which parts within the machine structure contribute most significantly to the total thermal displacement. Further analysis then concentrated on the influence coefficient of discrete points using the FCM method. The process is as follows:

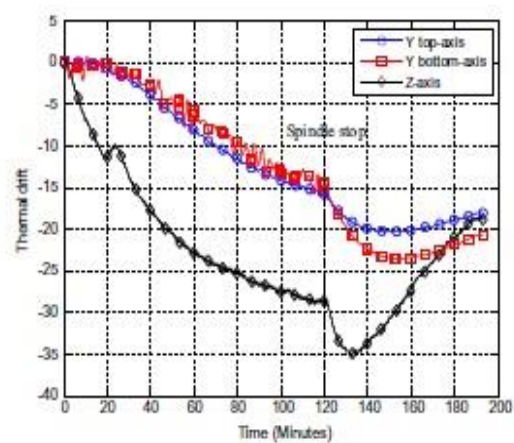Fig. 4. A general overview of the experimental setup.
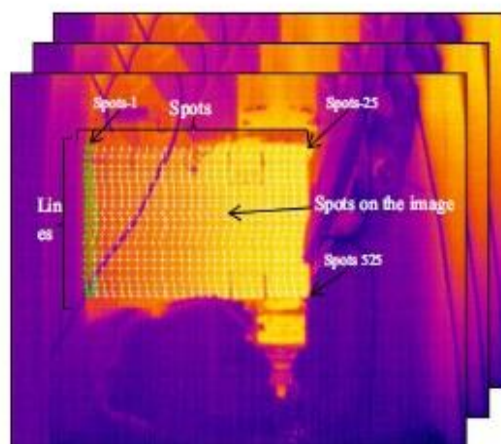

Fig. 5. Thermal drift of the spindle.

Fig. 6. Thermal images captured during the experiment with 525 selected spots.
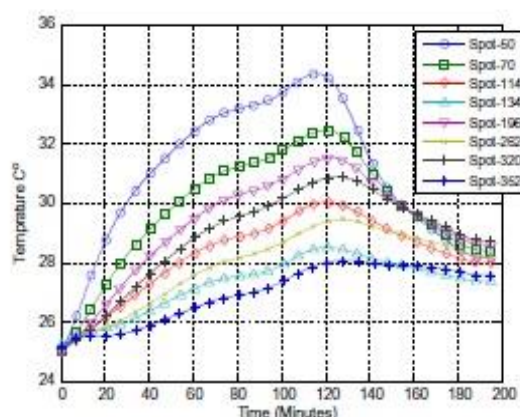
Fig. 7. Thermal data extracted from images using MATLAB.

First, the GM (0, N) model of Grey system theory is calculated using the temperature changes and displacement of spindle nose in the Z-axis.

Suppose that Spot-1∼Spot-525 represents the major variables (inputs) $x_2^{(0)} \sim x_{526}^{(0)}$ and the measurement of the NCDT sensors are the target variable (output) $x_1^{(0)}$. The norm values of the influence coefficient matrix $\hat{\theta}$ can be obtained using Eq. (8), as $|\theta_2| \sim |\theta_{526}|$, indicating the influence weighting of the input data against the output data, respectively. The greater the influence weight, the greater the impact on the thermal error, and the more likely it is that the temperature variable can be regarded as a possible modelling variable. Fig. 8 shows a 3D plot of the influence coefficient matrix.

From Fig. 8, the flow of heat across the carrier can be clearly seen. Different points have different influence on thermal error in the Z direction; the points near the motor are the highest factors. During the cooling cycle, it can be seen (Fig. 5) that the test bar shows some movement occurred immediately after the spindle was stopped. This movement is probably caused by the expansion of the test bar itself; the localised heat from the motor and spindle bearings flow into the bar and there is no cooling effect from air turbulence. This flow of heat into the test bar is a significant contributor to the drift in the Z direction as the tool continues to expand after the spindle has stopped. An investigation of the source of this growth of the test bar was carried out by extracting ten spots during the same heating and cooling test as show in Fig. 9. The GM (0, N) model of the Grey system theory was applied again on a specific period "snapshot" of the test as shown in Fig. 10.

Fig. 11 shows the GM (0, N) model output for the selected period. It can be observed that the temperature change of different selected spots on the carrier has different influence on the thermal error in the Z-axis direction and the spots 9 and 10 on the test bar are the most important factors, while spot 7 is the most significant location on the machine structure. The GM (0, N) model provides a method to analyse systems where traditional methods such as the correlation coefficient do not seem
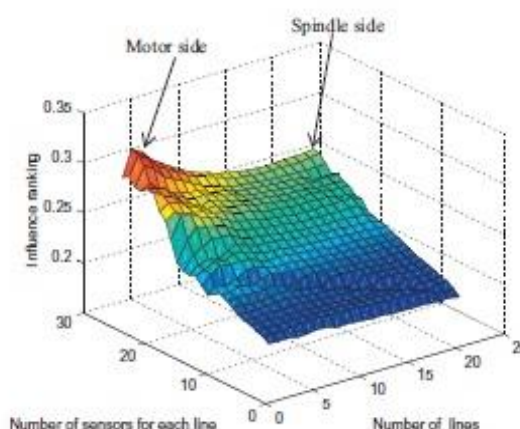
Fig. 8. Surface of Influence ranking of temperature data using GM (0,N).
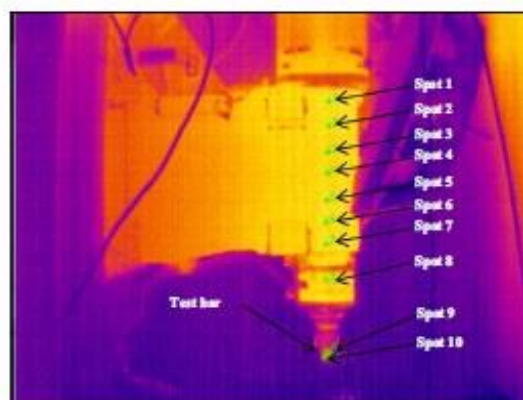
Fig. 9. Thermal image captured during the experimental with 10 selected points.
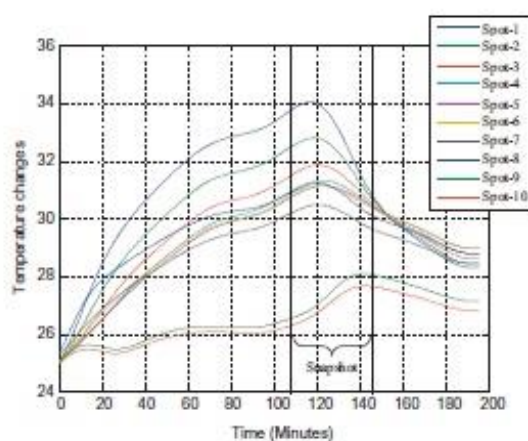
Fig. 10. Thermal data extracted from images with 10 selected points.
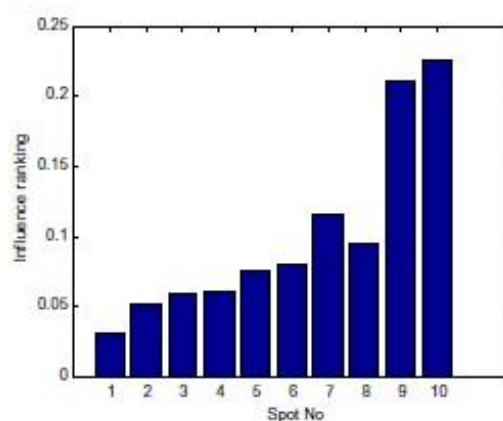
Fig. 11. Influence ranking of ten temperature spots using GM (0,N).

appropriate. It is applicable irrespective of the size of data sets and independent of requirement for a specific distribution. The results of this investigation indicate that the GM (0,N) model is a good optimisation tool for finding the proper selection of thermal sensors and their location.

Table 3
The cluster results.

No of groups	Representative spots
Group 1 (one cluster)	Spot-50
Group 2 (two clusters)	Spot-50, Spot-214
Group 3 (there clusters)	Spot-50, Spot-84, Spot-398
Group 4 (four clusters)	Spot-50, Spot-107, Spot-249, Spot-493
Group 5 (five clusters)	Spot-50, Spot-140, Spot-225, Spot-263, Spot-283
Group 6 (six clusters)	Spot-50, Spot-109, Spot-200, Spot-240, Spot-348, Spot-407
Group 7 (seven clusters)	Spot-50, Spot-96, Spot-136, Spot-305, Spot-335, Spot-443, Spot-474
Group 8 (eight clusters)	Spot-50, Spot-70, Spot-114, Spot-134, Spot-196, Spot-262, Spot-320, Spot-352

5.2. Thermal error modelling and discussion

The temperature sensors were clustered into a different number of groups using FCM as described in Section 5, starting with one cluster for group 1 up to eight clusters for group 8. Then, one sensor from each cluster was selected according to its correlation with the thermal drift to represent the temperature sensor of the same category (see Table 3); eight ANFIS models were constructed from these representative spots for evaluation. An example of the clustering procedure for four clusters is shown in Fig. 12.

It is important to understand any uncertainty that is created by variation of the model design. A parametric study was conducted by testing the accuracy of the models with variation in number of inputs and in number of membership functions. Eight models were developed as follows: representative temperature sensors from Table 3 were selected as input variables and the thermal drift in the Z-direction was considered as a target variable. The same test (120 min heating and 70 min cooling) was used for training and validation the models: experimental data are divided into training and checking datasets. The training dataset is used to train (or tune) a fuzzy model, while the checking dataset was used for over-fitting model validation. The Gaussian functions are used to describe the membership degree of these inputs, due to their advantages of being smooth and non-zero at each point [9]. After setting the initial parameter values in the FCM-ANFIS models, the models were adjusted using a hybrid learning scheme.

Extensive simulations were conducted to select the optimal number of MFs (clusters) and number of iterations (epoch number) for each model. The performance of the model depends on the combination of these different parameters. Too
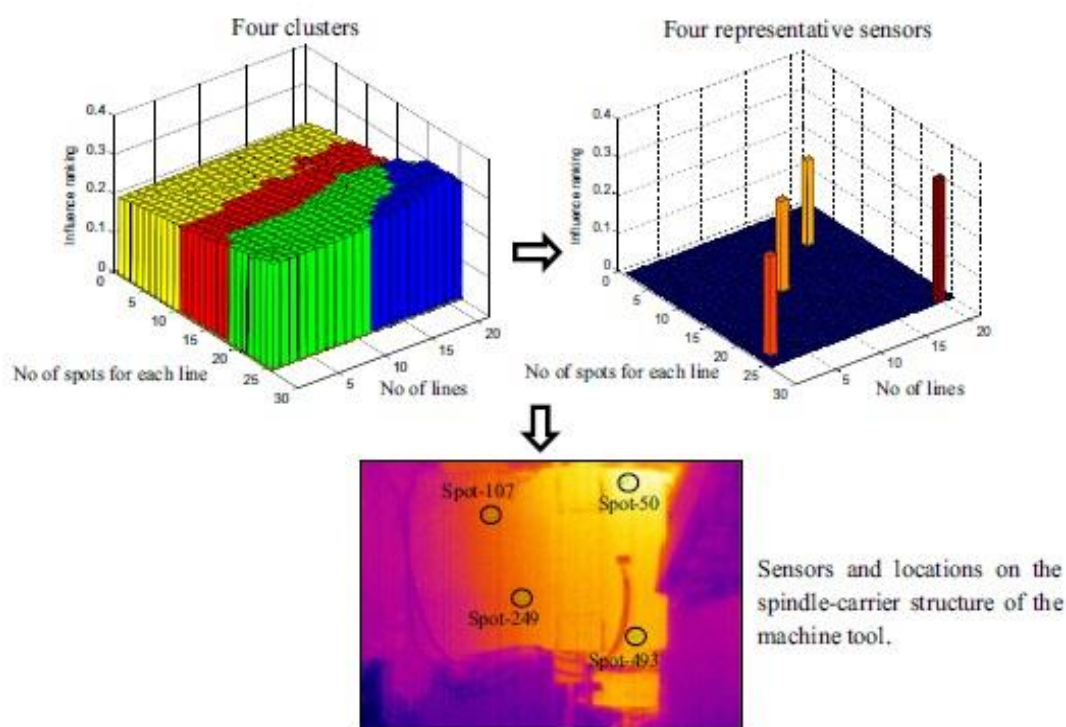

Fig. 12. An example of clustering procedure for four clusters.

1848   *A.M. Abdulshahed et al./Applied Mathematical Modelling 39 (2015) 1837–1852*

Table 4
Performance of FCM-ANFIS models with various numbers of MFs.

Models	Number of MFs	Convergence epochs	RMSE of the validation data	RMSE of the testing data
1	2	200	0.8314	3.8456
2	3	200	0.6064	2.0052
3	4	200	0.5380	2.4614
4	5	100	0.5793	2.0534
5	6	100	0.5327	1.7275
6	7	100	0.3494	4.1113
7	8	100	0.3232	4.8818
8	9	100	0.3058	5.0802

Table 5
The characteristics of the FCM-ANFIS models.

Model	No. of inputs	No. of MFs for each input	No. of iterations	Training stage		Testing stage			
				NSE	RMSE	NSE	RMSE	R	Residual
FCM-ANFIS 1	1	6	200	0.6780	4.4835	0.4070	5.8847	0.7636	14.0963
FCM-ANFIS 2	2	6	200	0.9838	1.0071	0.4929	5.5618	0.8302	13.7686
FCM-ANFIS 3	3	6	11	0.9941	0.6223	0.9585	1.5183	0.9904	3.3979
FCM-ANFIS 4	4	6	9	0.9939	0.6069	0.9764	1.4139	0.9912	2.9521
FCM-ANFIS 5	5	6	12	0.9941	0.6254	0.9351	1.8981	0.9806	4.5397
FCM-ANFIS 6	6	3	2	0.9881	0.8634	0.7154	3.9754	0.9595	8.002
FCM-ANFIS 7	7	3	2	0.9880	0.8659	0.7352	3.8346	0.9635	8.2159
FCM-ANFIS 8	8	3	10	0.9847	0.9789	0.6439	4.4463	0.9332	10.4211

few MFs do not allow the FCM-ANFIS models to be mapped well. However, too many MFs increase the difficulty of training and lead to over-fitting or memorising undesirable inputs such as noise. The prediction errors were measured separately for each model using the root mean square error (RMSE) index. By varying the simulations, it was determined that the optimal solution was six MFs in the first five models, and three MFs for the remaining models. Different numbers of epochs were selected for each model because the training process only needs to be carried out until the errors to converge. An example of selecting MFs with four inputs is presented in Table 4.

In order to examine the performance of all the FCM-ANFIS models on non-training data, another test was carried out on the same machine in an operational cycle as follows. The machine was programmed to run at spindle speed of 8000 rpm for 60 min and then 40 min with the spindle stopped. It was then run again at spindle speeds of 4000 rpm and 9000 rpm for 30 min and 40 min respectively. Finally, measurement continued for another 40 min with the spindle stopped. During the experiment, the thermal errors were measured by the NCDTs, and the predicted displacements were obtained using FCM-ANFIS models.

The performances of the models used in this study were computed using four performance criteria: root mean square error (RMSE), Nash–Sutcliffe efficiency coefficient (NSE), correlation coefficient (R) and also residual value. The equations of first two are defined as:

$$RMSE = \sqrt{\frac{\sum_{k=1}^{n}(Z-P)^2}{n}},$$ (11)

$$NSE = 1 - \frac{\sum(Z-P)^2}{\sum(Z-\bar{Z})^2},$$ (12)

where, Z: Thermal drift; P: The predicted thermal drift; $\bar{Z}$: Average of the thermal drift; and n: The number of measured data.

In Table 5, the prediction performance of eight FCM-ANFIS models was compared for training and non-training data respectively.

Table 5 illustrates the obtained results from all eight developed models. From these results, it can be observed that both NSE and RMSE have promising values during the training stage for all the models. However, during the testing stage the models with one and two input variables gave low efficiency, low correlation coefficient and high residual value due to insufficient data regarding the system behaviour. In addition, the seven and eight inputs models did not give as good results as the other models due to redundancy of input data. The FCM-ANFIS model with four inputs gives the best estimation, taking into account the performance indices (higher efficiency coefficient NSE = 0.97 higher correlation coefficient R = 0.9912, and lower mean square error RMSE = 1.4139) and lowest residual value amongst others as shown in Fig. 13.

The structure of the FCM-ANFIS model with four inputs is shown in Fig. 14. There are four input neurons, corresponding to the four selected representative sensors. In the second layer, six neurons are connected to each input neuron (in total 24
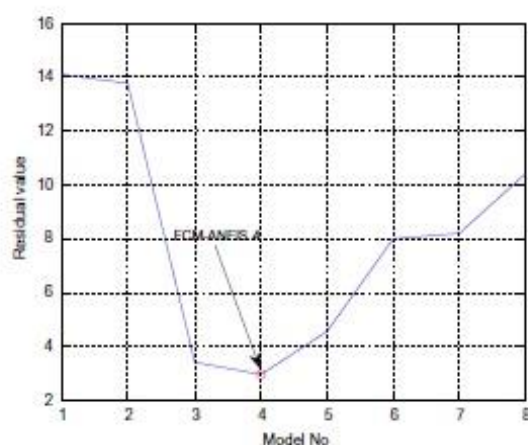
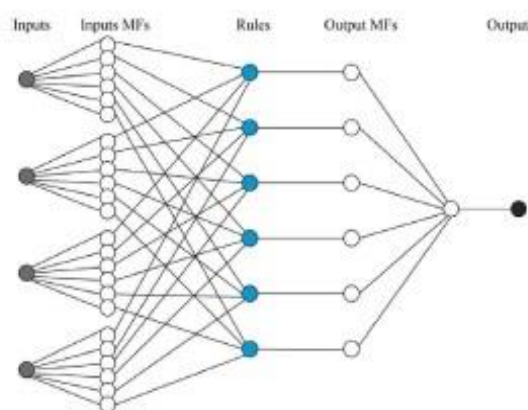**Fig. 13.** Residual values for all eight models.

Fig. 14. The structure of associated network model.

neurons), which correspond to six Gaussian membership functions for each input sensor as shown in Fig. 15. The next layer contains six neurons equivalent to six fuzzy "if-then" rules. The result of the prediction process is presented by six neurons in the output layer. A weighted average method is used for the defuzzification stage in order to obtain the final predicted thermal drift.

Fig. 16 describes the temperature rise during the testing experiment. It can be seen that the temperature extracted from the representative sensors fluctuated due to change of the spindle speed, which causes sudden change in the resultant displacement in the Z-axis direction. The simulation result shows that the proposed FCM –ANFIS model can predict the error accurately and can also track the rapid changes of thermal error precisely (the maximum residual is approximately ± 2 μm). Thus, a model with four representative temperature sensors is therefore a powerful and precise predictor of the thermal errors of the machine tool (see Fig. 17).

The prediction of the FCM-ANFIS model with four selected key temperature points can significantly reduce the thermal error from an independent test under different conditions of varying rotational spindle speeds and dwells on the machine tool. To emphasise the importance of correctly finding the optimal sensor locations, one of the virtual sensors was arbitrarily moved from the location determined by this method to another location that could have been selected intuitively, i.e. with some engineering justification. It is noticeable that by changing just one temperature point from the key temperature points gives unsatisfactory prediction ability (residual value ± 9 μm), which implies that the proposed methods (GM (0, N) and FCM) are a valid and important combination to build an accurate model.

5.3. Comparison with other models

In order to assess the ability of FCM-ANFIS model relative to that of a neural network model, an ANN model was constructed using the same input variables to the ANFIS with four inputs. Usually ANN model have three layers: Input, hidden and output layer. Although, for common engineering problems, one hidden layer is sufficient for model training, two or more
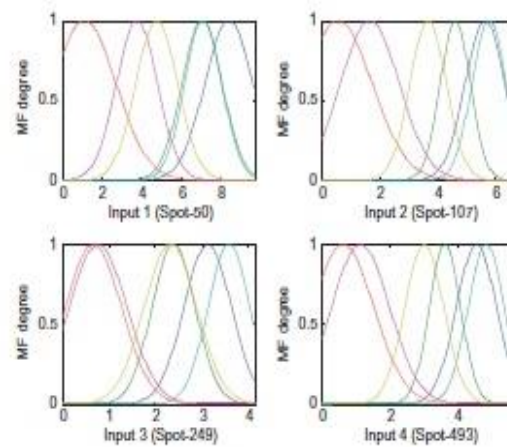
Fig. 15. Membership functions obtained through FCM.
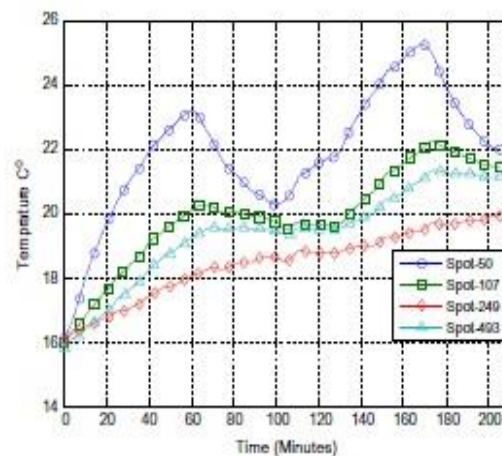

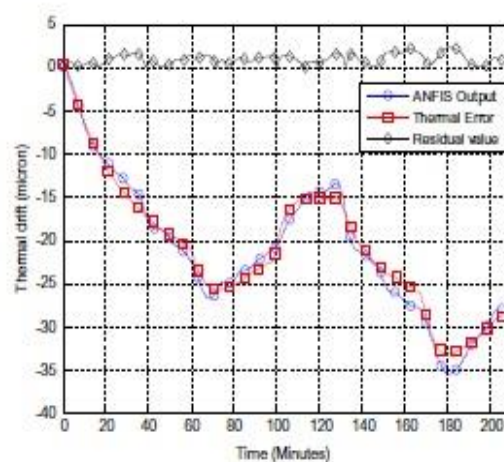Fig. 16. Thermal data extracted from images from selected points.

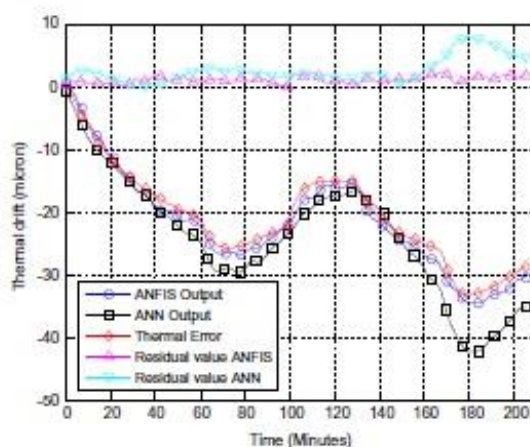Fig. 17. FCM-ANFIS model output vs the actual thermal drift.

Fig. 18. A Comparison of ANFIS and ANN for the prediction of thermal drift.

Table 6
Performance of ANFIS and ANN in modelling the thermal drift in Z direction.

Model	Testing stage			
	NSE	RMSE	R	Residual
ANFIS	0.9764	1.4139	0.9912	2.9521
ANN	0.9012	2.6071	0.9807	7.0210

hidden layers may be needed for very complex phenomena [9]. An ANN model with three layers was used in this study: the input layer has four input variables and the output layer has one neuron (the thermal drift in the Z-axis direction).

The same test (120 min heating and 70 min cooling) was used for training the model; the experimental data are divided into training and validation datasets. After a series of experiments to find the best architecture, an ANN model with 10 neurons in the hidden layer was constructed to predict the thermal drift in the Z-axis direction. Prediction results using ANFIS and ANN are shown in Fig. 18, where the two models were trained using the same training dataset and tested by the same testing dataset. The same four performance criteria of root mean square error (RMSE), Nash–Sutcliffe efficiency coefficient (NSE) and correlation coefficient (R) were used to judge the optimal model. According to the results in Fig. 18 and the evaluation criteria in Table 6 it is very clear that the ANFIS model has smaller RMSE and higher NSE compared to the ANN model. Therefore, the ANFIS model is shown to be a good modelling choice to predict the thermal error of machine tools. Moreover, the ANN model is a black box in nature and its relationships between inputs and outputs are difficult to interpret, while ANFIS is transparent and its "if–then" rules are easy to understand and interpret.

6. Conclusion

In this paper, a thermal imaging camera has been used to record temperature distributions across the spindle carrier structure during the experiments. The thermal images are saved as a matrix of temperatures with a specific resolution of one pixel (equivalent to 2.25 mm^2). This system equates to over 76,000 possible temperature measurement points. Averaging, which is used to decrease noise, reduces the number of temperature locations to the equivalent of 525 points, depending upon the field of view. This richness of data is exploited to find the optimal location for temperature measurement when designing a thermal error control model.

With the use of GM (0, N) and FCM methods, the influence rankings of recorded temperature data has been found to be applicable to determine which parts within the machine structure contribute most significantly to the total thermal displacement. This eliminates the need for intuitive locating of sensors and significantly reduces implementation time. The principal advantage of this novel technique is to use thermal imaging to assess a machine's thermal behaviour and to build compensation models with different numbers and configurations of sensors. An Adaptive Neuro-Fuzzy Inference System with FCM (FCM-ANFIS) has been employed for the prediction of the thermal error in machine tools. The models are built using data obtained from short heating and cooling test, with a wide variety of models being able to be assessed using multiple simulations.

The results on this machine indicate that FCM-ANFIS model with four inputs and six rules has the optimal capability to map the input–output data pairs; it can predict thermal displacement under different operational conditions depending on

the availability of the empirical data. Perhaps counter-intuitively, the ANFIS model is less well conditioned when additional sensors are included. Minimal effort is then required for practical application of discrete contact sensors that are used for on-line compensation.

The method was further tested by observing that the optimally-found model could compensate the thermal errors derived from the heat induced by running the spindle of the machine to better than $\pm 2\,\mu m$ for an arbitrary duty cycle. However, by varying the location of one sensor to another "intuitive" node, the accuracy of the model fell to $\pm 9\,\mu m$.

In addition to the better absolute accuracy, the FCM-ANFIS has been shown to have the advantage of requiring fewer rules, in this case requiring only six rules as opposed to the standard ANFIS model. This is a significant benefit, since the latter method is significantly more laborious to construct.

Finally, an ANN model was trained using the same sensor locations and same training dataset. The FCM-ANFIS model was shown to give better performance that the ANN model. In summary, the proposed FCM -ANFIS model is a valid and promising alternative for predicting thermal error of machine tools without increasing computation overheads.

Acknowledgements

References

[1] R. Ramesh et al, Error compensation in machine tools—a review: Part II: thermal errors, Int. J. Mach. Tools Manuf 40 (2000) 1257–1284.

[2] S. Postlethwaite et al, The use of thermal imaging, temperature and distortion models for machine tool thermal error reduction, Proc. Inst. Mech. Eng. Part II: J. Eng. Manuf. 212 (1998) 671–679.

[3] J. Li et al, Thermal-error modeling for complex physical systems: the-state-of-arts review, Int. J. Adv. Manuf. Technol. 42 (2009) 168–179.

[4] N.S. Mian et al, Efficient thermal error prediction in a machine tool using finite element analysis, Meas. Sci. Technol. 22 (2011) 085107.

[5] B. Bossmanns, J.F. Tu, A thermal model for high speed motorized spindles, Int. J. Mach. Tools Manuf. 39 (1999) 1345–1366.

[6] J. Chen et al, Thermal error modelling for real-time error compensation, Int. J. Adv. Manuf. Technol. 12 (1996) 266–275.

[7] J. Chen, G. Chiou, Quick testing and modeling of thermally-induced errors of CNC machine tools, Int. J. Mach. Tools Manuf. 35 (1995) 1063–1074.

[8] J.-H. Lee et al, Development of thermal error model with minimum number of variables using fuzzy logic strategy, KSME Int. J. 15 (2001) 1482–1489.

[9] A. Abdulshahed et al., Comparative study of ANN and ANFIS prediction models for thermal error compensation on CNC machine tools, in: Laser Metrology and Machine Performance X, Buckinghamshire, 2013, pp. 79–88.

[10] K.C. Wang, Thermal error modeling of a machining center using grey system theory and adaptive network-based fuzzy inference system (2006) 1–6.

[11] Y. Wang et al, Compensation for the thermal error of a multi-axis machining center, J. Mater. Process. Technol. 75 (1998) 45–53.

[12] A. Abdulshahed et al., Application of GNNMCI(1, N) to environmental thermal error modelling of CNC machine tools, in: Presented at the 3rd International Conference on Advanced Manufacturing Engineering and Technologies, Stockholm, 2013, pp. 253–262.

[13] K. C. Wang, Thermal error modeling of a machining center using grey system theory and HGA-trained neural network, in: Cybernetics and Intelligent Systems, Bangkok, 2006, pp. 1–7.

[14] J. Yan, J. Yang, Application of synthetic grey correlation theory on thermal point optimization for machine tool thermal error compensation, Int. J. Adv. Manuf. Technol. 43 (2009) 1124–1132.

[15] S. Eskandari et al, Positional, geometrical, and thermal errors compensation by tool path modification using three methods of regression, neural networks, and fuzzy logic, Int. J. Adv. Manuf. Technol. (2013) 1–15.

[16] J. Han et al, Thermal error modeling of machine tool based on fuzzy c-means cluster analysis and minimal-resource allocating networks, Int. J. Adv. Manuf. Technol. 60 (2012) 463–472.

[17] J. Han et al, A new thermal error modeling method for CNC machine tools, Int. J. Adv. Manuf. Technol. (2012) 1–8.

[18] S. Guillaume, Designing fuzzy inference systems from data: An interpretability-oriented review, Fuzzy Sys. IEEE Trans 9 (2001) 426–443.

[19] S. Fletcher et al, Measurement methods for efficient thermal assessment and error compensation, in: Proceedings of the Topical Meeting: Thermal Effects in Precision Engineering, Maastricht, 2007.

[20] J.S.R. Jang, ANFIS: Adaptive-network-based fuzzy inference system, Sys. Man Cybern. IEEE Trans. 23 (1993) 665–685.

[21] J. C. Dunn, A fuzzy relative of the ISODATA process and its use in detecting compact well-separated clusters, 1973, pp. 32–57.

[22] J.C Bezdek, Pattern Recognition with Fuzzy Objective Function Algorithms, Plenum Press, New York, 1981.

[23] S. H. Park et al., Comparison of recognition rates between BP and ANFIS with FCM clustering method on off-line PD diagnosis of defect models of traction motor stator coil, in: Proceedings of 2005 International Symposium on Electrical Insulating Materials, 2005. (ISEIM 2005), 2005, pp. 849–852.

[24] J.-L. Deng, Control problems of grey systems, Sys. Control Lett. 1 (1982) 288–294.

[25] S. Liu et al, Grey Systems: Theory and Applications, vol. 68, Springer, 2010.

[26] K. Wen, The Grey system analysis and its application in gas breakdown and VAR compensator finding, Int. J. Comput. Cognition 2 (2004) 21–44.

III CONCLUSIONS AND FUTURE PERSPECTIVES

1 FOUNDATION CONCLUSIONS

1.1 Specific foundation conclusions from the papers

1.1.1 Conclusions paper 2005-01

Measurement techniques for determining the static stiffness of foundations for machine tools.

Using conventional metrology equipment in a novel way it is was shown that the stiffness at the surface of a foundation can be measured and the results used to determine whether or not the foundations is able to support a large machine tool such that the machine will be capable to meeting its accuracy requirements

1.1.2 Conclusions paper 2005-06

Finite element analysis of the static stiffness of a foundation for large machine tool

This paper verified that FEA can be used to accurately predict foundation stiffness if the sub-soil stiffness is determined by use of bore holes or plate tests.

1.1.3 Conclusions paper 2007-02

Structural Analysis of a large Moving Gantry Milling Machine including its Work Support System and Foundation.

This paper clearly demonstrates that it is now possible to comprehensively analyse the static characteristics of large machine tools structures, their concrete foundations and the supporting subsoil to obtain a comprehensive understanding of their behaviour.

1.1.4 Conclusions paper 2009-04

Evaluation and Comparison of a Large Machine Tool Structure with ISO Standard Alignment tests

The paper describes how the information required to ensure foundations can be designed correctly can be drawn from the appropriate ISO and BSI machine tool accuracy standards.

1.1.5 Conclusions paper 2013-09

New low cost sensing head and taut wire method for automated straightness measurement of machine tool axes

The paper describes how a low cost, effective method has been developed for measuring the accuracy of machine tools traverse straightness, thereby enabling verification that the foundation supporting the machine is suitable or not

1.1.6 Conclusions paper 2014-06

Performance evaluation of a new taut wire system for straightness measurement of machine tools.

The paper shows that the taut wire with optical sensor method developed for measuring machine tool straightness is as accurate as the equivalent laser based equipment yet considerably less expensive and much easier to setup when used on large machine tools.

2. THERMAL CONCLUSIONS

2.1 Specific thermal conclusions from the papers

2.1.1 Conclusions paper 2005-07

Compensation of thermal errors on a small vertical milling machine

Use of thermal imaging for temperature measurement and offline model development was applied to a small vertical milling machine which gave reduced machine downtime and improved accuracy prediction.

2.1.2 Conclusions paper 2005-10

Flexible modelling and compensation of machine tool thermal errors

A flexible thermal compensation system was created and installed on two controllers and a PC. Machining trials were carried out in accordance with the ISO230 Part 3 standard and showed reductions of 70% for thermal errors.

2.1.3 Conclusions paper 2005-12

Practical compensation of all significant thermal errors in machine tools

Practical compensation system was implemented on a machine which subsequent machining trials resulted in workpiece errors of less than 5 micron.

2.1.4 Conclusions paper 2007-04

Measurement methods for efficient thermal assessment and error compensation
This paper describes measurement procedures for efficient assessment of thermal errors using strip sensors to measure thermal gradients. This resulted in error predication greater than 85% emphasising the benefits of this sensor technology development.

2.1.5 Conclusions paper 2007-05

Flexible compensation of thermal errors.
The performance of machine thermal compensation system was validated by tests and measurements of a machined NAS979 artefact which showed an 80% improvement of accuracy of machined features.

2.1.6 Conclusions paper 2011-05

Efficient thermal error prediction in a machine tool using finite element analysis
Studies showed significant reductions in machine downtime could be made by use of FEA to predict thermal errors rather than physical machine testing.

2.1.7 Conclusions paper 2012-06

An efficient offline method for determining the thermally sensitive points of a machine tool structure
FEA provides a very good assessment of machine thermal errors and prediction of sensitive nodal locations for efficient installation of sensors

2.1.8 Conclusions paper 2013-02

The significance of air pockets for modelling thermal errors of machine tools Air pockets in machine structures have significant effects and should be avoided by good design but where this is not possible they should be taken into account during development of predictive models.

2.1.9 Conclusions paper 2013-05

Comparative study of ANN and ANFIS prediction models for thermal error compensation on CNC machine tools

ANN and ANFIS models for error prediction were compared showing a range of advantages and disadvantages depending on circumstances

2.1.10 Conclusions paper 2013-06

Efficient estimation by FEA of machine tool distortion due to environmental temperature perturbations

Use of FEA has produced good environmental thermal error models and reduced machine downtime.

2.1.11 Conclusions paper 2013-13

Application of GNNMCI (1, N) to environmental thermal modelling of CNC machine tools

The Grey Neural Network model with Convolution Integral GNNMC AI is was used with a Particle Swarm Optimisation (PSO) algorithm and was shown to be capable of producing superior prediction results for thermal errors whilst being more practical and cost effective.

2.1.12 Conclusions paper 2015-03

Thermal error modelling on machine tools based on ANFIS with fuzzy c-means clustering using a thermal imaging camera

ANFIS is proving to give very good results for prediction of thermal errors

3. SUMMARY CONCLUSIONS

Research by the Centre for Precision Technologies (CPT) at The University of Huddersfield has produced an in-depth understanding of the factors that contribute to machine tool inaccuracy.

The research presented here discusses what are potentially the two main causes of inaccuracies of machine tools namely the concrete foundation that support them and their response to temperature changes caused by both their environment and self-induced heat sources.

3.1 FOUNDATIONS

The six "Foundation" papers presented in this thesis describe how the specification, design and testing of concrete foundations for large machine tools can be achieved in a manner such that process will ensure that the foundation will meet the functional needs of the machine.

The research describes how the uncertain nature of foundation subsoil can be overcome by following a specific testing protocol.

Additionally the development and testing of instrumentation that has been successfully developed to support the above mentioned protocols is described in the final two "Foundation" publications. The instrumentation is inexpensive, extremely accurate and will reduce testing time from days to hours.

Adherence to the procedures described, would ensure that the possibility of anyone of a large number of potential problems occurring will be avoided.

3.2 THERMAL EFFECTS

The reduction of thermal errors of machine tools has until recently been in the order of 70%. The culmination of the research and development that is described in the twelve thermal papers presented in this thesis is error reduction values of 95% are now being achieved. This

is due to the accumulated effect of the planned research activities which has led to the final
papers associated with the research and development of Artificial Intelligence methods.

The thermal compensation research was key to the CPT becoming a participant in the FP7
ADAMOD european project. The project needed a thermal compensation system with higher
levels of accuracy than achievalbe in any literature in the public domain. The CPT
successfully completed the project by data fusion of on-machine strain measurement into the
thermal compensation system. This led to a further FP7 grant EASE-R3.

This research has led to the design and development of a new machine tool compensation
system unit with all the capability of volumetric compensation and affordable bespoke
hardware for universal integration onto new and existing machine tools. This system has been
shown to reduce geometric errors by 90% and with recent developments thermal errors by
95% giving the capability for more accurate parts, with better functionality, less wear, longer
life, less re-work, fewer scrapped parts and lower unit costs which in turn reduce the need for
inspection, significantly lowered assembly times and enhanced inter-changeability of parts.

The underpinning technology of rapid geometric calibration and high accuracy temperature
measurement using thermal imaging and unique flexible temperature sensing strips, combined
with physics based algorithms enabled thermal errors to be reduced by 80%. Specialist
software, TempSpy was written to calibrate sensors and record large amounts of data along
with Virmach which evolved to simulate and communicate machine errors for customer
reports and became a further key tool for the compensation.

Finite Element Analysis (FEA) has played a significant role in more recent research, using
new techniques to model more accurately the thermal behaviour of complex structures. This
reduces the amount of empirical work require to optimise model variables. FEA has also been
used to understand the often ignored elastic effects when traversing the machines.

The final papers describe how the use of artificial intelligence (AI) based models of machine
tools have enabled thermal errors to be reduced by 95%.

3.3 OVERALL SUMMARY

The accuracy of machine tools is fundamental to the quality of the products they make. A
better understanding of why errors occur and how to minimise them is vital to ensuring higher
standards of manufacturing and increased productivity. The work described in this thesis has
delivered significant improvements in measuring and compensation for machine tool
inaccuracies and therefore the components that are manufactured by them.

This has led to predictive methods for assessing the capability of machines to produce specific
components and the development of a low-cost electronic Volumetric Compensation System
that can increase machine tool volumetric accuracy by a factor of 10, with significant cost
savings for factory temperature control. A contract has been signed to market this system
globally. Rapid calibration techniques have been developed, in collaboration with a UK
world-leading aerospace manufacturer, reducing timescales for days to less than one hour.

4. FUTURE PERSPECTIVES

4.1 FOUNDATIONS

Research and development is currently being carried out on the use of hydraulic levelling
units with capacitive sensors for determining horizontality, height variation and vertical
deflection.
It is envisaged this research is will produce the extremely high orders of accuracy needed for
modern large machine tools and their foundations.

It is thought that the surface stiffness of concrete foundations and also the sub-soil could be
more easily and efficiently measured by use of Laser trackers. The current technology is such
that they are not sufficiently accurate and that they are considerably more expensive than the
equipment described in this thesis.

However it is envisaged that both of these problems will be overcome and although there are
considerable uncertainties associated with the process, the benefits will fully warrant further
research and development which would form the basis of a significant project.

4.2 THERMAL EFFECTS

`With such high reductions in thermal error of 95% the future concentration will be focused on improving the efficiency of installation of compensation systems, reducing machine downtime and the cost of hardware associated with sensors.

Attention will move towards focus on work-piece thermal errors and the use of telemetry for communication with sensors.

4.3 OVERALL PERSPECTIVE

Current machine tool industrial technology uses individual feedback encoders systems which are axis specific. Future systems are envisaged which will be based on direct measurement of the cutting tool position relative to datums on the workpiece. Such systems will in principle be machine based equivalent of GPS and capable of eliminating all machine positional errors. To overcome problems of line of sight due to swarf, coolant and workpiece size and shape, they might involve the use of aerial drone reference units.